IONIC AND NEUTRAL HYDROGELS FOR DERMAL AND OPHTHALMIC APPLICATIONS

ANISA MAHOMED

Doctor of Philosophy

ASTON UNIVERSITY

October 2005

ASTON UNIVERSITY

IONIC AND NEUTRAL HYDROGELS FOR DERMAL AND OPHTHALMIC APPLICATIONS

ANISA MAHOMED

Submitted for the degree of
Doctor of philosophy

October 2005

SUMMARY

This thesis is concerned with the use of ionic and neutral hydrogels in dermal and ocular applications with particular reference to controlled release applications. The work consists of three interconnected themes. The first area of study is the use of skin adhesive bioelectrode hydrogels as ground plate electrodes for ophthalmic iontophoresis applications. The work described here provides a basis of understanding of the relative contributions made by ionic monomers (such as sodium 2-(acrylamido)-2-methyl propane sulphonate and acrylic acid-bis-(3-sulfopropyl)-ester, potassium salt) and neutral monomers (such as acryloylmorpholine, *N,N*-dimethylacrylamide and *N*-vinyl pyrrolidone) to adhesion, rheology and impedance of bioelectrode gels. The general advantage of neutral monomers, which have been used to successfully replace ionic monomers, is that they enable more effective control of independent anion and cation species (for example potassium chloride and sodium chloride) unlike ionic monomers where polymerisation produces an immobile polyanion thus limiting cation mobility.

Secondly, release from a completely neutral hydrogel under the influence of mechanical shaking was studied for the case of crosslinked polyvinyl alcohol (PVA) containing low concentration of linear soluble PVA in a contact lens application. The soluble PVA was observed to be eluting by reptation from the lens matrix due to the mechanical action of the eyelid. This process was studied in an *in vitro* model, which in this research was used as a basis for developing a lens made with enhanced release polymer.

The third area of work is related to the factors that control drug release (in particular non-steroidal anti-inflammatory drugs) from a hydrogel matrix. This links both electrotherapy applications, such as transcutaneous electrical nerve stimulation, in which the passive diffusion from the gel could be used in conjunction with enhanced transmission across the dermal surface with passive diffusion from a contact lens matrix and the development of therapeutic contact lenses.

Keywords: bioelectrode hydrogel, electrotherapy, macromolecular release, ocular release model, release from a hydrogel matrix, release modelling

For

Mum, Dad, Zita,

Mama and Papa

ACKNOWLEDGEMENTS

I would like to take this opportunity to thank Professor Brian Tighe for giving me the opportunity to carry out this research, for his guidance, enthusiasm, financial support throughout the course of this research, for the opportunities to attend many conferences within the U.K. and abroad and for organising a great fantasy football contest.

Thank you to First Water for their collaborative help with materials and the impedance meter used to carry out tests described in chapter 3.

Thank you to all those past and present members of Aston Biomaterials Research Unit and Chemical Engineering and Applied Chemistry Department who assisted me as and when I required.

I would like to make special mention of Ellie for teaching me the basics, Aisling for her invaluable advice, having to share her "space" with me at the office as well as away and her sense of humour, Fiona for her advice and for the education on pregnancy and childbirth and Val for taking care of all things administration related. Acknowledgements also go to Gareth Ross for his collaboration with chapter 4 of this project.

Last but not least many many many thanks to my parents, sister and grandparents for their love, support, a home and untimely distractions!

LIST OF CONTENTS

LIST OF FIGURES

LIST OF TABLES

NOTATION AND ABBREVIATIONS

Ab	absorbance
D	swollen diameter
D_o	original diameter
E	electrostatic potential
F	Faraday's constant
F_t	force causing movement
G'	elastic modulus
G"	viscous modulus
I	current
I_t	intensity of transmitted light
I_o	intensity of incident light
J	flux
J_i	flux of species i
J_C	flux electroosmotic contribution
J_E	flux electromigration contribution
J_P	flux passive contribution
J_T	total flux
J_v	flux convective contribution
K_a	acidity constant
$K_{o/w}$	octanol-water partition coefficient
K_{pc}	solute partition coefficient
MW	molecular weight of the species
$\overline{M}_c$	number average MW between crosslinks
M_r	MW of repeat unit
$\frac{M_t}{M_\infty}$	fractional release
R	resistance
V/Vo	swollen volume / original volume (volume swell)
U	acceleration potential
X	reactance
W	applied load
Z	impedance
X	crosslink ratio

a_i	thermodynamic activity of species i in its vehicle
c	concentration
c_i	concentration of species i
c^I	concentration of ionised species
c^N	concentration of unionised species
d	diffusion coefficient
d_i	diffusion coefficient of species i
$d_i(c_i)$	concentration-dependent diffusion coefficient
f^I	ionised fraction
h	thickness of the recipient membrane
k.e.	kinetic energy
$k_p{}^I$	permeability of the ionised species
$k_p{}^N$	permeability of the unionised species
l	length of light path
m	species mobility
a	electrical contact area
j	unit imaginary number
k	constant characteristic of the active-polymer system
l	hydrogel thickness
m	mass
n_i	RI of incident medium
n	diffusional exponent
p	permeability constant
pH	power of the concentration of hydrogen ions ($-\log[H^+]$)
pK_a	pH at which the active is 50 % ionised (see equation 5.13)
r	hydrodynamic radius of the active
r_c	radius of contact
s	solubility
t	release time
$\bar{v}$	specific volume
w/v	weight to volume
w/w	weight to weight
x	position normal to the effective area of diffusion (x axis)
z	ion charge (valence)
z_i	the valence of species i
n_r	RI of refracted medium
t	pulse length
v	sliding speed , velocity
v_i	speed of incident light
v_r	speed of refracted light

$\tan \delta$	tangent of phase shift, see equation 2.9
logD	see equation 5.19
$\log P^{I}$	see equation 5.22
$\log P^{N}$	see equation 5.18

AC	alternating current
AR	aqua release
C-C	carbon-carbon
CMC	critical micellar concentration
DC	direct current
DSC	dynamic scanning calorimetry
ECG	electrocardiograph
EWC	equilibrium water content
GC	gas chromatography
HPLC	high performance liquid chromatography
IC	ion chromatography
IPN	interpenetrating polymer networks
LC	liquid chromatography
MALDI-TOF MS	matrix-assisted laser desorption ionisation-time-of-flight mass spectrometry
MEC	minimum effective concentration
MS	mass spectrometry
MTC	minimum toxic concentration
NMR	nuclear magnetic resonance
NSAID	non-steroidal anti-inflammatory drug
PABS	phosphate-acetate buffered saline
PBS	phosphate buffered saline
PSA	pressure sensitive adhesive
RI	reactive index
SINs	simultaneous IPN
TDDS	transdermal drug delivery systems
TENS	transcutaneous electrical nerve stimulation
UV	ultraviolet radiation

AMPS	2-acrylamido-2-methyl propane sulphonate
COOH	carboxyl group
$CONH_2$	amide group
DOPC	dioleylphosphatidyl choline
HEC	hydroxyethyl cellulose
K^+	potassium ion
KCl	potassium chloride
KOH	potassium hydroxide
Na^+	sodium ion
NaCl	sodium chloride
NaOH	sodium hydroxide
OCOCH	acetate group
OH	hydroxyl group
OH_3^+	hydronium ions
PEG	polyethylene glycol
PVA	polyvinyl alcohol
PVAc	polyvinyl acetate
PMMA	polymethyl methacrylate
PVP	polyvinyl pyrrolidone
SO_3^-	sulphonate
SO_4^{2-}	sulphate

Please refer to section 2.1 for the following monomers and reagents:

AA	AMO	AZBN	DAA	DATr	DHB
Eb11	HEMA	Irgacure 184	$MPEG_{400}MA$	NaAMPS	NNDMA
NVP	TFA	TRIS	SPA		

Δc_i	transmembrane concentration difference
γ	effective activity coefficient in the skin barrier
δ	phase shift
$\delta_{o/w}$	partition log ratio of the neutral species to ionic species
ε	extinction coefficient
ξ	pore size
ρ_x	crosslinked density
θ_c	critical angle
θ_i	angle of incidence
θ_r	angle of refraction
η	viscosity
μ	coefficient of friction
μD	dynamic or sliding friction
μS	start-up or static friction
%	percent
$\leq$	less than or equal too
$>$	greater than
$<$	less than

µC	microcoulomb ($x10^{-6}$)
µJ	microjoule ($x10^{-6}$)
µl	microlitre ($x10^{-6}$)
µl/min	microlitre per minute
µm	micrometer ($x10^{-6}$)
µS/cm	microSiemens per centimetre
µs	microsecond ($x10^{-6}$)
Ω	ohm
MΩ.cm	megaohms ($x10^{6}$) centimetres

A	amperes (amps)
atm	atmospheres
°C	degrees celsius
cm	centimetre
cm^2	centimetre squared
cm/h	centimetre per hour
(k)Da	(kilo)dalton
g	gram
(k)Hz	(kilo)hertz
k	kilo ($x10^{3}$)
kg	kilogram
M	molar
m	metre
m^2	metre squared
m/min	metres/minute
m^2/N	metre squared per newton
mA	milliamps ($x10^{-3}$)
mA/cm^2	milliamps per centimetre squared
mA*min	milliamp minutes
mg	milligrams ($x10^{-3}$)
mg/cm^2h	milligrams per centimetre squared per hour
mg/ml	milligrams per millilitre
MHz	megahertz ($x10^{6}$)
min	minutes
ml	millilitres ($x10^{-3}$)
ml/min	millilitres per minute
mM	millimolar ($x10^{-3}$)
mm	millimetres ($x10^{-3}$)
mm/min	millimetres per minute
mN	millinewtons ($x10^{-3}$)
mN/m	millinewtons per metre
mOsm/L	milliosmoles per litre
ms	milliseconds ($x10^{-3}$)
mPa.s	millipascal ($x10^{-3}$) seconds
N	newton
N/m^2	newton per metre squared
N/mm	Newton per millimetre
nm	nanometres ($x10^{-9}$)
mOsm	milliosmoles ($x10^{-3}$)
Pa	pascal
pps	pulses per second
psi	pounds per square inch
rpm	revolutions per minute
s^{-1}	per second (1/s)
(k)V	(kilo)volt, potential difference
W/cm	watts per centimetre

Chapter One

Introduction

1. INTRODUCTION

1.1 Hydrogels

Biomaterials are substances other than food or drugs contained in therapeutic or diagnostic systems that are in contact with biological fluids.[1] The work resulting in the discovery of hydrogels, specifically polymers of 2-hydroxyethyl methacrylate (HEMA) as a new class of biomaterials, was pioneered by Wichterle and Lim[2] circa 1960. The term *hydrogel* does not have a precise and limiting definition. However a useful definition may describe hydrogels as three-dimensional hydrophilic polymeric networks, either natural or synthetic in origin, capable of imbibing large amounts of water or biological fluids and do not dissolve due to the presence of crosslinks.[3, 4]

Hydrogels are synthesised by the copolymerisation of one or more monomers or polymers with a crosslinker to form a hydrogel network. Alternatively they can be produced by polymerising a monomer within a polymer network to form an interpenetrating network as portrayed in figure 1.1.

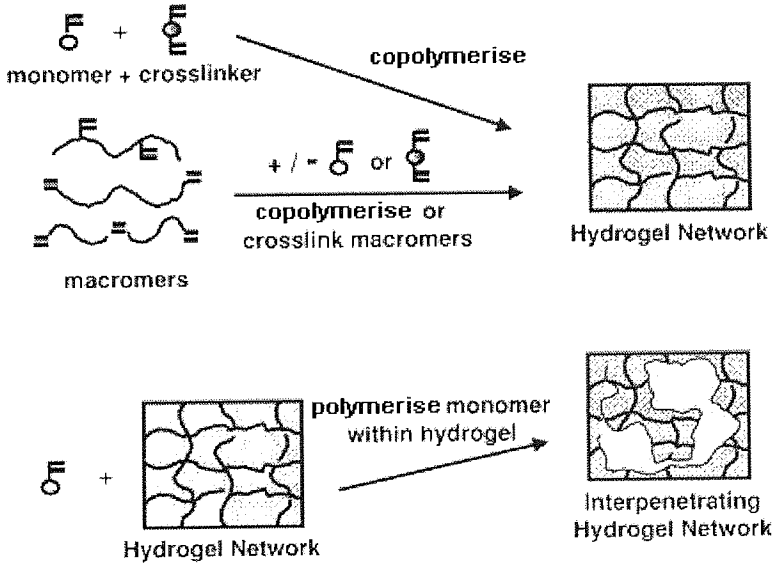

Figure 1.1 Schematic of methods for formation of crosslinked hydrogels.[5]

Crosslinks may be ionic or covalent bonds; in addition association bonds such as hydrogen bonds and strong van der Waals forces can serve as crosslinks.

Hydrogels can be classed in various ways[6-10] as summarised in table 1.1.

Classification	Contents
i. source	• natural • synthetic
ii. component	• homopolymers (single monomer) • copolymers (two monomers) • multipolymer (several monomers) • interpenetrating (one crosslinked polymer is swelled in a second monomer that is reacted to form a second intermeshing network)
iii. method of preparation	• simultaneous polymerisation • crosslink polymer
iv. nature of the side groups	• ionic (anionic or cationic) • non ionic (neutral) • ampholytic (both anionic and cationic)
v. mechanical or structural characteristics	• affine network (junctions are firmly embedded in the medium) • phantom network (junctions are mobile in the medium)
vi. network morphology	• amorphous (randomly ordered polymer chains) • semi crystalline (containing dense regions of ordered polymer chains) • hydrogen bonded structures (three-dimensional network held together by hydrogen bonds) • supermolecular structures (large polymer, repeating units are not necessarily same)

	• hydrocolloidal aggregates
vii. network structure	• macroporous (pore size between 0.1 and 1 μm) • microporous (pore size between 0.01 and 0.1 μm) • nonporous (pore size between 0.001 and 0.01 μm)
viii. physical structure	• physical (sol→ gel reversibility) • chemical (covalently bonded) • composite gels
ix. crosslink	• covalent bond • intermolecular force
x. function	• biodegradable • stimuli responsive • super absorbent

Table 1.1 Possible classification of hydrogels.

1.2 Water in hydrogels

The water contained within a hydrogel strongly influences the behaviour of the material. When immersed in water hydrogels swell to form a soft elastic water containing gel. It is this water that governs the unique mechanical, surface and permeability properties that give them the interface compatibility with blood and tissue. Hence this water bestows hydrogels their *biocompatibility*. Biocompatibility is defined as "the ability of the material to perform with an appropriate host response in a specific application".[4] Given that biological surfaces and many constituents of biological fluids are polar, charged monomers would not only affect hydrogel bulk properties but also their behaviour in a biological environment. Thus water content and structure are believed to be the most important properties of a hydrogel.[4, 11]

1.2.1 Equilibrium water content

When placed in water hydrogels swell until equilibrium is reached. This is when the thermodynamically driven swelling force is counterbalanced by the elastic retractive force of the crosslinked structure. The water content of a fully hydrated and equilibrated hydrogel is given as the equilibrium water content (EWC). This is quantified by the ratio of the water in the hydrogel to the total weight of the hydrogel and is expressed as a percentage.[11]

$$\mathbf{EWC(\%)} = \frac{\mathbf{weight\ of\ water\ in\ hydrogel}}{\mathbf{Total\ weight\ of\ hydrated\ hydrogel}} \times \mathbf{100} \qquad \text{Equation 1.1}$$

Water in hydrogel acts as a:[4, 12]

i. plasticiser, behaving as an "internal lubricant" allowing chains to rotate, hence conferring flexibility
ii. transport medium for dissolved species such as oxygen and water-soluble metabolites
iii. "bridge" between the surface energies of natural and synthetic systems, thereby enhancing biotolerance
iv. lubricant, reducing the coefficient of friction at the surface.

In the context of the present research, to this may be added the ability to act as an ionic conduction medium.

The EWC of a hydrogel is influenced by the nature of the hydrophilic monomer, the nature and density of the crosslinking agent used in the hydrogel and external factors such as temperature, tonicity (and nature of the constituent ions) and pH of any hydrating medium. The balance of contributing steric and polar effects for a given composition also influences the EWC.[4, 11] These factors can be varied to obtain an EWC to suit the application.

1.2.2 Water structure

Besides EWC, other structural aspects that are capable of exerting a dominating influence on hydrogel properties are the water structures within the hydrogel coupled with chain stiffness and inter-chain forces of the constituent polymer.

Varying the molecular interactions within a hydrogel can result in thermodynamically different classes of water. Different terms have been used to describe the classes, but it is generally suggested that water present in a polymer network exists in a continuum of states between two extremes. On the one extreme when a dry hydrogel begins to imbibe water the most polar hydrophilic groups will be hydrated first, this water is strongly associated with the polymer network through hydrogen bonding, and is referred to as *primary* bound. The network swells as the polar groups become hydrated abd this exposes the hydrophobic groups which interact with the water molecules resulting in hydrophobically or *secondary* bound water. These can be combined and referred to as *total* bound water. Further water absorption, resulting from the osmotic driving force of the network towards infinite dilution, is opposed by the crosslinks resulting in an elastic network retraction force allowing the hydrogel to reach an equilibrium swelling level. This is the other extreme referred to as *free* or *bulk* water. This water has a greater degree of mobility as it is unaffected by the polymeric environment.[5, 13] A literature review shows that various authors use a variety of terms to describe the state of water in hydrogels.[13] These are listed in table 1.2.

Primary Bound Non-freezing		Secondary Free Freezing	
Bound Non-freezing X W_3	Interfacial Freezable bound Y W_2	Free/ bulk Free Z W_1	
Primary bound Bound water which rejects salts	Secondary bound Bound water which can contain salts	Free Free water completely interacting with polymer	Bulk Completely free water

Table 1.2 Various descriptions of water binding states.

Conversely, it has also been suggested that different fractions of water undergo phase transitions at different temperatures although the existence of different states of water at or above 0°C cannot be presupposed. Additionally it is postulated that due to reorientation, the mobility of water molecules increases when surrounded by other water molecules instead of the polymer.[14]

The techniques used to study water binding in hydrogels are based on small molecular probes, differential scanning calorimetry (DSC) and nuclear magnetic resonance (NMR).[5] It has also been noted that the technique used influences, to a certain extent, the ratio of the water states.[4]

For the molecular probe technique, the hydrogel is equilibrated in a solution of probe molecules and at equilibrium the concentration of the probe molecules are measured. The amount of free water content can then be deduced from the amount of absorbed probe molecule and the measured external probe molecule concentration. The bound water content is obtained from the difference between total and free water content. However this is based on the assumption that:

i. only free water in the hydrogel can dissolve the probe solute
ii. the solute does not affect free and bound water distribution
iii. all free water is accessible to the solute
iv. the solute concentration in the free water is equal to solute concentration in external solution and
v. the solute does not interact with the matrix.

DSC is based on the supposition that only free water is frozen. Thus the measured endotherm seen when warming a frozen gel is representative of the amount of free water. Again the bound water content is obtained from the difference between total and free water content. This method does not, however, take into account the contribution of the heat of polymer-water mixing when the melting endotherm is recorded.

It has been suggested[15] that NMR can probe the behaviour of bound water. In addition it can qualitatively and quantitatively distinguish between water that freezes closer to its normal freezing point of 0 °C and water that retains mobility at lower temperatures.

1.2.3 Water content

In addition to EWC and water states in a hydrogel, the volume of water in a hydrogel also has an influence on its properties.[16] Partially hydrated hydrogels are adhesive due to an increased affinity for water. Hence the extent of adhesion is influenced by the quantity of water within the hydrogel. Partially hydrated, high EWC hydrogels are therefore useful as adhesives for soft and moist tissue. Thus EWC and degree of hydration can be optimised to provide the required adhesion for a given application.[16, 17]

1.3 Mechanical strength

A characteristic advantage of hydrogels is that their properties can be tailored by modifying the ratio of copolymers to obtain different degrees of hydrophilicity. On the contrary, a disadvantage intrinsic to hydrogels is their low mechanical strength, although this is overcome by altering the degree of crosslink or by forming interpenetrating networks.

1.3.1 Crosslink ratio

Hydrogels acquire the majority of their mechanical strength from the crosslinks within the polymer network. An important parameter used to identify crosslinked structures is the crosslink ratio: *X*. This is the ratio of crosslinker moles to the moles of polymer repeat units. From this, the number average molecular weight between crosslinks, $\overline{M}_c$, is defined as:

$$\overline{M}_c = \frac{M_r}{2X} \qquad \text{Equation 1.2}$$

where M_r is the molecular weight of the repeat unit.[3] The crosslinked density, ρ_x, can then be determined from equation 1.3:

$$\rho_x = \frac{1}{\bar{v}\overline{M}_c} \qquad \text{Equation 1.3}$$

where $\bar{v}$ is the specific volume of the polymer.[6] These equations can be applied on the assumption that all crosslinking agent has reacted with the polymer.

Increasing the concentration of crosslinking agent creates a hydrogel with greater mechanical strength. This however causes the hydrogel to become brittle. In addition this causes an increased elastic network retraction force resulting in decreased diffusivity within the hydrogel; thereby causing a reduction in release and swelling rates as well as EWC.[9, 18] Thus an optimum degree of crosslinking that achieves a relatively strong, yet elastic hydrogel, will need to be determined for each system.

1.3.2 Interpenetrating polymer networks

Polymer blends are known to possess enhanced mechanical properties; the same can be said for hydrogel polymer blends known as interpenetrating polymer networks (IPNs).[4]

IPNs are a combination of two polymers in network form, at least one of which has been synthesised and/ or crosslinked in the presence of the other. Depending on their method of synthesis they can be divided into three classes.[19]

Firstly, a sequential IPN is produced when pre-polymerised and crosslinked monomer I is swollen in a mix containing monomer II, crosslinker and initiator, and is subsequently polymerised in the presence on monomer I.

The second class are semi-IPNs. A preformed linear polymer is dissolved in a second monomer, the solution is then polymerised to crosslink the second monomer around the linear polymer. In this category only one of the two polymers is crosslinked.

The final category, simultaneous IPNs (SINs), entails the simultaneous polymerisation of a mix of two monomers with their respective crosslinkers and initiators but by different non-interfering methods.

Figure 1.2 illustrates possible two-polymer combinations of IPNs.

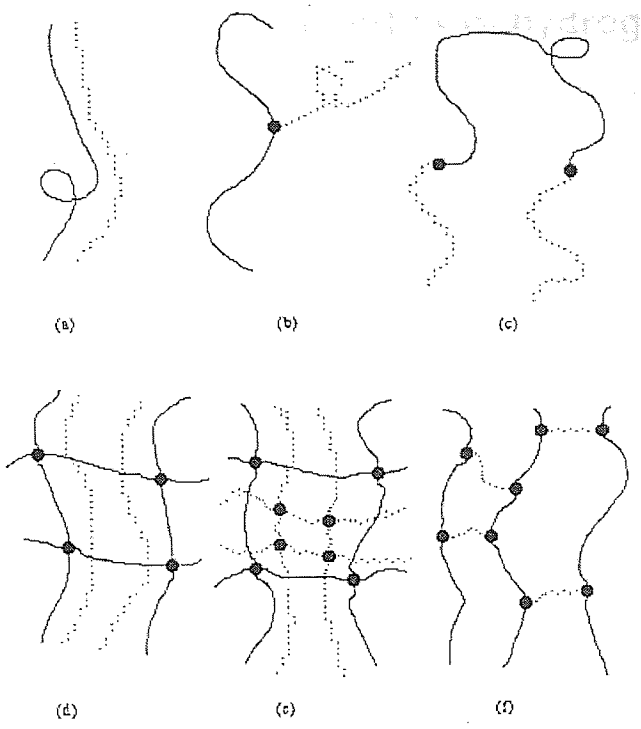

(a) polymer blend (b) graft copolymer (c) block copolymer (d) semi-IPN (e) full IPN (f) AB crosslinked polymer.

Figure 1.2 Possible two-polymer combinations.[4]

Interpenetrating polymer networks provide an interesting means to strengthen hydrogels although, yet again, other properties such as water binding, surface and optical properties are affected. Notably IPNs create hydrogels with increased strength and stiffness but less elastic in comparison to copolymers of similar water content.[4]

1.4 Biomedical applications and properties of hydrogels

The use of crosslinked, covalently bonded, synthetic hydrogels has grown considerably in recent years in biomedical applications such as contact lenses, ocular prostheses, synthetic articular cartilage, implant and reconstructive materials, wound dressings, skin adhesives, sensors, perm-selective membranes, drug delivery systems and the list goes on.[1, 4, 16, 17] This is attributed to the biocompatibility of hydrogels resulting from their ability to simulate natural tissue by virtue of their high water content and special surface properties.[20] This thesis focuses in particular on hydrogels used in applications requiring skin adhesives and contact lenses.

1.4.1 Skin adhesives

Skin adhesives may be defined as pressure sensitive adhesive (PSA) materials that adhere to the skin by applying a light pressure but which should leave no residual adhesive upon their removal.[21] In principal a functional skin adhesive requires adequate tack, peel adhesion and cohesive strength. In terms of applied pressure, tack is a measurement of how easily and quickly an adhesive can be applied to a chosen adherend. Peel adhesion is then used to evaluate the degree of difficulty of removing the adhesive (adhesive failure). Cohesive strength gives an indication of the ability to peel the adhesive off cleanly (cohesive failure) and this is determined by measuring its shear strength or dynamic mechanical properties.

1.4.1.1 Mechanism of adhesion

Adhesion can be defined as the state in which two surfaces are held together by interfacial forces.[22] The interfacial forces may range from valence forces to mechanical interactions, or some combination of chemical and physical interactions. When one or both of the adherends are of a biological nature this interaction is known as *bioadhesion*. A *bioadhesive* can therefore be defined as a substance that has the ability to adhere to a biological material and is capable of being retained on the biological substrate for a protracted period. One distinctive feature of bioadhesion is that adhesion usually occurs in the presence of water.[23]

It has been suggested[23] that it is more appropriate to refer to bioadhesion as a phenomenon rather than a mechanism. Hence different types of bioadhesion have been grouped from a phenomenological perspective. The adhesion between biological objects has been classed as Type I adhesion. The adhesion of biological substances to an artificial substrate has been categorised as Type II adhesion. The reverse, that is the adhesion of an artificial substrate (such as a hydrogel) to a biological substrate, has been classed as Type III adhesion. Furthermore this perspective allows for one or more theories to explain the formation of a bioadhesive bond, as the pertinence of each theory is not exclusive as it depends upon the system concerned.[23] Theories of bioadhesion have already been reviewed[23, 24] in detail, thus will not be discussed further. Nevertheless it is widely accepted that for an adhesive to adhere to a substrate it must satisfy thermodynamic and kinetic conditions. Thermodynamically its measured surface energy must be equal or less than that of the adherend. The surface energy of clean and dry human skin is quoted[25] to be within the region of 28 to 29 mN/m. Kinetically the adhesive must *flow* sufficiently to promote intimate contact between the adhesive and the adherend. A guideline, the Dahlquist criterion, states that:[25]

the adhesive's compliance should be $> 10^{-6}\ m^2/N$,
equally its (elastic) modulus should be $< 10^5\ N/m^2\ (Pa)$, *ideally between* 10^3 *and* $10^4\ N/m^2\ (Pa)$.

In an attempt to generalise the bioadhesion phenomenon it has been proposed that bioadhesion in the presence of an optimum amount of water maintains a dynamic state; whereby hydrated polymer chains are free to move and stretch thereby becoming entangled or twisted when in close contact with a substrate. This allows for the matching of adhesive sites between the polymer and substrate; subsequently allowing the formation an adhesive bond.[23] The adhesive bond may result from either:[23, 26]

i. primary ionic or covalent chemical bonds of the functional groups
ii. secondary chemical bonds such as van der Waals dispersive interactions or hydrogen bonding or
iii. physical or mechanical bonds as a result of surface roughness.

1.4.1.2 Adhesive bioelectrodes

Bioelectrodes are electrodes applied onto biological surfaces. Adhesive bioelectrodes should possess the ability to form an adhesive bond with biological surfaces. Therefore when used as an electrode the adhesive should also be electrically conductive; this may be achieved by the addition of ionic components, such as sodium or potassium chloride, with water acting as the conduction fluid. Adhesive bioelectrodes have been used widely within the medical field, for example electrosurgery, which requires high frequency electrical currents (radio frequencies of 1 to 5 MHz)[27] for cutting tissue and causing coagulation of haemostasis in tissues. Other examples of adhesive bioelectrodes used in electrotherapy are for wound healing, medical diathermy, transcutaneous electrical nerve stimulation (TENS), direct nerve stimulation, muscle stimulation[27] and more recently in transdermal drug delivery (section 1.5.2). The composition of a hydrogel can be manipulated to provide the electrical conducting interface required for adhesive biomedical electrodes.

The structure of a bioelectrode is illustrated in figure 1.3.

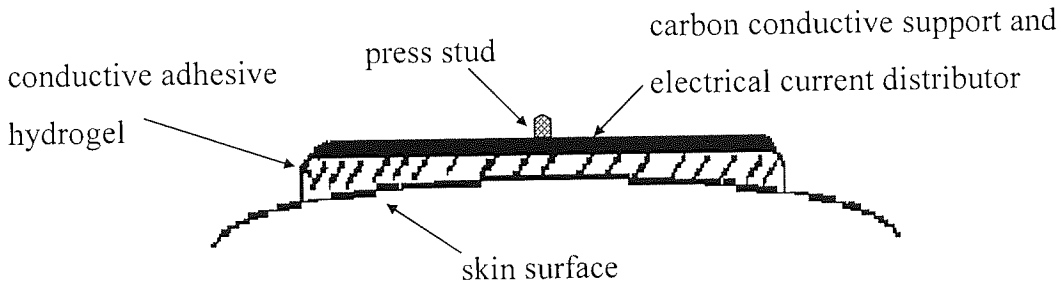

Figure 1.3 Typical components of a bioelectrode.

1.4.1.3 Suitability of hydrogels as skin adhesives

A skin adhesive ought to adhere to the skin for the duration of intended use, usually between twenty-four hours and seven days. Additionally it should be easy to apply and remove from the skin and ought to remain adhesive if removed for repositioning. In theory it is feasible to improve the cohesive strength of a hydrogel through crosslinking, yet maintaining its tack and adhesive properties. It is already known that the strength of adhesion is affected by the molecular weight of the adhesive, crosslink density,

hydration, hydrophilicity, charge, applied force, initial contact pressure and time and temperature.[22, 28] Hence by controlling the surface chemistry of the adhesive hydrogel, through compositional manipulation, molecular contact and interactions at the interface between the skin and the adhesive can be maximised.

Three main factors have been identified that are responsible for the importance of hydrogels as skin adhesive materials. These are the presence of a hydrophilic component, the short-range interactions via hydrophobic domains on flexible side chains and the rheological properties.[16]

i. hydrophilicity

The hydrophilic component is desired in order to remove the lubricating interfacial water layer between the hydrogel and the skin allowing for maximum interaction at the interface. Hydrogels prepared with hydrophilic monomers contain chains with hydrophilic groups, such as hydroxyl (-OH), carboxyl (-COOH), amide ($-CONH_2$) and sulphate ($-SO_4^{2-}$) groups. When partially hydrated these hydrogels encompass an outstanding capacity for water uptake; hence potentially a high EWC that promotes their adhesiveness when applied to the skin.

ii. hydrophobic domains

In comparison to other polymers, hydrogels have a low crosslink density enhancing the flexibility of the hydrophobic groups on the external hydrogel chain branches. In air, for example, when the environment is relatively hydrophobic compared to that within the hydrogel, the hydrophobic groups rotate thereby exposing their side chains. In contrast to this, in a relatively hydrophilic environment, such as water, the chains rotate thereby exposing their hydrophilic side chains. This feature enhances skin adhesion resulting from "matching" of the hydrophobic side chain with the hydrophobic lipids and proteins of the skin resulting in a hydrophobic interaction.

iii. dynamic mechanical properties

The rheological properties of hydrogels can be tailored to allow close conformation to the skin surface. These properties give the hydrogel sufficient cohesive mechanical strength to remain consistent on removal or for replacing. Ideally a skin

adhesive hydrogel should have dominant elastic forces at low frequency stresses, such as when being applied to the skin. This facilitates close shaping of the hydrogel to the skin contours. The viscous component should be dominant at high frequency stresses, such as during its removal. This minimises the extension of the hydrogel (*"legging"*) and allows for removal in one piece. However, it should be noted that a combination of high adhesive strength and high mechanical strength may cause trauma to the skin on removing the hydrogel. This can be controlled by the crosslink density, which permits fine adjustment of mechanical and rheological behaviour. The issue of painful removal of the adhesive hydrogel can be overcome by adding a water-soluble interpenetrate polymer, which acts as a plasticiser and increases the flexibility of the gel as well as the molecular contact at the interface, without deterioration of the mechanical strength.

In context of this research, hydrogels for use as adhesive sensors or electrodes must be electrical conductors. This can be achieved by incorporating ionic monomers or salts, whilst the presence of water within the polymer matrix acts as the conduction media. In terms of an economically viable product, hydrogels also allow for production of sterile samples, are disposable, have ample shelf life and are aesthetically pleasing.

1.4.2 Contact lenses

Contact lenses, external prosthetic devices for vision correction, were historically made from glass. In the late 1940s however this was replaced by a thermoplastic, polymethyl methacrylate (PMMA). Thermoplastics are shaped under applied heat and pressure, but are rigid at room temperature showing some flexibility but not elasticity. Synthetic elastomers, which are flexible and show rubber-like behaviour, have also been considered. However these produce polymers with hydrophobic surfaces resulting in poor wettability and a high affinity for surface deposits. Since hydrogels can be formulated to possess a wide range of properties it is possible to purposely design hydrogel polymers for contact lenses.

1.4.2.1 Contact lens requirements

A contact lens should ideally behave as an extension of the cornea. It should allow the cornea to respire without undue physiological stress, resist the deforming force of the eyelid and permit the maintenance of a continuous tear film on the lens whilst minimising the accumulation of lipoidal and denatured protein deposits.[29, 30]

Oxygen permeability

Oxygen permeability is vital as the cornea is avascular and lack of oxygen may lead to cell death and possible lack of vision. The oxygen permeability of hydrogels containing 30% or less of water is dependent on the nature of the polymer backbone and the state of the water.[29] However, at higher water contents it is dependent on the EWC. It can therefore be concluded that EWC is an important element in governing the oxygen permeability of a hydrogel.

Mechanical properties

To remain visually stable, a contact lens must resist deformation resulting from the shear and compressive forces produced by the eyelid during the blink cycle. Hydrogels containing 50% or more of water and low effective crosslink density exhibit rapid initial deformation that does not reach equilibrium in a minute and tend to have high deformation and poor recovery.[29] This in turn gives rise to lenses with unacceptable visual instability.

Surface wettability

The maintenance of a precorneal tear film as a thin capillary layer is of prime necessity for the physiological compatibility between the lens and cornea. The wetting properties of a contact lens are predictably important. In order for the tear layer to spontaneously wet the surface of the contact lens, its surface tension should be equal or less than the lens' critical surface tension. This may be the reason why hydrophobic contact lenses are unable to maintain a continuous tear film over its anterior surface. Although tear fluid has a higher surface tension (approximately 46 mN/m) than the cornea (approximately 35 mN/m) it is just able to wet the cornea due to the mechanical action of the eyelid.[29] This may be further assisted by the complex nature of tear fluid and its interaction with the epithelium. Hydrogels do not present a wettability issue and the low coefficient of friction between the contact lens and the eyelid contributes to the

comfort of hydrogels. However tear fluid contains a mixture of proteins, mucopolysaccharides, lipids and electrolytes and this creates a problem, as hydrophilic hydrogels tend to accumulate amongst others proteinacious debris. It therefore, may be desirable to slightly reduce the wettability of the hydrogel.[30]

In addition to these aspects, other factors that need to be considered when designing a contact lens are the dimensional stability, optical transmittance, density, refractive index, ocular compatibility, toxicity, chemical stability along with method and ease of sterilisation.[30] The relative significance of these requirements depends upon whether the lens is designed for daily or extended wear.

In conclusion, hydrogels were first developed as general-purpose biomaterials due to their compatibility with tissue, however, with time it has been realised that their greatest potential is in applications requiring a balance of properties. This is because by controlling their EWC, mechanical properties and surface characteristics their structure can be modified to fulfil a wide range of functions. Other important design variables unique to this class of materials are pore size, pore size distribution and nature of water binding.

For the purpose of this study, skin adhesives were synthesised and evaluated for use as return electrodes in iontophoretic drug delivery (chapter 3) and commercial contact lenses were considered as vehicles for drug delivery (chapters 4 and 5).

1.5 Controlled drug delivery

During the 1950s pharmaceutical research was exclusively focused on novel drug development but due to cost and regulatory issues new drug creation has diminished. Although this continues to be an important area of research, there is an ever-increasing focus in controlled delivery techniques to exploit the full potential of existing drugs.[31] Agricultural drugs were incorporated into polymers in the 1950s and this *modus operandi* was extended to medicine in the mid 1960s. Soon after it was discovered that drugs could be continuously released from polymers and that by using different polymers or modifying the drug incorporation method release rates can be modified.[32]

Controlled drug delivery entails the release from a vehicle with a *zero-order* kinetic release profile in order to maintain stable drug plasma at a level where effectiveness is optimal. In addition, to eliminate overdosing and minimise side effects, the drug ought to act solely on the desired site, hence act as a "magic bullet", and a single application must suffice to sustain plasma level over a specified period of treatment. Conventional dosing regimes, such as periodic oral doses or other parenteral administration, cause drug plasma levels to oscillate. The levels may fluctuate above the minimum toxic concentration (MTC) as well as below the minimum effective concentration (MEC); thereby resulting in a "sawtooth" or "pulsed" profile of active agent level in plasma[7] as demonstrated in figure 1.4.

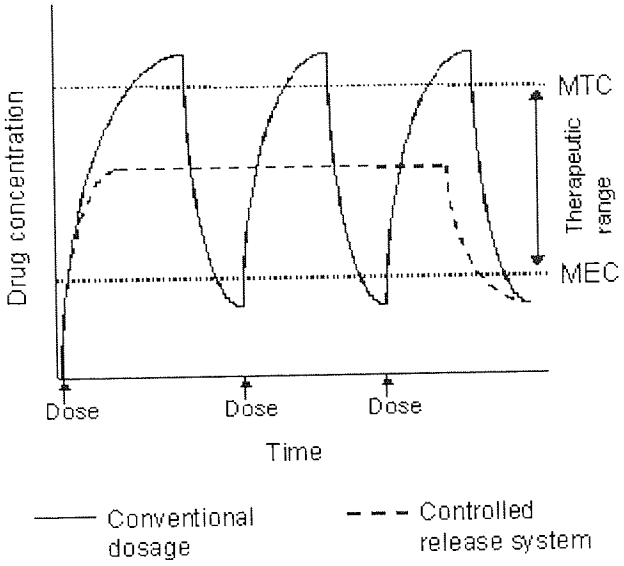

Figure 1.4 Comparison of blood drug levels for conventional and controlled delivery dosing.

Drug release from polymeric systems can be classified according to the mechanism which controls the release as shown in table 1.3.[33]

Type of system	Rate control mechanism
Diffusion controlled	
reservoir devices	diffusion through membrane
monolithic (matrix) devices	diffusion through bulk polymer
Water penetration controlled	
osmotic systems	osmotic transport of water through semi-permeable membrane
swelling systems	water penetration into glassy polymer
Chemically controlled	
monolithic systems	pure polymer (surface) erosion or combination of erosion and diffusion (bulk erosion)
pendant chain systems	combination of hydrolysis of pendant group and diffusion from bulk polymer
Regulated systems	
magnetic or ultrasound	external application of magnetic field or ultrasound to device

chemical	use of competitive desorption or enzyme-substrate reactions, rate control built into device

Table 1.3 Classification of controlled release systems.

Although controlled release devices provide an ideal drug administration method the pros and cons, as outlined in table 1.4[32], of such devices, particularly when implanted, must be weighed against each other.

Advantages	Limitations
• drug plasma levels are maintained within the desired therapeutic range • local administration reduces harmful systemic administration side effects • drugs with short in vivo half lives may be protected from degradation • administration of small amounts continuously by controlled delivery could eliminate discomfort associated with several large doses by parenteral administration • improved patient compliance due to reduction of dosing schedules • potentially less expensive and reduced drug wastage • improved drug administration where there is a lack of medical supervision	• toxicity or lack of biocompatibility of polymer material • production of harmful by products from biodegradable polymers • need for surgical procedure to implant device in the appropriate location • pain caused by presence of implant • expense of particular drug-polymer formulation due to cost of polymer or fabrication procedure • difficulty in stopping release post implantation if the need arises • assurance of adequate safety features so that leaks and other factors leading to inadequate control are eliminated

Table 1.4 Pros and cons of implanted controlled drug delivery systems.

1.5.1 Controlled release mechanism

This thesis (chapter 5) explores the properties of monolithic (matrix) diffusion controlled systems for use as transdermal or ocular delivery systems.

In matrix systems the drug is uniformly distributed throughout a polymer matrix, as shown in figure 1.5.

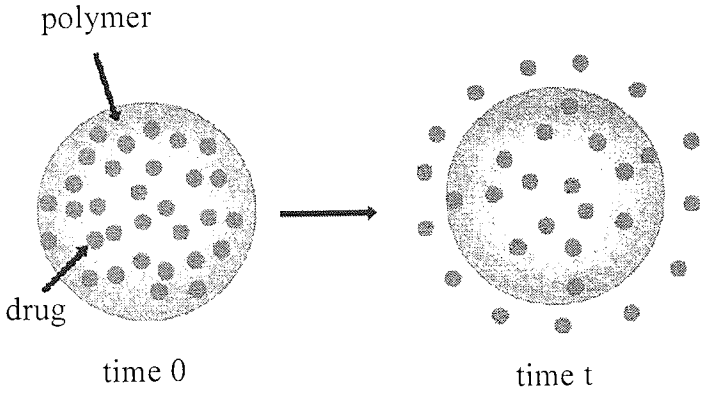

Figure 1.5 Matrix release system.

In this type of system the drug can be either molecularly dissolved or dispersed, that is loaded above solubility limit. Drug permeation occurs by a solution-diffusion mechanism.[32] This has two distinct processes: the solubility of the drug in the polymer is a thermodynamic quantity and the diffusion of the drug through the matrix is a kinetic property.[13] Diffusion may also occur through water filled pores.[32] For diffusion-controlled systems, the rate-limiting step is the diffusion of the drug through the polymer. Solubility, molecular weight, partitioning coefficient and melting point of a drug will have a large influence on its diffusion rate.

Matrix drug delivery systems require long-term compatibility between the vehicle, active and any excipient in the formulation. When designing matrix systems consideration must also be given to the manufacturing process to ensure that it does not alter the potency of the active.

1.5.2 Transdermal drug delivery

Skin has been extensively used for topical administration of dermatological drugs to achieve localised pharmacological action in skin tissues. More recently its use as a site

for the systemic delivery of therapeutic agents has been acknowledged since it has the lowest enzymatic activity compared to other delivery routes[34, 35] in addition, as detailed in section 1.5.3, it is an easily accessible organ with a large surface area.

Transdermal drug delivery systems (TDDS) are drug-loaded PSAs that deliver the therapeutic agent through the skin to the target organs via the systemic circulation. Ultimately they are intended to deliver the drug at a predetermined rate for a predefined period. In 1980 the first transdermal controlled delivery system, Transderm-Scop® containing scopolamine for managing motion sickness, was commercialised by Alza Corporation. Since then at least seven other drugs and twenty-five transdermal delivery systems have been marketed.[21]

Compared to the corresponding oral or injectable dose, TDDS offer various advantages in addition to those mentioned in table 1.3 and again these need to be weighed against their limitations. These are summarised in table 1.5.

Advantages	Limitations
• exclusion of variables associated with oral administration, such as pH, transit times and presence of food and enzymes • bypass hepatic first-pass metabolism and gastrointestinal incompatibility • reversibility of drug delivery as drug source can be easily removed • minimised inter- and intrapatient variation • self administration	• human skin functions as a chemical barrier limiting dosage that can be administered through skin • contact dermatitis or skin irritation caused by excipients and drug enhancers used in the formulation • there needs to be a clinical need for a successful product

Table 1.5 Advantages and limitations of transdermal drug delivery systems.

Drug permeation across human skin is not yet fully understood as it is a complex process. Penetration of a drug through the skin's stratum corneum may occur by diffusion via transcellular, intercellular or transappendegeal routes particularly the

sebaceous pathway of the pilosebaceous apparatus.[36] This is discussed further in sections 1.5.5 and 1.5.6. In addition as the drug diffuses through skin it may bind with potential sites forming a reservoir with fickle release kinetics.[36, 37] The location of application of the device can also influence drug plasma levels as body sites vary in permeability according to the following trend:[35]

genitals > head and neck > trunk > arm > leg

In addition barrier properties of skin vary with health and integrity of skin, that is grazed or removed compared to intact skin.[38] Although during normal lifespan it is unlikely that a mature stratum corneum's barrier properties are modified, unless it has been damaged by chemicals or UV radiation, there is a reduction in moisture content and blood flow with age, which could contribute to transdermal drug flux.[35] On the other hand the stratum corneum of a preterm infant is not fully matured and has an imperfect barrier allowing for easier delivery of actives.[35, 39] The disadvantage of this is that noxious chemicals may be absorbed and regulation of body temperature and water loss becomes problematic. Other factors that may affect barrier properties such as race and sex have not been fully investigated. An increase in hydration of the stratum corneum and the temperature of skin increases the permeability of hydrophilic drugs.[35]

Various interactions between drug, PSA and skin may also influence overall percutaneous absorption. Invariably the thermodynamic activity of a drug in the PSA and the intrinsic ability of the drug to pass through skin are important factors to consider in the design of transdermal drug delivery devices. It has been previously identified[40] that the force required to peel a PSA from skin increases as a function of adhesion time until a plateau is reached. For a drug concentration of 0 to 3% in the adhesive, peel force is independent of the amount of drug in the adhesive. Nonetheless the amount of drug released increases with adhesion time until a plateau is reached. However drug release is dependent on adhesion strength as well as number of bonds formed between the adhesive and skin.[40] The tighter the interface between the adhesive and skin the greater the release. Therefore periodically removing and reapplying the adhesive will result in a reduction in drug release as the adhesive-skin adhesion becomes weaker. Once adhesion has developed the drug is easily released until it reaches the limit imposed by the generally accepted octanol-water partition coefficient (section 1.5.6).

To design a successful TDDS, it is necessary for the PSA to show consistency on a highly variable substrate (skin) over a broad range of temperature, relative humidity, application time and mechanical movement.

1.5.3 Human skin physiology[35]

Skin is the body's largest organ. For an average person it contributes approximately 10% of body mass and covers an average area of $1.7m^2$. It is designed to act as a shield against heat, light, injury and microorganisms. It is also designed to regulate body temperature, store water and fat, prevent water loss and act as a sensory organ.

Skin may be regarded as having various barriers in series, as exemplified in figure 1.6. The three major layers are the innermost *hypodermis*, a fat layer, the overlying *dermis*, a dense fibroelastic connective tissue and the outermost *epidermis*, a stratified squamous epithelium.

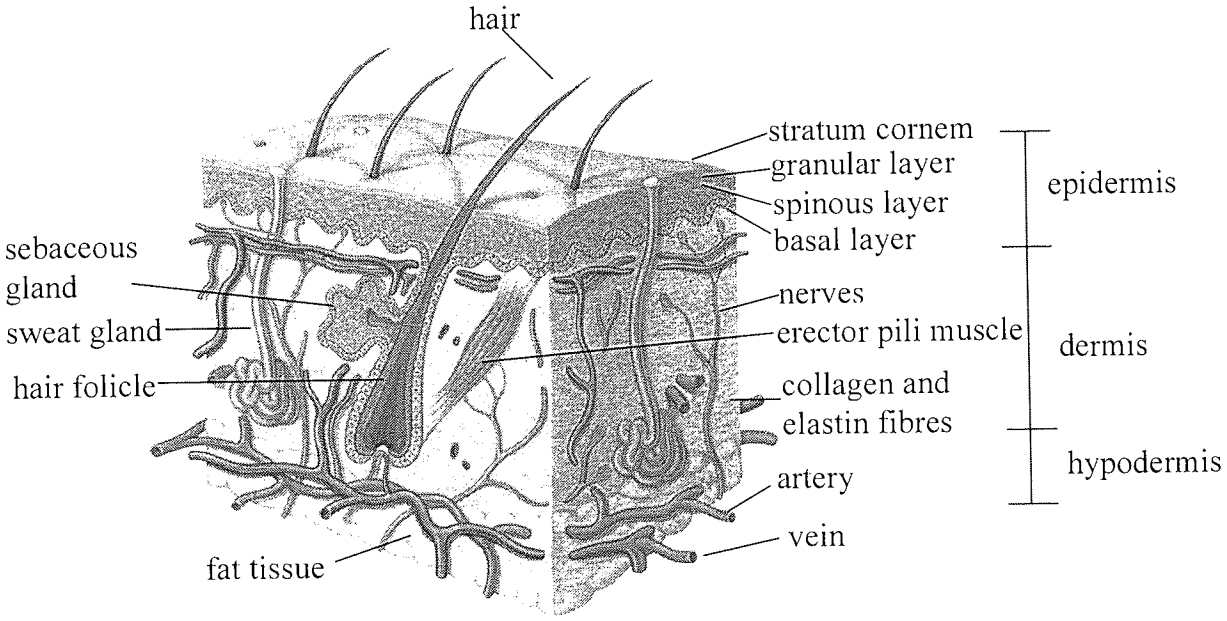

Figure 1.6 Skin morphology.

Hypodermis

The innermost layer of skin is variably composed of loose fatty (adipose) connective tissue. It allows the skin to freely envelope muscles and bones thereby forming a "bridge" between the overlying dermis and underlying body elements. Additionally it helps conserve body heat and may provide physical protection by acting as a "shock absorber". It can also readily supply high-energy molecules as principle blood vessels and nerves are carried within this layer to the non-vascular outer layers. Its thickness varies in different regions of the body from several millimetres to none at all, such as at the eyelids.

Dermis

The dermis is the major component of human skin and typically it is 3 to 5 mm thick. It houses a dense mat of collagen fibres, that supports blood vessels, lymphatic vessels, nerves (pain and touch receptors), pilosebaceous units (hair follicles and sebaceous glands) and sweat glands, and elastic tissue providing flexibility. There is a disparity in the amount and type of hair follicles: most are found on the head while load-bearing regions, such as the palm or soles, and lips have none. Sweat glands also vary in frequency and control mechanism, generally there are 100 to 200 sweat glands per cm^2 of skin.

In relation to transdermal drug delivery the appendages (hair follicles and sweat ducts) may offer possible entry routes, known as "shunt routes", to lower skin layers without having to cross the "intact" outer barrier. Additionally this layer is unlikely to form a barrier for the delivery of polar drugs but the same cannot be said for highly lipophilic molecules. Its rich blood flow, approximately 0.05 ml/min per mg of skin, allows for efficient transportation of drugs that have penetrated the outer skin layer. Blood vessels come to within 0.2 mm from the skin surface thereby ensuring that dermal concentrations of small drugs, such as lidocaine, are very low thereby maintaining a concentration driving force between the skin surface and the uppermost inner layer. The same applies to presence of lymphatic vessels which aid the clearance of larger molecules, such as interferon, a protein displaying antiviral activity.

Epidermis

The non-vascular epidermis varies in thickness from 0.06 mm on the eyelids to 0.8 mm on the load bearing area. It is a complex boundary consisting of four layers, the *basal*, *spinous* and *granular* layers and the *stratum corneum*. The structural integrity of the epidermis is disrupted when it dips into the dermis to produce sweat glands, hair follicles and sebaceous glands that open into the follicles.

The basal layer, also known as the "viable epidermis", is the only epidermal layer that is comprised of metabolically active cells, keratinocytes. These cells replicate by mitosis once every 200 to 400 hours after which one daughter cell remains in the basal layer and the other migrates towards the skin surface. Melanocytes, Langerhans cells and Merkel cells are found in the basal layer. Melanocytes synthesise melanin pigment, a free radical scavenger that absorbs harmful ultraviolet (UV) radiation. Langerhans cells are antigen-presenting cells; therefore have an important role in conditions such as allergic dermatitis. Merkel cells are associated with nerve endings having a role in cutaneous sensation, especially in the lips and fingertips.

The overlying spinous layer is composed of between 2 and 6 rows of keratinocytes. These cells begin to differentiate, changing from columnar to polygonal cells, and synthesise keratins that form tonofilaments. These condense to form desmosomes which maintain an approximate 20 nm gap between the cells.

The granular layer's thickness is only 1 to 3 cell layers deep. It contains enzymes that begin to decompose the viable cells which acquire granular structures. Keratohyalin granules cause the keratins within the cells to mature. In addition membrane-coating granules are also produced, these contain precursors for the intercellular lipid lamellae seen in the stratum corneum.

The uppermost skin layer is the stratum corneum or horny layer, which consists between 10 and 15 cell layers having a total depth of 10 μm when dry. It is thickest on palms and soles and thinnest on the lips. The cells referred to as corneocytes are dead, anucleated and keratinised. They are staggered in a lipid bilayer matrix, similar to a "brick and mortar" assembly. This layer regulates fluid loss from the body and averts the entry of noxious agents including microorganisms. These barrier properties depend

on the composition of the stratum corneum. The constituents of this layer are listed in table 1.6.

Component	% (dry weight basis)
Protein	75-80
of which cellular alpha-keratin	±70
beta-keratin	±10
proteinaceous cell envelope	±5
enzymes and other proteins	±15
Lipid	5-15
Unidentified	5-10

Table 1.6 Stratum corneum composition.

The proteinaceous cell layer is very much insoluble and resistant to chemical attack. In addition the mixture of lipids and the continuous multiply bilayered lipid component regulates drug flux through the skin. The main lipid components are ceramides, fatty acids, cholesterol, cholesterol sulphate and sterol or wax esters. These vary between individuals and body site. Notably, phospholipids are a rarity as compared to other lipid bilayers found in the body. The combination of a "brick and mortar" assembly and unusual lipid matrix causes molecules applied to the skin to follow a complex diffusion pathway; thereby making the stratum corneum 1000-times less permeable to water with respect to other biomembranes.[41]

Water also has an important task in maintaining the integrity of the barrier as the activity of hydrolytic enzymes involved in the desquamation process is affected by humidity. In addition its plasticising effect prevents the stratum corneum from cracking. It also regulates enzymes involved in the production of natural moisturising factor, a humectant that retains moisture and helps maintain suppleness.

1.5.4 Ocular drug delivery

Drugs for treating ocular diseases are administered systemically (oral or intravenous routes), topically (eye drops, ointments, gels or solid inserts) or via intraocular routes

(direct injection into the eye).[42, 43] Various methods of drug administration have been employed in an attempt to facilitate the therapeutic agent reaching its target site. The target sites may vary within the globe, for example, specific sites for miotics and mydriatics are in the iris-ciliary body whilst those for sulphonamides, antibiotics and steroids may be an infected or inflamed region within the eye.[44] However these receptors are not unique to the eye and may give rise to undesirable side effects. Additionally repeated dosing to induce the desired therapeutic effect may result in the "pulsed" profile, discussed previously in section 1.5. Furthermore, as several drugs used for treating eye disorders were developed for systemic use they do not easily penetrate ocular membranes.[42]

The periodic application of eye drops into the lower cul-de-sac has been the preferred form of application due to better patient compliance. Once applied the drug should ideally diffuse across the cornea to inner binding sites. However it has been reported[45-47] that ocular bioavailability of topically applied eye drops is only 1 to 10 %. This is a net result of a limited corneal surface area for penetration and poor corneal permeability, the presence of absorption barriers (mainly lipophilic corneal epithelium) and reduced contact time between vehicle and corneal factors due to various pre-corneal elimination factors.[47]

Elimination features are characteristic of typical eye function, which is designed to purge foreign bodies from the ocular surface. These include drainage of instilled solution via lacrimation and tear turnover, reflex blinking, drug metabolism, tear evaporation, non-corneal absorption or adsorption and binding to lacrimal proteins. Non-corneal absorption is the diffusion across the sclera and conjuctiva followed by removal to general circulation by local capillary beds bypassing the aqueous humour.[48] The drug that does reach the aqueous humour is removed by aqueous humour turnover and blood circulation of the anterior uvea.[42, 46]

The volume of one to two drops from conventional eye droppers varies between 50 and 100 µl.[44, 47] Given that normal tear volume is 7 to 10 µl and the cul-de-sac may hold momentarily 30 µl,[46] excess liquid is rapidly removed by spillage or via the nasolacrimal drainage system (figure 1.7) in order to restore normal volume. This lessens the residence time of the solution; thus reducing the period of activity or

persistence of a therapeutic agent between the tear film and anterior eye surface to two minutes.[47] Furthermore mildly irritating solutions stimulate lacrimation and tear turnover consequentially diluting the drug and accelerating drainage. Once again repeated dosing to achieve the desired therapeutic effect may result in the "pulsed" profile due to systemic absorption, mainly through the nasolacrimal duct, since more than 50 % of the instilled dose is systemically absorbed.[46, 47]

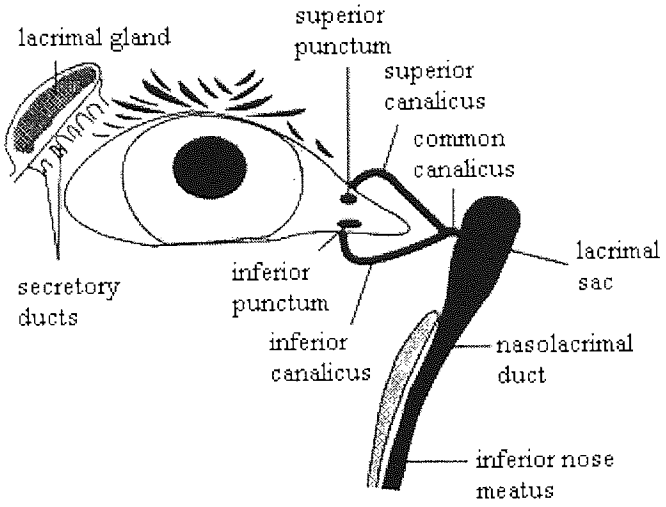

Figure 1.7 Nasolacrimal drainage system.[49]

Precorneal fluid dynamics have a huge effect on ocular drug absorption and disposition; hence in formulating ophthalmic drug delivery devices not only does the stability of a drug in the formulation need to be considered, but so does the influence of the formulation on the precorneal fluid dynamics. Characteristics of the human precorneal fluid are summarised[50] in table 1.7.

Tear volume	7-8 µl, 20-30 µl without blinking
Tear flow rate	1 µl/min
Tear turnover	16 %/min
Blink rate	15-20 /min
Drainage rate constant, 50 µl solutions	1.40 µl/min
Protein content of tears	0.7 %
Tear pH	6.5-7.4

Table 1.7 Precorneal fluid characteristics.

It has been established by a mass transport theorem[51] that by reducing the instilled volume to 25 µl ocular bioavailability of drugs with low corneal permeability increases four fold. This is due to a prolonged contact time between drug and anterior eye surface, as normal tear volume is not disturbed.[44] Realistically this is not achievable as it is difficult to design and produce small volume droppers. Furthermore the application of small volumes may not be detected and repeated applications may result in overdosing.[52] A possible solution is to increase the adhesion; thereby promoting wetting between the therapeutic agent's vehicle and the eye. Eye therapy formulations use polymers to form adhesive non-covalent bonds with the mucin layer (*mucoadhesion*) coating the corneal-conjunctival epithelium. Theories of adhesion, as mentioned in section 1.4.1.1, have been suggested[24] but generally to bond with this glycoprotein layer the polymers should possess:

i. hydrophilic functional groups, such as hydroxyl (-OH), carboxyl (-COOH), amide ($-CONH_2$) and sulphate ($-SO_4^{2-}$) groups
ii. strong anionic charges, for example sulphate ($-SO_4^{2-}$) and sulphonate ($-SO_3^-$) groups
iii. high molecular weight and viscoelastic properties when hydrated
iv. sufficient chain flexibility
v. surface energy properties that favour spreading on mucous surfaces.

It is thought that the hydrophilicity allows them to attract water from mucousal surfaces; thereby forming a strong bond when used in a dry form or to form a viscous liquid when

hydrated allowing it to increase its retention on the eye's surface. Similarly to PSAs (section 1.4.1.1) the hydrophilic groups can establish[47] electrostatic, hydrophobic, van der Waals intermolecular interactions and hydrogen bonding with the glycoprotein mucin layer. An increase in viscosity corresponds to an increased contact time between drug and anterior eye. This may be due to a reduction in non-productive drainage and improved retention of a more viscous tear film.[44] On the other hand, viscosity changes with shear rate (blinking) may affect the retention pattern on the ocular surface, hence flow properties cannot be overlooked.[53] Shear thinning polymers may drain quicker, whereas shear thickening agents are likely to cause pain during blinking when shear rates vary between 10k to 40k s^{-1}.[53] Theoretically Newtonian systems are the best as their viscosity is independent of shear rate. Pseudoplastics are recommended as tears show pseudoplastic behaviour, although at low viscosity they are probably ineffective due to their shear thinning and consequential accelerated drainage. Plastic flow is hypothetically better than pseudoplastic as these resist shear thinning provided that the yield is not exceeded. Previous work has shown[53] that there is a restricted viscosity range for which bioavailability is at a maximum whilst minimising visual effects, avoiding obstruction of the puncti and canaliculi, and allowing for easy filtration and sterilisation. It has been suggested[52] that viscosity should be between 1.5 and 1.8 mPa.s.

Given that methods of delivering drugs to the eye have not yet fully achieved the aims of controlled drug delivery, there is a growing professional and technical interest in the extension of optometric technology and practice into the therapeutics field. Although soft contact lenses were initially used for drug delivery to the eye in 1965[54] this area is still under-exploited. Initial publications in the area have suggested that *zero-order* release from a contact lens is achievable and provide higher drug penetration compared to subconjuctival injections.[54] However the success of a contact lens as a drug delivery vehicle depends on the compatibility of the lens material and the nature of the drug.[55] Controlled drug release from contact lenses offers various benefits compared to conventional administration methods; nonetheless these need to be weighed against their limitations as summarised in table 1.8.[54]

Benefits	Limitations
• higher drug penetration compared to subconjuctival therapy (injections) • lenses with higher water content show greater drug penetration • smaller amount of drug required for desired therapeutic effect, therefore fewer side effects, hence drugs that result in adverse side effects at high concentrations can be considered • better patient compliance	• prolonged wear of contact lens may lead to intolerance, corneal vascularisation, protein deposits and spoilage, giant papillary conjunctivitis and corneal ulceration • potential to loose lens

Table 1.8 Benefits and limitations of contact lenses as drug delivery vehicles.

1.5.5 Anatomy of the eye

The eyeball is not a true sphere but two spheres: one set in the other[50] as shown in figure 1.8. The larger inner sphere is a casing consisting of three layers:[49] the inner *retina*, the middle *choroid layer* and the outer *sclera*. The smaller frontal sphere is bordered by the *cornea*.

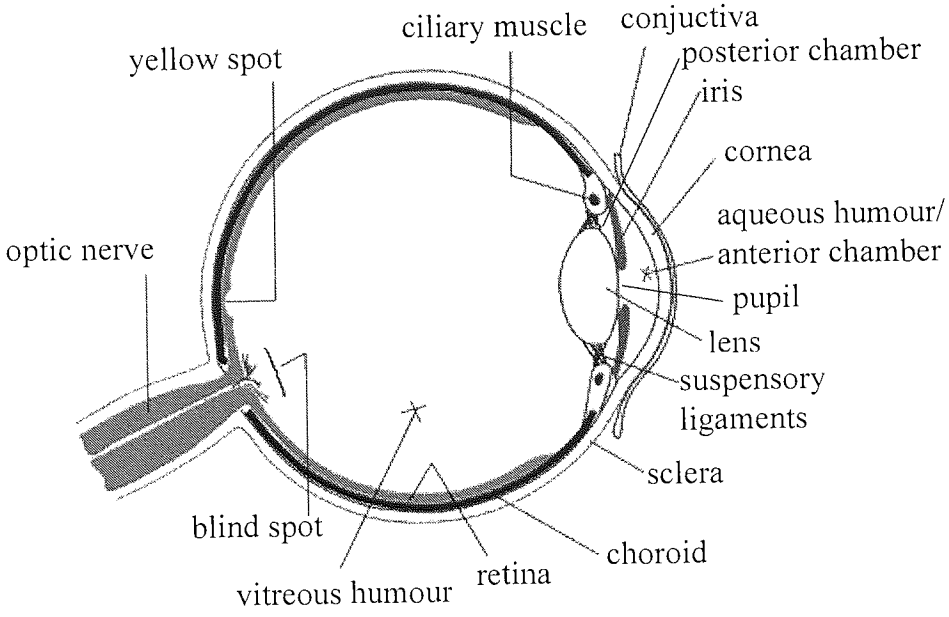

Figure 1.8 Cross-section of the human eye.

The eyeball houses an optical apparatus consisting of a frontal and inner section. The inner section consists of the *aqueous humour*, *pupil*, crystalline *lens*, *vitreous humour*, *retina*, *choroid* and *sclera*. The aqueous and vitreous humour are gelatinous substances; the vitreous humour occupies 80 % of the eyeball. The pupil is a centric hole that acts as a variable aperture of the system, it is located in the iris: a contractile membranous partition. The lens is a refractive element with variable power which is controlled and supported by the *ciliary muscle*. The light-detecting retina is supported by the choroid.[56] The sclera is a tough fibrous coating that protects the inner layers.[50] There are two main openings in the sclera: the posterior opening accommodates the *optic nerve* and the anterior opening surrounds the cornea. There are also approximately twenty small openings which carry ciliary nerves as well as arteries and veins.[50]

The frontal section of the eye consists of the *precorneal film*, *cornea* and *conjuctiva*.

Tear film

The tear film is a specialised lacrimal fluid layer that covers the outer cornea and conjunctiva (figure 1.9). It is involved in removing unwanted matter and provides a lubricating film between the eyelids and anterior surface of the eye. Historically, the tear film has been suggested to have a trilaminer structure. The layer in contact with the cornea is composed of mucin (glycoprotein) which stabilises the tear film and assists tear spreading. The middle layer is an aqueous phase making up about 98 % of the tear film and the outermost layer is a lipid monolayer which reduces evaporation.[50]

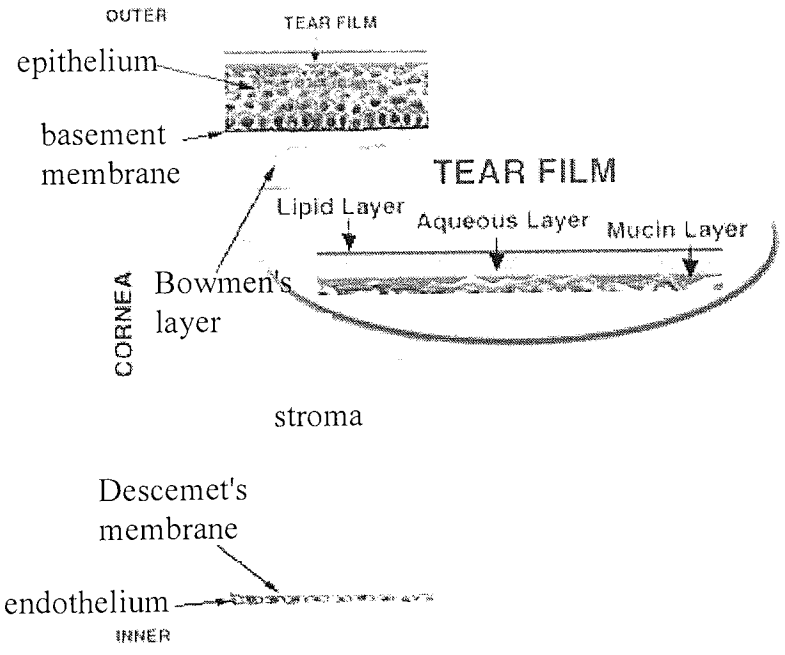

Figure 1.9 Cross-section of the tear film and cornea.[57]

Cornea

The cornea covers about one-sixth (16 cm^2) of the total surface area of the eyeball. The outer surface has a diameter of 11.5 mm and a 7.8 mm radius of curvature. Its thickness varies between 0.5 to 0.7 mm.[49] Essentially the cornea is a hydrophilic layer (*stroma*) sandwiched between two lipophilic layers, the *epithelium* and *endothelium* (figure 1.9).

The corneal epithelium is 50 to 100 μm thick[49] and consists of five to ten cell layers, which are continuous with those of the conjuctiva,[50] and has a cell turnover of one layer per day. The corneal epithelium has a basal layer of columnar cells, two to three layers of wing cells and one to two outermost layers of squamous polygonal cells.[46, 50]

Similar to the skin's epidermis (section 1.5.3) cell division occurs in the basal layer and cell differentiation occurs gradually as cells move towards the corneal surface.[46] The tight junctions and hydrophobic domains make it the main barrier of drug diffusion into the eye; hence for effective permeation across the cornea the drug needs to be small and have both hydrophilic and lipophilic properties.[49]

The stroma contributes 90 % of the corneal thickness. It is approximately 85 % water and contains 200 to 250 collagenous lamellae that are superimposed onto one another providing physical strength. Its relatively open structure should allow the diffusion of hydrophilic solutes.[49]

The endothelium consists of a layer of flattened hexagonal cells that are 5 μm thick and 20 μm wide, it is responsible for maintaining corneal hydration. Since it is in contact with the anterior chamber it is subject to an influx of water from the aqueous humour towards the stroma.[49]

The cornea is an avascular tissue; thus it receives nutrients and oxygen via bathing the epithelium with lacrimal fluid and the endothelium with aqueous humour as well as from blood vessels that line the junction between the cornea and sclera.

Conjuctiva

The conjuctiva is a thin vascularised mucous membrane that lines posterior surface of the eyelids and anterior surface of the globe except the cornea. The conjuctival epithelium is thicker than the cornea and contains mucus-secreting goblet cells. It is 2 to 30 times more permeable to drugs compared to the cornea. It is involved in the formation and maintenance of the tear film as well as physically protecting the eye and potentially combating infection. It has four important qualities that make it suited to fighting infection, these are:[50]

i. ability to mobilise and deliver defence cells and antimicrobial agents due to its rich blood supply
ii. contains many immunocompetent cells
iii. contains different cell types that can initiate and participate in inflammatory reactions

iv. anatomy and biochemistry of cells enable phagocytisation and neutralisation of foreign substances.

1.5.6 Passive drug delivery

Passive drug delivery can be described as the penetration of a drug across a membrane without any mechanism of enhancement. The thermodynamic force driving this is the concentration gradient of the drug and the partitioning of the drug between the adhesive and membrane. This phenomenon is known as Fick's law of diffusion (equation 1.4):

$$\textbf{Flux} = \frac{(\textbf{concentration gradient})(\textbf{surface area} \times \textbf{partition coefficient})}{\textbf{thickness of diffusion path}} \quad \text{Equation 1.4}$$

An important parameter in drug delivery is the octanol-water partition coefficient. Most organic liquids are immiscible with each other or with water at standard temperature and pressure. When a third component is added to a system of two immiscible liquids it distributes itself between the two and reaches equilibrium by achieving a concentration ratio between the two liquids.[58] The baseline ratio commonly referred to is the octanol-water partition coefficient (Ko/w). This is defined as:

$$\textbf{Partition coefficient}\,(\textbf{Ko/w}) = \frac{\textbf{concentration of molecule in octanol}}{\textbf{concentration of molecule in water}} \quad \text{Equation 1.5}$$

Generally the larger the partition coefficient the higher the lipid solubility of the drug and hence the greater its diffusion through a hydrophobic membrane. With respect to hydrogels, the fraction of total water it contains as well as the ratio of "free" to "bound" water will ascertain the partitioning and diffusion of solutes through it.

Passive drug permeation across cellular barriers can be through either an intercellular or transcellular pathway[59]. The intercellular path is through tight junctions between cells which is filled with a lamellar lipid-aqueous mixture. This is the main permeation route of hydrophilic compounds with small partition coefficients. Rates and extent of intercellular transport are influenced by structure and size of the tight junctions as well as by the size of the molecules. The transcellular route is diffusion through protein-

filled cell cytoplasm and protein-lipid cellular envelope. The surface area available for the transcellular route is much larger than the surface area of the intercellular route. This route is generally limited to relatively small lipophilic compounds with higher partition coefficients. In conclusion rate and route of permeation is influenced[46] by the physicochemical properties of the drug, such as lipophilicity, solubility, molecular size and shape, charge and degree of ionisation. For ideal passive transdermal drug delivery, log Ko/w should range between one and three, aqueous solubility should be greater than 1 mg/ml and molecular weight less than 500 Da.[41] Similarly the maximum penetration across the cornea is achieved with actives having a log Ko/w in the region of 2 to 2.5[60] and a molecular diameter less than 1 nm.[61]

It is also worthy to note that both skin[62] and cornea[46] are negatively charged membranes; hence are naturally permselective to cations. It is anticipated that lower charged cations will have a higher mobility compared to those of a higher charge, as they may tend to associate more strongly with a negatively charged membrane. In contrast anions will have a lower mobility due to repulsion.

The pore volume fraction, pore sizes and interconnections, size of active molecule and the type and strength of interaction of the active with the polymer chains of the hydrogel are other factors that control the passive release of drugs from hydrogels. Thus it is necessary to match the composition and crosslink density of the hydrogel, which in turn determines pore volume fraction, size and interconnections, to the size and composition of the active.[5]

1.5.7 Active drug delivery

Epithelial barriers provide a natural impediment to the passage of drug; consequently the amount of drug released passively is only a fraction of the total available for release. Furthermore the number of drugs delivered passively via the transdermal route is currently restricted and mainly confined to small (<500 Da) and persuasive lipophilic drugs that are effective at low doses. These are listed in table 1.9.[62, 63]

Drug	Function
clonidine	antihypertensive, antidysmenorrheal
estradiol	antineoplastic, ovarian hormone therapy
estradiol + norethisterone / levonorgestrel	
fentanyl	analgesic
hyoscine (scopolamine)	anticholinergic, cycloplegic, mydriatic
nicotine	smoking cessation adjunct
nitroglycerine	antianginal, vasodilator
testosterone	androgen, antianaemic, antineoplastic
lidocaine	local anaesthetic
oxybutynin	antispasmodic, anticholinergic

Table 1.9 Commercialised transdermal drugs.

Therefore, it is logical to postulate that the amount of drug release may be increased if movement of the drug across an epithelial layer is assisted by either incorporating enhancing factors into the formulation or by "physical" mass transfer enhancement. Possible methods for maximising transdermal drug delivery are presented in figure 1.10; similar strategies can be employed to facilitate ocular drug delivery.

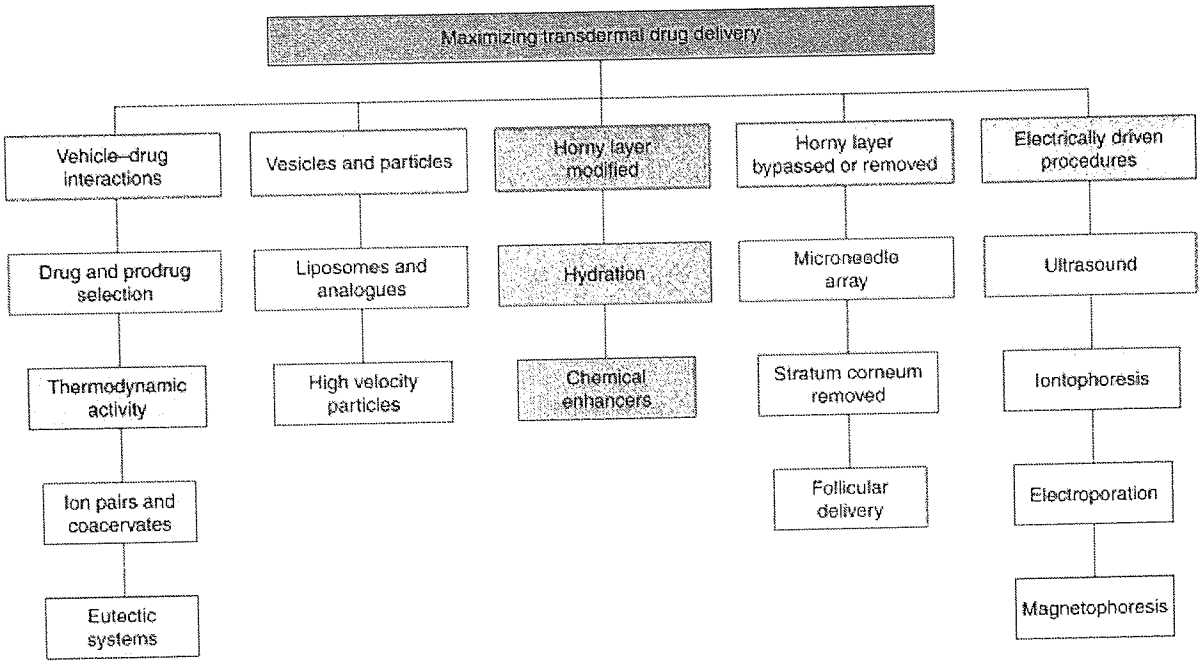

Figure 1.10 Methods for maximising transdermal drug delivery.[62]

Electrotherapy is a term used to encompass clinical treatments based on the movement of charged particles in an electric field. One application of this technique, which has been researched in recent years, is its use in the delivery of ionised drugs into or across skin for systemic delivery or the eye to treat posterior eye diseases. This concept was the first described by Veratti in 1747, although the first biomedical applications using electricity were prescribed by Etius to treat gout using torpedo (electric fish) shocks.[64] Possible electrically driven procedures used for drug delivery are iontophoresis, electroporation, ultrasound and magnetophoresis. Iontophoresis, a method that increases the penetration of charged molecules, is fairly well established, whereas electroporation, a method used for transdermal or topical drug delivery, has only been developed within the last two decades.[64] The first controlled experiments demonstrating the iontophoresis of strychnine sulphate and potassium cyanide were performed in 1901 by Leduc.[64] Skin adhesives were investigated in this study for use as potential return electrodes in ocular iontophoresis, thus this technique is discussed further.

1.5.7.1 Iontophoresis

Iontophoresis is an effective method of delivering medication to a localised tissue area by applying an electrode with low voltage (10V or less) and constant current (current density of 0.5 mA/cm^2 or less) to a solution of the medication.[65] An oppositely charged *ground* (return) electrode is placed elsewhere on the body to complete the circuit.[62]

Iontophoresis uses three mechanisms to enhance drug transport when a potential difference is applied to tissue.[62, 63, 66] These are:

i. electromigration by electrical repulsion from the driving electrode; thereby applying a positive current will drive positively charged (cationic) molecules away from the anode electrode and into the tissues (electrophoresis). The converse is also true. The salt form of the drug is usually used because when it dissociates it is highly soluble and has a high charge density.

ii. electroosmosis, the convective flow of water, in the anode to the cathode direction resulting from the electric field imposed on a negatively charged membrane. Consequently this could also move uncharged molecules and large polar peptides.

iii. easier passive penetration of molecules as the electric current enhances the permeability of skin arising from electroporation of the appendageal epithelial layer.[65]

In summary,

$$\textbf{Total Flux } (J_T) = J_E + J_C + J_P \qquad \text{Equation 1.6}$$

where:

J_E = electromigration contribution

J_C = electroosmotic contribution

J_P = passive contribution

These mechanisms are illustrated in figure 1.11.

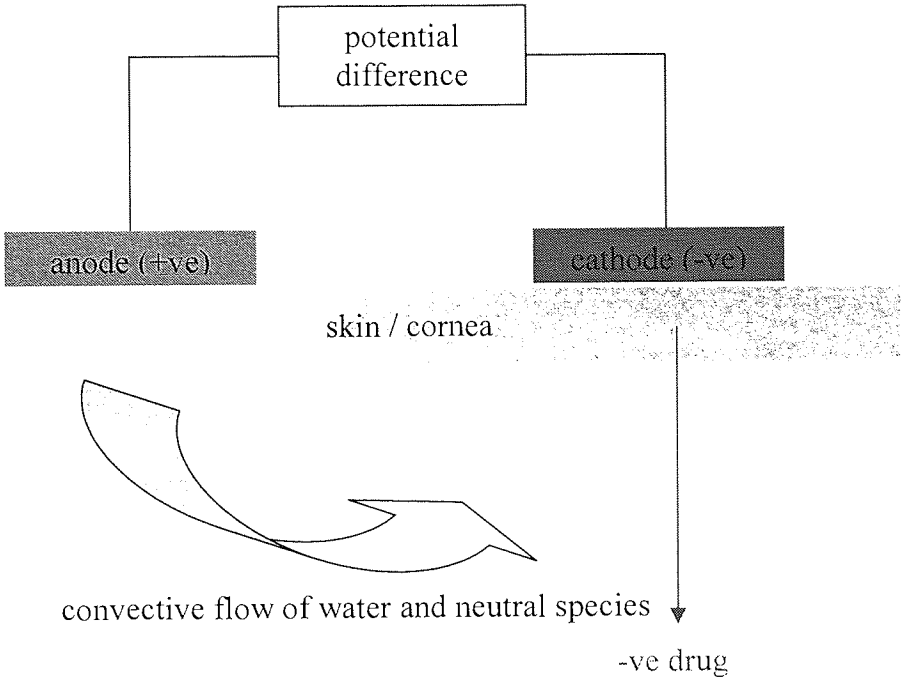

Figure 1.11 The iontophoresis mechanism.

During transdermal iontophoresis ionised drugs are transported through pre-existing shunt pathways, such as sweat glands and hair follicles. In addition, even with the low to moderate voltage, new pores or shunt pathways are induced at the level of appendageal epithelia during transdermal iontophoresis. The dominant pathway of electric current flow through skin is likely to be via the sweat ducts. However, the final pathway of the drug is intercellular, between hair follicles and epidermal cells.[64]

The amount of drug delivered via iontophoresis is dependent on the following:[34]

i. location of the loaded hydrogel electrode

   Abdominal skin, for example, has higher drug permeation compared to dorsal skin.

ii. pattern of current application

   Iontophoretic skin permeation of a molecule is likely to be higher when current is applied continuously as opposed to frequently and intermittently, due to the time dependent electrochemical potential during current application. The different waveforms of current application are unlikely to have an enormous effect on drug permeation.

iii. on / off ratios and duration of current

A higher on / off ratio results in faster voltage decrease indicating a faster reduction in skin's resistance, thereby yielding higher iontophoretic permeation. Duration of current application also appears to be of higher significance compared to amplitude and intensity of current.

For commercial iontophoretic devices dosage is expressed as follows:[64]

$$\textbf{Dosage (mA * min)} = \textbf{Current (mA)} \times \textbf{time (min)} \qquad \text{Equation 1.7}$$

Depending on the manufacturer, the maximum dosage varies from 80 to 160 mA*min.

Advantages of iontophoresis are:[65]

i. reduced physical risk as it is non-invasive
ii. direct delivery of drug solutions to the treatment site without disadvantages of injections or orally administered drugs
iii. relatively pain-free
iv. minimises the potential for further tissue trauma that may occur with increased pressure from a fluid bolus injection
v. potential to program delivery as drug is delivered in proportion to current output.

The characteristics of drugs that could potentially be delivered using iontophoresis are:[67]

i. drugs used for localised solutions
ii. water-soluble drugs
iii. strongly positive or negative charged drugs
iv. relatively small molecular size drugs.

With ocular iontophoresis, for example, the drug is applied to the eye by an electrode carrying the same charge as the drug. The return electrode has the opposite charge and is placed elsewhere on the body to complete the circuit. For ocular drug delivery there are two forms[68] of iontophoresis: transcorneal or transcleral, depending on the location requiring treatment. Transcorneal iontophoresis has the potential to treat the anterior segment namely the cornea, anterior chamber, iris, crystalline lens and ciliary body, of

the eye as it yields an ideal and sustainable concentration of drug in the cornea and aqueous humour. However with transcorneal iontophoresis the drug cannot reach the vitreous body due to the crystalline lens. Consequently infections of the posterior segment, specifically the retina and choroids, are treated by transcleral iontophoresis that can by-pass the lens and deliver the drug to the vitreous body in sufficient therapeutic amounts. This method is preferable to intra-vitreal injections that may cause retinal detachment, vitreous haemorrhage and endophthalmitis.

An interesting application of iontophoresis in medical diagnostics is reverse iontophoresis.[62, 64] This can be used for back iontophoretic extraction, by electroosmotic flow, of a molecule from the body instead of forward delivery into the body; hence allowing for non-invasive sampling of biological fluids. This technique may be useful in determining the level of glucose in diabetics and is still under investigation, thus will not be discussed any further.

1.5.7.2 Electroporation

In contrast to iontophoresis, electroporation uses high voltage (100 to 1000 V) short duration (μs to ms) pulses creating localised regions of membrane permeabilisation resulting from the apparent formation of transient aqueous pathways in lipid cell membrane bilayers.[62, 64] Hence the estimated 100-multimellar bilayers of stratum corneum need at least 1 V per bilayer for electroporation. Essentially, it is a physical method where cells are exposed to the current causing artificial shunts to open within the cell membrane providing a more energetically favourable straight through path for drug penetration. Drug fluxes increase 10 to 10^4 fold[62], depending on the polarity of the pulse, for neutral and highly charged molecules up to 40 kDa. With this method drug transport is likely to occur by iontophoresis and electroosmosis during a pulse and by enhanced diffusion in between pulses due to lowered resistance of the stratum corneum.[69] Iontophoresis will act on hydrophilic drugs with a larger charge while diffusion prevails with neutral or weakly charged drugs. Forward polarity (same charge to that of the drug) has a higher flux as compared to alternating polarity (alternating between positive and negative charges), which in turn is larger than reverse polarity (opposite charge as of drug).[69] Drug movement during forward flux is mainly by

electrophoresis and mostly by diffusion between pulses for reverse flux. With alternating pulses both types of drug movement are likely to occur.[69]

The possible course taken by a charged species during electrotherapy is illustrated in figure 1.12.

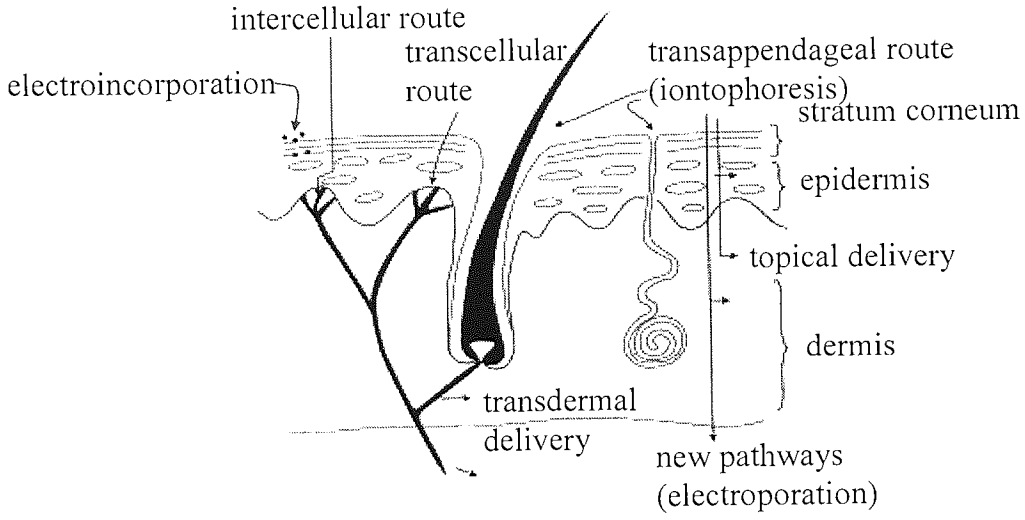

Figure 1.12 Possible routes for charged species during electrotherapy.[64]

By and large iontophoresis is used for clinical dermatological applications for drug delivery. On the other hand electroporation is used for physical therapy, mainly for transcutaneous electrical nerve stimulation (TENS). With respect to drug delivery, electroporation is quantitatively more effective *in vitro* compared to iontophoresis.[41] A combination of both may produce a yet more efficient result. Iontophoresis acts mainly on the drug, whereas electroporation acts on the skin with some driving force on the drug during a pulse. The use of electroporation for drug delivery in clinical dermatological applications is still under investigation; nonetheless as shorter pulses are used during electroporation, much higher voltages as compared to iontophoresis can be used before a sensation is felt.[64]

1.5.7.3 The electrical circuit

A complete circuit is required for current to flow. The circuit begins from the source of the current, the *generator*, goes via a conductible cable to the conductible bioelectrode

and into the body, the *load*. The current then returns to the generator through a second bioelectrode, known as the *ground* or *return* electrode.

The initial stage of this study involved formulating adhesive hydrogels for use as bioelectrodes that could potentially minimise the painful sensation experienced at the point of the return electrode used in ocular iontophoresis. The method used by the Optis System to treat ocular diseases uses a battery powered generator supplying constant current across two electrodes: the hydrogel drug delivery device is placed on the eye and the adhesive hydrogel return electrode placed on another area of the body. The Optis System is shown in figure 1.13.

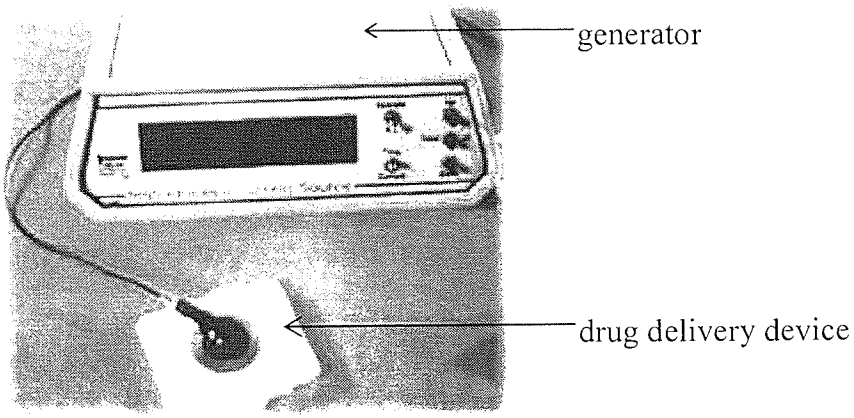

Figure 1.13 The Optis System.[70]

The electric field of the Optis System is limited to a maximum of 9V direct current (DC). The system delivers the drug to the eye by iontophoresis, a technique discussed in section 1.5.7.1. With this system pain is not felt in the eye itself, but undesirable pain is felt at the location of the hydrogel return electrode although no epithelium burns were noted. This pain is reported to be mild when compared to that of conventional techniques, but should ideally be minimised. For Optis the ideal hydrogel electrode should have an impedance lower than 500 Ω at 2.5 mA current and maximum of 9V DC.[71]

1.5.7.4 Effect of electric current on skin morphology

The stratum corneum protects the more permeable parts of the skin (part of the epidermis and all of the dermis) and deeper tissues. It is also highly electrically resistant, thus when current is applied to skin the concentration of the electric field on the stratum corneum induces electroporation.[64] Post iontophoresis and electroporation the stratum corneum becomes disorganised. For both, two observations were made:[72]

i. increased hydration of the stratum corneum
ii. disordered lipid bilayers .

The degree of these disturbances is proportional to the amount of charge passed and results in a reduction in skin electrical resistance (impedance).[69, 73] A reduction in skin impedance generally reflects an increase in skin permeability.[64, 74] Skin impedance reduces with time and either current density (for iontophoresis[73]) or pulse voltage (for electroporation[69]). It has also been suggested that the reduction of skin's impedance during electrotherapy is a result of an increase in the stratum corneum's local ion concentration.[72, 73] On cessation of current application this local ion concentration returns to its normal physiological level. Skin's natural impedance gradually returns as the ions diffuse into the deeper skin layers. Compared to iontophoresis, electroporation induces a greater decrease in skin impedance. These changes are considered to be completely reversible for low iontophoretic current density[72] and low electroporation pulse voltages (~100 V), whereas partial reversibility occurs for higher electroporation pulse voltages.[64, 69] For the most part these techniques are not considered damaging to the skin.[64, 73]

Comparing electrotherapy and a conventional injection, the needle leaves a hole big enough to allow bacteria to pass through, whereas electrotherapy creates several submicroscopic holes unlikely to pose a risk to infection.[69] It is worth noting that skin responds to any physical damage to its barrier by triggering a sequence of biochemical reaction to repair the damage. The resulting level of irritation is a reflection of the disturbance caused by the onset of these reactions.[64]

1.5.7.5 Skin-electrode interface

The main drawback in the use of ocular iontophoresis has been the pricking pain sensation that occurs at the location of the return electrode at low current levels. The sensation caused by current applied to skin is a result of the direct nerve electrical excitation.[74] In order to minimise this effect the return electrode should provide a low impedance and current density path for the return current.[27] If this is not satisfied, the "excess" current will travel through alternate routes of lower resistance ensuing equally high local current density, which may cause, for example, damage to viable hair follicles or in extreme cases tissue heating and burns arising from resistive heating. Initial skin temperature is in the order of 29 to 33 °C and that of skin burn threshold is around 45 °C; therefore a 12 °C rise in skin temperature could be hazardous.[74]

The minimum current applied to the skin that induces a sensation is termed the perception threshold and likewise that causing pain is termed the pain threshold. A minimum transmembrane voltage must be applied to stimulate a nerve and cause an action potential due to membrane depolarisation. For long pulses a constant current termed the rheobase current is required to achieve the minimum voltage. For short pulses only a minimum charge is required. The additive effect of multiple pulses results in varying levels of perception thresholds and sensation, depending on the spacing and rate of the pulses. Multiple pulses of the same polarity can increase sensation, whereas sequential pulses with opposite polarity (biphasic pulses) reduce sensation. Generally as pulse rate is increased, stimulation thresholds decrease and then plateaus.[74]

Current and frequency of pulses have a strong influence on the quality of the sensation experienced. Currents slightly above the perception threshold mainly cause painless sensations described as a tingle, itch, pinch, prick or vibration. On the other hand greater currents can cause sharp and burning pain. Sensation is reduced as AC current pulse frequency is increased.[74]

Pain thresholds depend on physical as well as physiological factors; thus tend to be more variable than perception thresholds. Pain thresholds are usually 3 to 35 times greater than perception thresholds, with larger differences at higher frequencies. For transdermal iontophoresis the limit of tolerable sensation is a current density of 0.5 mA/cm^2. However, there are differences between overall and local current densities.

The overall current density is based on the total area of electrical contact. The local density varies under an electrode, with greater current densities experienced along the edges. Even larger localised differences are found due to variations in microscopic skin structure, with higher current densities obtained in low resistance areas through sweat ducts and hair follicles. Poor electrode-skin contact also leads to localised spots of high current density resulting in pinpoint burns. A proposed equation for the maximum painless current during iontophoresis is:[74]

$$\mathbf{I} = \frac{\mathbf{28.6}a}{\mathbf{48.3} + a} \qquad \text{Equation 1.8}$$

where:

I = current (mA)

a = electrical contact area (cm^2)

Another equation based on the Weiss-Lapicque relationship is:

$$\mathbf{I} = \frac{\mathbf{19.3}}{\mathbf{1} - \mathbf{e}^{t/1.11}} \qquad \text{Equation 1.9}$$

where:

I = current (mA)

t = pulse length (ms)

The quality and threshold of sensation varies very little at different sites on the body. The face, however, is the most sensitive whereas the fingertips and the soles are the least sensitive. In order to be distinguished as separate sensations electrodes should be placed at least 1 cm apart. However the level of pain and sensation thresholds increases with an increase in pulse frequencies as well as with time due to habituation. Pain thresholds increase by at least a factor of two. Differences of these thresholds based on gender could be a result of the sensation threshold being dependent on body weight. Temperature also has a mild effect, a 10 °C drop increases the threshold current to a maximum of 30 %.[74]

The return electrode can be placed on most parts of the body due to the body's low impedance to surface current.[27] However, ideally an electrode should possess rapid depolarisation of internal charged layers caused by defibrillation of pulses and should

have a relatively low and constant DC offset and constant impedance with fluctuating voltages applied at various frequencies. Low impedance provides a higher signal to noise ratio. The hydrogel coated on the electrode should be even and hydrophilic to enable uniform electrical conduction. The hydrogel should also be able to retain its shape and be compliant to shape of body contours. To maintain low production costs, an electrode should have a minimum number of layers, which also prevents chemical changes occurring as it avoids soluble substances diffusing from one layer to the next.[17]

1.6 Hydrogels as delivery systems

Macromolecular release from a completely neutral hydrogel and an analysis of release of small molecules from hydrogels is explored in this thesis. Hydrogels have been under study for their potential as controlled release delivery devices for at least three reasons.

Firstly, the water within the polymer network gives them their biocompatibility allowing them to perform with an appropriate host response in a specific application. This biotolerance is enhanced because hydrogels are permeable to ions and metabolites in body fluids. The water can also act as a transport medium for hydrophilic species

Secondly, by varying the monomers, crosslink density and water content the properties of a hydrogel can be manipulated to suit a particular application. This enables the hydrogel to be designed so that it is compatible with the drug. In principle it also allows for the design of a system that reduces the risks of achieving high concentrations that produce undesired side effects or such low concentrations that the drug is rendered ineffective. Keeping the amount of drug required to achieve the desired therapeutic response at a minimum level reduces both costs and waste.

Thirdly, hydrogels can be moulded into different physical forms such as solid (contact lenses), pressed powder matrices (pills), microparticles, coatings, membranes, encapsulated solids and liquids.[5] Thus, their physical shape can also be tailored for a specific purpose.

1.7 Research objectives

This thesis is split into three sections.

The first section (chapter 3) investigates the use of conventional bioelectrodes and skin adhesive hydrogels in electrically mediated release applications. This section addresses the problem of inadequate compatibility of conventional bioelectrodes for use as a grounding electrode in ocular iontophoresis, as they produce a great deal of discomfort on application of the current due to the resultant high current density. The work is intended to provide a basis of understanding of the relative contributions made by a selection of ionic and neutral monomers to adhesion, rheology and impedance of bioelectrode gels.

In the second section (chapter 4) the release of water-soluble macromolecules from a neutral hydrogel is studied. This has not been previously examined and an opportunity exists to develop an *in vitro* model to observe the phenomena of macromolecular release from a contact lens matrix. Focus® Dailies®, which consists of a neutral PVA based crosslinked matrix and leaches linear PVA (by chance rather than by design!) will be used for the study.

The third section (chapter 5) outlines the importance of release models for determining factors which control drug release. This section serves to link electrotherapy applications, where passive diffusion from the hydrogel could be enhanced across the dermal surface, to passive diffusion from a contact lens matrix. Furthermore the ability to monitor release of surrogate drugs from various contact lenses provides a platform for developing therapeutic contact lenses.

Chapter Two

Materials, Methods and Method Development

2. MATERIALS, METHODS AND METHOD DEVELOPMENT

2.1 Materials

Hydrogels are synthesised using a combination of monomers and a crosslinker dissolved in water, as shown in figure 1.1, in the presence of an initiator. Depending on their application they may additionally contain various therapeutic agents for use as drug delivery vehicles or, in the case for skin adhesives, metal ions for use as bioelectrodes.

2.1.1 Monomers

For the purpose of this study the monomers used to synthesise pressure sensitive adhesives were either anionic or neutral. These are detailed in table 2.1 and their structures are shown in section 2.1.1.1. Throughout this thesis monomers are referred to using their abbreviation.

Anionic monomers	**Abbreviation/ Generic name**	**Molecular weight**	**Supplier**
acrylic acid-bis-(3-sulfopropyl)-ester, potassium salt	SPA	232.29	Raschig
sodium 2-(acrylamido-2-methyl propane sulphonate	NaAMPS	229.23	Lubrizol
Neutral monomers			
acryloylmorpholine*	AMO	141.17	Sigma-aldrich
diacetone acrylamide*	DAA	169.22	Sigma-aldrich
2- hydroxyethyl methacrylate*	HEMA	130.14	Cognis Performance
methacrylic acid	MA	86.09	Sigma-aldrich
N,N-dimethylacrylamide*	NNDMA	99.13	Sigma-aldrich
N-(tris (hydroxymethyl) methyl) acrylamide*	TRIS	175.18	Sigma-aldrich

N-vinyl pyrrolidone**	NVP	111.14	Vickers
poly(ethylene glycol)$_n$ mono methyl ether monomethacrylate ave. M_n=400*	$MPEG_{400}MA$	496.59 (approx.)	Polysciences

Table 2.1 Monomers utilised, molecular weights and suppliers.

Note:
* indicates reagent stored in refrigerator
** indicates reagent stored in refrigerator below 5°C

2.1.1.1 Monomer structures

ANIONIC MONOMERS

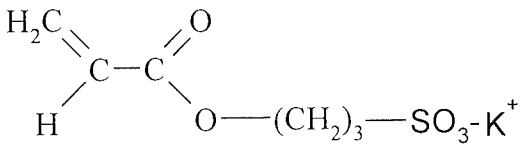

acrylic acid-bis-(3-sulfopropyl)-ester, potassium salt (**SPA**)

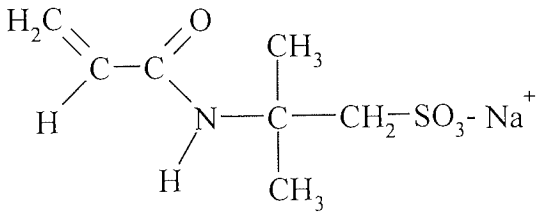

sodium 2-(acrylamido)-2-methyl propane sulphonate (**NaAMPS**)

NEUTRAL MONOMERS

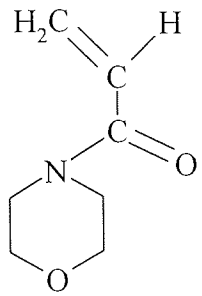

acryloylmorpholine (**AMO**)

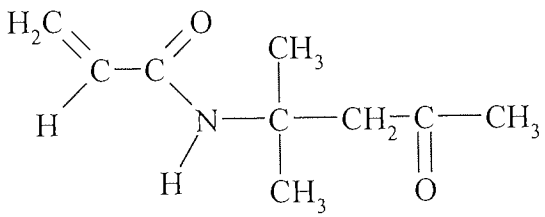

diacetone acrylamide (**DAA**)

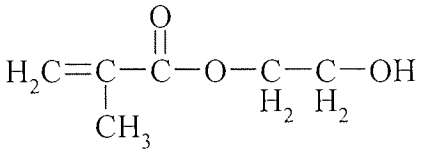

2- hydroxyethyl methacrylate (**HEMA**)

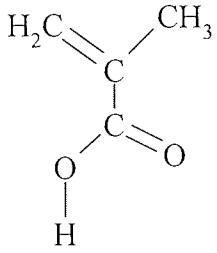

methacrylic acid (**MA**)

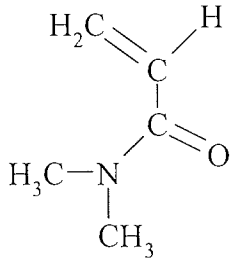

N,N-dimethyl acrylamide (**NNDMA**)

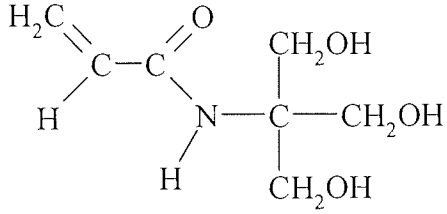

N-(tris (hydroxymethyl) methyl) acrylamide (**TRIS**)

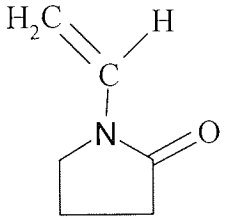

N-vinyl pyrrolidone (**NVP**)

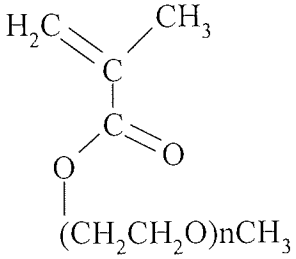

poly(ethylene glycol)$_n$ monomethyl ether monomethacrylate ave. n = 9 (**MPEG$_{400}$MA**)

2.1.2 Initiators and crosslinkers

In addition to a crosslinker, a thermal initiator was used to thermally polymerise hydrogel membranes that were subsequently fully hydrated. Likewise a photo initiator was used to photo-polymerise partially hydrated skin adhesive hydrogels. These are listed in table 2.2 with structures shown in section 2.1.2.1. Throughout this thesis the crosslinkers and initiators are referred to using their abbreviation.

Initiators	**Abbreviation**	**Molecular Weight**	**Supplier**
azo-iso-butyronitrile* (thermal)	AZBN	164.21	BDH
1-hydroxycyclohexyl phenyl ketone# (photo)	Irgacure 184	204.27	Ciba
Crosslinkers			
N,N'-diallyltartardiamide*	DATr	288.25	Aldrich
ebecryl 11#	Eb 11	confidential	U.C.B

Table 2.2 Initiators and crosslinkers utilised, molecular weights and suppliers.

Note:
* indicates reagent stored in refrigerator
# indicates reagent stored in darkness

2.1.2.1 Initiator and crosslinker structures

INITIATORS

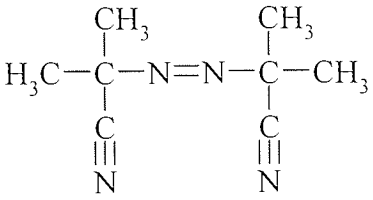

azo-iso-butyronitrile (**AZBN**)

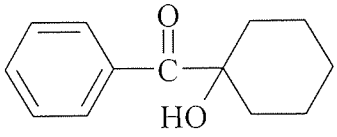

1-hydroxycyclohexyl phenyl ketone (**Irgacure 184**)

CROSSLINKERS

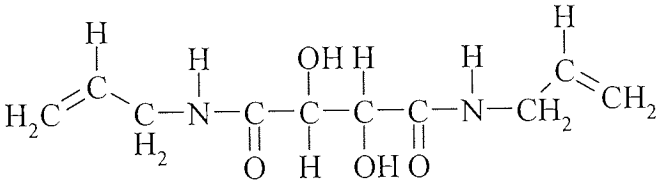

N,N'-diallyltartardiamide (**DATr**)

ebecryl 11

The structure of this polyethyleneglycol diacrylate photo crosslinker has not been published by its suppliers.

2.1.3 Other reagents and therapeutic agents

Distilled water was used for both thermal and photo-polymerised hydrogels. Glycerol was used in partially hydrated skin adhesive hydrogels only as this serves to reduce evaporation effects as its polar groups interact strongly with water.[17] Other reagents and therapeutic agents discussed in this thesis are listed in table 2.3 and the structures are shown in section 2.1.3.1.

Other reagents	Abbreviation	Molecular Weight	Supplier
acrylic acid*	AA	72.06	Sigma-aldrich
2,5-dihydroxybenzoic acid	DHB	154.12	Sigma-aldrich
1,2,3-propanetriol	Glycerol	92.09	Sigma-aldrich
trifluoroacetic acid	TFA	114.02	Sigma-aldrich
Model compounds/ therapeutic agents			
basic fuchsin (lidocaine model compound)	none	323.82	Sigma-aldrich
2-diethylamino-N-(2,6-dimethylphenyl)acetamide	lidocaine	234.34	Sigma-aldrich
2-isopropyl-5-methylcyclohexanol	menthol	156.27	Sigma-aldrich
α-methyl-4-(isobutyl) phenylacetic acid	ibuprofen	206.28	Sigma-aldrich

Table 2.3 Other reagents and therapeutic agents utilised, molecular weights and suppliers.

Note:
* indicates reagent stored in refrigerator

2.1.3.1 Structures of other reagents and therapeutic agents or models

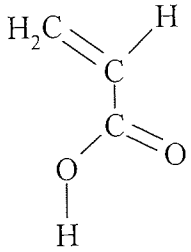

acrylic acid (**AA**)

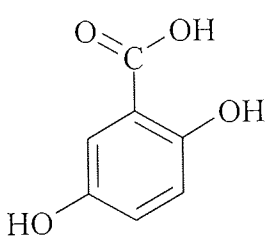

2,5-dihydroxybenzoic acid (**DHB**)

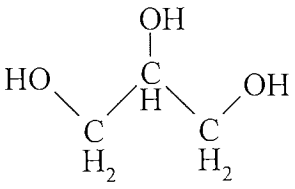

1,2,3-propanetriol (**glycerol**)

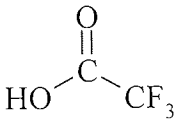

trifluoroacetic acid (**TFA**)

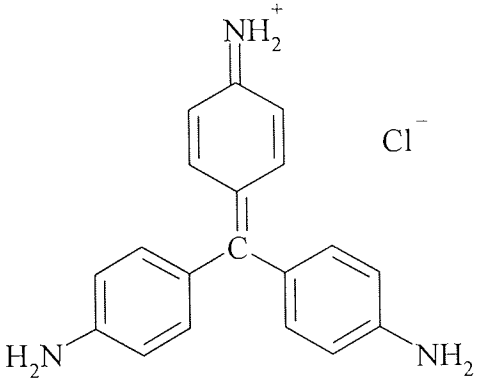

basic fuchsin

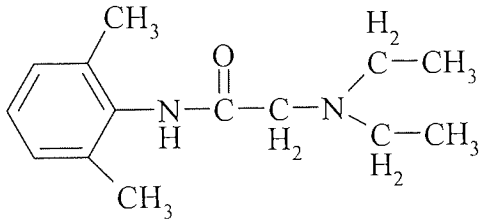

2-diethylamino-N-(2,6-dimethylphenyl)acetamide **(lidocaine)**

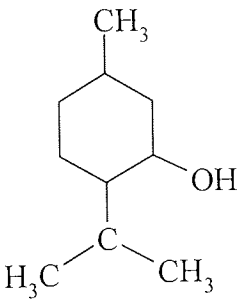

2-isopropyl-5-methylcyclohexanol **(menthol)**

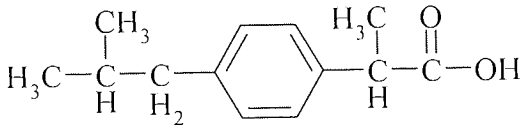

α-methyl-4-(isobutyl) phenylacetic acid **(ibuprofen)**

2.2 Methods

The synthesis and characterisation of hydrogels for use as skin adhesive bioelectrodes in release applications is discussed in this section. In addition analytical techniques used to quantify release from contact lenses and measure changes in surface properties as a result of release are reviewed.

Hydrogels are synthesised by free radical polymerisation of hydrophilic monomers. There are various methods of polymerisation; thus it is necessary to identify the one most suited for the required application.

The adhesive performance as well as the material properties of a skin adhesive can be evaluated. The adhesive performance provides an indication of the strength of the bond formed between the adhesive and the adherend. This entails measurements such as peel strength. Material properties are valuable for quality control purposes and to detect lot-to-lot variability. They are determined by viscoelastic measurements using a dynamic-mechanical technique.

Techniques that enable quantification of the release of therapeutic polymers, such as refraction index, and release of dyes used as models of actives, such as colorimetry, are necessary for obtaining information on release kinetics. In addition techniques that can detect the effect of release on surface wear are useful, in say contact lens wear where changes to surface characteristics as a result of release may have detrimental effects on comfort related issues.

2.2.1 Polymerisation

There are three basic steps in free radical polymerisation namely: initiation, propagation and termination in sequential order. Initiation is the decomposition of the initiator to form radicals, which then attack a monomer molecule. Propagation involves the addition of many monomer molecules producing a long chain radical. Termination then occurs when two radicals react by recombination or disproportionation to complete the process. A schematic representation of these steps is shown in figure 2.1.

$I \rightarrow R\bullet + R\bullet$	**Initiation**	where: I = initiator
$R\bullet + M \rightarrow RM\bullet$		R = radical
$RM\bullet + M \rightarrow RMM\bullet$	**Propagation**	M = monomer
$RMM\bullet + nM \rightarrow RMM(M)n\bullet$		• = reactive species
$RMM\bullet + RMM\bullet \rightarrow RMMMMR$	**Termination**	

Figure 2.1 Steps involved in a polymerisation reaction.

For this investigation two types of free radical initiation systems were used: thermal initiation for hydrogel membranes, which were subsequently fully hydrated and photo initiation for skin adhesive hydrogels.

2.2.1.1 Synthesis of hydrogel membranes by thermal initiation

During thermal polymerisation, thermal initiators within the monomer mixture absorb heat energy causing the initiator to become electronically excited, as an outer electron is promoted to a higher state. This excitation results in the initiator becoming unstable; thus it reacts swiftly, either by decaying back to its original state and emitting the excess energy as heat or by participating in a reaction to generate a reactive intermediate such as a free radical, to regain a stable state. The radicals produced in this manner react with each other in turn to initiate polymerisation of the monomers as illustrated in figure 2.1.

A range of compositions containing neutral and anionic monomers were thermally polymerised and subsequently fully hydrated to enable the effects of different monomer groups on EWC to be determined. Samples (5 g) were made with varying amounts of monomers and distilled water, 0.5 % w/w (0.025 g) thermal initiator (AZBN) and 1 % w/w (0.05 g) thermal crosslinker (DATr).

The initiator (AZBN) and TRIS were dissolved in NVP and NNDMA in a vial. The vial was placed on a shaker until the TRIS had dissolved. The contents of this vial constituted the organic phase of the mixture.

In a second vial the SPA and crosslinker (DATr) were dissolved in distilled water, NaAMPS and acrylic acid. The vial was placed on a shaker until a homogenous mixture was formed. The contents of this vial comprised the aqueous phase of the mixture.

The aqueous and organic mixtures were then mixed together and the vial shaken until no residue remained. The mixture was then degassed with a slow stream of nitrogen and then injected into a membrane mould.

A diagram of the membrane mould is shown in figure 2.2. Two glass plates, approximately 10 cm by 15 cm in size, were each covered by a Melinex® (polyethylene terephthalate) sheet and separated by two polyethylene gaskets, each one 0.2 mm thick. Spring clips were placed around the mould to hold it together.

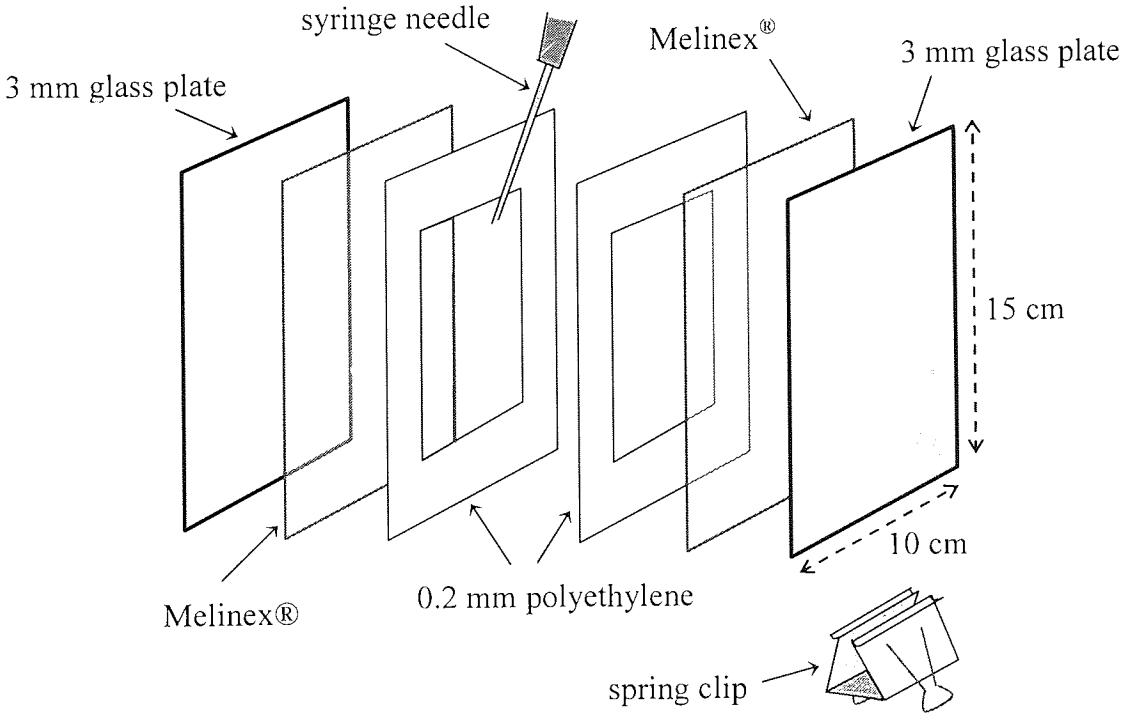

Figure 2.2 Membrane mould (exploded view).

The homogeneous monomer mixture was injected into the cavity of the mould via the G22 syringe needle inserted into the cavity space between the Melinex® sheets. The needle was removed and the mould placed in an oven at 60 °C for three days followed

by a three hour post-cure at 90 °C. The membrane was then removed from the mould and separated from the Melinex® sheets. It was allowed to hydrate in distilled water for at least seven days, changing the water daily. This allowed for equilibrium hydration to be reached and for the extraction of any water-soluble residual monomers.

2.2.1.2 Synthesis of skin adhesive hydrogels by photo initiation

The principle of photo curing is similar to that of thermal polymerisation, described above. However, with photo curing photo initiators are used which become electronically excited when they absorb ultraviolet (UV) light. The photo initiator then either decays back to its original state and emits the excess energy as light or heat or participates in a reaction to generate a reactive intermediate, such as a free radical, to regain a stable state.

Partially hydrated skin adhesive hydrogels were made using photo-polymerisation technique. This form of polymerisation was chosen over thermal polymerisation as it has the following advantages:[75]

i. spatial and temporal control over polymerisation
ii. fast curing rates
iii. minimal heat production
iv. possibility of curing hydrogels in situ

Radical generation is through a chain reaction; thus only very small quantities of the photo initiator are necessary to polymerise the monomers to form a skin adhesive hydrogel. Uniform polymerisation is important in the production of hydrogels with continuous material and adhesive properties. This requires uniform initiation and production of radicals; however achieving equivalent polymerisation of both the bulk and the surface of a gel can be problematic, partly because the larger light intensity experienced at the surface causes greater decomposition of the initiator here. Conversely going further away from the surface there is an increase in optical density impeding polymerisation of the lower layers. Oxygen in the atmosphere can also inhibit photo-polymerisation by reducing the amount of radicals available either by deactivating them or reacting with them. This can be minimised by increasing the concentration of the photo initiator or by polymerising under a vacuum or in an inert

atmosphere. This, however, may not prove practical in some circumstances when amount and cost of production are taken into consideration.

A range of skin adhesives containing anionic and neutral monomers were photo-polymerised and their functional differences characterised by peel testing and dynamic mechanical measurements. Samples (100 g) were made with varying amounts of monomers, glycerol and distilled water and 0.15 % w/w (0.15 g) of crosslinker-photo initiator mix.

A crosslinker-photo initiator mixture was made up in a vial with UV crosslinker (Eb 11) and UV initiator (Irgacure 184) in the ratio of 10:3 and placed on a shaker for about thirty minutes. To prevent the decay of the initiator by any UV light rays in the laboratory the vial was kept in darkness. Any unused mixture was not regarded to be effective after fourteen days. Irgacure 184 initiator has been found to be one of the initiators least affected by oxygen, a radical formation inhibitor.[76]

The monomers, glycerol and distilled water were weighed out into a vessel. The crosslinker-photo initiator mix was added to the bulk mixture after all the monomers had dissolved and was thoroughly shaken. The mixture was immediately poured onto the underside of silicone coated release paper placed in a metal tray. The tray was then placed on the conveyor belt of a GEW laboratory UV curing unit. The belt was set at minimum speed (approximately 5 m/min) and the tray allow to pass under a UV lamp 310, which has an output equivalent to 100 W/cm, until the monomers had completely polymerised to form an adhesive hydrogel. To protect the skin adhesive hydrogel from contamination and water loss it was covered with the coated side of the silicone coated release paper and stored in a polythene bag.

2.2.2 90 Degree peel strength

The adhesion performance of pressure sensitive adhesives can be determined by tack and peel strength. Given that tack and peel strengths are comparable in a number of aspects[77] only peel tests were carried out on the adhesives produced during this investigation.

Peel strength testing measures the strength of the adhesive bond between the hydrogel and substrate. It measures the difficulty of adhesive removal taking into account that, as stated in section 1.4.1.1, for an adhesive to adhere to a substrate its measured surface energy must be equal to or less than that of the substrate. The peel test is subject to several variables such as variations characteristic of the substrate, contact area, contact pressure and time, the angle of peel and the speed of removal. The shear strength measured by the peel test is a measure of force required to induce adhesive failure between the adhesive and the substrate. If the adhesive extends ("legs") or leaves sticky residue the adhesive is said to fail cohesively.

It has been suggested[78] that at a peel angle of 90° the test is less sensitive to backing material failures. Thus a 90° peel strength test was used to determine the difficulty of the adhesive's removal from a substrate. This perpendicular peel test consists of a wooden tray sliding over a wooden base. The tray enables the substrate to remain in position at the same time as it slides over the base to allow the angle of peel to remain constant. This test allows the adhesive to leave the substrate directly below the peel grip. A diagrammatic representation of the test is shown in figure 2.3.

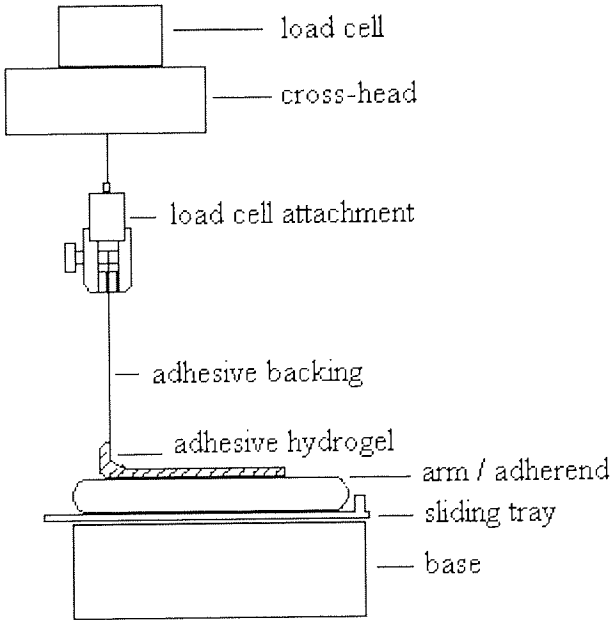

Figure 2.3 90° Peel test set up.

The substrate chosen to determine the peel strength of the adhesives synthesised for the purpose of this study was the researchers forearm. The skin adhesive hydrogel was cut into a strip with dimensions of approximately 2.5 cm by 12 cm. The strip, with its backing sheet still in place, was then placed on the forearm and a 2 kg weight was rolled over the strip to warrant consistent adhesion, the arm was then placed on the sliding tray. A Hounsfield Hti tensometer grip was attached to the backing sheet and the strip peeled off after one minute of placement on the arm at a speed of 500 mm/min using a 100 N load cell, as shown in figure 2.3. All strips were, therefore, removed after equal times of adhesion. During testing the arm moved along the sliding tray to ensure that the peel angle remained constant at 90°. A sample trace obtained with peel strength measured in N/25mm is shown in figure 2.4.

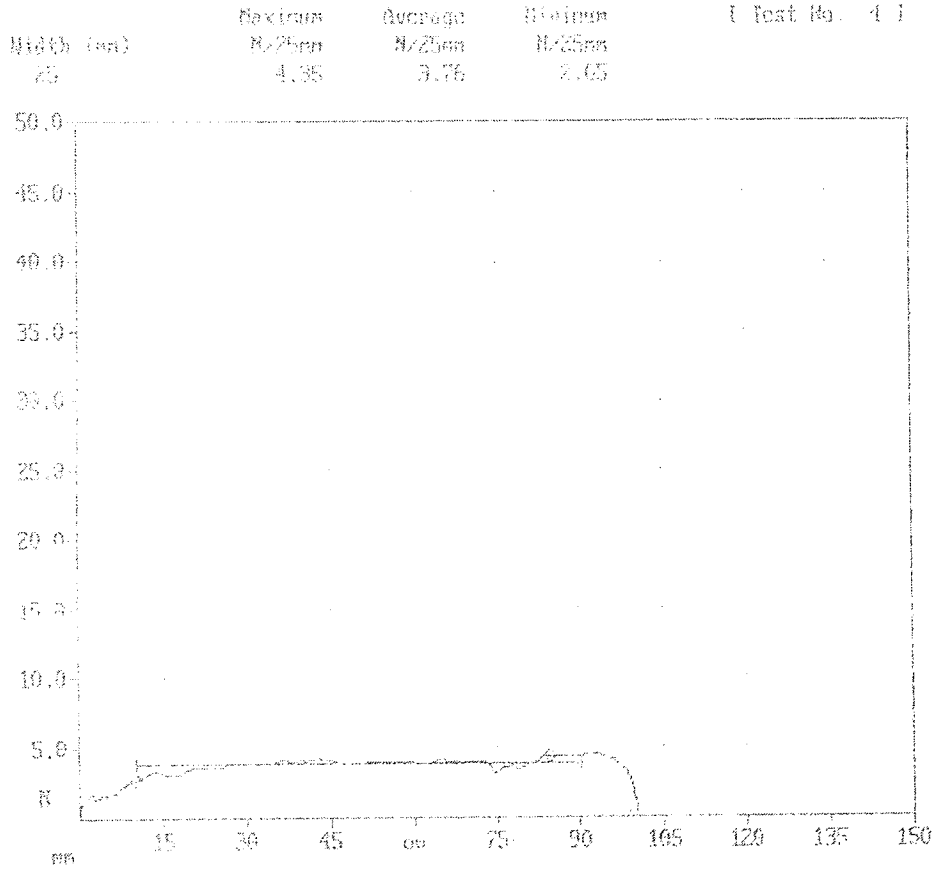

Figure 2.4 A sample trace from a 90° peel test.

For each samples at least three peel tests were carried out to establish the degree of reproducibility of the results. The mean maximum, mean average and mean minimum

values were used in the results. The forearm was cleaned with methanol in between in each test to remove any residual adhesive as well as to minimise lipid variation.

2.2.3 Dynamic mechanical testing

Rheology is the study of deformation and flow of matter under an applied sheared stress. There are two types of deformation a material can undergo: viscous and elastic. The viscosity of a material is its resistance to flow; hence the viscous or loss modulus (G") describes the viscous dissipation of energy through permanent deformation in flow. Elasticity is the property that enables it to return to its original dimensions after an applied stress has been removed; hence the elastic or storage modulus (G') signifies the amount of elastic storage of energy, as in an elastic solid the strain is recoverable. Most materials have a combination of both viscous and elastic components hence they are viscoelastic. However if a material is subjected to a high enough strain its structure becomes permanently destroyed and further deformation is entirely viscous. Viscoelastic properties provide information on how the material is likely to flow under an imposed constant or cyclic shear stress or rate. The viscoelastic properties of the material are assessed by applying a torque and deforming the gel with an applied stress, which in turn causes a strain.

Shear stress is defined as the force applied divided by the area of the gel. Shear strain is the displacement of the gel caused by the force divided by the height of the gap. Shear rate is the rate of change of strain as a function of time.

$$\textbf{shear stress} = \frac{\textbf{force}}{\textbf{area}} \qquad \text{Equation 2.1}$$

$$\textbf{shear strain} = \frac{\textbf{gel displaced}}{\textbf{gap height}} \qquad \text{Equation 2.2}$$

$$\textbf{shear rate} = \frac{\partial\,\textbf{shear strain}}{\partial\,\textbf{time}} \qquad \text{Equation 2.3}$$

Since flow resistance is proportional to force and displacement, viscosity is the quotient of shear stress and shear rate, that is:

$$\textbf{viscosity} = \frac{\textbf{shear stress}}{\textbf{shear rate}} \qquad \text{Equation 2.4}$$

Hooke's law states that the shear modulus (G) is the ratio of the stress to the strain.

$$\mathbf{G} = \frac{\textbf{shear stress}}{\textbf{shear strain}} \qquad \text{Equation 2.5}$$

The ratio of the stress amplitude to the strain amplitude is termed the complex modulus (G*). This is the sum of G' and G".

$$\mathbf{G^* = G' + jG''} \qquad \text{Equation 2.6}$$

where:

j = a unit imaginary number called the j operator = $+\sqrt{-1}$

An oscillatory technique was used to assess the hydrogels viscoelastic characteristics, thereby, providing information on how a material is likely to behave under imposed shear stress conditions. The principle of this technique is to apply a stress or strain with values changing continuously according to the sine wave equation, y = sin x. The complete cycle of a sine wave is taken to be 360°. The induced strain or stress also follows a sinusoidal response. With this technique the material can be continuously excited without exceeding the strain value that destroys its structure; hence the applied stress is continuously adjusted so that the resultant strain is kept at a specific value. The difference between the stress and strain sine waves is referred to as the phase shift or phase angle (δ). The strain response of a pure solid is directly related to the stress, and thus will be in phase with the applied stress giving a phase angle of 0°. The closer the phase angle is to 90° (the phase angle of a pure viscous liquid) the more fluid the behaviour of the material.

The values of G' and G" can be obtained from those of G* and δ.

$$G' = G * \cos\delta \qquad \text{Equation 2.7}$$

$$G'' = G * \sin\delta \qquad \text{Equation 2.8}$$

The viscoelastic properties of the skin adhesive hydrogels were measured on a Bohlin CVO Rheometer. A 20 mm disc of each sample was cut using cork borer number 13 and placed on the lower plate of the rheometer. The top plate was lowered to the thickness of the hydrogel. Correct loading of the sample is important, as measurements should only be taken from the area directly beneath the parallel plate (figure 2.5).

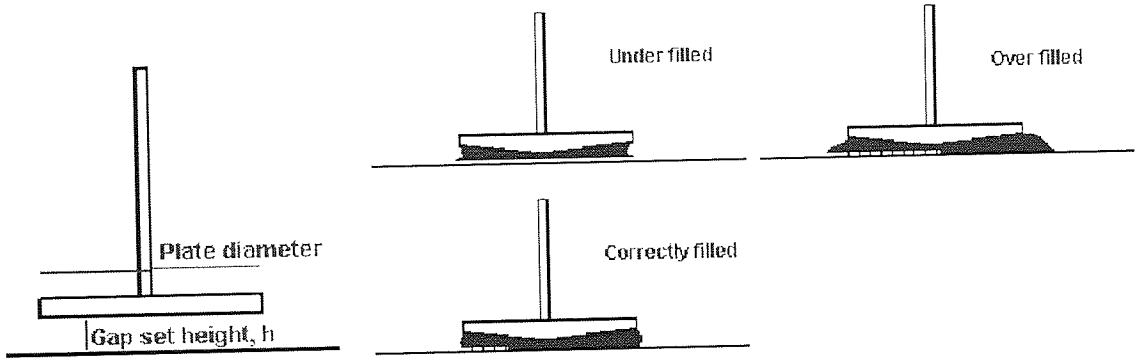

Figure 2.5 Correct loading of a parallel plate measuring system.[79]

The viscoelastic properties of the adhesive gels were measured as a function of frequency. For each test the frequency to complete a sine wave was set to increase from 0.5 Hz to 25 Hz. The lower frequencies were intended to mimic the properties of the gel when it is applied to the skin and higher frequencies when the gel is removed from the skin. Compression was set at 12 %, the target strain at 0.003 and the initial stress at 62 Pa. Tests were carried out at 37 °C, normal body temperature. Measurements of the of the applied torque and angular velocity were relayed from the rheometer to a computer with Bohlin software enabling the shear stress and shear rate to be calculated which in turn allowed the G', G", δ and the tangent of the phase shift (tan δ) to be evaluated. The tangent of the phase shift is defined as:

$$\tan\delta = \frac{\text{viscous modulus}}{\text{elastic modulus}} = \frac{G''}{G'} \qquad \text{Equation 2.9}$$

A sample of the trace obtained is illustrated in figure 2.6.

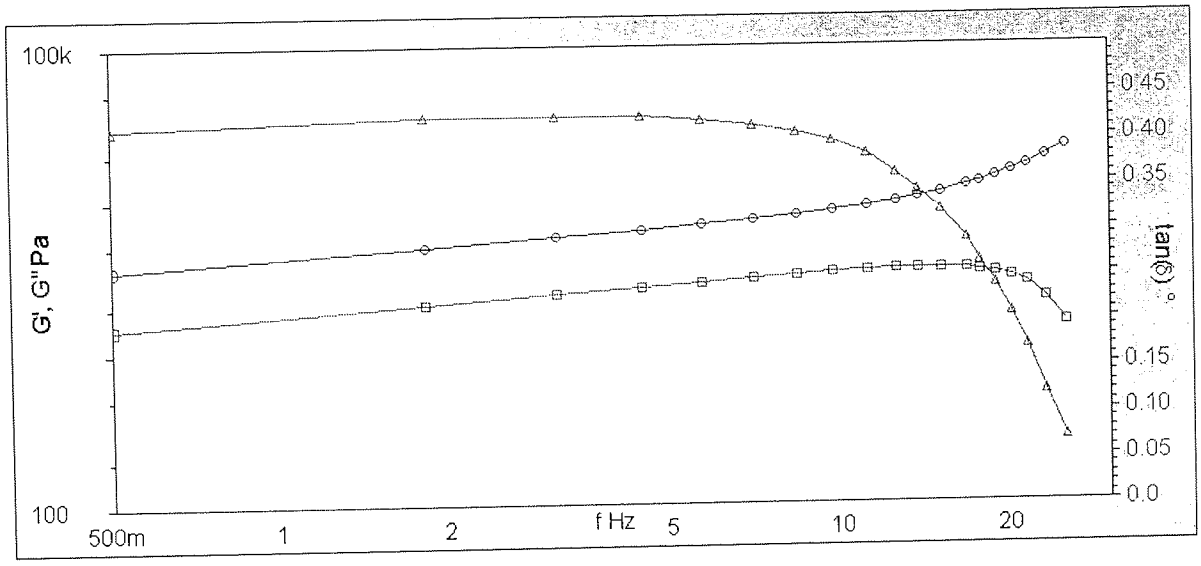

Figure 2.6 A sample trace from oscillatory flow characterisation.

At least three discs form each sample were tested and their average quoted in the results.

2.2.4 Impedance

Impedance is a measure of a circuit's ability to resist the flow of an alternating or direct current. It is a vector quantity consisting of two independent scalar (one-dimensional) phenomena, namely resistance and reactance, expressed by:

$$\mathbf{Z} = \mathbf{R} + j\,\mathbf{X} \qquad \text{Equation 2.10}$$

where:

Z = impedance, Ω (ohm)

R = resistance, Ω

X = reactance

Resistance is the property of a material that reduces the flow of electricity through it. It is defined by Ohm's law as the ratio of the potential difference (V) between the ends of a conductor to the current (I) flowing through it.

$$\mathbf{R} = \frac{\mathbf{V}}{\mathbf{I}}$$ Equation 2.11

Reactance is the property of an electric circuit to oppose a voltage change. It is an expression to which electric systems store and release energy as the current and voltage fluctuate with an alternating current (AC) cycle and is not valid for direct current (DC). When an AC passes through a component that contains reactance energy might be stored and released in the form of a magnetic field, in which case the reactance is inductive (denoted $+ jX_L$), or energy might be stored and released in the form of an electric field, in which case the reactance is capacitive (denoted $- jX_C$).

Thus Z can be expressed as a complex number of two forms:[80]

i. $R + jX_L$ when the net reactance is inductive or
ii. $R + jX_C$ when the net reactance is capacitive.

A Holman Design gel electrode impedance meter number 04 was used to determine the impedance of the adhesive hydrogels. The frequency of the current could be set at 10 Hz, 50 Hz, 2 kHz, 30 kHz and 200 kHz. The three lower frequencies were thought to be equivalent to those of a transcutaneous electrical nerve stimulation (TENS) machine. The maximum potential of the meter was 1.99 V and the maximum current 999 mA.

Prior to each test the machine was calibrated at a potential of 1.94 V using a 100 Ω and 200 Ω resistance box. The potential and current values were entered into a spreadsheet provided by Holman Design to determine coefficients used to evaluate impedance.

The adhesive hydrogel was placed on a metal plate and covered with a metal backing. A potential difference of approximately 1.94 V was then applied between the bottom and backing plate. The actual potential and current readings were taken every thirty seconds for a period of eleven minutes. The readings were subsequently entered into the spreadsheet and the impedance calculated.

The effect of composition, thickness and area of the adhesive hydrogel electrode were investigated at a frequency of 50 Hz. The effect of frequency on impedance was also studied.

2.2.5 Sensation

Sensation is the experience felt when current passes through the adhesive. Sensation that causes discomfort is undesirable in certain applications such as ocular iontophoresis, which is described in section 1.5.7.3. A possible method of comparing the level of sensation produced by different hydrogels is to use a TENS machine, as in a TENS application sensation in desirable.

TENS is a common clinical tool used to treat chronic conditions such as low back pain, arthritis and pain caused by neurological disorders as well as acute conditions such as pain during childbirth and post-operative pain. It works by applying gentle electrical pulses to block pain signals sent to the brain and encourages the body to produce endorphins, natural painkillers.

With a TENS machine various pulsed waveforms can be employed using surface electrodes. The current employed is generally less than or equal to ($\leq$) 200 mA, pulse duration $\leq$ 6 ms and pulse rate $\leq$ 200 pps (pulses per second). The recommended minimum treatment time is twenty minutes and the maximum is one hour. The waveforms are designed to pass no net current, as the pulses are biphasic, in order to reduce irritation. According to the American National Standard for TENS devices the maximum allowed charge per pulse based on an electrode area of 25 cm^2 is 75 μC.[74]

A Boots TENS machine was used to evaluate the sensation felt for the skin adhesive hydrogels produced. The Boots TENS machine requires two 1.5 V size AA batteries. The biphasic waveform produced is rectangular and symmetrical. Its amplitude over a 500 Ω load is 100 mA with a peak voltage of 250 V. The machine utilises up to four hydrogel electrodes on carbon based backing pads connected to the unit via wires. The electrode connected to the white snap is the cathode and that connected to the red snap is the anode. The machine has seven modes, A to G, of various pulse rates and durations with either constant, burst or modulated output. Each mode has fifteen levels of intensity.

Tests were carried out using Mode F of the Boots TENS machine. This mode has a constant output pulse rate of 110 Hz and pulse duration of 200 μs. The intensity of the current was set at fifteen as this was thought to be the setting that would most closely simulate iontophoresis. Both anode and cathode electrodes were used for the tests.

The adhesive gels were cut into a similar size and shape of Boots TENS electrodes and then placed on top of the Boots' electrode gel thereby over coating it. To evaluate the effect of increasing the thickness of the gel several layers of gel were placed on top of each other. To study the effect caused by increasing or decreasing electrode surface area an MSB neutralect electrode, normally used for defibrillation, was cut in half. The adhesive hydrogels made were also cut to larger sizes and then over coated the gel on the Boots TENS electrode.

Once the electrode had been prepared as above, depending on the parameter investigated, the electrode pads were placed on either side of the right shoulder. Current was then allowed to pass through for ten minutes during which time the sensation was noted.

2.2.6 Refractive index

Refractive index (RI) refers to the ratio of the speed of light in a vacuum (incident light) to that in the medium (refracted light). When light passes from vacuum through another medium such as glass, liquid, solid or gas its speed changes at the boundary. The change in speed causes a change in direction of travel (figure 2.7). However for purposes of convenience air (at 1 atm) instead of vacuum is used as the reference medium.

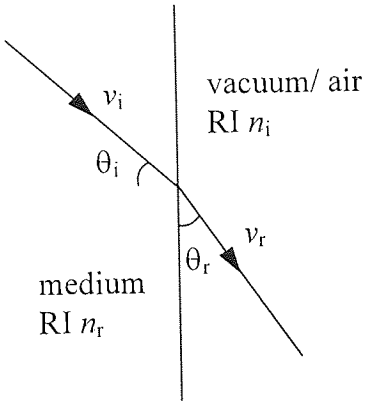

Figure 2.7 Differences in the refraction of light as it passes through different media.

It is not necessary to determine the ratio of the speed of incident light (v_i) to refracted light (v_r) in order to determine the RI of a medium, as this ratio is related to the ratio of the sine of the angle of incidence (θ_i) to the sine of the angle of refraction (θ_r) in the medium; whereby the angles are measured relative to the normal of the interface between the two media (equation 2.12).

$$\mathbf{RI} = \frac{n_r}{n_i} = \frac{v_i}{v_r} = \frac{\sin\theta_i}{\sin\theta_r} \qquad \text{Equation 2.12}$$

where:

n_r = refractive index of the refractive medium

n_i = refractive index of the incident medium

RI is a physical property of the medium that varies with temperature and with the wavelength of the light used. In general refractometers (RI measuring instrument) contain a lamp that emits light at a wavelength equal to that of the yellow sodium D line (a doublet 589.0 to 589.6 nm) and are attached to a water bath to maintain a constant temperature. Density is temperature dependent thus as temperature rises the medium becomes less dense and this results in a decrease in RI.

The principle for measuring RI is based on the determination of the critical angle (θ_c) of reflection. This is the incident angle at which the angle of refraction is 90^o (figure 2.8).

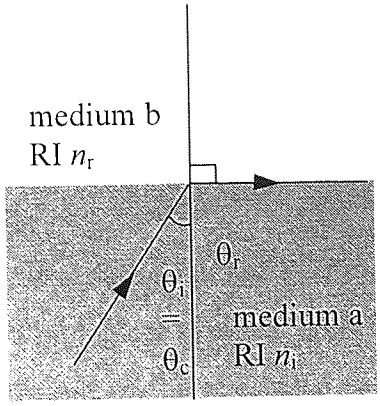

Figure 2.8 The critical angle of reflection.

When the angle of incidence is larger than the critical angle, the light undergoes total internal reflection at the same angle as the angle of incidence. Refractometers contain a high resolution optical sensor that measures the total reflection of the light beam. This is used to determine θ_c. The sine of 90^o is 1, this can be substituted into equation 2.12 and re-arranged (equation 2.13) to determine the RI of the refractive medium (n_r) since that of the incident medium (n_i) is known.

$$n_r = \frac{\sin\theta_c}{\sin 90^\circ} n_i = \sin\theta_c n_i \qquad \text{Equation 2.13}$$

An Index Instruments automatic GPR 11 – 37X micro-refractometer was used for measuring RI. Prior to testing the refractometer and the water bath were turned on until a steady temperature of 25 °C had been achieved (approximately one hour). To calibrate the machine a sufficient amount of sample (approximately 100 µl) of high performance liquid chromatography (HPLC) grade water was placed onto a synthetic sapphire prism (incident medium), ensuring that it was fully covered. The instrument automatically measured the RI of the HPLC grade water and once this remained steady the instrument was zeroed. The prism was subsequently cleaned and dried and 100 µl of the sample to be analysed was placed on it. The RI of the sample was automatically measured to five decimal places.

2.2.7 Biotribology

The term "*tribology*", derived from the Greek word "*tribos*" which means rubbing, is defined as the science and technology of interacting surfaces in relative motion. The main subjects of study are lubrication, friction and wear.

A second term, "*biotribology*" was defined in the 1970s as the study of all aspects of the subject of tribology related to biological systems, so it is wide ranging. The study of biotribology involves measurement of the resistance to motion of contacting surfaces expressed in terms of the coefficient of friction (μ). This is the ratio of the force causing movement (F_t) to the applied load (W).

$$\mu = \frac{F_t}{W} \qquad \text{Equation 2.14}$$

In order to understand the breakdown in lubrication reference can be made to the Stribeck curve, which was originally developed in 1970s for a solid-fluid-solid system.

The Stribeck curve (figure 2.9) shows the evolution of μ versus the Sommerfeld number; a parameter consisting of the lubricant's viscosity (η), the sliding speed (v), the load or normal force (W) and the radius of contact (r_c).

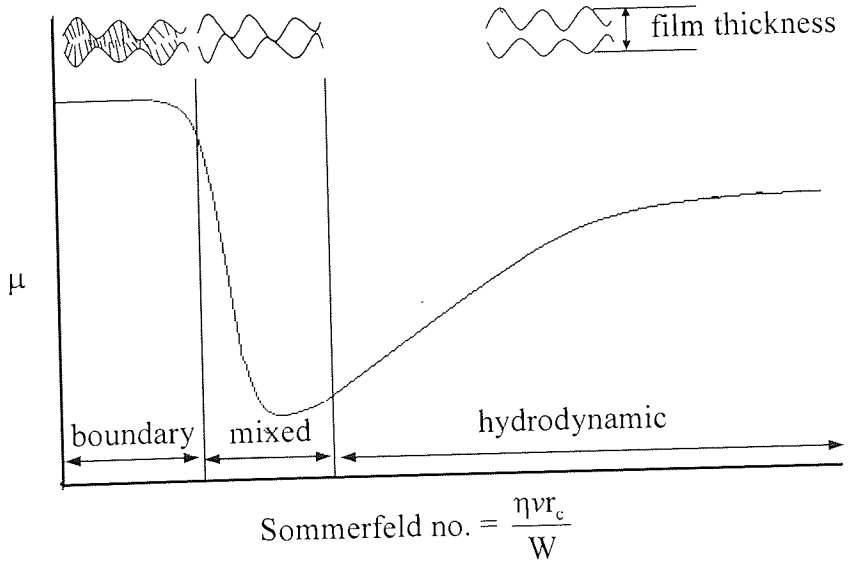

Figure 2.9 The Stribeck curve.

This plot shows that three regimes can be identified to describe lubrication. Each regime is characterised by the degree of contact between the two solid surfaces.

In the boundary lubrication regime the lubricant film thickness approaches zero as the lubricant is adsorbed onto the surfaces; thus there is a high degree of contact between the two solids. The friction forces are attributed to surface attractions and the effects of deformation and recovery of the asperities on one of the surfaces as they pass over the asperities of the other surface, which in turn are dependent on the surface roughness. In this lubrication regime μ is fairly large and remains constant as the η, v, W or r_c are varied.

The other extreme is the hydrodynamic lubrication regime. Here the film thickness is greater than the combined surface roughness of both surfaces; hence the surfaces are completely separated from each other. For this type of lubrication μ rises with an increase of the η of the lubricant and or v but decreases as W increases.

In between the two extremes is the mixed lubrication (or elastohydrodynamic) regime where both the boundary and fluid film mechanisms act simultaneously, either supporting or competing with each other. The average film thickness is less than the combined surface roughness of both surfaces; thus there is partial contact between the asperities of the two surfaces. In this case W is supported by the asperity contact and the hydrodynamic pressure forces.

Although there are as yet no established *in vitro* techniques to measure the μ of contact lenses, a high sensitivity tribometer, Nano-Scratch Tester with Scratch Software V3.46 data management system, for the study of contact lens biotribology was identified and adapted in conjunction with an instrument manufacturer. With this nanobiotribometer (figure 2.10) the lens is placed on the convex mould and a chosen substrate is clipped onto a moving table in the optional presence of an appropriate lubricating solution. The table is raised until the contact lens comes into contact with the lubricating solution. Thus the meniscus of the lubricating solution is "carried" over the lens, similarly to the eyelid carrying the tear meniscus over lens or cornea, and μ is determined from equation 2.14. A significant development is that the whole instrument sits on an air table to

isolate it from vibration; therefore it can measure low values of μ due to the reduced background "noise".

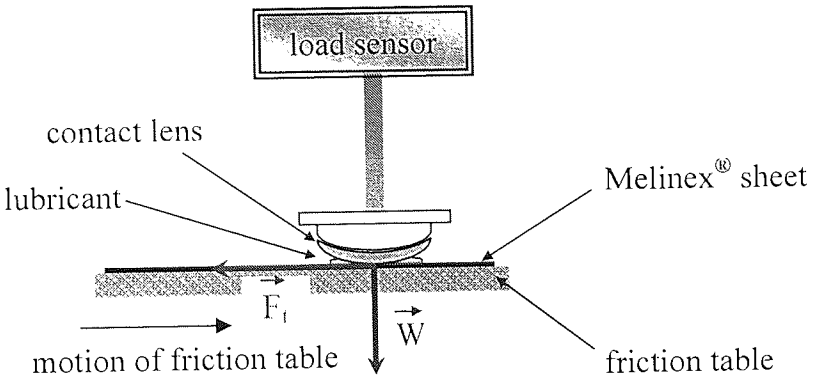

Figure 2.10 Schematic representation of a nanobiotribometer for contact lenses.

Figure 2.11 illustrates a typical μ-distance measurement output indicating difference between μS ("start-up" or "static") and μD ("dynamic" or "sliding") friction.

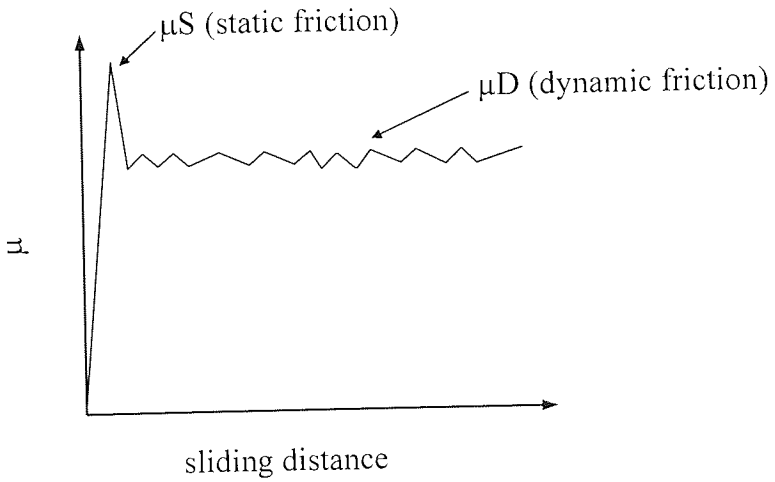

Figure 2.11 A schematic of a typical μ-distance trace.

Experimental set-up values such as the applied load and the sliding speed as well as the properties of the material, lubricant and substrate will influence the value of the μ. Thus

to enable the comparison of the μ for different materials and lubricants the applied constant load was set at 60 mN, the sliding speed at 30 mm/min, sliding distance 20mm and substrate used was a sheet of Melinex®, which was changed for each lens.

2.2.8 Photometric chemical analysis

Colorimetric analysis, a branch of photometric chemical analysis, is used to determine low concentrations of coloured substances by visually matching the colour of a coloured solution against the colour of solutions containing known concentrations of the coloured species. When a beam of monochromatic light is directed through a coloured solution some of the light (incident light) is transmitted and the rest is absorbed. By comparing the intensity of the incident light to the intensity of the light transmitted through the sample, the absorbance of the sample at that particular light wavelength can be determined.

The Beer-Lambert law relates the extent of absorption to concentration by the following expression:

$$\mathbf{Ab} = \mathbf{log}\frac{\mathbf{I}_0}{\mathbf{I}_t} = \mathbf{\varepsilon cl} \qquad \text{Equation 2.15}$$

where:

Ab = absorbance

I_0 = intensity of incident light

I_t = intensity of transmitted light

ε = extinction coefficient (substance and wavelength specific)

c = concentration of sample

l = length of light path

A Cecil CE404 spectrophotometer was used to measure the absorbance of coloured solutions. A simple diagrammatic representation of the instrument is shown in figure 2.12.

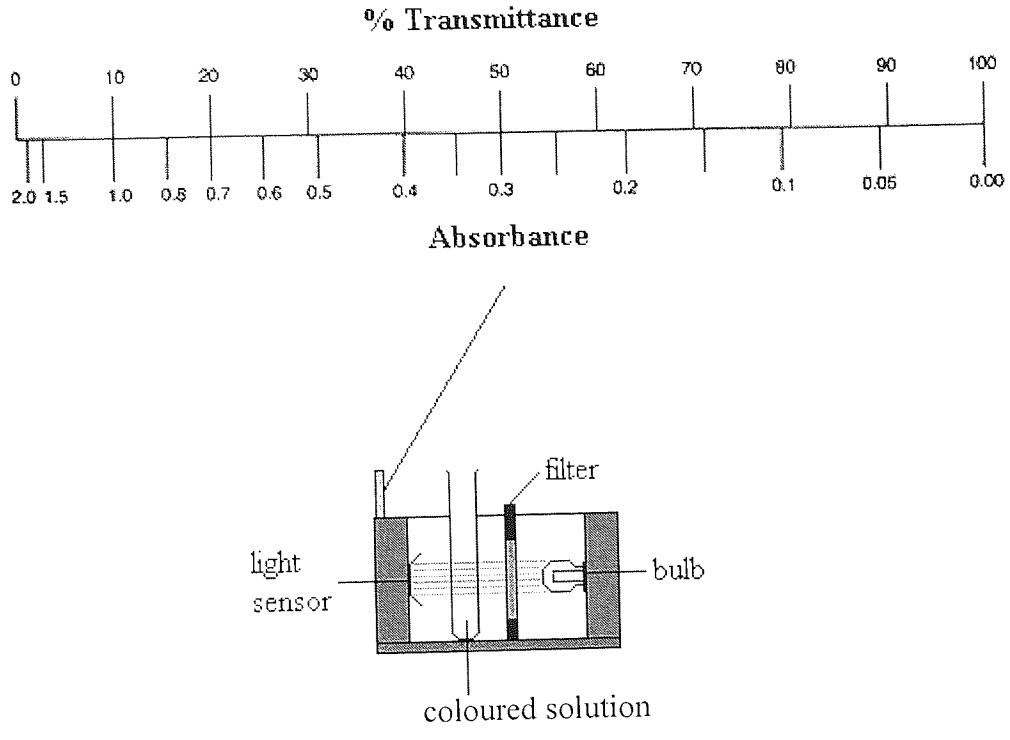

Figure 2.12 Diagrammatic representation of a colorimetric instrument.

The colorimetric filter chosen was that which selected the range of wavelengths most strongly absorbed by the dye, as this would be the most sensitive to changes in concentration. The filter can be chosen using figure 2.13 if the maximum absorption wavelength of the coloured species is known.

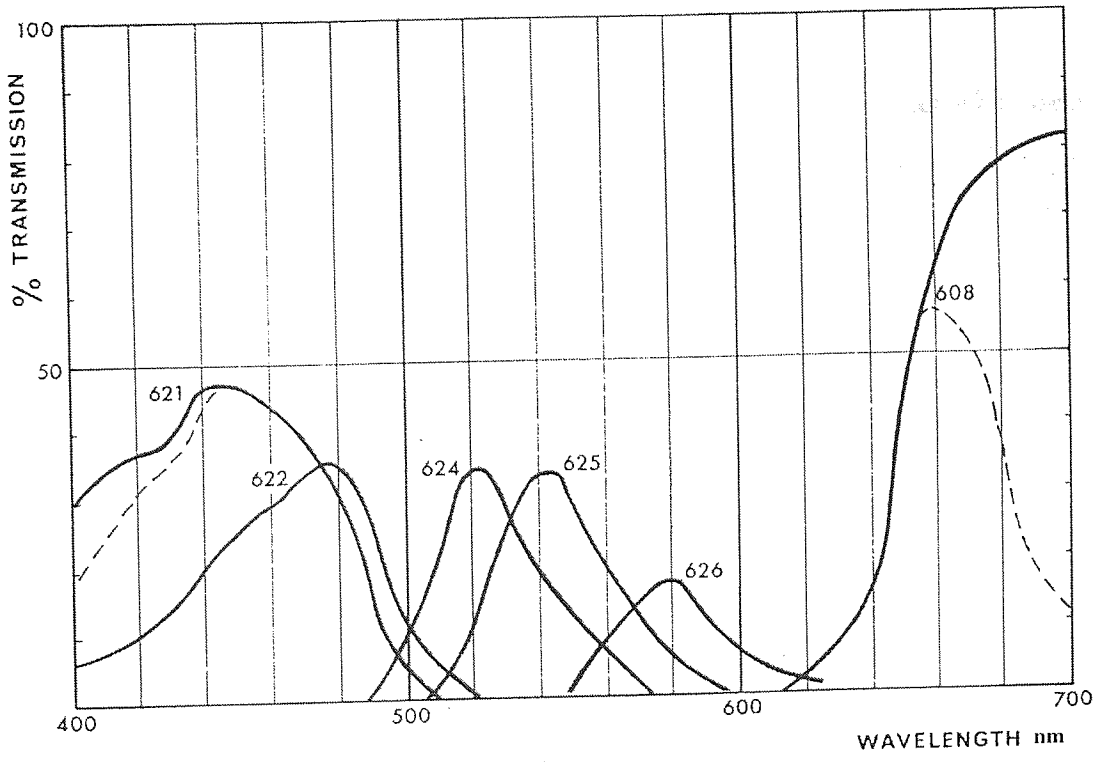

Figure 2.13 Transmission characteristics of Ilford Bright filters.[81]

In order to calibrate the colorimeter a control sample is required. The control sample used in this investigation was an uncontaminated sample of phosphate buffered saline (PBS). The PBS was poured into a cuvette and placed between the chosen filter and photocell and the absorbance scale subsequently zeroed. In order to plot a calibratrion chart of absorbance as a function of concentration, the absorbance of samples of known concentration of the coloured species to be studied was measured. At least three measurements for each concentration were taken and the average absorbance value used. The absorbencies of samples of unknown concentrations were measured using the same procedure as with samples of known concentration and their concentration determined using the calibration plot. The absorbance of the control was checked prior to measuring each sample.

2.3 Method development

The selection of appropriate analytical techniques is a fundamental aspect when dealing with research. However once an appropriate technique has been selected the method may require modifications, particularly with novel applications. For this study it was desired to detect and quantify three different substances. These were:

i. unpolymerised monomers remaining within a cured adhesive hydrogel. This is desired as residual unpolymerised monomers are generally toxic and cause adverse reactions.
ii. water-soluble polymers used for improving contact-lens related comfort
iii. actives released from a hydrogel matrix to satisfy a therapeutic need

The use of gas and ion chromatography (for i and iii) and mass spectrometry (for ii) was investigated.

2.3.1 Gas chromatography

Chromatography is a technique used to separate, identify and quantitate the components of a mixture by differences in their partitioning behaviour between a flowing mobile phase and a stationary phase. A major benefit of this technique is that it generally requires only very small amounts of sample.

There are various types of chromatographic techniques which are classed according to the physical states of the two phases. With gas chromatography (GC) the mobile phase is a gas. The principle of this technique involves injecting an amply volatile sample into the head of a chromatographic column. The sample is subsequently vaporised and then carried through the column by a regulated stream of inert gas, known as the carrier gas. The column contains a liquid stationary phase that enables the components to separate independently according to their relative solubility in the liquid. Hence the components travel through the column at a different pace. The separated components pass through a detector on leaving the column and produce an electrical signal, which is in turn fed to an amplifier producing a trace, known as a chromatogram, on a recorder. A schematic diagram of a gas chromatogram is shown in figure 2.14

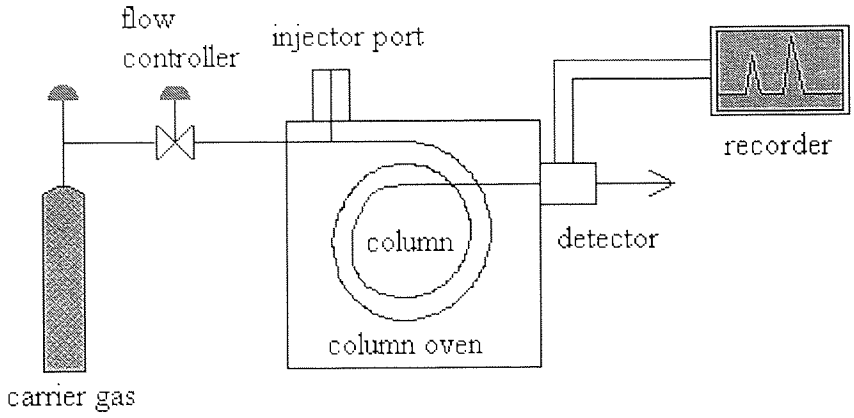

Figure 2.14 Schematic diagram of a gas chromatogram.[82]

GC was chosen as an appropriate technique for detecting menthol; as menthol is sufficiently volatile and only 10^6 molecules, a tiny fraction of a mole, are needed to be able to smell thus detect the presence of menthol. Menthol is used as an antiseptic or local anaesthetic and in herbal medicine it is used as a spasmolytic.

A Perkin Elmer ATI Unicam gas chromatogram was used to quantitatively determine the amount of menthol released from a skin adhesive hydrogel. It was fitted with a fused silica bonded phase non-polar capillary column (BPX 5). The column had an internal diameter of 0.32 mm, an outer diameter of 0.43 mm, a length of 25 m and a film thickness of 25 microns.

The column and injector were set at a temperature close to the boiling point of substance to be detected; for this study this was set at a temperature of 210 °C close to that of the boiling point of menthol (216 °C). The temperature of the flame ionisation detector was set 20 °C higher than this, that is at 230 °C. The carrier gas used was helium at 9 psi and the make up gas was nitrogen (split). Air at 20 psi and hydrogen at 12 psi were used to fuel the flame ionisation detector. The detector was interfaced to a computer with Unicam 4880 chromatography data handling software, which produced a trace. An example of a trace of a mixture containing two components is shown in figure 2.15.

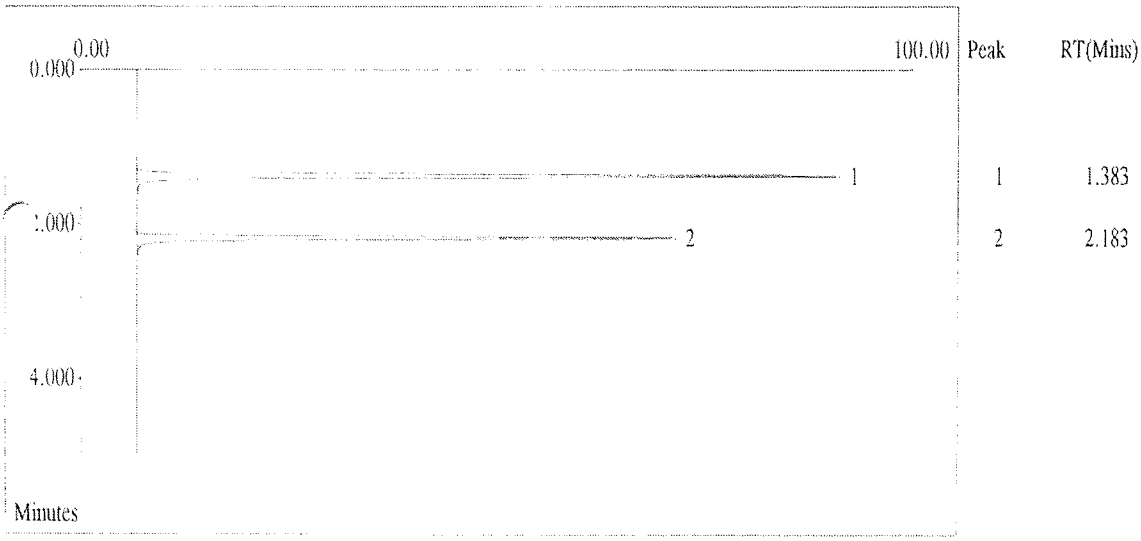

Figure 2.15 Gas chromatography trace of a sample of solvent containing an active.

For a solute-solvent mixture, one of the peaks corresponds to the solvent and the other the solute peak. These are differentiated by retention time, as different substances peak at different times. Determining the retention time of the pure solvent a priori enables the identification of the solvent peak and by process of elimination the remaining peak is that of the active. The software is also able to determine the area under the peak. Thus a calibration chart of area under the active peak as a function of its concentration can be plotted.

2.3.1.1 Effect of varying the solvent with menthol

Samples of methanol and ethyl acetate containing 0.5 %, 5 % and 10 % w/w of menthol were prepared, as per compositions detailed in appendix 1, and allowed to equilibrate overnight. A 1 ml sample size of each mixture was injected through the capillary column and the test carried under the conditions stated above.

By maintaining the solvent peak area constant (353.5 units^2) the peak areas of the various menthol concentrations were recalculated, see appendix 1. The peak areas of the three different concentrations in two solvents, methanol and ethyl acetate, were compared (figure 2.16).

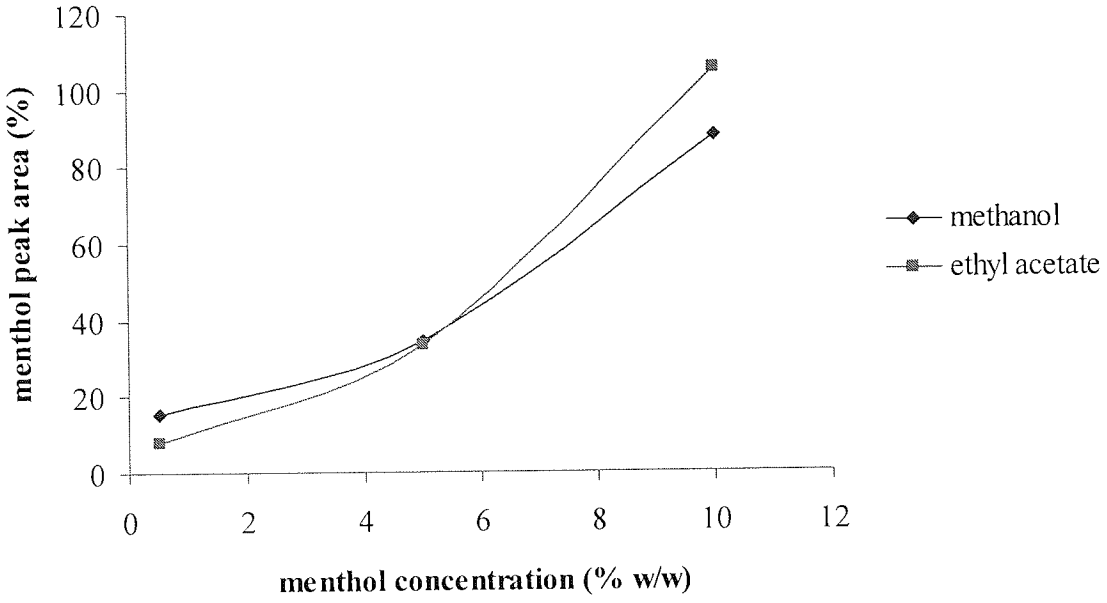

Figure 2.16 Menthol peak areas for various concentrations using two solvents.

These results show that menthol peaks for both solvents were detected by the system and method used. Differences in percentage peak area at the same menthol concentration but different solvent may be due to differences in the degree of solubility of menthol in the solvent.

In conclusion, GC is thought to be a viable technique for determining the amount of menthol released. It is proposed that a menthol loaded hydrogel may be placed in either menthol or ethyl acetate and that at certain time intervals a sample of the solvent could be analysed to determine the w/w % of the menthol from a calibration curve, similar to that of figure 2.16 but with at least five data points corresponding to five menthol concentrations. The same principle could therefore be applied to other volatile actives however a column with a stationary phase that the active under investigation binds to should be used. The temperature of the detector should be set at a temperature similar to that of the boiling point of active to ensure that it vaporises.

This technique was also investigated for determining residual neutral monomer as outlined in section 3.6.2.

2.3.2 Ion chromatography

Ion chromatography (IC) is a subdivision of high performance liquid chromatography (HPLC). IC involves separating and quantifying anions and cations using liquid chromatography (LC). LC is an analytical technique based on the separation of a mixture in solution using a liquid mobile phase to carry the mixture through a chromatographic column, which separates the components of the mixture by selective absorption.

With IC the ions dissolved in a solvent are injected into a column. The column contains a stationary bed with a surface of opposite charge to the sample ions. The stronger the charge on the sample, the stronger its attraction to the ionic surface thus the longer it takes to elute. Both the pH and ionic strength of the mobile phase control elution time. Once the ions are separated they are detected and quantified by a conductivity detector.

The suitability for using IC to detect anionic monomers was investigated in this study. The ability to detect and quantify anionic monomers would provide a method for determining the amount of residual monomer that remains post curing. This is desired as residual unpolymerised monomers are generally toxic and cause adverse reactions (see chapter 3). A Dionex DX600 supported by Chromeleon Client 6.50 software to process the acquired data was used. The main advantages of this system are the online generation of the mobile (eluent) phase as well as its counter ion auto suppression technology. A schematic of the system is shown in figure 2.17.

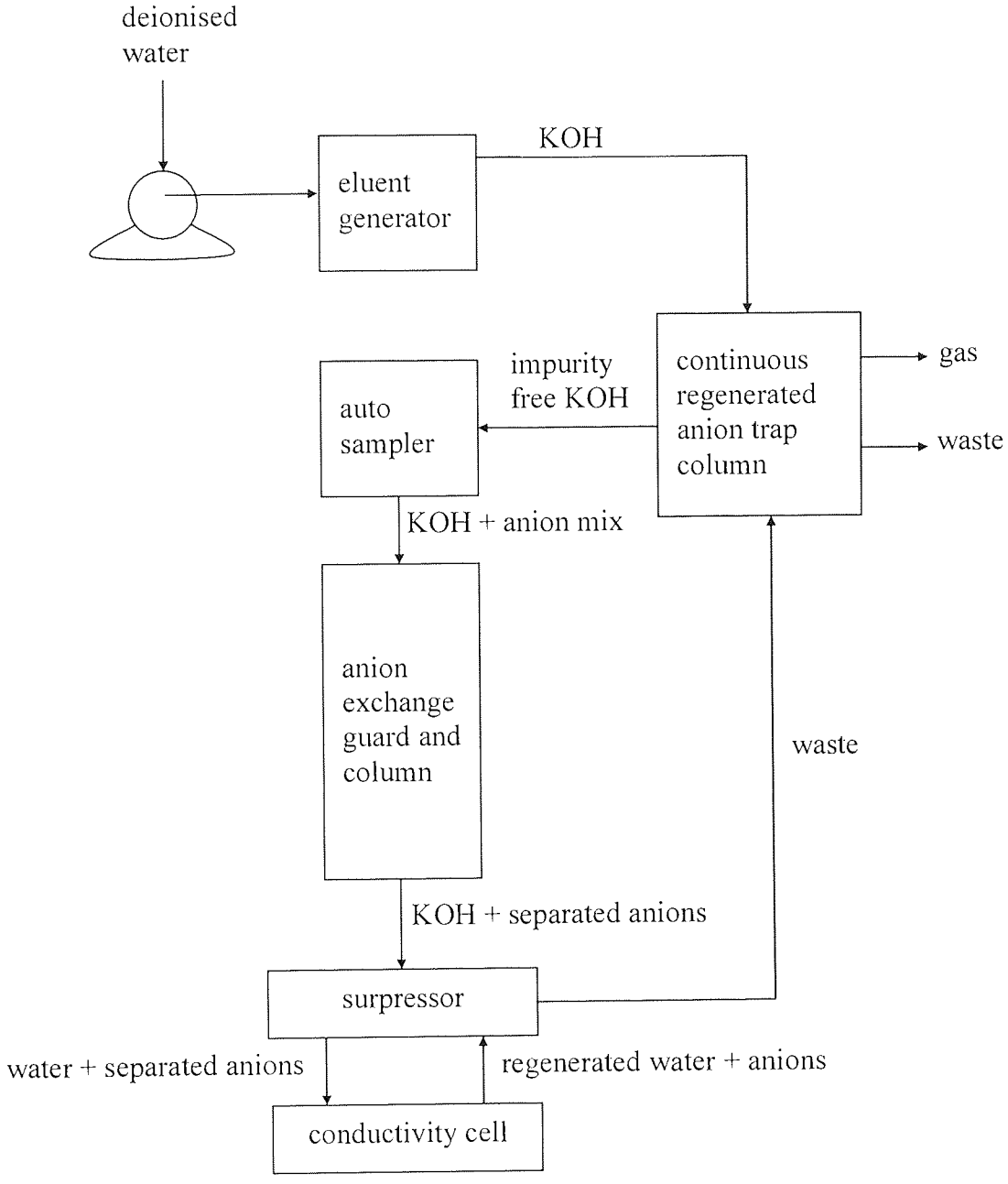

Figure 2.17 Flow diagram of the Dionex DX600 ion chromatograph.

2.3.2.1 Online eluent generation

Dionex eluent generators use electrolysis to convert pure water into potassium hydroxide (KOH) eluent for anion separation. The eluent's counter ion (potassium, K^+), which is stored in an EluGen® cartridge reservoir, diffuses across a membrane into the

cartridge's high-pressure chamber during electrolysis. A degasser built into the cartridge outlet removes by-product gas (hydrogen) from the eluent stream. The concentration of the eluent is delivered as a function of the applied voltage, eluent flow rate, concentration of the species in the reservoir and other factors; however these are automatically adjusted according to the flow rate and concentration specified. Thus a contaminant-free eluent is delivered on demand at the exact concentration required for the application.

By eliminating variability associated with manual eluent preparation and by eliminating the possibility of eluent contamination, online eluent generation enhances reproducibility of results. Furthermore absorption of atmospheric carbon dioxide or ammonia is virtually eliminated; thus eluent contamination is reduced resulting in lower background signal, reduced noise, smaller baseline shifts and better peak resolution.

2.3.2.2 Counter ion auto suppression

Suppression works to achieve the absolute best sensitivity (signal-to-noise ratio) and corresponding lowest detection limits for inorganic analysis by:

i. decreasing background eluent conductivity (lowers noise)
ii. increasing analyte conductivity (increases signal)
iii. eliminating sample counterions

The anion suppressor behaves like a cation exchanger by replacing K^+ from the eluent with hydronium ions (OH_3^+); thus when the analytes leave the suppressor they are in a water solution. Water is only weakly ionised so the background conductivity is very low. The analyte response is also enhanced because the OH_3^+ counterion is about seven times more conductive than the K^+. This water is regenerated back to the surpressor to wet the cells; hence this section of the process has been termed auto-surpression.

2.3.2.3 Anion separation

An evaluation of the ability to use ion chromatography to detect and quantify water-soluble anionic monomers (NaAMPS and SPA) was carried out. A sample of 0.058%

monomer dissolved in 18.2 MΩ.cm (0.055 μS/cm) water was placed in the autosampler. 2.5 μl of the monomer-water mixture was injected into a 2 mm IonPac AS11 column containing a 13 μm diameter microporous resin bead functionalised with quaternary ammonium groups. The KOH eluent concentration was ramped from 5 mM to 60 mM over 30 minutes with the eluent flowrate set at 0.38 ml/min. Post separation the anions were detected by an electrochemical detector. The chromatograms obtained for NaAMPS and SPA are illustrated in figures 2.18 and 2.19.

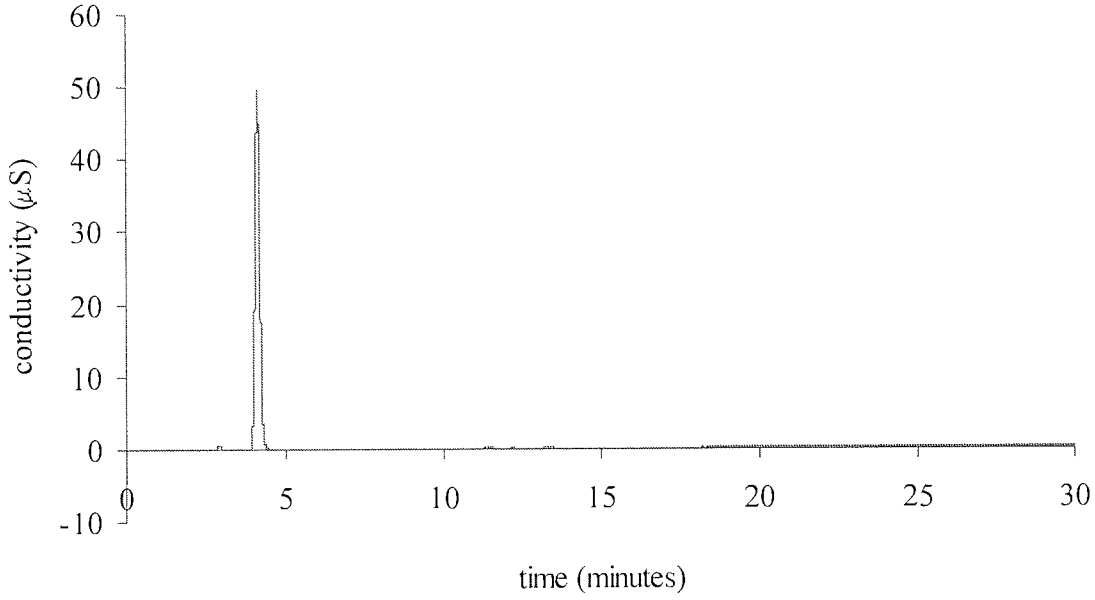

Figure 2.18 NaAMPS ion chromatogram.

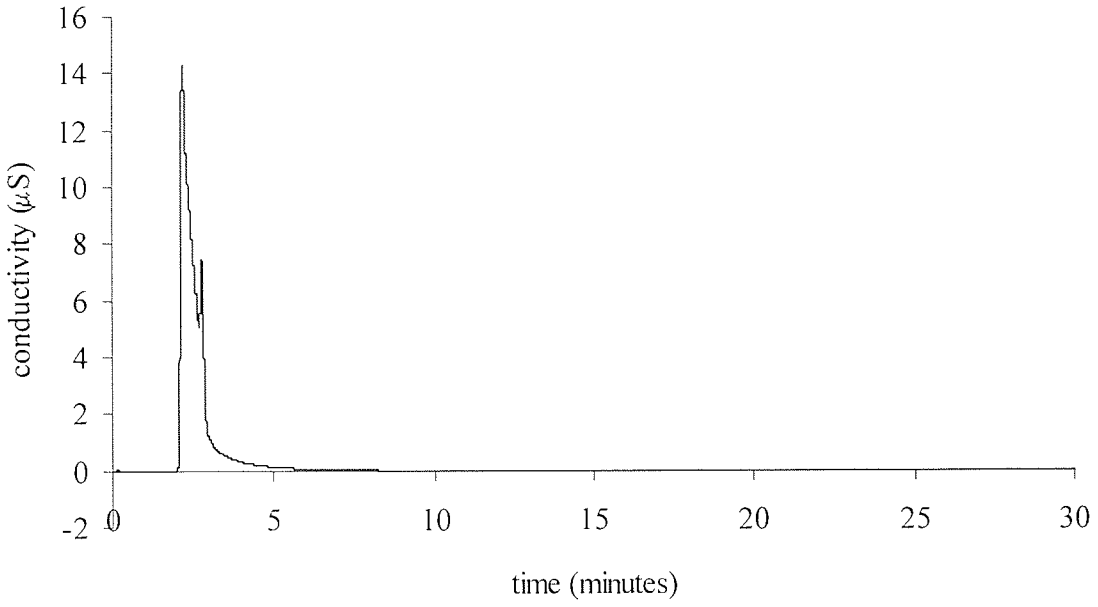

Figure 2.19 SPA ion chromatogram.

The peak obtained for SPA was not as sharp as that of NaAMPS. Attempts were made to reduce the volume injected into the column, but a peak of similar broadness was acquired. This suggests that although both SPA and NaAMPS anion contain a sulphonate anion (SO_3^-) there seem to be compatibility issues with the column. This may only be verified by testing various anions columns; a feat too costly as well as time consuming but feasible nonetheless.

2.3.2.4 Sensitivity issues

Further exploration of the use of IC for determining anionic monomers or actives was hindered because issues related to sensitivity emerged. Initially there was a steady rise in the baseline (figure 2.20) suggesting an increase in the signal-to-noise ratio therefore reducing the ability of the software to detect the peaks.

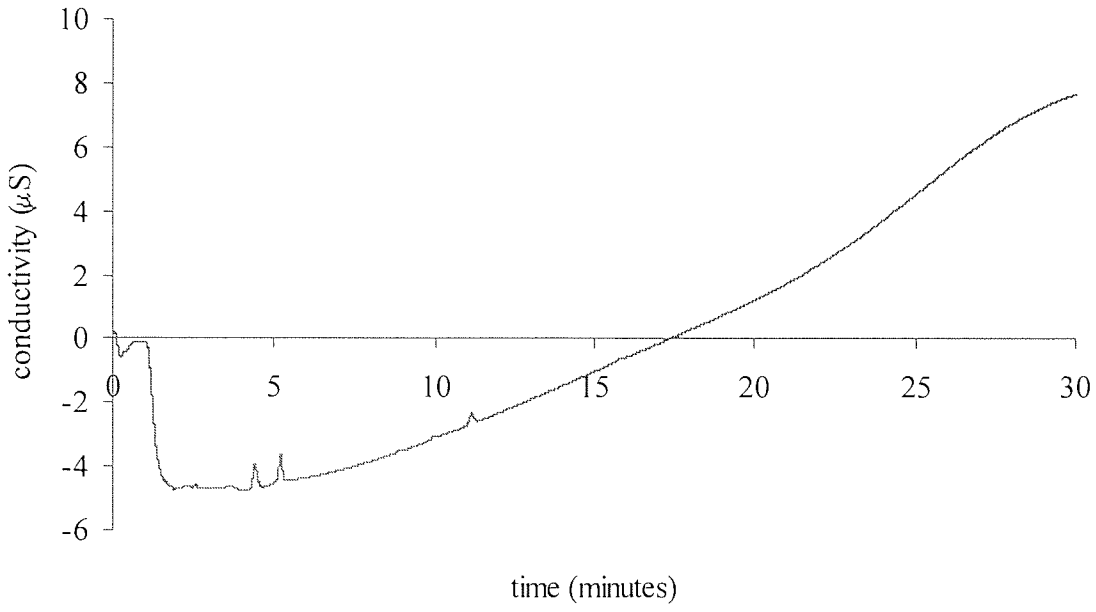

Figure 2.20 Rise in baseline.

After substantial investigation it was discovered that the helium used to pressurise the deionised water was contaminated. This resulted in the installation of a direct helium feed to the water bottles. Initially this seemed to resolve the problem however retention times began to drift making it difficult to differentiate peaks of similar retention time (figure 2.21).

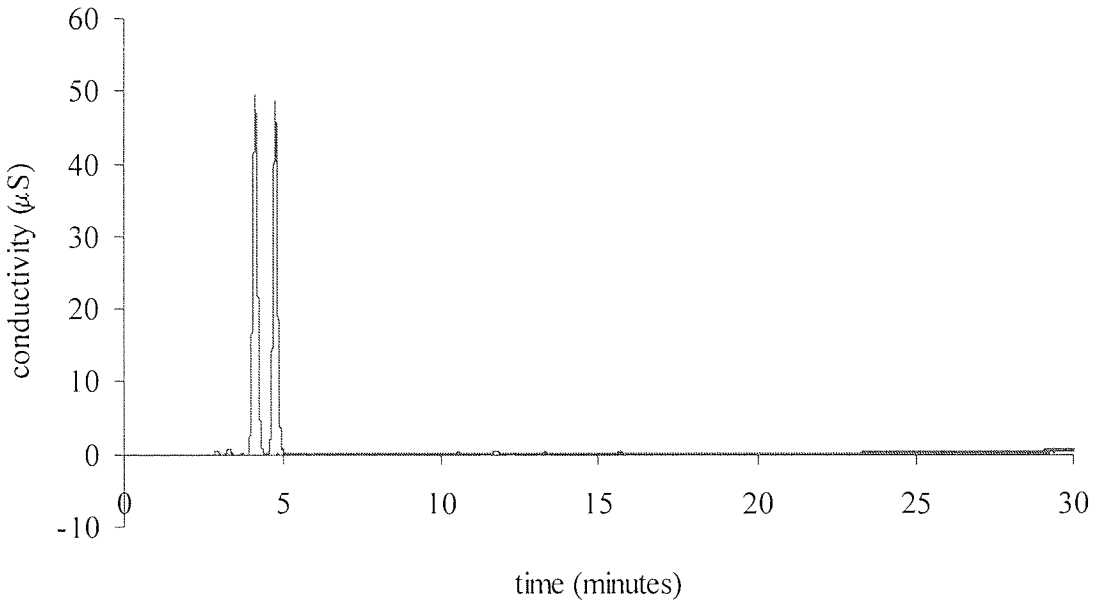

Figure 2.21 Atypical retention times of the same ion.

This has been attributed to the water quality. Given the sensitivity of this system it is necessary that the system is supplied with fresh 18.2 MΩ.cm (0.055 μS/cm) water. Additionally, the previous use of contaminated water may have caused poisoning of the anion column resulting in atypical retention times of the same species. Nonetheless it is anticipated that once water quality issues are resolved ion suppression chromatography has the potential for detecting and quantifying anionic monomers and actives.

2.3.3 MALDI-TOF MS

Mass spectrometry (MS) is the analysis of a polymer to obtain its average molecular weight, molecular weight distribution, mass of end groups and even sample purity. Matrix-assisted laser desorption ionisation-mass spectrometry (MALDI-MS) is a soft ionisation technique; that is it produces intact pseudomolecular ions of the molecule. This is done by dissolving the molecule in a suitable matrix compound followed by co-crystallisation of the mixture, which is then irradiated with a pulsed laser beam. After that the ions are introduced into a time-of-flight (TOF) mass analyser and separated according to their mass to charge (m/z) ratios; since the larger its mass the lower its velocity and the longer it takes the ion to reach the detector. The ions entering the mass

analyser are subjected to a fixed kinetic energy; thus their mass can be calculated from the following equation:

$$\text{k.e.} = \tfrac{1}{2} mv^2 = zU \qquad \text{Equation 2.18}$$

where:

k.e. = kinetic energy

m = mass

v = velocity

z = ion charge (valence)

U = acceleration potential

A schematic representation of the process is illustrated in figure 2.22.

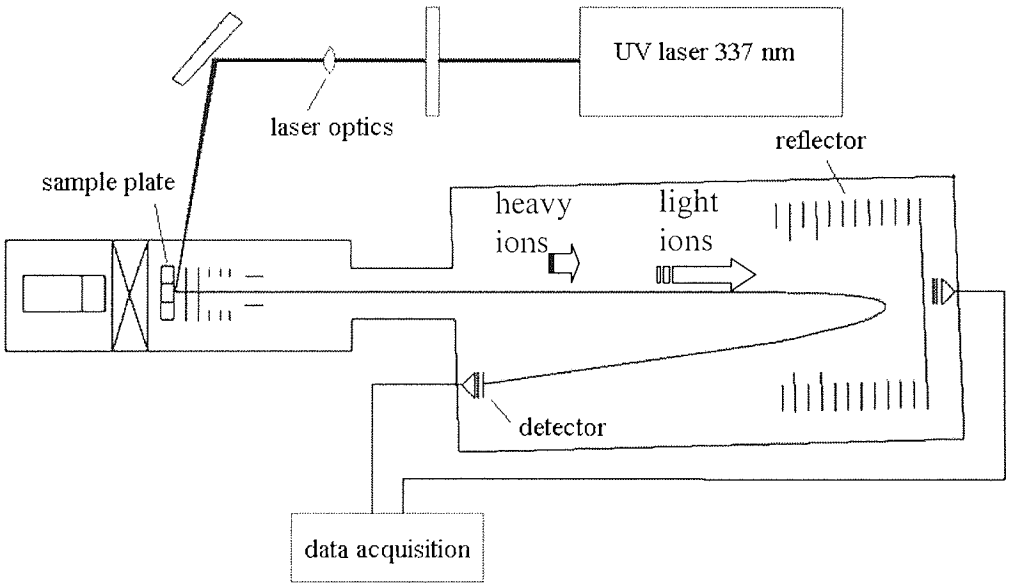

Figure 2.22 Schematic representation of a Maldi-TOF MS.

This technique requires only small samples and has short analysis times; hence its effectiveness in determining various molecular weights of polyvinyl alcohol (PVA) was investigated. This would enable the detection of PVA released from a contact lens (chapter 4) by molecular weight, as refractive index (RI) does not discriminate different molecular weights. Mass spectral data was collected from a Bruker OmniFLEX MALDI-TOF MS equipped with a UV nitrogen laser that emits 337 nm radiation in 3 ns

pulses at 175 μJ. The instrument was operated in positive mode at high voltage (9 kV). The number of laser shots was averaged at 200 used since PVA of higher molecular weights were investigated. Acquired spectra data was managed with OmniFLEX TOF control software.

2.3.3.1 Sample preparation

Samples analysed by MALDI are generally prepared by combining the polymer, matrix and cationising agent in a common solvent. Mixing the polymer with a matrix compound improves the efficiency of desorption into the gas phase of non-volatile polymers. This is because the matrix molecules absorb the laser energy and rapidly convert it to heat causing sublimation of the matrix molecules followed by expansion of the matrix molecules and co-crystallised polymer molecules into the gas phase. The primary means of forming gas-phase ions is by proton or metal ion attachment. This is achieved through cationising the polymer with metal ions. Sample preparation requires a uniform formation of a solid solution between the matrix and the polymer; hence the use of a solvent to prepare the polymer-matrix mixture is required for successful analysis. For water-soluble polymers a polar matrix of 2,5-dihydroxybenzoic acid (DHB) and an alkali-metal salt solution are generally used.[83]

2.3.3.2 PVA analysis

Initial MALDI-TOF MS analysis of PVA with a molecular weight of 61000 (61k) was carried out by preparing two samples:

i. 0.05 % of 61k PVA in HPLC grade water and
ii. 0.05 % of 61k PVA in PBS.

The ability to detect PVA in PBS solution was desired as this was the preferred *in vitro* release medium (chapter 4).

Highly hydrolysed PVA only dissolves in water above 70 °C thus both samples were prepared by heating in the respective solvent. After cooling one of the samples was spotted very thinly (0.5 to1 μl) along several rows and columns of a 10x10 MALDI

target and allowed to air-dry overnight. The target was then placed into the sample arm of the Scout100™ ion source, and a high vacuum applied. A strong electrical field was applied and a laser fired onto the sample to cause desorption. At the end of the test the target was sonicated in the presence of acetone and then rinsed in distilled water. The next sample was then placed as before.

For both samples PVA was not detected. Thus sample preparation was optimised by using conditions similar to those used for polyvinyl acetate[84] and those successfully used with other hydrocarbon based polymers.[83] In addition a lower molecular weight PVA (47000) was analysed. The recipe used for investigating MALDI analysis of PVA was:

solvent : 50 % water : 50 % methanol with 0.1 % trifluoroacetic acid (TFA)
matrix : 50 mg/ml DHB
polymer : 5 mg/ ml
salt : 5 mg/ml sodium chloride (NaCl)

Highly hydrolysed PVA only dissolves in water above 70 °C. Thus the polymer solution was prepared by heating 0.05 g PVA in 5 ml water until the PVA dissolved then 5ml of methanol with 0.1 % TFA was added to the PVA-water solution. The matrix, polymer and salt were mixed at a ratio of 10:10:1 and as before placed on a clean target.

The change in sample preparation still did not detect PVA. It has been suggested[85] that MALDI is limited to analysing polymers with a polydispersity index below 1.2. The polydispersity index of PVA with molecular weight ranging from 10700 and 88900 and with varying degrees of hydrolysis is between 1.7 and 2.1.[86] It has also been suggested that sensitivity for polymers with higher molecular weights can only be maintained by increasing the matrix to polymer ratio several hundreds fold.[87] Furthermore there may be a contribution from equipment limitations resulting from detector saturation, due to a continuous stream of particles impacting the detector.[88] Although MALDI-TOF MS analysis of high molecular weight polydisperse PVA was not successful further investigation may prove otherwise. Modification of sample preparation by increasing

the ratio of matrix to polymer should be investigated. Failure for this to succeed requires the need to experiment the use of other matrices such as dithranol.[85]

Chapter Three

Novel Skin Adhesives for Bioelectrode Applications

3. NOVEL SKIN ADHESIVES FOR BIOELECTRODE APPLICATIONS

This section is concerned with the use of adhesive electrodes (described in section 1.4.1.2) in electrical techniques such as iontophoresis and electroporation (section 1.5.7), which are emerging applications that can be used to, for example, prevent or relieve pain. This is achieved either by aiding the delivery of an anaesthetic or analgesic agent (iontophoresis) or by the application of a chosen current intensity, pulse rate and duration, at the site of pain (TENS, which is also an example of electroporation). The delivery of other types of drugs for other disorders by electrotherapy is currently under development.

One novel application for the use of conductive adhesive hydrogels in drug delivery is found in iontophoretic ocular drug delivery. For this application the drug is applied to the eye by an electrode carrying the same charge as the drug. The return (ground) electrode has the opposite charge and is placed elsewhere on the body to complete the circuit. In recent years there has been an increased interest in pain-free non-invasive methods, such as iontophoresis, for the delivery of drugs to specific ocular sites, because although relatively pain-free techniques such as topical administration via eye drops are valuable in treating diseases on the eye's exterior surface they do not assist drug penetration to the back of the eye, for example for treating retinal diseases. On the other hand invasive methods, such as intravitreal, periocular and intracameral injections as well as sustained-release implants, which can achieve therapeutic levels of drugs in ocular tissues, are innately risky due to the potential for the drug to reach toxic levels. In addition these may cause vitreous haemorrhage, endophthalmitis, infection, retinal detachment and other local injuries. Furthermore these techniques subject the patient to immense pain.

Since this application is relatively new and is as yet employed on a modest scale (the Optis System, section 1.5.7.3, is one example), the devices have used conventional sodium 2-(acrylamido)-2-methyl propane sulphonate (NaAMPS) medical electrodes to complete the circuit. The main drawback of these electrodes however is the prickling sensation and pain that occurs at the location of the return electrode at low current

levels. Although sensation is a requirement for some applications such as TENS it is not desired for ocular iontophoresis. Thus in order to minimise this effect and improve the usefulness of this potentially valuable technique the return electrode should provide a low impedance, preferably below 500 Ω at 2.5mA current and maximum of 9V DC,[71] and low current density path for the return current. If this is not satisfied the "excess" current travels through alternate routes of lower resistance ensuing equally high local current density that may cause, for example, erythema, damage to viable hair follicles or in extreme cases tissue heating and burns arising from resistive heating.

Conventional adhesive bioelectrode hydrogels contain, as mentioned above, NaAMPS. Although these hydrogels possess the required adhesiveness and a large amount of sodium ions (Na^+), the conductivity aspects are limited as the Na^+ is linked to a large acrylamido-2-methyl propane sulphonate anion, as illustrated in chapter 2. When polymerised the large sulphonate anion become fixed to the polymer backbone; hence a NaAMPS polymer is associated with a fixed charge density that is composition dependent. In order to extend the range of adhesive hydrogels for use as bioelectrodes in therapeutic applications the aim of the work carried out here was to design conductive skin adhesives containing neutral monomers in an attempt to "dilute" the fixed charge density. The potential to design an adhesive containing neutral monomers would produce a more versatile skin adhesive as the effect of adding different types and amounts of mobile charge carriers, for example alkali salts, on impedance could be investigated.

3.1 Physical requirements of a skin adhesive hydrogel

A skin adhesive should adhere to skin, by application of light pressure, for the duration of intended use, which can vary from a few minutes to several days. It should also be easy to apply and remove and ought to remain adhesive if removed for repositioning. Therefore a good adhesive has to have high adhesive force and high cohesive strength in order to minimise deformation on removal which involves the mechanical transfer of force to the substrate via the adhesive bond. The ability of the adhesive to flow easily and "wet" the surface of the adherend is vital for the formation of an adhesive bond. There are three physical properties, as mentioned in section 1.4.1, that determine the

performance of a pressure sensitive adhesive (PSA): tack, peel strength and viscoelasticity (rheology).

Tack is the ability of a PSA to form a bond of measurable strength to another material under low contact pressure and short contact time.[89] This renders PSA's easy and safe to handle as additional solvent or a heat source is not required for the adhesive to bond with skin. Tack measurements serve to establish how quickly and easily and adhesive can be applied.

Peel strength measurements serve to determine the relative ease of gel removal from skin (section 2.2.2), although in practice they are required to bond firmly with skin and remain firmly adhered in situ for the intended duration. On removal from skin it is desirable that the adhesive fails adhesively, that is at the skin-adhesive interface, rather than cohesively, that is to "leg". Since tack and peel strengths are comparable in a number of aspects[77] only peel tests were carried out on the adhesives produced during this investigation.

Viscoelastic measurements provide details on how a material is likely to flow under an imposed constant shear stress or rate (section 2.2.3). This property also gives an indication as to the cohesive strength of the gel. It is desired that there is a slow increase in elastic (G') and viscous (G") moduli with increasing frequency at lower shear rates followed by a rapid increase of G' and conversely a rapid reduction of G" with increasing frequency at high shear rates.

In addition a skin adhesive for use as a bioelectrode should be a good conductor of electricity and enable even distribution of current over its entire surface to prevent the formation of hot spots and therefore skin burns.

3.2 Key ingredients for adhesive hydrogels

The patent literature provides compositions used to produce adhesive hydrogels, but they rarely provide mechanistic interpretations of the role of each component. Previous work within this laboratory[16, 17] has identified that partially hydrated (skin adhesive) hydrogels consist of three main components: unsaturated water-soluble monomer, plasticiser and water. The following description provides a basis for understanding the separate contribution of each one.

i. hydrophilic monomer

A skin adhesive is required to have an exceptional ability to absorb water (as discussed in section 1.4.1.3); therefore at least a monomer with a hydrophilic functional group is essential to impart a high EWC on the hydrogel. Functional groups are important as they also influence properties, such as the cohesive strength of a hydrogel which is provided by its polymer backbone. In addition ionic monomers may enhance the conductivity of an adhesive hydrogel.

iii. water

When water is absorbed by a hydrogel the free volume of the polymer chains within the hydrogel is increased which aids the rotation of polymer backbone; hence water acts as a plasticiser, rendering the hydrogel more flexible. However the degree of covalent crosslinking within the hydrogel will influence the extent of this translational mobility.[90] The water within a hydrogel also provides a conductive and transport medium allowing diffusion of solutes across the hydrogel. It was mentioned previously (section 1.4.1.3) that adhesive hydrogels are only partially hydrated in order to retain their high ability for water uptake; thus enhance the adhesion of the hydrogel by rapidly absorbing the water at the skin-hydrogel interface.

iii. humectant

Humectants are hygroscopic compounds that promote the retention of moisture. They are traditionally incorporated into foods and cosmetics for that purpose and serve a similar function in adhesive hydrogels. The most widely used compound of this type is glycerol, which contains three hydrophilic hydroxyl groups enabling it to

interact strongly with the water within the hydrogel and in doing so reduce the effects of evaporation. Glycerol also acts as a plasticiser, although of the three components it is the least favoured for improving the cohesion of the hydrogel.[17] Plasticisers may also be used to adjust the tackiness and wetting behaviour of the hydrogel surface.[78]

In addition to the specific roles of these components it is important to understand the effect of variations in their constituent ratios. Although patents give a broad indication of composition requirements there is little information therein relating to the underlying structure-property relationship. That is the way in which the behavioural changes in the adhesive hydrogels are related to specific component ratios and quantities. A recent study[16] of the underlying principles involved in the design and synthesis of synthetic skin adhesive hydrogels identified three important behavioral requirements (see also section 1.4.1.3). These are that an adhesive hydrogel must:

i. have a residual hydrophilic "appetite" to enable rapid removal of interfacial moisture from skin on contact
ii. be able to undergo chain rotation to present both hydrophobic and polar chain segments allowing for "matching" with respective skin sites
iii. have rheological properties that allow it to conform to the skin's surface at low shear rate, specifically on application to prevent adventitious removal, but become stiffer as the shear stress is increased, particularly on removal to prevent extension ("legging") of the adhesive hydrogel.

3.2.1.1 Influence of composition on properties of a skin adhesive

Previous research within this laboratory[17] using simple conventional skin adhesive compositions, containing NaAMPS, water and glycerol whilst maintaining the crosslink density at 0.08 %, was used to effectively illustrate the effect of varying the ratios on a three-coordinate graph (figure 3.1).

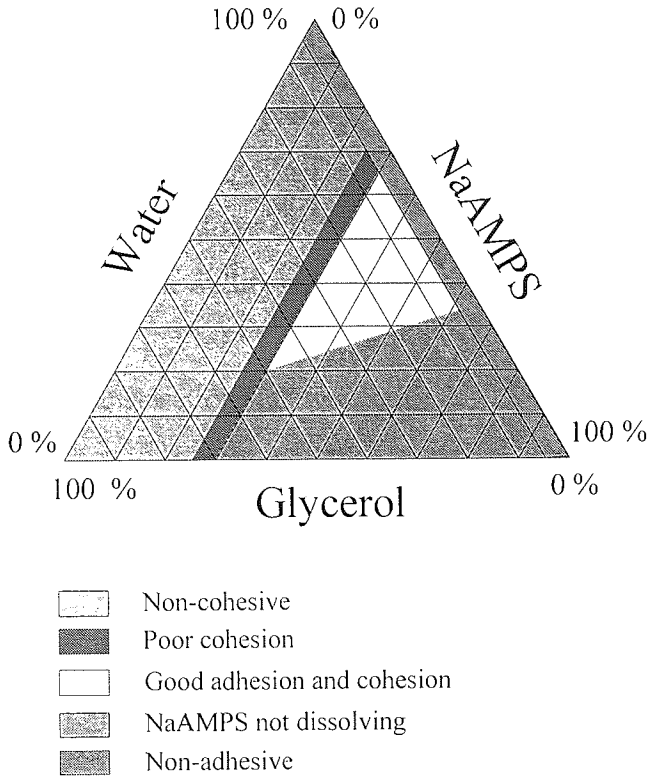

Figure 3.1 Triangular graph showing properties of a skin adhesive composed of various monomer, glycerol and water compositions (w/w).

This is useful as a guide to determine upper and lower limits of the three key components in order to develop new skin adhesive compositions with acceptable cohesive and adhesive characteristics. Hence a suitable combination would be one that falls within the white zone. The compositions discussed in this chapter contain approximately:

40 % monomer, 25 % glycerol and 35 % water

3.2.1.2 Strategy proposed to design conductive adhesive hydrogels

The aim of this research is to extend the range of skin adhesive hydrogels for use as bioelectrodes that are not wholly dependent on ionic monomers as this reduces the ability to vary the amount of cations and therefore conductivity of the skin adhesive. However, the adhesiveness similar to that of a NaAMPS skin adhesive is desired. Thus the effect of substituting anionic monomers by hydrophilic nitro-carbonyl containing monomers was investigated. Furthermore the total replacement of anionic monomers,

which carry a mobile counter cation (K^+ of Na^+), by neutral monomers was explored in order to study the effect of adding salts (KCl and NaCl) on impedance and to suggest an ideal composition for a conductive skin adhesive. In addition an important question to be answered was what would be the effect of replacing anionic monomers by neutral ones on the peel strength and rheology of the adhesive hydrogel. These properties are important because they define the ability of the hydrogel to function as a skin adhesive.

The optimisation of polymerisation has previously been explored[16] thus for the purposes of this research it is not intended to optimise the polymerisation method. Furthermore under manufacturing conditions this is a fast throughput process. Hence, most of the focus has been directed towards the shortcomings of the monomers, of which there are many variables, as success is not going to depend on one parameter, such as hydrophilicity, but at ease that it can be used to synthesise a standard hydrogel.

Ionic and neutral skin adhesive hydrogels were formulated using various combinations of conventional anionic monomers (see chapter 2 for monomer details) namely: NaAMPS, SPA and neutral monomers, namely: acrylic acid, AMO, $MPEG_{400}MA$, NNDMA, NVP and TRIS. The initiator and crosslinker were added as a mixture of Irgacure 184 and Ebecryl 11 at a corresponding ratio of 3:10 with 0.015 % of this mixture added to the system. This had been previously established[17] as the optimum amount of crosslinker-initiator required to produce an adequately cohesive skin adhesive hydrogel.

Prior to producing and testing skin adhesives, hydrogel membranes were produced by thermal polymerisation and then fully hydrated in order to determine the equilibrium water content (EWC) of the formulations proposed for skin adhesive hydrogels. This served to determine the relative ability of the proposed adhesive hydrogels to absorb interfacial moisture, which in turn promotes adhesion.

3.3 Equilibrium hydration of hydrogels

The equilibrium water content (EWC) of the formulations proposed for skin adhesive hydrogels was investigated by allowing hydrogels to fully hydrate, as this served to determine the relative hydrophilicity of the adhesive hydrogels even though they are only used partially hydrated for skin adhesive applications. A set of seven hydrogel membranes, FH1 to FH7 (FH for fully hydrated) were formulated as per table 3.1 and thermally polymerised in the presence of (w/w) 0.5 % AZBN initiator and 1 % DATr crosslinker (actual weight compositions are detailed in appendix 2).

Sample Reference	SPA	NaAMPS	TRIS	NVP	Acrylic Acid	NNDMA
	(w/w %)					
FH1	5	25	10	45	5	10
FH2	10	20	10	42.5	5	12.5
FH3	15	15	10	40	5	15
FH4	5	25	10	0	5	55
FH5	10	20	10	0	5	55
FH6	15	15	10	0	5	55
FH7	10	20	10	55	5	0

Table 3.1 Makeup monomers of thermally polymerised hydrogel membranes.

Monomer preparation and polymerisation were carried out as outlined in section 2.2.1.1. The hydrogel membranes were subsequently placed in distilled water and hydrated to equilibrium.

To determine the effect of changes in osmolality on swelling the EWC of hydrogels FH1 to FH7 in various salt concentrations were compared. Each fully hydrated hydrogel membrane was divided into three equal parts and placed into vessels with 0.9 %, 2 % and 5 % w/v (approximately 0.15, 0.34 and 0.86 M) saline solution, made with 99 % w/w sodium chloride (NaCl) crystals and distilled water, and left for a week.

3.3.1 Equilibrium water content

Two 2 cm diameter discs were cut from each of the seven hydrogel samples hydrated in the various saline solutions. Excess surface liquid on the discs was absorbed onto filter paper and each disc weighed to obtain the weight of the fully hydrated disc. The discs were then dehydrated in a vacuum oven at approximately 30 °C for three days after which they were reweighed in order to calculate the equilibrium water content, EWC, of each gel at each salt concentration using equation 1.1 (section 1.2.1).

Figures 3.2 to 3.5 present the data in ways that illustrate the effect of the compositional variations on EWC with 2 % error bars shown. A discussion of these results follows.

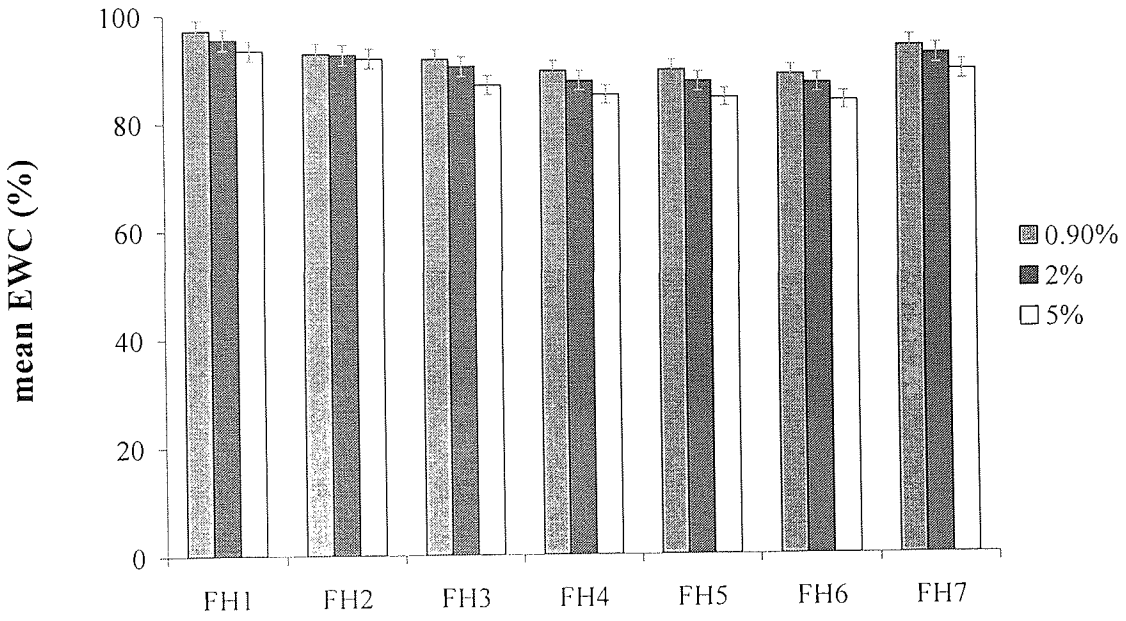

Figure 3.2 Mean EWC for all samples placed in 0.9 %, 2 % and 5 % saline solution.

Figure 3.2 shows that the EWC decreased as saline concentration increased for all compositions. Furthermore the EWC of all the seven hydrogels studied was above 80 %; thereby indicating that substituting anionic monomers by neutral hydrophilic monomers maintained the high residual capacity for moisture uptake.

The EWC of samples in which the amounts of NVP and NNDMA were varied, although their sum as well as those of the remaining monomers remained constant, as outlined in table 3.2, were compared as shown is figure 3.3.

Sample Reference	SPA	NaAMPS	TRIS	NVP	Acrylic Acid	NNDMA
	(w/w %)					
FH7	10	20	10	55	5	0
FH2	10	20	10	42.5	5	12.5
FH5	10	20	10	0	5	55

Table 3.2 Family of hydrogel compositions consisting of varying amounts of NVP and NNDMA.

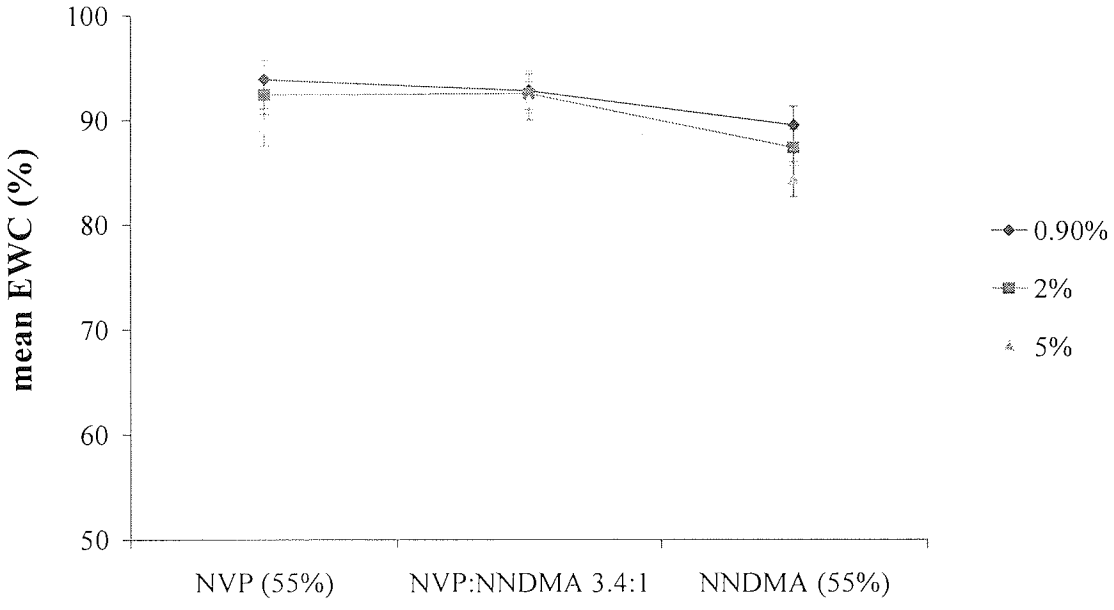

Figure 3.3 Effect of reducing NVP and increasing NNDMA on EWC.

Figure 3.3 illustrates that the EWC of compositions containing higher NVP content benefited from a greater EWC by approximately 4.5 % as compared to those with more NNDMA.

The EWC of samples in which the amounts NaAMPS and SPA were varied, although their sum as well as those of the remaining monomers remained constant, as outlined in table 3.3, were compared as shown is figure 3.4.

Sample Reference	SPA	NaAMPS	TRIS	NVP	Acrylic Acid	NNDMA
	(w/w %)					
FH4	5	25	10	0	5	55
FH5	10	20	10	0	5	55
FH6	15	15	10	0	5	55

Table 3.3 Family of hydrogel compositions consisting of varying NaAMPS and SPA amounts.

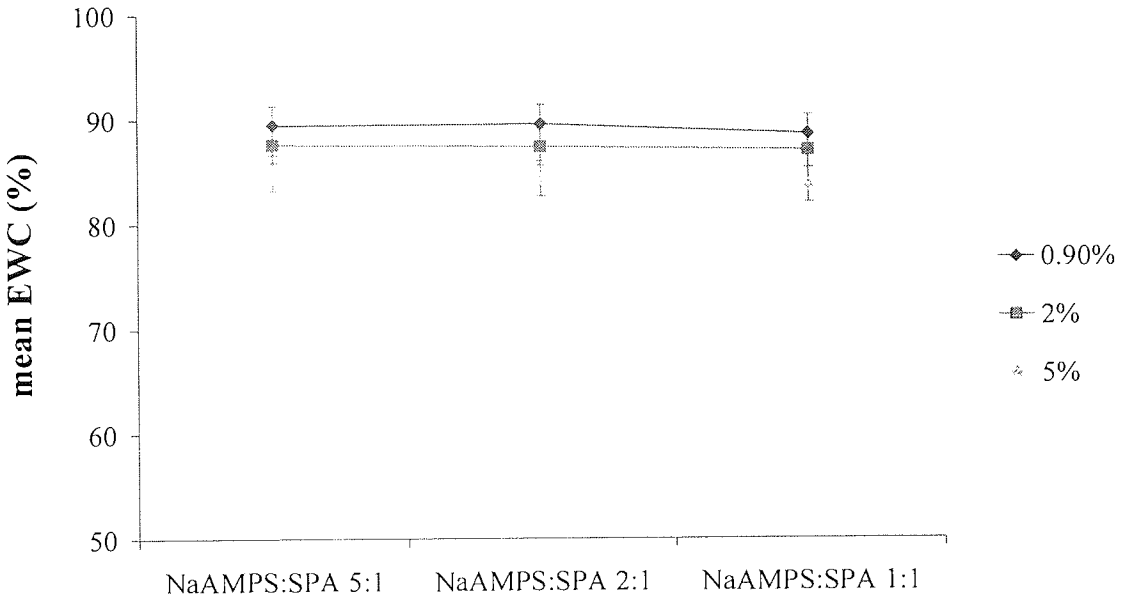

Figure 3.4 Effect of reducing NaAMPS whilst increasing SPA on EWC.

Figure 3.4 shows that the EWC of compositions containing varying amount NaAMPS and SPA, as portrayed in figure 3.4, had a similar EWC.

The EWC of samples in which the amounts NNDMA, SPA, NVP and NaAMPS were varied, although their sum as well as those of the remaining monomers remained constant, as outlined in table 3.4, were compared as shown is figure 3.5.

Sample Reference	SPA	NaAMPS	TRIS	NVP	Acrylic Acid	NNDMA
	(w/w %)					
FH1	5	25	10	45	5	10
FH2	10	20	10	42.5	5	12.5
FH3	15	15	10	40	5	15

Table 3.4 Family of hydrogel compositions consisting of varying NaAMPS and SPA amounts in tandem with varying NVP and NNDMA.

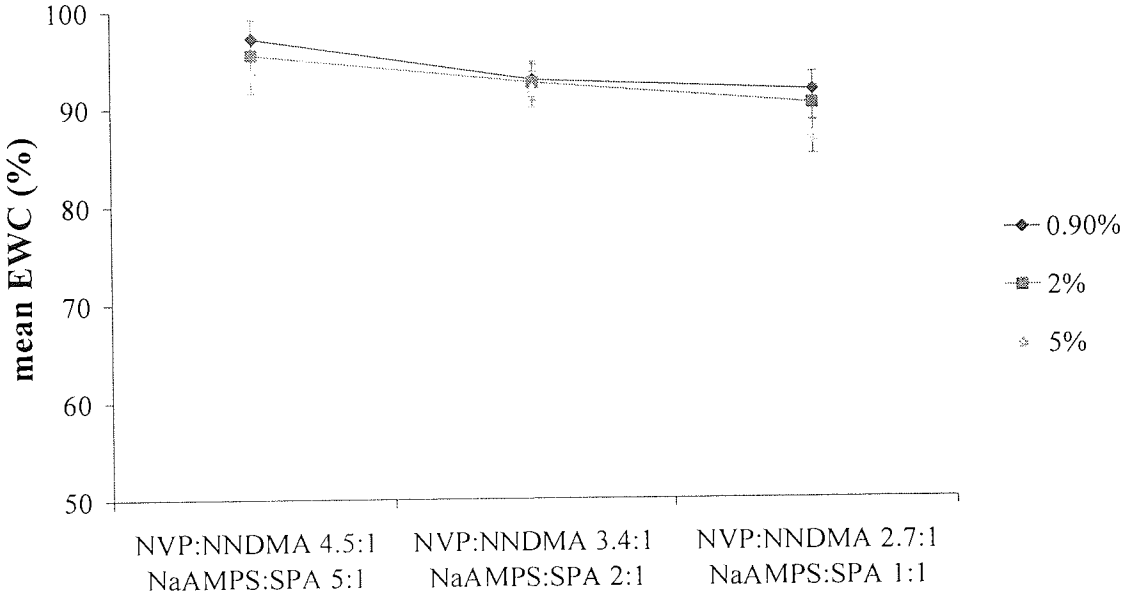

Figure 3.5 Effect of reducing both NVP and NaAMPS in tandem with increasing both NNDMA and SPA on EWC.

Figure 3.5 illustrates that the EWC of compositions containing increasing amounts of NNDMA and SPA, coupled with decreasing amounts of NVP and NaAMPS showed a reduction in EWC by approximately 5 %.

3.3.2 Effect of composition on EWC in physiological saline and more concentrated systems

All seven compositions exhibited EWCs above 80 % (figure 3.2). Thus partially hydrated skin adhesive hydrogels based on these formulations would have an immense appetite for water, which would in turn give them a strong residual capacity to absorb interfacial water and thereby promote adhesiveness.

Comparing the set of compositions with decreasing amounts of NVP, while increasing that of NNDMA indicated that EWC dropped by approximately 4.5 % (figure 3.3). Although at such high values of EWC this may be considered negligible it is suggested that NVP is slightly more hydrophilic as compared to NNDMA.

A similar evaluation carried out with formulations with decreasing amounts of NaAMPS and increasing SPA content showed that EWC is reduced by approximately 1 %, as illustrated in figure 3.4. Again this reduction can be considered negligible given an experimental error of about 2 %. However the slightly greater hydrophilicity of NaAMPS may result from it containing a hydrophilic nitrogen-carbonyl group (see section 2.1.1.1) or that the Na^+ causes a larger increase in the osmotic drive compared to K^+.

The effect of increasing both NNDMA and SPA while decreasing NVP and NaAMPS on EWC was also assessed. The result, as shown in figure 3.5, suggests that EWC drops by approximately 5 %. Thus the increase in SPA and NNDMA is not sufficient to compensate for the reduction in NVP and NaAMPS. According to the results shown in figures 3.3 and 3.4 it can be suggested that this reduction in EWC is mainly due to lowering NVP content while increasing that of NNDMA, as the hydrophilicities of SPA and NaAMPS are similar. The marked increase in hydrophilicity of hydrogels with the addition of NVP to hydrogels is in agreement with published results.[4]

Although for all seven compositions EWC decreased with increasing saline concentration (figure 3.2), the decrease was not as large as anticipated. This may be explained in terms of the evolution of the forces that contribute to swell as the osmolarity of the hydrating medium increases. This is neatly explained by examining

the swelling profile (figure 3.6) of 70 % NaAMPS copolymerised with 30 % diacetone acrylamide (DAA) in different NaCl concentrations. DAA is similar in all aspects to AMPS except that it does not contain the sulphonate group (section 2.1.1).

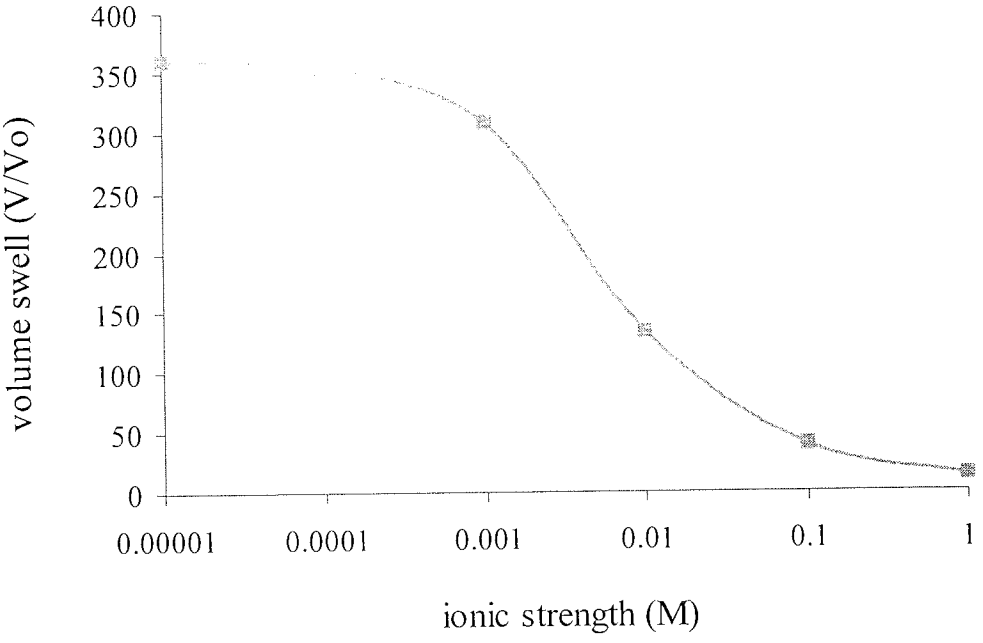

Figure 3.6 Swelling behaviour of NaAMPS copolymers as ionic strength of the swelling medium increases.

Figure 3.6 shows that the swelling curve is sigmoidal in shape with a rapid transition in the region of 0.01 M NaCl. The region beyond this is interesting as it illustrates the swelling behaviour when hydrogels come into contact with different biological environments. Thus an understanding of the effects that contribute to swell would also be important for other applications because the osmolarity of biological fluids ranges between 100 to 1000 mOsm[91] (approximately 0.1 to 1 M) in different environments. Between 0.1 and 1 M there is a reduction in volume swell, however this reduction is not as significant as that at lower concentrations. The potential contributory effects for this type of behaviour are described in figure 3.7.

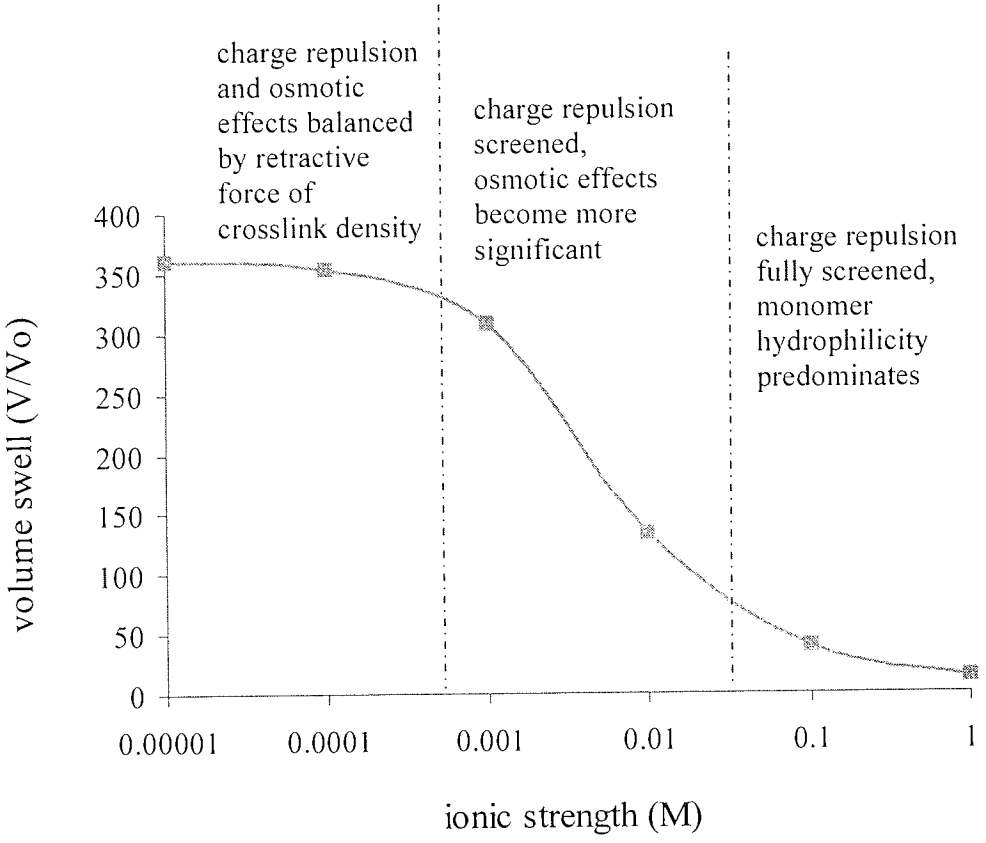

Figure 3.7 Factors that influence the swelling behaviour of hydrogels.

At low saline concentrations the repulsion between fixed polymer anion charges is great and as the polymer has a higher cation concentration than the swelling medium it has a tendency to absorb a lot of water. In this region the principle counterbalancing actions are the retractive forces of the crosslinks and the hydrophobic association of the hydrophobic monomers and groups.

When the salt concentration increases the fixed polyanion repulsion is reduced as it is screened by the cations and swell due osmotic effects becomes dominant in this region, but it is still counterbalanced by the retractive forces of the crosslinks.

At higher salt concentrations the shielding effect is even greater, but there is no osmotic drive as the salt concentration is greater than or equal to the charge density, thus swelling in this region is determined by the hydrophilicity rather than the ionicity of the monomers.

In view of the fact that "diluting" anionic monomers with neutral monomers produced hydrogels with a high tendency to absorb interfacial water the next aim at this stage was to determine whether formulations containing a combination of both types of monomers formed suitable adhesive hydrogels. Thus skin adhesive hydrogels were produced by photo-polymerisation and functional changes in peel strength and rheology were observed.

3.4 Skin adhesive hydrogels containing ionic and neutral monomers

Given that the formulations detailed above demonstrated a high level of hydrophilicity when allowed to fully hydrate, hydrogels IN1 to IN18 were formulated (as summarised in appendix 3) containing anionic (NaAMPS and SPA) and neutral (NVP, NNDMA, acrylic acid) hydrophilic monomers.

The monomers were photo-polymerised, as described in section 2.2.1.2, in the presence of distilled water, glycerol and 0.15 % initiator (Irgacure 184) and crosslinker (Ebecryl 11) in a 3:10 respectively mixture, to produce skin adhesive hydrogels.

The effect of "substituting" anionic monomers by neutral monomers on the ability of the hydrogels to function as conventional skin adhesives was evaluated by measuring the force required to peel the adhesive from skin and by characterising their dynamic mechanical behaviour (rheology). The impedance characteristics of these skin adhesives were then assessed for use as bioelectrodes.

3.4.1 Peel strength

To determine the effect of varying the backbone of the skin adhesives on peel strength (adhesive failure), skin adhesives IN1 to IN18 were peeled from the skin at 90° at a speed of 500 mm/min using a 100 N load cell, as discussed in section 2.2.2. Mean maximum, mean average and mean minimum N/25mm values from at least three peel strengths per hydrogel were taken (see appendix 3). Figures 3.8 to 3.13 present the data in ways that illustrate the effect of the compositional variations on peel strength with 10 % error bars shown. A discussion of these results follows.

The peel strength of adhesive hydrogels in which the amounts of NVP and NNDMA were varied, yet the summation of the two and of the other monomers remained constant as outlined in tables 3.5 and 3.6, were compared as shown in figures 3.8 and 3.9 respectively.

Sample Reference	SPA	NaAMPS	NVP	NNDMA	Acrylic Acid	Glycerol	Water
	w/w %						
IN7	5	14.5	15	5	5	25	30.5
IN1	5	14.5	10	10	5	25	30.5
IN4	5	14.5	5	15	5	25	30.5

Table 3.5 Family of hydrogel compositions consisting of varying NVP and NNDMA amounts.

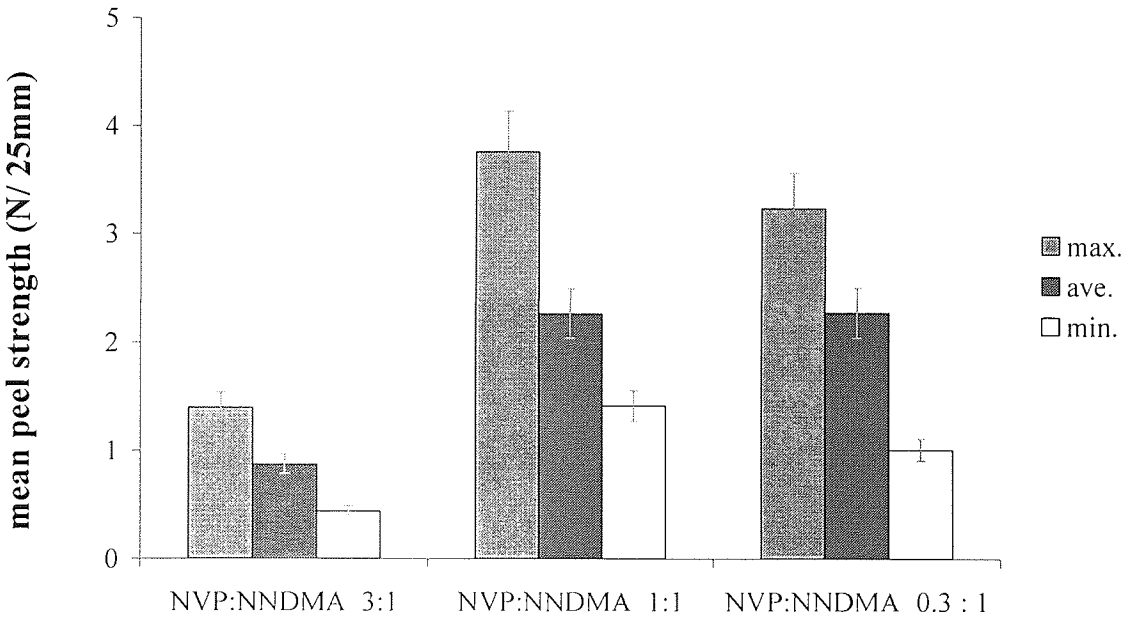

Figure 3.8 Effect of increasing NNDMA while reducing NVP on peel strength.

Sample Reference	SPA	NaAMPS	NVP	NNDMA	Acrylic Acid	Glycerol	Water
	w/w %						
IN8	10	11.6	15	5	5	25	28.4
IN2	10	11.6	10	10	5	25	28.4
IN5	10	11.6	5	15	5	25	28.4

Table 3.6 A second set of hydrogel compositions consisting of varying NVP and NNDMA amounts.

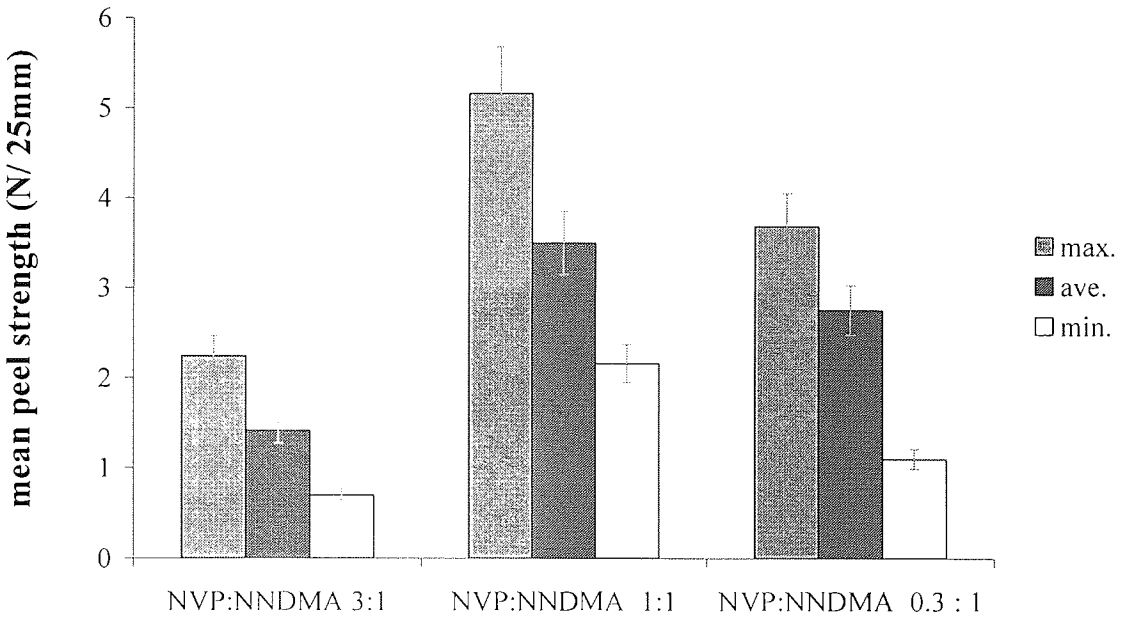

Figure 3.9 A second set of compositions demonstrating the effect of increasing NNDMA while reducing NVP on peel strength.

Figures 3.8 and 3.9 show that the peel strengths of skin adhesives with increasing amount of NNDMA, in tandem with decreasing amount of NVP peaked when the ratio of NVP to NNDMA was 1:1.

The peel strength of adhesive hydrogels in which the amounts of SPA, NaAMPS and water were varied, yet the summation of the three and those of the other monomers remained constant as outlined in tables 3.7 and 3.8, were compared as shown in figures 3.10 and 3.11 respectively.

Sample Reference	SPA	NaAMPS	NVP	NNDMA	Acrylic Acid	Glycerol	Water
	w/w %						
IN1	5	14.5	10	10	5	25	30.5
IN2	10	11.6	10	10	5	25	28.4
IN3	15	8.7	10	10	5	25	26.3

Table 3.7 Family of hydrogel compositions consisting of varying SPA, NaAMPS and water amounts.

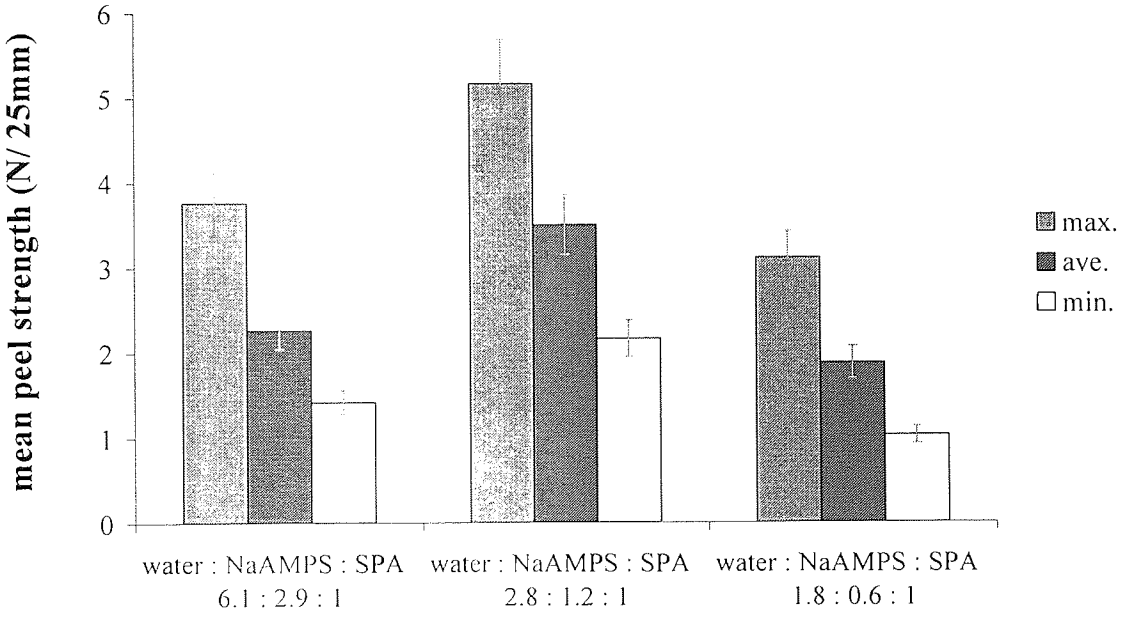

Figure 3.10 Effect of increasing SPA while reducing NaAMPS and water on peel strength.

Sample Reference	SPA	NaAMPS	NVP	NNDMA	Acrylic Acid	Glycerol	Water
	w/w %						
IN7	5	14.5	15	5	5	25	30.5
IN8	10	11.6	15	5	5	25	28.4
IN9	15	8.7	15	5	5	25	26.3

Table 3.8 A second set of hydrogel compositions consisting of varying SPA, NaAMPS and water amounts.

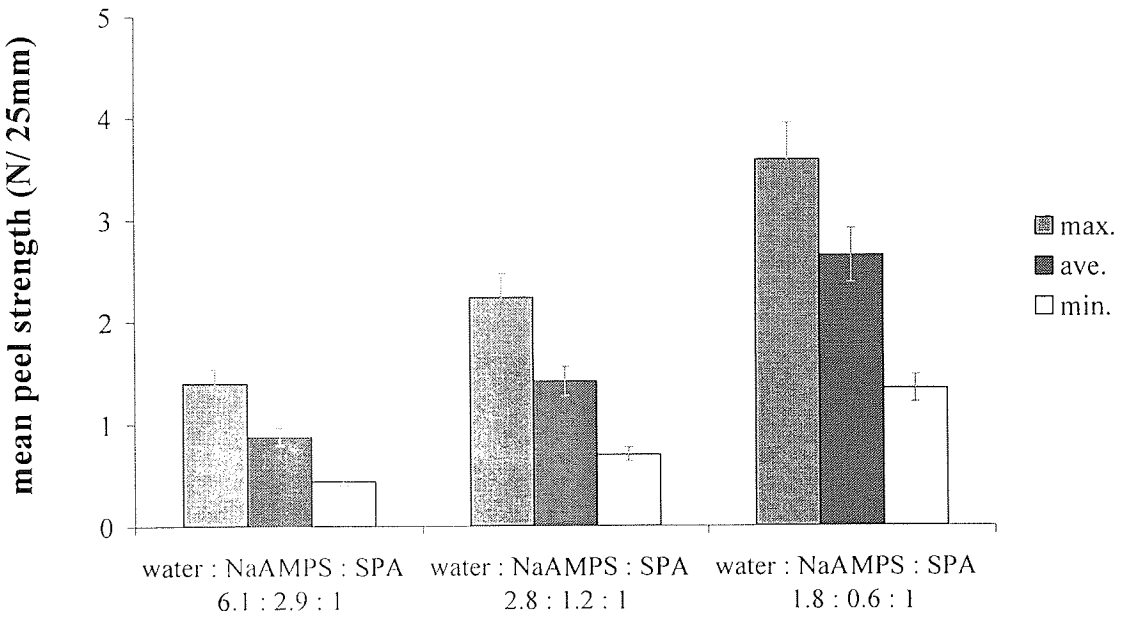

Figure 3.11 A second set of compositions demonstrating the effect of increasing SPA while reducing NaAMPS and water on peel strength.

Figure 3.10 demonstrates that the peel strengths of skin adhesives with increasing amount of SPA, in tandem with decreasing amount of NaAMPS and water peaked when the NaAMPS to SPA ratio was close to 1:1. However the same trend does not occur in figure 3.11 where the peel strength increased with increasing amounts of SPA while decreasing amount of NaAMPS and water. It should be noted that although the actual SPA, NaAMPS and water amounts are the same in both figures 3.10 and 3.11, those of the other monomers differ.

The peel strength of adhesive hydrogels with increasing amounts of NVP and SPA while decreasing amounts of water and NNDMA (maintaining the sums of NVP with NNDMA and SPA with water) as detailed in table 3.9 were evaluated as outlined in figure 3.12.

Sample Reference	SPA	NaAMPS	NVP	NNDMA	Acrylic Acid	Glycerol	Water
	w/w %						
IN11	12.5	8.7	2.5	7.5	5	25	38.8
IN14	15	8.7	5	5	5	25	36.3
IN17	17.5	8.7	7.5	2.5	5	25	33.8

Table 3.9 Family of hydrogel compositions consisting of varying NVP, SPA, NNDMA and water amounts with 8.7 % NaAMPS.

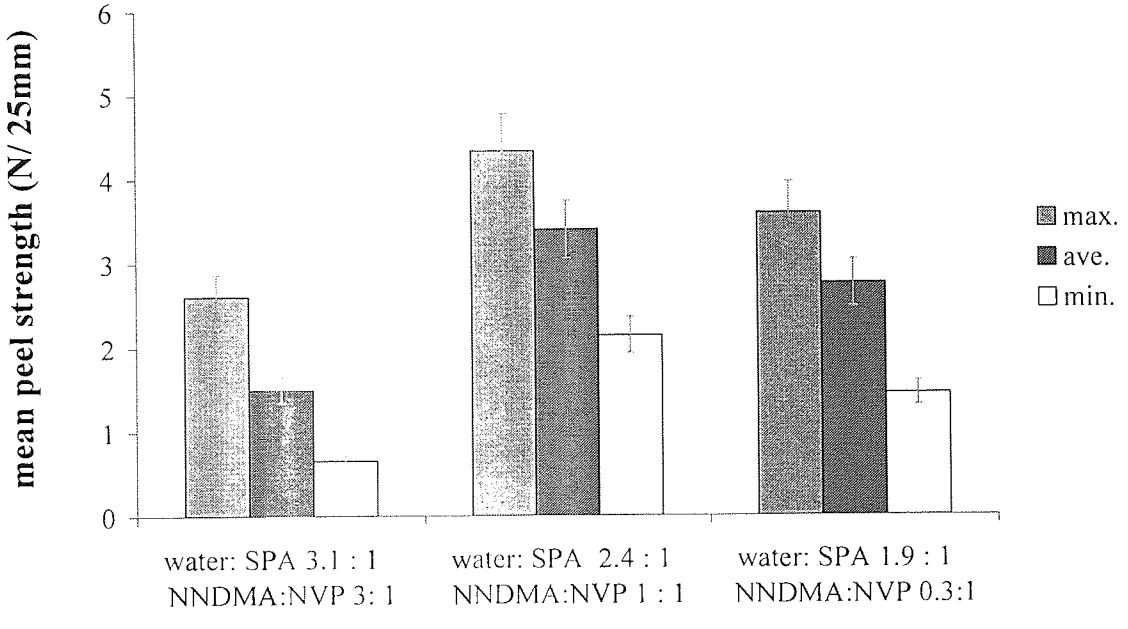

Figure 3.12 Effect of increasing NVP and SPA while reducing water and NNDMA on peel strength.

Figure 3.12 illustrates that the peel strengths of skin adhesives with increasing amounts of NVP and SPA while decreasing amounts of water and NNDMA peaked when the

ratio of NNDMA to NVP was 1:1. The same trend also occurred with (w/w) 5.8 % (IN12, IN15 and IN18) and 11.6 % (IN10, IN13 and IN16, table 3.11) NaAMPS.

The peel strength of adhesive hydrogels with increasing amount of water content coupled with decreasing amount of NaAMPS (yet maintaining their total) as in table 3.10 were contrasted (figure 3.13).

Sample Reference	SPA	NaAMPS	NVP	NNDMA	Acrylic Acid	Glycerol	Water
	w/w %						
IN13	15	11.6	5	5	5	25	33.4
IN14	15	8.7	5	5	5	25	36.3
IN15	15	5.8	5	5	5	25	39.2

Table 3.10 Family of hydrogel compositions consisting of varying NaAMPS and water amounts.

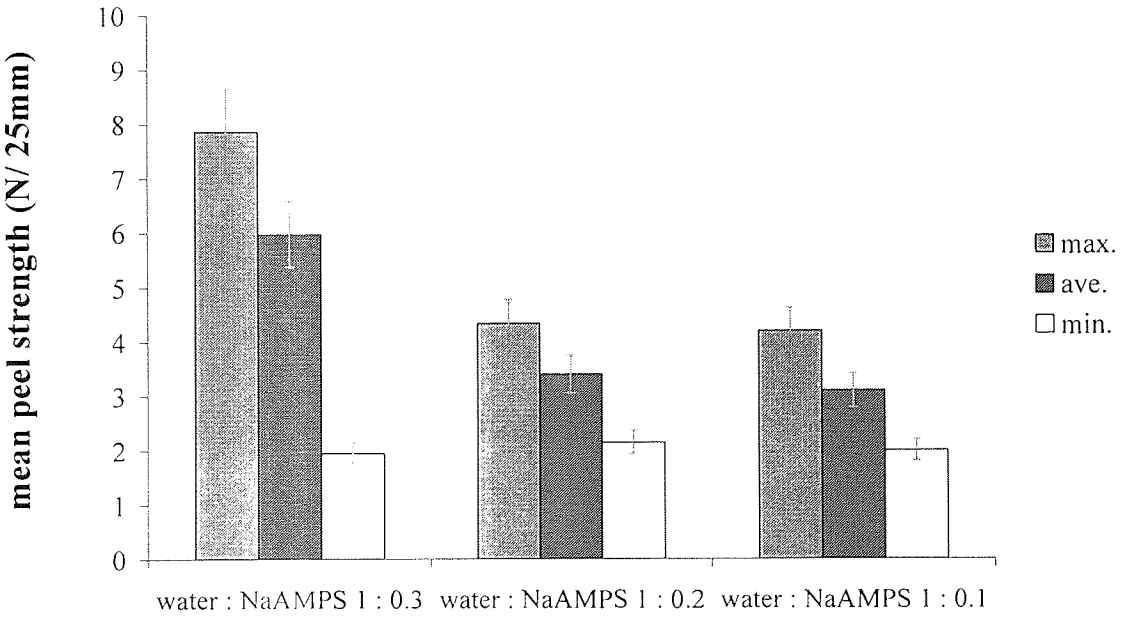

Figure 3.13 Effect of increasing water while reducing NaAMPS on peel strength.

Figure 3.13 shows that the peel strength of adhesive hydrogels with increasing amount of water content coupled with decreasing amount of NaAMPS decreased and then appeared to level off. A similar tendency was also noted with (w/w) 12.5 % SPA, 7.5 % NNDMA, 2.5 % NVP (IN10, IN11, IN12) and with 17.5 % SPA, 7.5 % NVP (IN16, IN17, IN18).

3.4.1.1 Effect of skin adhesive composition on peel strength

The mean maximum peel strengths for all samples were below 8 N/25mm. Pain, normally felt at values above 10 N/25mm,[16] was not felt on removal of the adhesive hydrogels. The target peel strength value is 3 N/25mm.[16] Generally the trend followed by the mean maximum, average and minimum peel strengths were the same and standard deviations were below one.

Figures 3.8 and 3.9 demonstrate that mean peel strength of adhesive hydrogels with increasing amount of NNDMA coupled with decreasing amount of NVP peaked when the NVP to NNDMA ratio was 1:1. Since the same trend occurred with two sets of formulations containing different amounts of the remaining components, it is suggested that when the ratio of NVP to NNDMA is approximately one, mean peel strength is at its maximum. At any other ratio mean peel strength is lower and possibly affected by other components. The influence of the other components is clearly illustrated by comparing both figures. In figure 3.8 the mean maximum peel strengths were between approximately 1.5 N/25mm and 3.5 N/25mm (0.06 and 0.14 N/mm) and for those in figure 3.9 they were somewhat higher, around 2 N/25mm and 5 N/25mm (0.08 N/mm and 0.2 N/mm), implying that presence of other components influences peel strength.

Figure 3.10 shows that mean peel strength of adhesive hydrogels with increasing amount of SPA and decreasing amount of NaAMPS and water in the presence of (w/w) 10 % NVP, 10 % NNDMA peaked when the NaAMPS to SPA ratio was approximately 1:1. However figure 3.11 illustrates that with (w/w) 15 % NVP, 5 % NNDMA mean peel strength increased with increasing amount of SPA and decreasing amount of NaAMPS and water. Although none of these gels were "leggy" (see appendix 3) the difference in these results may be caused by several factors. Firstly, there are errors associated with the technique, such as the substrates arm not moving at the same speed as the tensometer; thus the peel angle is not consistently at ninety degrees. Secondly, the bond formed with skin is likely to vary as the number of peels increase due to the "stripping effect",[78] whereby the outermost layers of the *stratum corneum* are peeled off on removal of the adhesive. Thirdly, the amount of the remaining components varied.

Comparing the differences in mean maximum peel strengths showed that they varied between about 3N/25 and 5 N/25mm (0.12 N/mm and 0.2 N/mm) for figure 3.10, whereas in figure 3.11 they varied between 1.5 N/25mm and 3.5N/25mm (0.06 N/mm and 0.14 N/mm). The apparently higher mean peel strengths for the set in figure 3.10 may be because this set of compositions also contained NVP and NNDMA at a ratio of 1:1. Thus it can be inferred from figure 3.10 that mean peal strength is greater when both the ratios of NaAMPS to SPA and NVP to NNDMA are approximately 1:1. This in turn provides a potential explanation for the fact that compositions in figure 3.9 have marginally higher mean peel strengths than those of figure 3.8. At this ratio it is possible that induced dipolar attractions, which have an effect of a secondary crosslink thereby strengthening the network, between polar groups of NVP and NNDMA molecules (figure 3.14) or NaAMPS and SPA molecules (figure 3.15) on opposing polymer chains are at a maximum. The higher mean peel strengths may be due to the hydrogels having improved cohesiveness allowing them to comply better with skin surface.

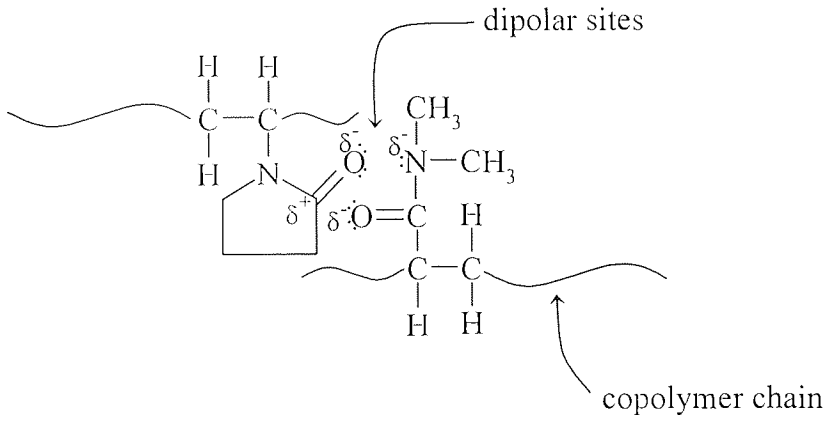

Figure 3.14 Proposed sites for dipolar interactions between NNDMA and NVP molecules on adjacent molecular chains.

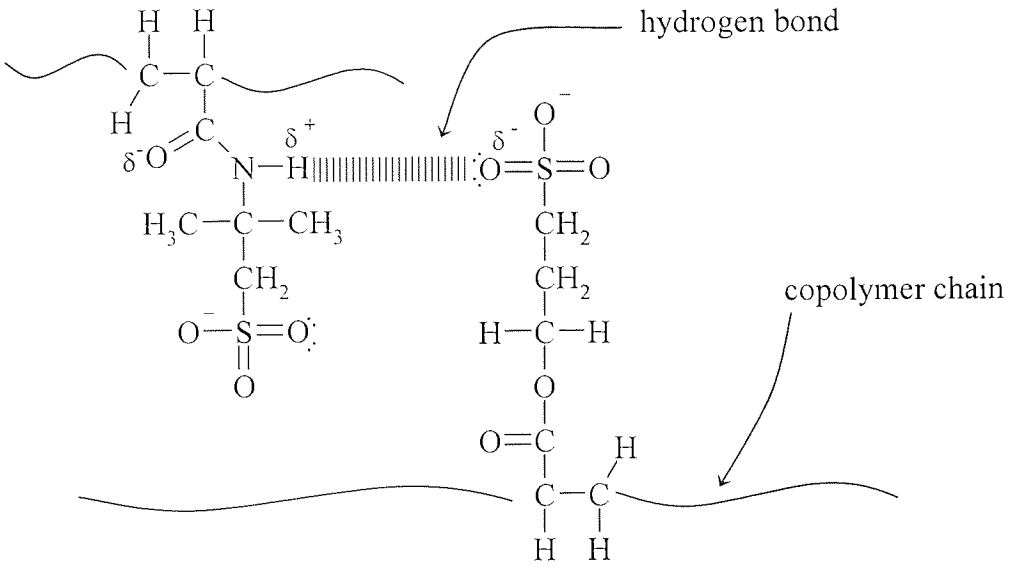

Figure 3.15 Proposed hydrogen bonding between NaAMPS and SPA molecules on opposing molecular chains. [92]

Mean peel strengths of adhesive hydrogels with increasing amounts of NVP and SPA, while decreasing amounts of water and NNDMA, peaked when the ratio of NVP to NNDMA was 1:1, as shown in figure 3.12. The same tendency was seen at different compositions. However, during polymerisation it was observed that hydrogels with higher amounts of both water (>35 %) and NNDMA (>5 %) were slightly "leggy" (section 1.4.1.3).

Increasing amount water coupled with decreasing that of NaAMPS lowered mean peel strengths as shown in figure 3.13. This trend was consistent with different compositions. Thus water content directly affects peel strength. This may due to the increase in water content causing a reduction in residual hydrophilicity by some degree, thereby reducing the adhesiveness of the hydrogel to skin making it easier to remove. This agrees with previously published results.[17] Although the amount of water seems to have a well-defined effect on peel strength it is proposed that the combination of all components within the adhesive hydrogel will have a dominating effect on peel strength.

3.4.2 Rheology

To determine the effect on viscoelasticity as the polymer backbone is varied, the elastic (G') and viscous (G") moduli of ionic skin adhesive hydrogels IN1 to IN18 were measured as a function of frequency. For each test the frequency to complete a sine wave was set to increase from 0.5 Hz to 25 Hz. The lower frequencies were intended to mimic the properties of the gel when it is applied to the skin and higher frequencies when the gel is removed from the skin. Tests were carried out as discussed in section 2.2.3. Mean values of at least three G' and G" are detailed in appendix 3. A summary of tan delta (tan δ), the ratio of G" to G' (see section 2.2.3 for theory), obtained for the various compositions is presented in figures 3.16 to 3.21. A discussion of these results follows.

Tan δ for adhesive hydrogels with increasing amount of NNDMA and decreasing amount of NVP, whilst maintaining their sum, in the presence of (w/w) 10 % SPA and 11.6 % NaAMPS as detailed in table 3.6, was evaluated as shown in figure 3.16.

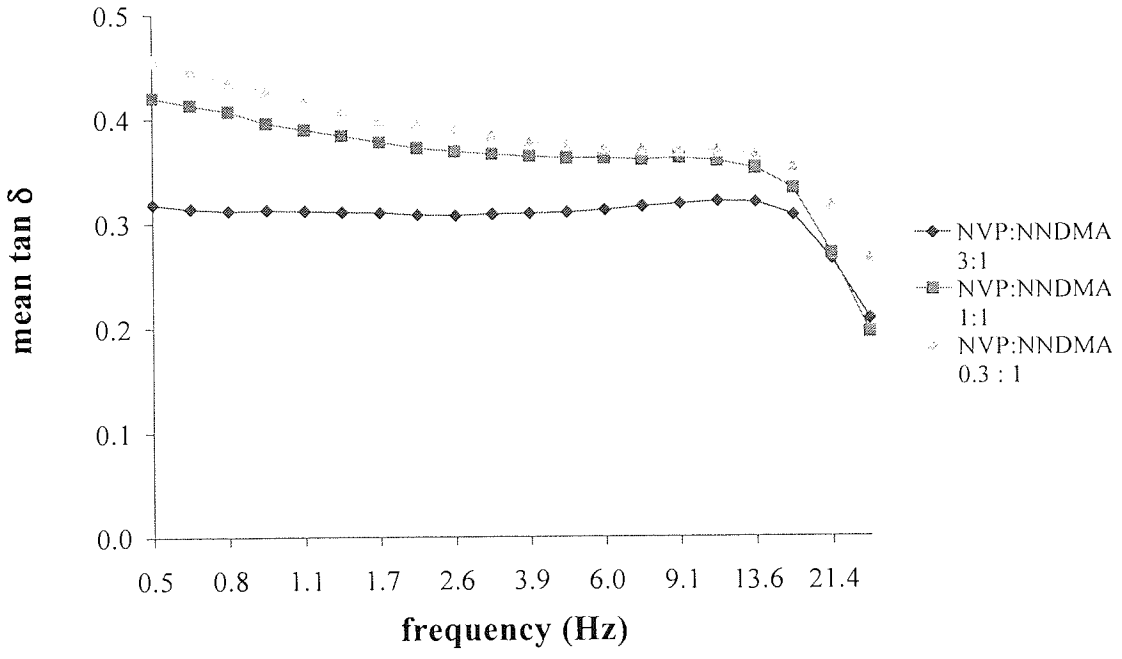

Figure 3.16 Effect of increasing NNDMA while reducing NVP on tan δ.

Figure 3.16 demonstrates that tan δ was higher for the hydrogel containing more NNDMA, particularly at the lower frequencies. At the highest frequency tan δ was lower for the hydrogel containing equal amounts of NVP and NNDMA. The same tendency was noted with formulations containing (w/w) 5 % SPA and 14.5 % NaAMPS as detailed in table 3.5.

Tan δ values for adhesive hydrogels with increasing amount of SPA whilst decreasing amount of NaAMPS and water, although the sum of three remained the same, in the presence of (w/w) 10 % NVP and 10 % NNDMA (table 3.7) were compared as illustrated in figure 3.17.

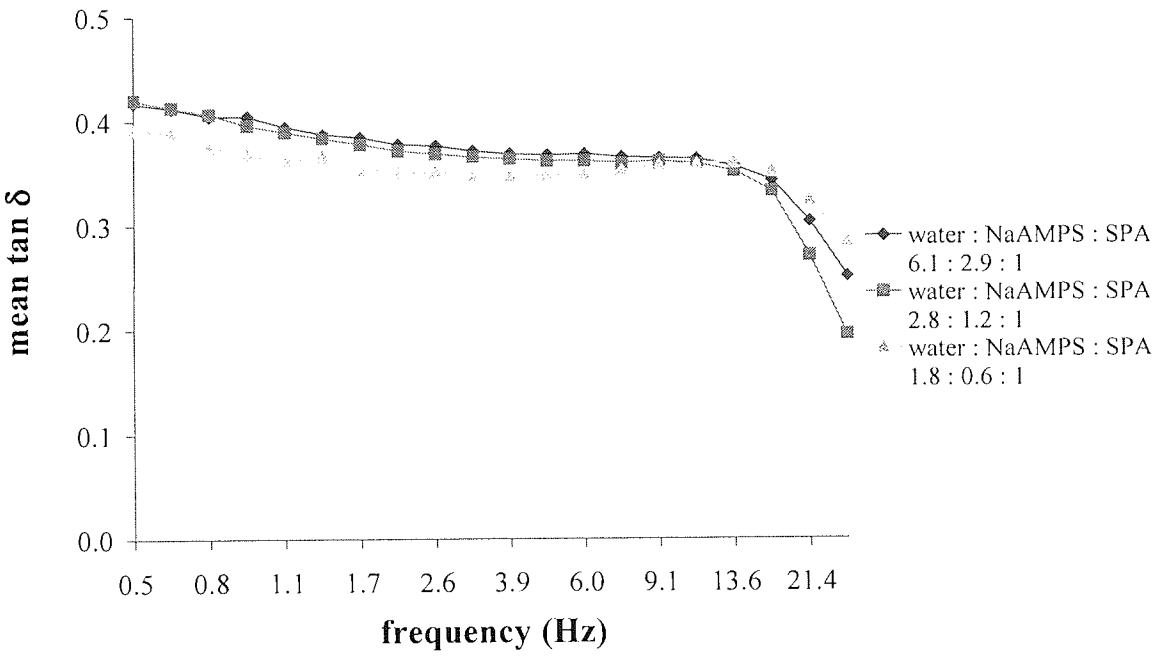

Figure 3.17 Effect of increasing SPA while reducing NaAMPS and water on tan δ.

At low to medium frequencies tan δ for adhesive hydrogels was somewhat lower for the hydrogel containing least NaAMPS (figure 3.17), however, at higher frequencies the hydrogel containing equal parts of NaAMPS and SPA had the lowest tan δ. The same trend occurred in the presence of 15 % NVP and 5 % NNDMA as per table 3.8.

The effect on tan δ as a result of increasing amounts of SPA and NVP whilst decreasing those of water and NNDMA (sum of NVP and NNDMA, SPA and water remained constant) as detailed in table 3.11 was investigated as shown in figure 3.18.

Sample Reference	SPA	NaAMPS	NVP	NNDMA	Acrylic Acid	Glycerol	Water
	w/w %						
IN10	12.5	11.6	2.5	7.5	5	25	35.9
IN13	15	11.6	5	5	5	25	33.4
IN16	17.5	11.6	7.5	2.5	5	25	30.9

Table 3.11 Family of hydrogel compositions consisting of varying SPA, NVP, NNDMA and water amounts with 11.6 % NaAMPS.

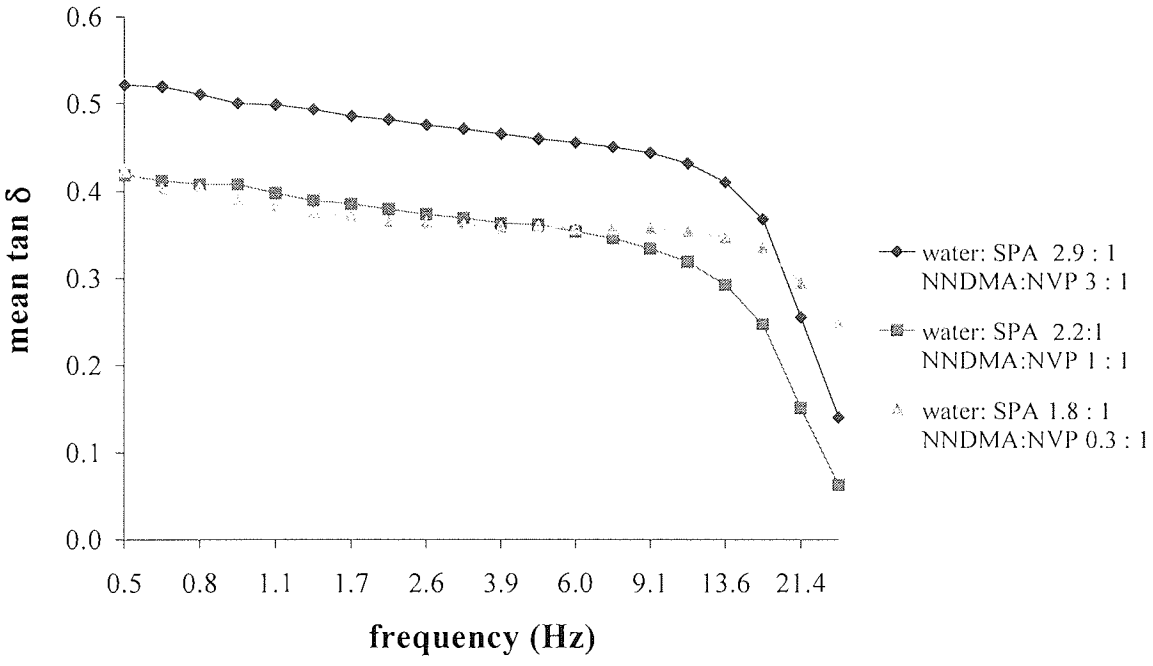

Figure 3.18 Effect of increasing NVP and SPA while reducing water and NNDMA on tan δ.

Figure 3.18 illustrates that at lower frequencies tan δ decreased with increasing amounts of SPA and NVP whilst decreasing amounts of water and NNDMA. However at higher

frequencies the hydrogel with a 1:1 ratio of NVP to NNDMA had the lowest tan δ. The same tendency was seen with (w/w) 8.7 % NaAMPS (table 3.9) and 5.8 % NaAMPS (IN12, IN15 and IN16).

Tan δ for adhesive hydrogel compositions with increasing water content whilst decreasing amount of NaAMPS, maintaining their total constant, as detailed in table 3.10 were compared in figure 3.19.

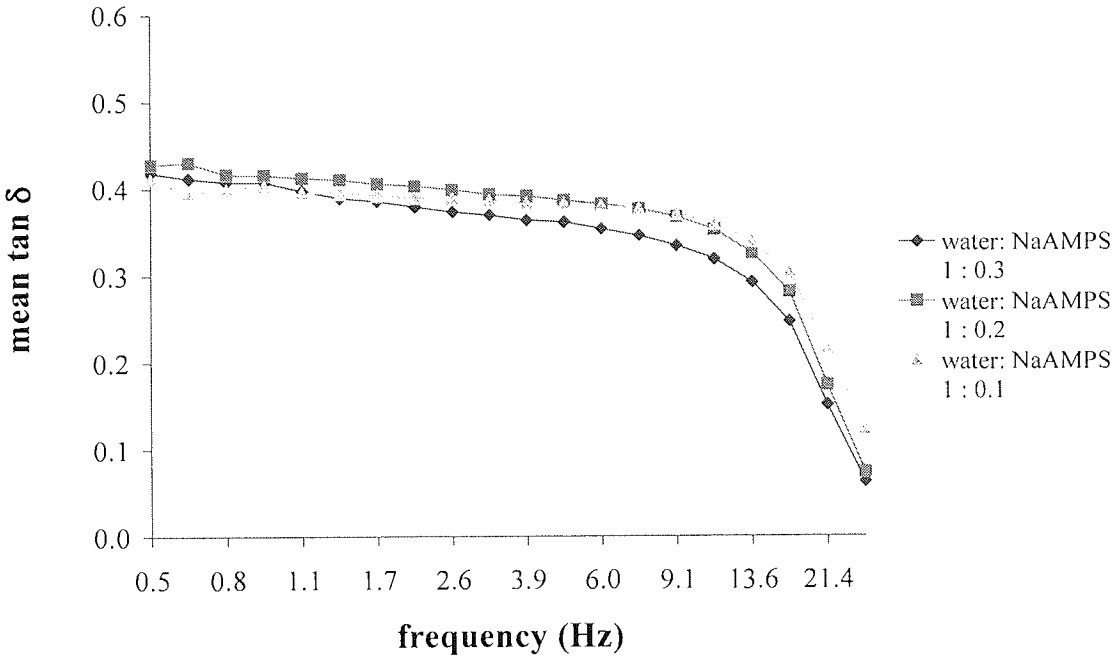

Figure 3.19 Effect of Increasing water while reducing NaAMPS on tan δ.

Figure 3.19 illustrates that tan δ increased slightly as frequency increased with increasing water content whilst decreasing that of NaAMPS.

The effect on tan δ on increasing water, NaAMPS and NNDMA content while decreasing those of SPA and NVP (total of water, NaAMPS and SPA, NVP and NNDMA remained constant as shown in table 3.12) was assessed as exemplified in figure 3.20.

Sample Reference	SPA	NaAMPS	NVP	NNDMA	Acrylic Acid	Glycerol	Water
	w/w %						
IN17	17.5	8.7	7.5	2.5	5	25	33.8
IN10	12.5	11.6	2.5	7.5	5	25	35.9

Table 3.12 Family of hydrogel compositions consisting with varying NaAMPS, NNDMA NVP, SPA, and water amounts.

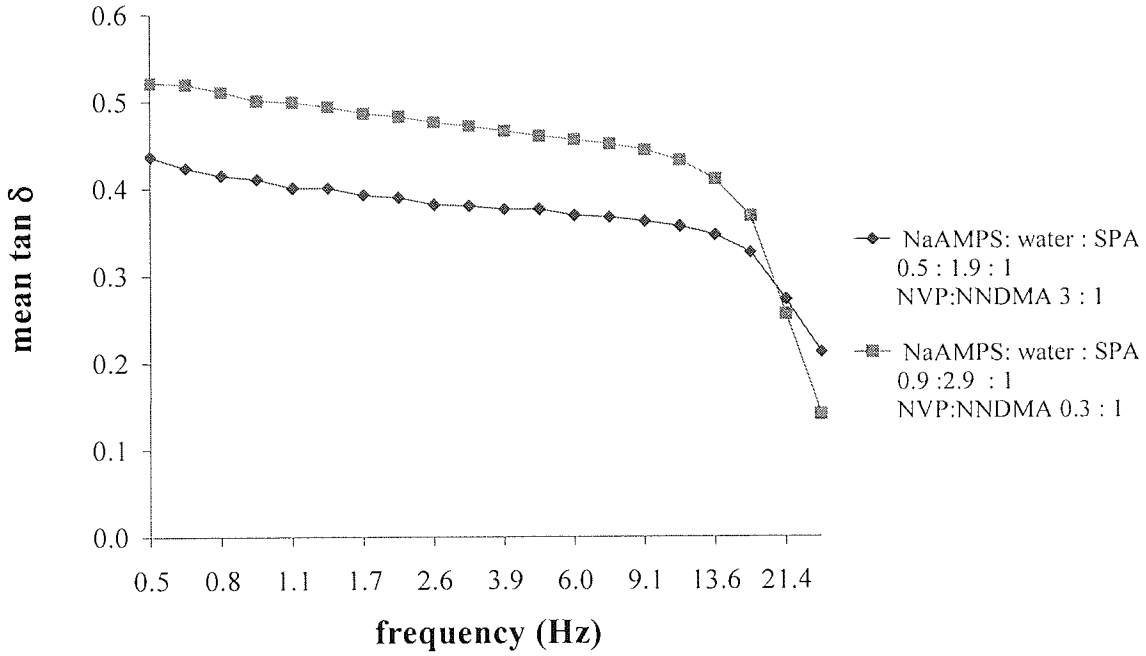

Figure 3.20 Effect of increasing water, NaAMPS and NNDMA while reducing SPA and NVP on tan δ.

Figure 3.20 illustrates that at lower frequencies a higher value of tan δ was noted with the skin adhesive containing a similar NaAMPS to SPA ratio. However, at higher frequencies the inverse was true.

The existence of a possible relationship between tan δ and mean average peel strength values was investigated. The values of mean tan δ at 5 Hz and mean average peel strength were plotted as displayed in figure 3.21.

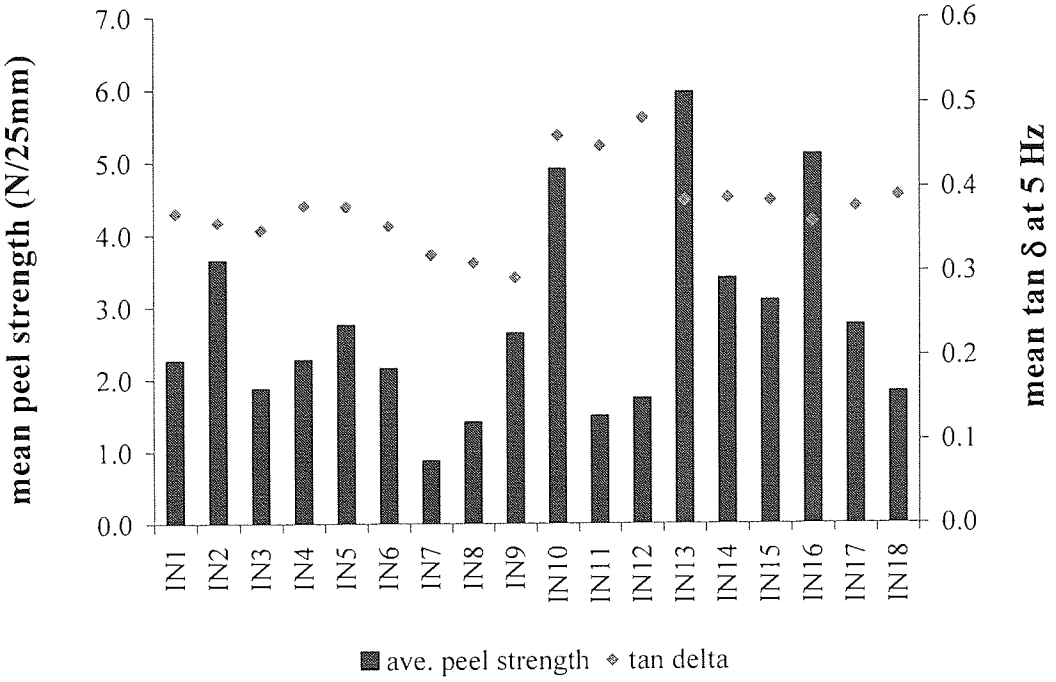

Figure 3.21 Variation in tan δ at 5Hz and peel strength for hydrogels IN1 to IN18.

On inspecting figure 3.21 it was noted that for tan δ values at 5 Hz between 0.29 and 0.4, mean average peel strength varied between 1 N/25mm (0.04 N/mm) and 4 N/25mm (0.16 N/mm). Furthermore, these hydrogels did not "leg". At higher tan δ values the hydrogels were prone to "leg" and peel strengths became unpredictable.

3.4.2.1 Effect of composition on rheological properties

In order for the hydrogels to remain cohesive they should have a dominant elastic component specifically tan δ (G":G') should be less than 1. All eighteen anionic adhesive hydrogels had maximum tan δ values below 0.55 thus these hydrogels can be considered to be sufficiently cohesive. However, those with tan δ at 5 Hz above 0.40 were "leggier" and so were less cohesive compared to those with lower tan δ values.

The G' for all these anionic adhesive hydrogels satisfied the Dahlquist criterion (section 1.4.1.1) as they were below 10^5 Pa (see appendix 3). For these adhesive hydrogels G' varied between 1.6×10^3 Pa at the lower frequency and 39×10^3 Pa at higher frequency. It was also noticed that "leggier" adhesive hydrogels had a significantly lower G' thereby resulting in a higher tan δ value. G", on the other hand, varied between 8×10^2 Pa and

$13x10^3$ Pa. "Leggy" adhesive hydrogels also had a lower G" although the difference was not as large compared to the G'. Thus, ideal values of G' (10^3 to 10^5 Pa) were satisfied at all frequencies. However, the ideal values of G" (10^2 to $5x10^3$ Pa[16]) were fully met by the less cohesive gels and only achieved at lower frequencies for the more cohesive gels.

Figures 3.16 to 3.20 show that tan δ declined gently and then sharply as it reached maximum frequency. This trend is desirable as it demonstrates that the adhesive hydrogel is likely to be malleable during application (lower frequencies) allowing it to form a good bond with skin. However on removal (higher frequencies) it is likely to remain adequately cohesive therefore is removed in a single piece.

Similarly to peel strength, tan δ is also somewhat sensitive to composition. Figure 3.16 shows that increasing amount of NNDMA whilst reducing that of NVP increases tan δ. Figure 3.17 illustrates that increasing SPA content while reducing that of NaAMPS causes a small reduction in tan δ. These results are complimented by those shown in figure 3.20; whereby increasing amounts of water, NaAMPS and NNDMA coupled with reducing those of SPA and NVP resulted in an increase in tan δ. It was also noted that as maximum frequency approached hydrogels containing equal parts of NVP and NNDMA or equal parts of SPA and NaAMPS had lower values of tan δ. This is desirable as it suggests that these hydrogels are cohesive at higher frequencies, which correspond to removal of the adhesive from skin, thus the adhesive fails adhesively and not cohesively. This cohesiveness may again be explained by the possible induced dipolar attraction shown in figures 3.14 and 3.15.

An increase in both NVP and SPA and a reduction in water and NNDMA resulted in a decrease of tan δ, as illustrated in figure 3.18. An increase in water content accompanied by reduction in NaAMPS resulted in a slight increase in tan δ, as shown in figure 3.19. This compliments previous studies[17] showing that the higher the ratio of monomer to water the better the cohesion.

Comparing tan δ to mean average peel strength, as characterised in figure 3.21, suggested that at tan δ values lower tan 0.4 mean average peel strength was moderately

consistent as the adhesive hydrogels did not have a tendency to "leg". However, at higher tan δ values mean average peel strength tended to become unpredictable, as the adhesive hydrogels were likely to "leg". Generally adhesive hydrogels that "leg" are likely to have inconsistent peel strengths, as the area of peel measured is likely to vary due to the tendency of the gel to cling to the adherend preventing it from being peeled off smoothly and thus failing cohesively. On the other hand "non-leggy" (desired) adhesive hydrogels fail adhesively, that is to say adhesion fails at the bond with skin.

3.5 Skin adhesive hydrogels containing neutral monomers

The previous formulations containing anionic and neutral hydrophilic monomers on the whole produced reasonably cohesive skin adhesives. Thus formulations containing solely neutral nitrogen-carbonyl containing monomers were designed and the ability of the hydrogels to function as conventional skin adhesives was evaluated as before. Furthermore the ability to incorporate smaller and therefore much more mobile ions into the formulations would enable the effect of ion mobility on impedance to be investigated.

Skin adhesive hydrogels, N19 to N24, containing a combination (see appendix 4) of neutral hydrophilic monomers (AMO, $MPEG_{400}MA$, NVP and NNDMA), distilled water, glycerol and initiator (Irgacure 184) and crosslinker (Ebecryl 11) in a 3:10 respectively mixture were photo-polymerised as described in section 2.2.1.2. It was observed that by replacing the anionic monomers with neutral monomers clear, glassy looking adhesive hydrogels were produced.

3.5.1 Peel strength

To determine the effect of varying the neutral backbone of an adhesive hydrogel on its peel strength (adhesive failure) skin adhesives N19 to N22 were peeled from the skin at 90^{o} at a speed of 500 mm/min using a 100 N load cell, as discussed in section 2.2.2. Mean maximum, mean average and mean minimum N/25mm of at least three peel strengths per hydrogel were taken (see appendix 4). Figures 3.22 to 3.25 present the data in ways that illustrate the effect of compositional variations on peel strength with 10 % error bars shown. A discussion of these results follows.

The effect of increasing the amounts of glycerol, AMO and NVP whilst decreasing amounts of $MPEG_{400}MA$ and NNDMA (sum of glycerol, AMO and $MPEG_{400}MA$, NVP and NNDMA remained the same), as tabled in table 3.13, was determined as shown in figure 3.22.

Sample Reference	AMO	$MPEG_{400}MA$	NVP	NNDMA	TRIS	Glycerol	Water
	w/w %						
N19	12.5	20	2.5	7.5	5	27.5	25
N20	15	15	5	5	5	30	25

Table 3.13 Family of hydrogel compositions consisting of varying amounts of glycerol, AMO, NVP, $MPEG_{400}MA$ and NNDMA.

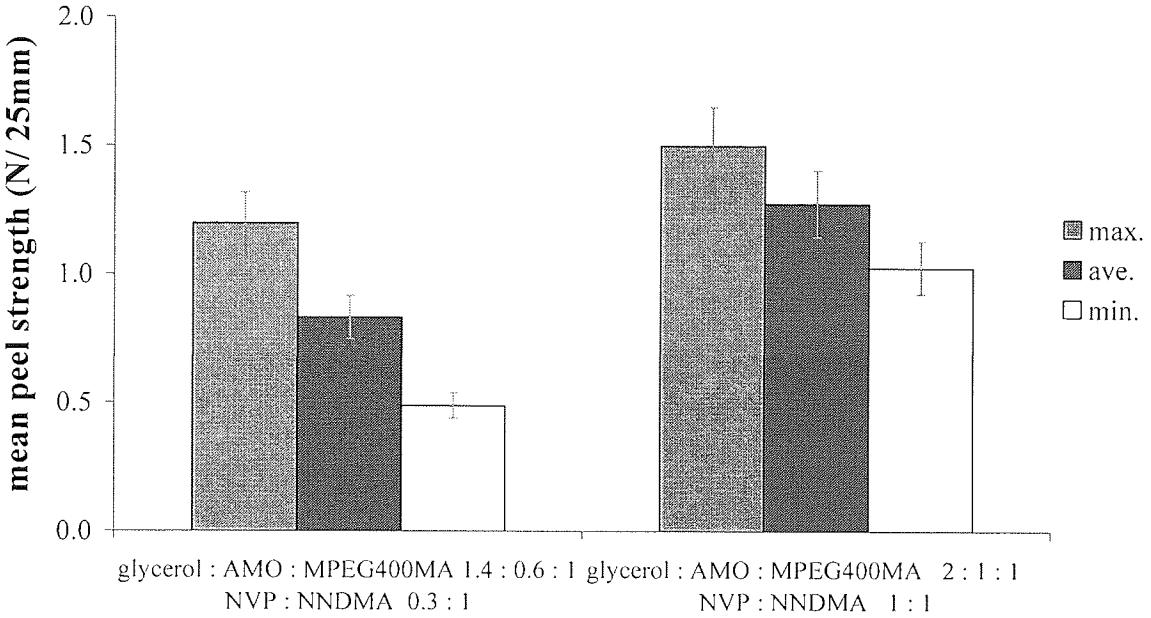

Figure 3.22 Effect of increasing glycerol, AMO and NVP whilst decreasing $MPEG_{400}MA$ and NNDMA on peel strength.

Increasing the amounts of glycerol, AMO and NVP whilst decreasing amounts of $MPEG_{400}MA$ and NNDMA resulted in an increase of mean peel strength as shown in figure 3.22.

The same comparison, as illustrated in figure 3.23, was made with increasing amounts of water, AMO and NVP whilst decreasing amounts of $MPEG_{400}MA$ and NNDMA

(sum of water, AMO and $MPEG_{400}MA$, NVP and NNDMA remained the same), as detailed in table 3.14.

Sample Reference	AMO	$MPEG_{400}MA$	NVP	NNDMA	TRIS	Glycerol	Water
	w/w %						
N21	12.5	20	2.5	7.5	5	25	27.5
N22	15	15	5	5	5	25	30

Table 3.14 Family of hydrogel compositions consisting of varying amounts of water, AMO, NVP, $MPEG_{400}MA$ and NNDMA.

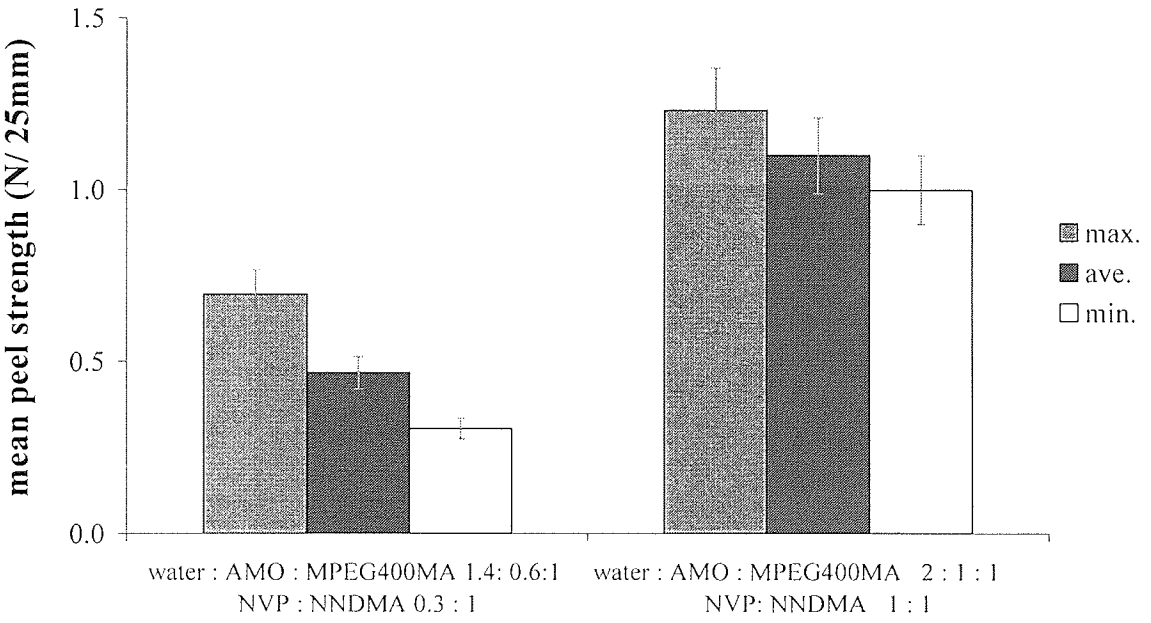

Figure 3.23 Effect of increasing water, AMO and NVP whilst decreasing $MPEG_{400}MA$ and NNDMA on peel strength.

Increasing the amounts of water, AMO and NVP whilst decreasing amounts of $MPEG_{400}MA$ and NNDMA also demonstrated an increase in mean peel strength as shown in figure 3.23.

The consequence of increasing the amount of water whilst decreasing that of glycerol, yet their total remained the same as shown in table 3.15, on peel strength is shown in figure 3.22.

Sample Reference	AMO	$MPEG_{400}MA$	NVP	NNDMA	TRIS	Glycerol	Water
	w/w %						
N19	12.5	20	2.5	7.5	5	27.5	25
N21	12.5	20	2.5	7.5	5	25	27.5

Table 3.15 Family of hydrogel compositions consisting of varying amounts of water and glycerol.

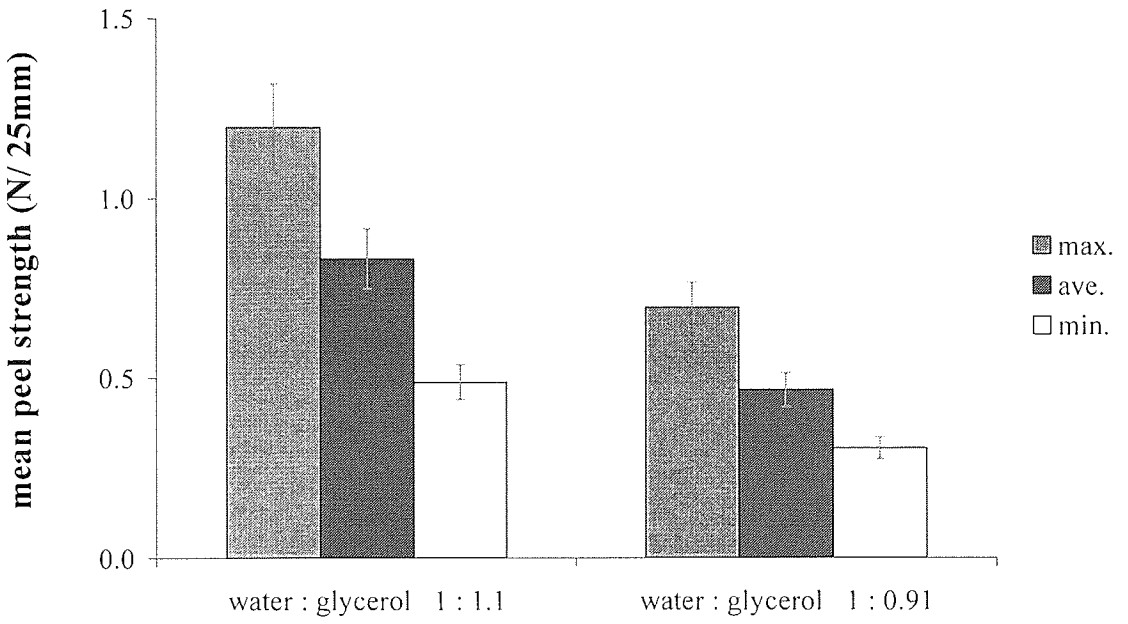

Figure 3.24 Effect of increasing water whilst decreasing glycerol on peel strength.

Figure 3.22 shows that increasing the amount of water whilst decreasing that of glycerol caused a reduction in mean peel strength. The same trend occurred with (w/w) 15 % AMO, 15 % $MPEG_{400}MA$, 5 % NVP and 5 % NNDMA (N20 and N22).

3.5.1.1 Effect of neutral monomers on peel strength

Mean peel strength values obtained for most of these neutral adhesive hydrogels were below 2 N/ 25mm. In addition, these hydrogels were physically non-cohesive; hence peel strength values were likely to have a much higher degree of error as compared to ionic adhesive hydrogels. Furthermore a dermal response emerged forty-eight hours post-application of these hydrogels to the subject's forearm. This suggested that, unlike the anionic skin adhesive hydrogels, residual monomers were precipitating from the bulk hydrogel.

Figures 3.22 and 3.23 show that a reduction in amounts of $MPEG_{400}MA$ and NNDMA, whilst increasing amounts of AMO, NVP and either glycerol or water increases mean peel strength. It was also noted that mean peel strengths are higher when the ratio of NVP to NNDMA was 1:1, similar to that found with anionic skin adhesives (section 3.4.1). Given that an increase in water reduced mean peel strength (figure 3.22) the increase in mean peel strength in figure 3.23 was probably influenced by an increase in AMO and NVP. Hence it is suggested that either a reduction in NNDMA or $MPEG_{400}MA$ in neutral hydrogels possibly reduces the residual effect, thus mean peel strength of neutral hydrogels increases. A reduction in peel strength with a reduction in glycerol (figure 3.22) is not surprising as glycerol acts as a humectant aiding absorbance of interfacial moisture thereby enhancing the adhesive bond.

3.5.2 Rheology

To determine the effect on viscoelasticity as the polymer backbone is varied, the elastic (G') and viscous (G") moduli of neutral skin adhesive hydrogels N19 to N22 were measured as a function of frequency. For each test the frequency to complete a sine wave was set to increase from 0.5 Hz to 25 Hz. The lower frequencies were intended to mimic the properties of the gel when it is applied to the skin and higher frequencies when the gel is removed from the skin. Tests were carried out as discussed in section 2.2.3. Mean values of at least three G' and G" are detailed in appendix 4. A summary of tan delta (tan δ), the ratio of G" to G' (see section 2.2.3 for theory), obtained for the various compositions is presented in figures 3.25 to 3.28. A discussion of these results follows.

Tan δ of neutral adhesive hydrogels with increasing amounts of glycerol, AMO and NVP whilst lowering amounts of $MPEG_{400}MA$ and NNDMA, as detailed in table 3.13 were compared (figure 3.25).

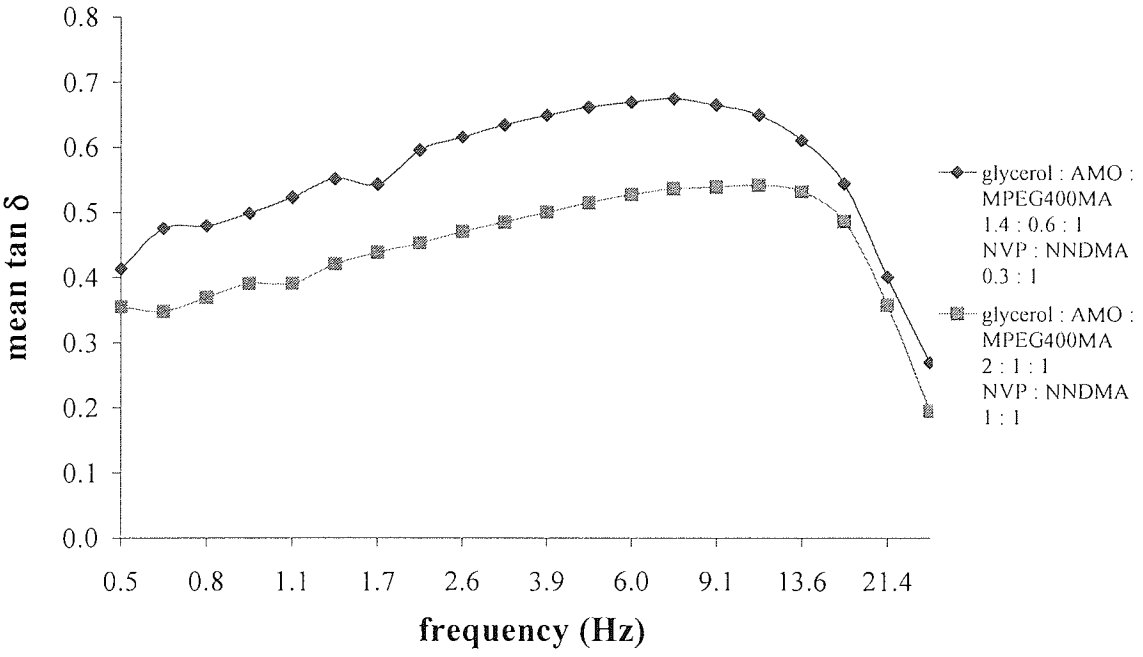

Figure 3.25 Effect of increasing glycerol, AMO and NVP whilst decreasing $MPEG_{400}MA$ and NNDMA on tan δ.

The adhesive hydrogel with a higher amount of glycerol, AMO and NVP had lower values of tan δ as demonstrated in figure 3.25.

The same comparison (figure 3.26) was made for adhesive hydrogels with increasing amounts of water, AMO and NVP whilst decreasing amounts of $MPEG_{400}MA$ and NNDMA (table 3.14).

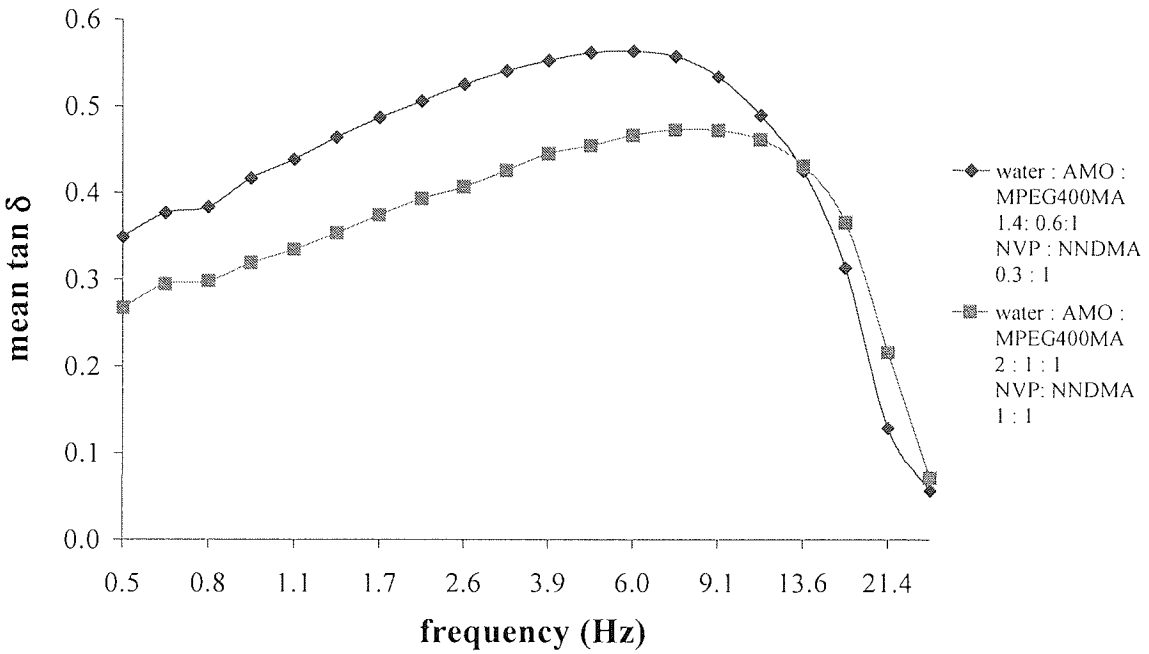

Figure 3.26 Effect of increasing water, AMO and NVP whilst decreasing $MPEG_{400}MA$ and NNDMA on tan δ.

At lower frequencies, an increase in water, AMO and NVP resulted in a reduction of tan δ values. However at higher frequencies the adhesive with lower amount of water, AMO and NVP had lower values of tan δ (figure 3.26).

The effect of increasing the water whilst decreasing glycerol, as detailed in table 3.15, on tan δ was also studied (figure 3.27).

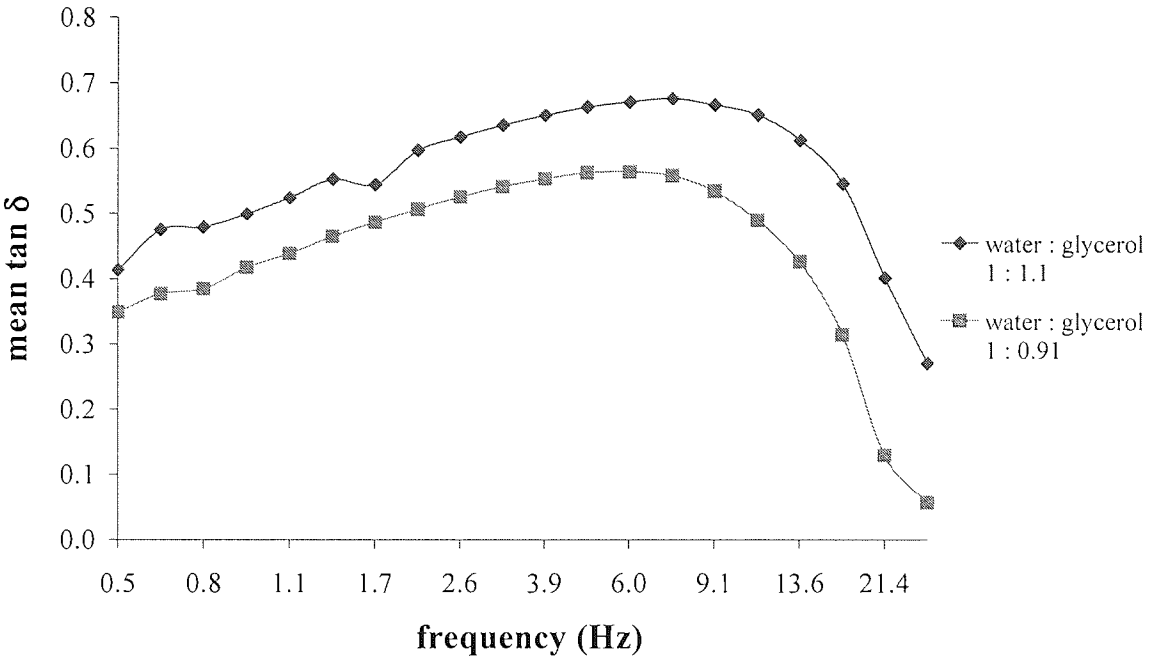

Figure 3.27 Effect of increasing water whilst decreasing glycerol on tan δ.

An increase in water content whilst reducing that of glycerol caused a reduction on tan δ as illustrated in figure 3.27. The same trend occurred with (w/w) 15 % AMO, 15 % $MPEG_{400}MA$, 5 % NVP and 5 % NNDMA (N20 and N22).

A contrast between tan δ of a neutral (N20) and an ionic (IN12) adhesive hydrogel is illustrated in figure 3.28.

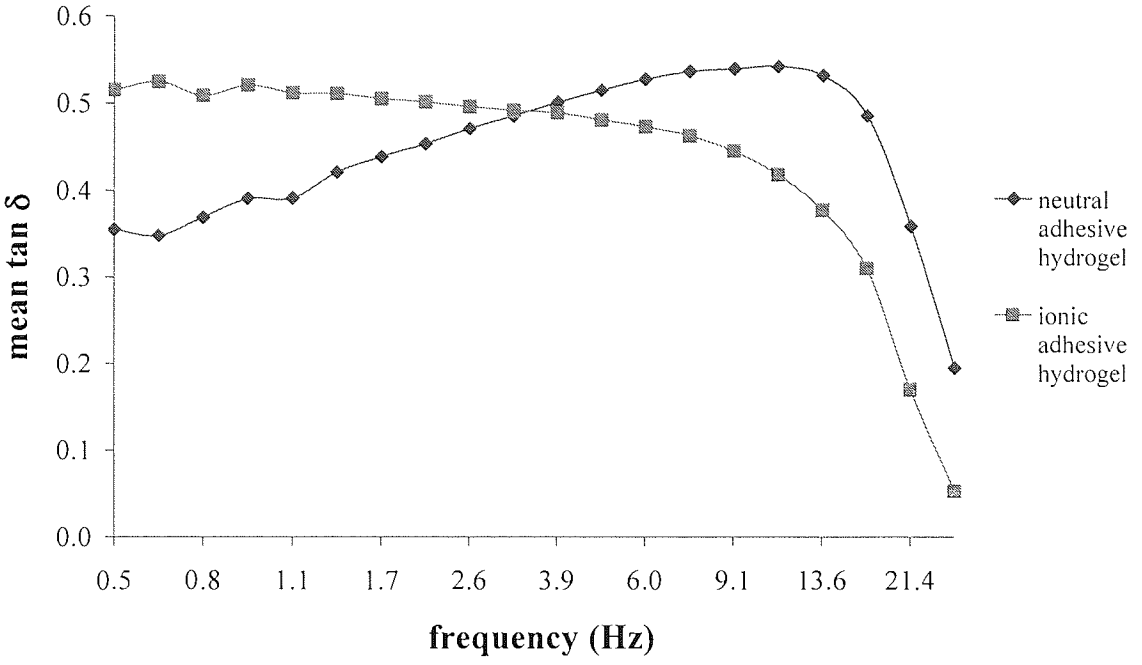

Figure 3.28 Comparison of tan δ between a neutral and an anionic adhesive hydrogel.

Figure 3.28 illustrates that tan δ for the neutral hydrogel increased with frequency and then fell sharply at very high frequencies. In contrast that of the anionic hydrogel decreased gently with frequency and then at very high frequency it also decreased steeply.

3.5.2.1 Effect of neutral monomers on dynamic mechanical properties

G' for all neutral adhesive hydrogels satisfied the Dahlquist criterion as they were below 10^5 Pa, as shown in appendix 4. G' of the neutral hydrogels ranged between 7.8×10^2 Pa at lower frequencies and 6×10^3 Pa at higher frequencies. This is significantly lower than those of the ionic hydrogels (1.6×10^3 Pa and 39×10^3 Pa). Values of G'' varied between 2.7×10^2 Pa and 2.5×10^3 Pa. Although these values are also lower than that of the ionic adhesive hydrogels (8×10^2 Pa and 13×10^3 Pa) the difference is not as large compared to G', thus resulting in somewhat higher values of tan δ for the neutral hydrogels.

For neutral adhesive hydrogels ideal values of G' (10^3 to 10^4 Pa) were only satisfied as frequency increased. Therefore these hydrogels can be considered weak and non-

cohesive. The ideal values of G" (10^2 to $5x10^3$ Pa) were fully met. Furthermore it was noted that compared to ionic hydrogels neutral ones were "leggier".

Figures 3.25 to 3.27 illustrate that tan δ increased and then declined sharply as maximum frequency approached. These figures also show that tan δ is somewhat sensitive to composition. Figure 3.25 suggests that by increasing the quantity of glycerol, AMO, NVP whilst reducing that of $MPEG_{400}MA$ and NNDMA reduces tan δ. Furthermore the adhesive gel with the ratio of NVP to NNDMA at 1:1 had lower tan δ values at higher frequencies.

A similar pattern was seen with increasing the percentage of water, AMO, NVP whilst reducing that of $MPEG_{400}MA$ and NNDMA (figure 3.26), although at the higher frequencies the adhesive with lower amount of water had lower values of tan δ. This is in agreement with the three point graph (figure 3.1) which illustrates that the higher the percentage of water the lower the cohesiveness of a hydrogel as it is more "dilute" and this overpowers the effect of the remaining components.

A reduction in glycerol with an increase in water content (figure 3.27) lowered the values of tan δ. This is not wholly surprising as it has been reported[117] that the additional hydrogen bonding water donates, as well as its ability to "loosen" the network aiding rotation of polymer chains enhances intermolecular interaction between polymer chains, thereby improving cohesion. Furthermore glycerol acts a radical scavenger subsequently decreasing the crosslinking density of the network.[93]

Figure 3.28 demonstrates that tan δ for a neutral adhesive hydrogel increased with frequency and then fell sharply at very high frequencies. In contrast that of an anionic adhesive hydrogel decreased gently with frequency and then sharply at very high frequencies. This indicates that with neutral adhesive hydrogels there is a steady increase in G":G' as frequency increases at the lower end of the frequency range. This is due to the much lower G' differences than G" differences of neutral adhesive hydrogels compared to anionic adhesive hydrogels as highlighted at the beginning of this section. Hence this suggests that an anionic monomer is desired for cohesion. Furthermore the lack of acrylic acid in neutral adhesive hydrogels may have added to

their lowered cohesiveness. Acrylic acid has been shown to increase peel strength as well as cohesive strength of skin adhesives.[17, 89] Furthermore the optimum amount of crosslinker-initiator mixture was the same as that used for anionic adhesive hydrogels; however this value might not be optimum for a neutral system.

Furthermore it was evident that residual monomers remained post polymerisation, more so with neutral rather than the anionic adhesive hydrogels. Thus determining which monomers were least likely to polymerise within the given environment would enable the optimisation of a formulation to produce cohesive adhesive hydrogels.

3.6 Residual monomers

In order to determine the monomers that were least likely to polymerise within the given aqueous-organic environment, the presence and effect of residual monomers had to be established. Initially this was achieved by cutting a disc of hydrogel, with a number 13 cork borer, and placing it in approximately 50 ml of its constituent monomers. The diameter of the disc was subsequently monitored. This was based on the assumption that the monomer most likely to render the hydrogel "leggy" would cause the polymer backbone to swell the most.

A disc of anionic adhesive hydrogel, IN4 (table 3.5), was placed in both its makeup and non-makeup monomers for an extended period of 400 hours. The change in ratio of the diameter (D) to original diameter (D_o) is illustrated in figure 3.29.

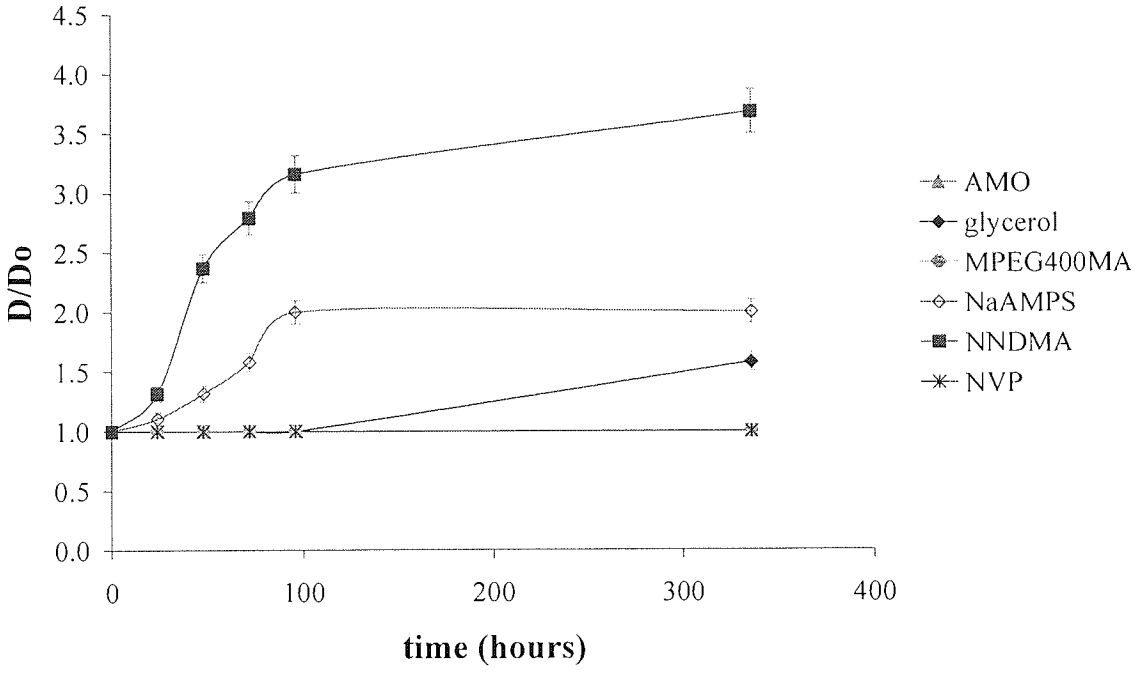

Figure 3.29 Effect of monomers on diameter of ionic hydrogel, IN4, disc (5 % error bars shown).

The diameter of the anionic hydrogel remained relatively unchanged in $MPEG_{400}MA$, AMO and NVP. However it doubled in NaAMPS and grew to about three and a half

times its original diameter in NNDMA. In glycerol its diameter began to increase slightly after 100 hours.

A similar test was carried out with neutral hydrogel, N20 (table 3.13), as shown in figure 3.30.

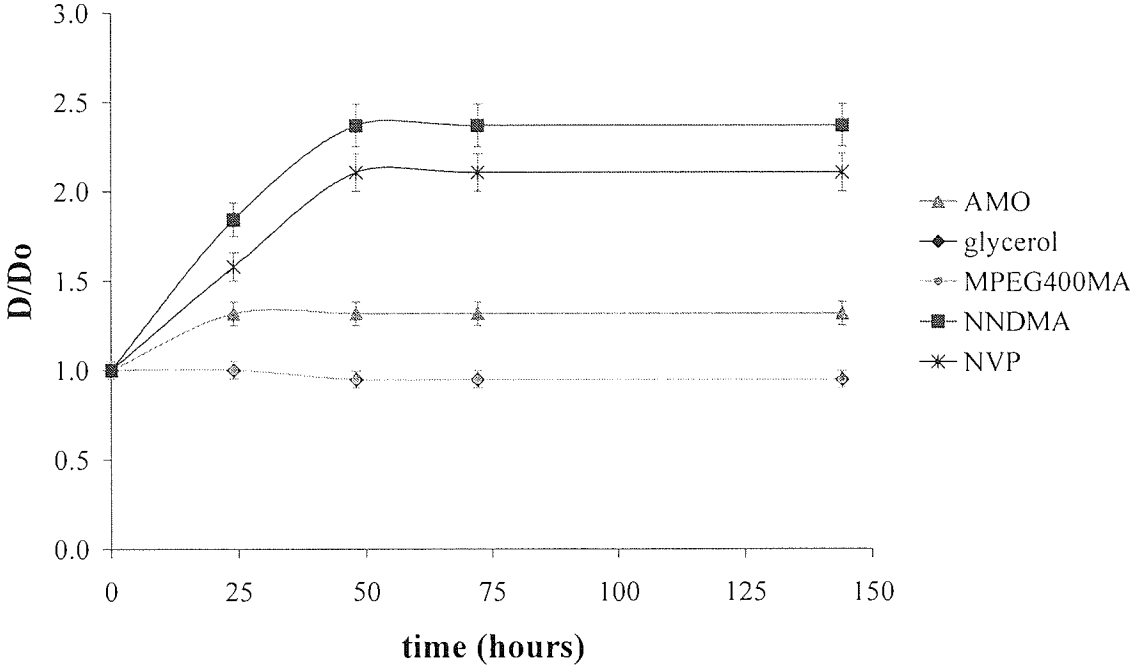

Figure 3.30 Effect of monomers on diameter of neutral hydrogel, N20, disc (5 % error bars shown).

The diameter of the neutral hydrogel remained relatively unchanged in $MPEG_{400}MA$ and glycerol, while it increased by approximately a third in AMO, doubled in NVP and grew by nearly two and a half times in NNDMA.

3.6.1 Relative effect of residual monomers

For the anionic hydrogel, swell increased along the series glycerol < NaAMPS < NNDMA after 350 hours. The extended period of swell for the anionic hydrogel showed that after about 100 hours glycerol also begins to cause the hydrogel to swell. The ionic hydrogel did not swell in AMO or NVP.

With the neutral hydrogel, after 150 hours swell increased along the series AMO < NVP < NNDMA. The neutral hydrogel did not swell in glycerol or $MPEG_{400}MA$. In both monomers a slight reduction was noted but this may have been due to a slight degree of difficulty in determining the edge, as it tended to become very clear and frill.

From the above results (figures 3.29 and 3.30) it is evident that for both types of hydrogels NNDMA caused the most swell; hence it is the monomer most likely to cause adhesive hydrogels to "leg". For the neutral hydrogel NVP was the second monomer to cause the most swell followed by AMO. In contrast NVP and AMO did not seem to cause the anionic hydrogel to swell. All three monomers contain, as illustrated in section 2.1.1.1, a polar carbonyl group and hydrogen atoms enabling the formation of hydrogen bonds. The higher degree of swell caused by NNDMA suggests that compared to NVP and AMO it undergoes polar interaction with a polymer backbone, more readily; this is not necessarily equivalent to its polarity with water. This was attributed to the structure of the monomer's molecules, since the carbonyl group on NNDMA is less shielded as the amide group is less sterically hindered. In contrast the carbonyl group on NVP and AMO has a higher degree of shielding, preventing it from forming hydrogen bonds easily, because the ring structure sterically obstructs the amide group. Thus, NNDMA is the most polar of the three neutral monomers and is likely to interact with the same sites as water within the hydrogel.

NaAMPS is marketed as a 58 % ionic solution therefore, as it caused the ionic hydrogel to swell it has a lower osmotic strength than the hydrogel. In this case the swell resulted from an osmotic drive. Since the anionic hydrogel did not contain AMO this monomer did not cause it to swell. This is desirable as it illustrates that "legginess" is caused by the swelling of the polymer by its monomer; therefore residual monomer must be present in order for it to cause its polymer to swell. NVP did not cause the anionic adhesive hydrogel to swell, suggesting that either NVP fully polymerised within the anionic system or that NVP is not a strong swelling solvent for the gel. It has been discovered[16] that NVP has an increased reactivity ratio in an aqueous environment (as distinct from the neutral gel system shown in figure 3.31 for instance) and it may be that both extent of polymerisation and swelling ability contribute to this effect. In the anionic system the ratio of organic to aqueous phase was 1:3, whereas in the neutral

system it was 1:0.9. Thus the ability to determine the ease of monomer polymerisation is desirable.

3.6.2 Determining amount of neutral residuals

Having established the monomer most likely to cause the adhesive hydrogel to "leg", the relationship between this and ease of monomer polymerisation was explored. The suitability of gas chromatography to quantify the relative amounts of neutral residual monomers was investigated.

A 1 ml sample size of pure propanol and various propanol and neutral monomer mixture was injected through the column, and the test carried out as described in section 2.3.1, to determine each monomer's retention time in order to enable identification of the individual monomer from the propanol residual mixture as discussed in section 2.3.1 (technique development).

Samples of neutral hydrogels N20, N23 and N24, compositions as detailed in table 3.16, were cut and weighed into a known weight of propanol. This was to ensure that the hydrogel weight to solvent weight ratio remained the same for all hydrogels. The hydrogels in propanol were allowed to equilibrate overnight. A 1 ml sample size of each propanol and residual monomer mixture was injected through a capillary column. The column was set at a temperature of 210 °C, the flame ionisation detector at 230 °C and the injector at 210 °C (isothermal). The test was carried out as described in section 2.3.1 and the raw results are tabulated in appendix 4.

Sample Reference	AMO	$MPEG_{400}MA$	NVP	NNDMA	TRIS	Glycerol	Water
	w/w %						
N20	15	15	5	5	5	30	25
N23	12.5	15	2.5	7.5	5	32.5	25
N24	17.5	15	7.5	2.5	5	27.5	25

Table 3.16 Family of hydrogel compositions consisting of varying amounts of AMO, NVP, NNDMA and glycerol.

The amount of residual in the propanol was expressed as a percentage area. By keeping a constant ratio of residual (percentage area) to feed (percentage) of AMO at 3:3 for

convenience, as AMO was the least likely nitrogen containing monomer to swell the hydrogels, a comparison of residual to feed for NNDMA and NVP was obtained as illustrated in figure 3.31.

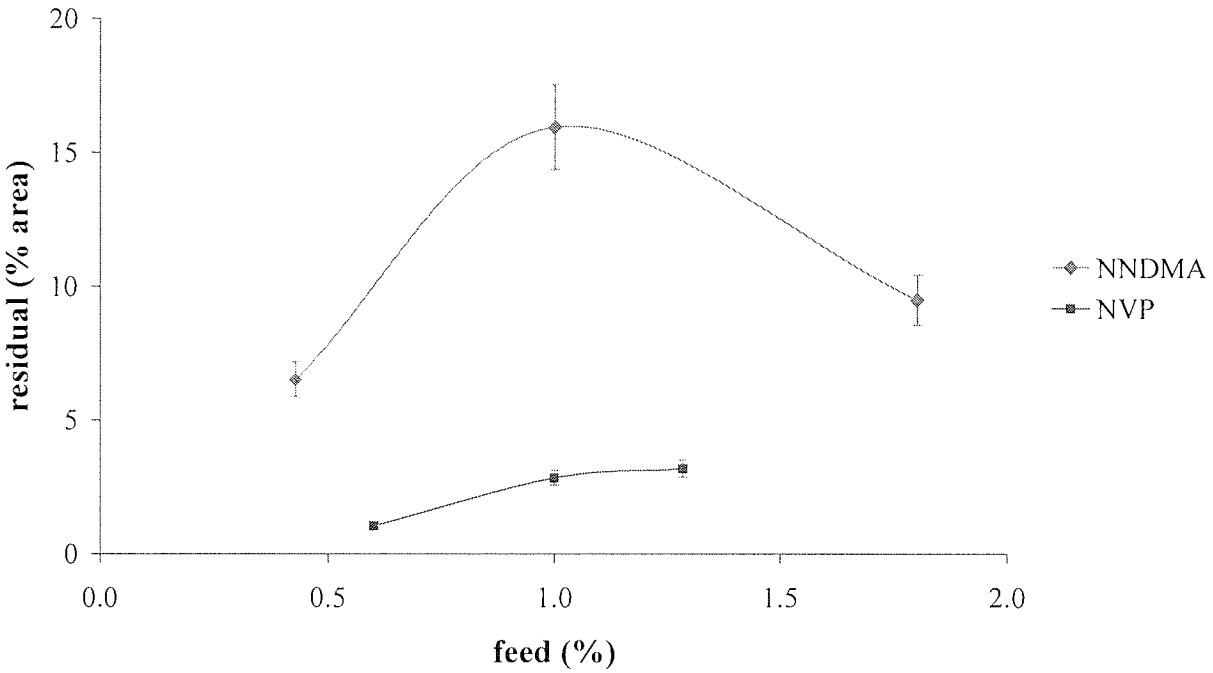

Figure 3.31 Determining the relationship between feed and residuals for NNDMA and NVP (10 % error bars shown).

For NNDMA an increase in feed showed an increase in residual until it peaked, when further increase in feed resulted in a reduction of residuals. For NVP increasing the feed increased amount of residual.

3.6.3 Factors influencing amount of residual monomers

Inspection of the results showed that residual NNDMA % area peaked and then declined with an increase in feed %. In contrast residual NVP % area increased with an increase in feed %.

At a similar monomer feed (%) residual NNDMA (%) is greater than that of residual NVP (%), indicating that NNDMA is less likely to polymerise under the conditions used. NNDMA contains an alternating double bond system that is able to stabilise the propagating free radical. In contrast the double bonds in NVP do not alternate (that is

they are not conjugated) hence, they are not as effective in radical stabilisation as those of NNDMA. Although NNDMA is thought of as a more readily polymerisable monomer there are two complications here. The first is the fact that this is an aqueous system and little direct work on rates of polymerisation of these monomers in aqueous media has been carried out. The second is that this is a copolymerisation involving a complex set of monomers in which (for example) the possibility of alternation of NVP and NaAMPS has been suggested.[94]

The fact that such high levels of residual monomer were obtained indicates that more effective polymerisation would be needed before these adhesive hydrogels could be used by humans. This may be achieved by gamma-radiation, which is commonly used by skin contacting medical devices, or simply by more efficient photo-polymerisation such as those found in commercial photo systems. Due to this and other observations NNDMA containing systems were considered (within the confines of this project) to be unsuitable for further consideration.

The use of gas chromatography to identify and separate neutral monomers appeared to be successful. The use of ion suppression chromatography to identify and quantify anionic monomers was also investigated (section 2.3.2) but met with limited success due to sensitivity issues. However, it is anticipated that once these are resolved the use of ion suppression chromatography would enable the identification of residual anionic monomers.

3.7 Impedance and sensation evaluation

Impedance measurements provide details on the variation of current flow (section 2.2.4). In order to minimise the discomfort felt at the location of the return electrode during ocular iontophoresis, the return electrode should possess low impedance and current density path for the return current, as mentioned previously (section 1.5.7.5). The effects of composition, area, thickness of the adhesive hydrogel as well as frequency of current on impedance were investigated. A summary and discussion of results obtained for the various compositions follows.

3.7.1 Anionic skin adhesives

Impedance measurements were evaluated at a frequency of 50 Hz and a potential difference set at approximately 1.94 V (refer to section 2.2.4). The current and actual potential difference readings were taken every thirty seconds for a period of eleven minutes. These values were entered onto a spreadsheet provided by Holman Design and the impedance calculated, the raw results are detailed in appendix 3.

A comparison was made between anionic adhesive hydrogels IN1 and IN3 (compositions as per table 3.7) and commercialised adhesive hydrogels (figure 3.32).

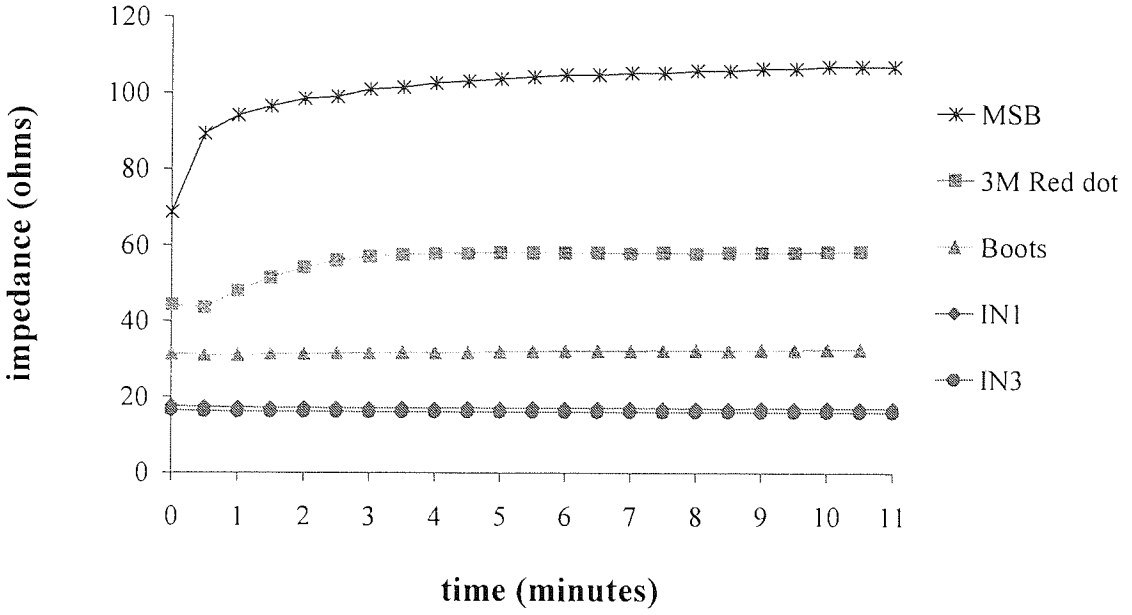

Figure 3.32 Impedance profile of hydrogels IN1, IN3 and commercialised electrodes.

Impedance did not change significantly between IN1 and IN3. In addition impedance remained constant during the eleven minutes of test. However, in comparison to the impedance of the Boots TENS machine, MSB neutralect and 3M Red dot electrodes, adhesive hydrogels IN1 and IN3 had significantly lower impedance. The large MSB neutralect electrode was cut down to ensure that surface area remained constant while compositions varied.

A similar comparison was made between adhesive hydrogels IN4 and IN7 (table 3.5) and commercialised electrodes (figure 3.33).

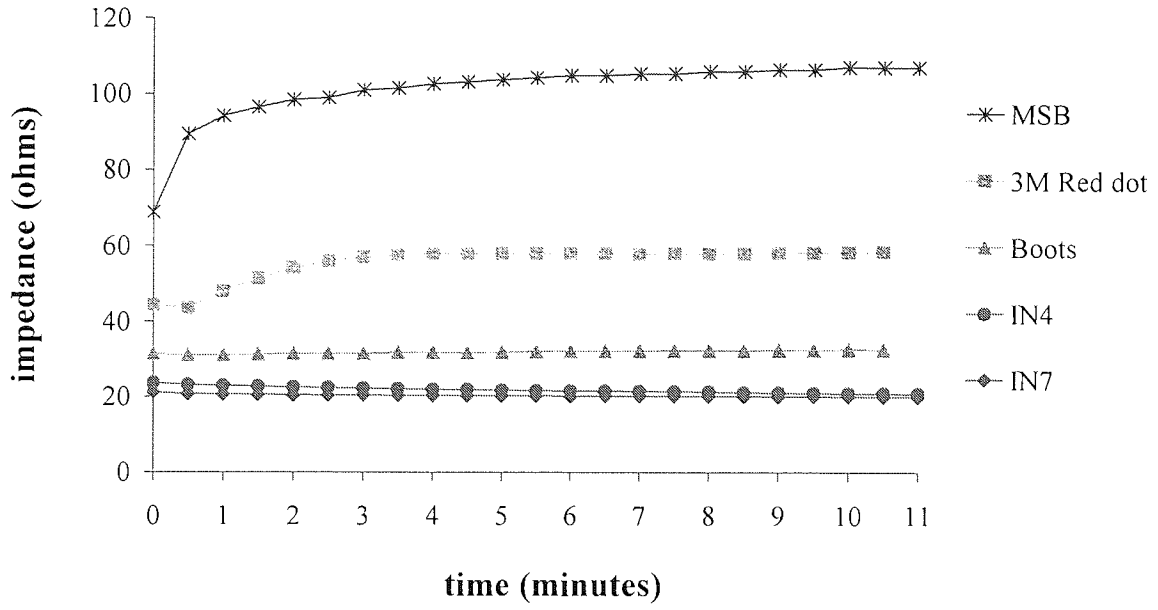

Figure 3.33 Impedance profile of hydrogels IN4, IN7 and commercialised electrodes.

The same trend was noted again, whereby impedance did not alter significantly between adhesive hydrogels IN4 and IN7, however their impedance was lower than commercialised electrodes.

The same comparison was made between adhesive hydrogels IN13, IN14 and IN15 (table 3.10) and commercialised electrodes (figure 3.34).

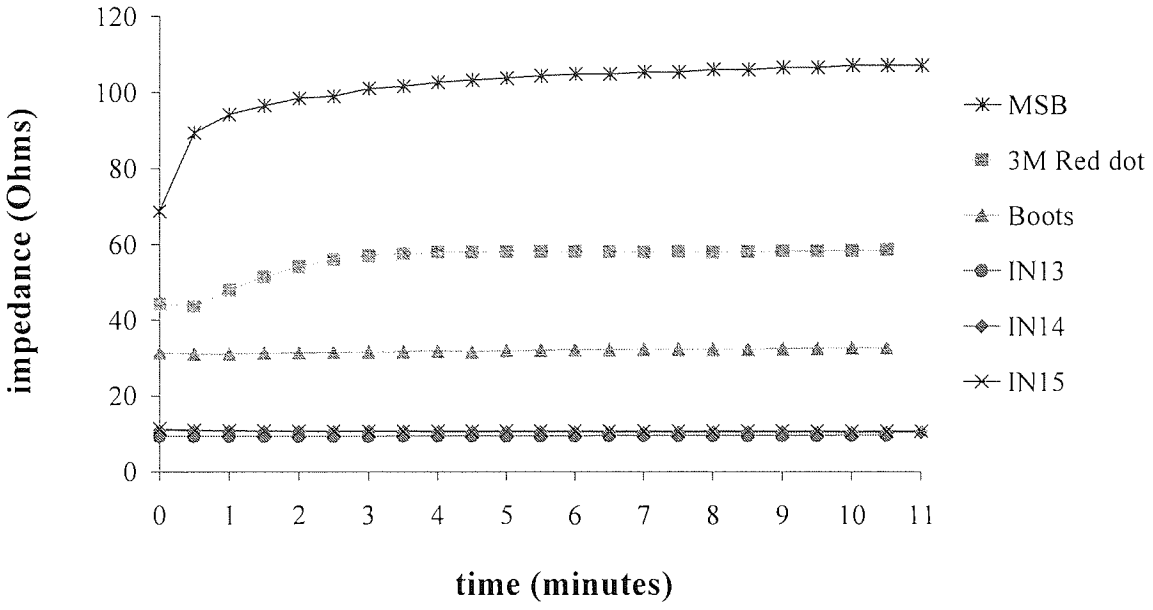

Figure 3.34 Impedance profile of hydrogels IN13, IN14, IN15 and commercialised electrodes.

Once more it was demonstrated that although impedance remained virtually unchanged between adhesive hydrogels IN13, IN14 and IN15 their impedance was significantly lower than commercialised electrodes.

The effect of hydrogel thickness, surface area as well as current frequency on impedance was investigated for the same hydrogel, IN3, as shown in figures 3.35 and 3.36.

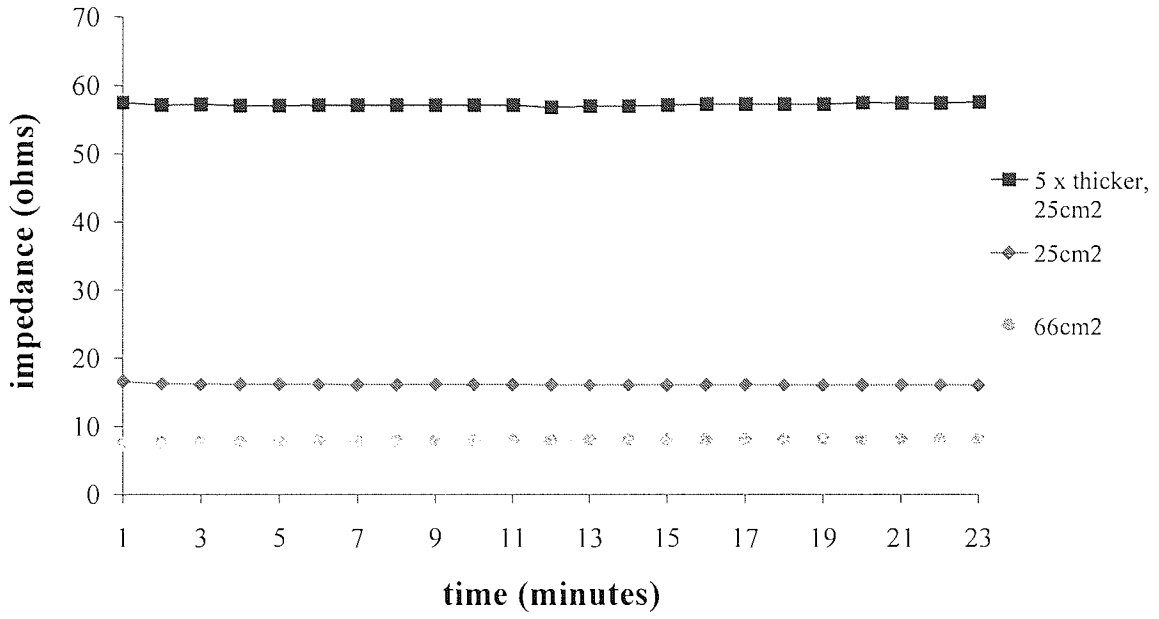

Figure 3.35 Effect of varying thickness and surface area on impedance of hydrogel IN3.

Increasing the thickness of hydrogel IN3 caused impedance to increase; however increasing surface area resulted in a decrease in impedance. Thickness of the hydrogel had a bigger influence on impedance compared to surface area.

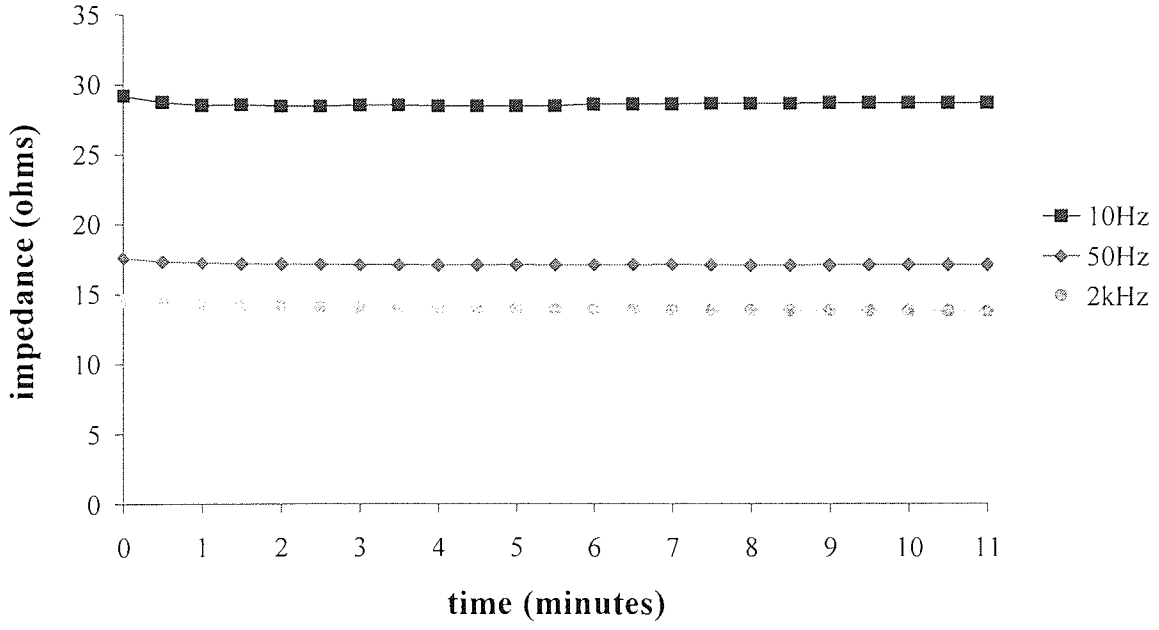

Figure 3.36 Effect of frequency on impedance of hydrogel IN1.

Impedance reduced with an increase in frequency. However, the reduction was greater at lower frequencies.

3.7.1.1 Factors influencing impedance and sensation

The results showed that impedance of the adhesive hydrogels IN1, IN3, IN4, IN7, IN13, IN14 and IN15, compositions as detailed in appendix 3, was lower than the 3M red dot electrode, which was not deemed acceptable by Optis.[71] The impedance of these skin adhesive hydrogels was also significantly lower compared to other commercialised electrodes. This difference indicates that composition is likely to influence impedance, despite very little difference noted when amounts of SPA, NaAMPS, NVP, NNDMA and water were varied.

Varying SPA and NaAMPS (figure 3.32) did not produce a significant change to impedance, as total number of moles of these monomers did not change considerably, thus the number of charge carrier moles (fixed charge density) remained comparable. Varying amount of NVP and NNDMA (figure 3.33) did not affect impedance as these monomers are neutral and so do not contain charge carriers. Since increasing amount of water did not affect impedance (figure 3.34) it may be suggested that a certain amount of water is sufficient to conduct charge and larger amounts do not have a significant effect on impedance. Likewise, significant differences in sensation was not felt when these adhesive hydrogels were tested in place of Boots TENS machine electrodes and a subjective sensation evaluation was carried out as described in section 2.2.5.

Figure 3.35 illustrates that increasing the thickness of the adhesive hydrogel caused impedance to increase. This could be a result of polarisation increasing in the direction of current. However increasing surface area reduced impedance, possibly due to a reduction in current density. This compliments equation 1.8, which suggests that by increasing the electrode surface area the current threshold at which pain is felt increases. Similarly when a MSB neutralect electrode, normally used for resuscitation and electrosurgery, with an original surface area of 170cm^2 was cut and used in place of a 25 cm^2 Boots TENS machine electrode the level of sensation felt increased. In addition, skin's electrical resistance increases[73] with current density; thus more pain is likely to

be felt at higher current densities. However, thickness of the hydrogel seemed to have a bigger influence on impedance compared to surface area.

Increasing current frequency caused a reduction in impedance as shown in figure 3.36. This result is comparable to electrosurgery and resuscitation techniques, which have high current frequencies and are not reported to inflict pain. However the difference in impedance with a frequency increase from 10 Hz to 50 Hz was higher compared to that increased from 50 Hz to 2 kHz. Therefore, within a certain frequency range there is significant impedance reduction; however beyond this further frequency increases may not reduce impedance considerably. This clearly demonstrates the need to design adhesive bioelectrodes for the intended application. In addition it has been reported[74] that stimulation thresholds decrease and then plateau with an increase in pulse rate. Most significantly, however, these results emphasize the need to design the adhesive hydrogel for each particular electrotherapeutic application. Different electrotherapeutic applications have different current frequencies thus, although an adhesive hydrogel used at a frequency of 2 kHz may not inflict pain, when the same adhesive hydrogel is used at a lower frequency, such as 10 Hz, pain may be experienced as a result in an increase of the adhesive's impedance.

It should be noted that it was not possible to remove the backing of the commercialised electrodes thus their impedance values may have a higher degree of error. In addition, although these results provide a good indication on the comparative polarisation of the hydrogels they are based on TENS rather than iontophoresis current specifications.

3.7.2 Neutral skin adhesives

Impedance and sensation tests were carried out on the neutral adhesive hydrogels (N19 to N22) as discussed in sections 2.2.4 and 2.2.5. For these neutral hydrogels there were no readings for either potential or current on the impedance meter. This indicated that current was not passing through these hydrogels. This suggests that water only is not sufficient as a conducting medium. The presence of charge carriers is probably required to pass on current thus the impedance of electrolyte containing neutral hydrogels was evaluated.

3.7.3 Effect of metal ions and polyanion on impedance

Skin adhesive hydrogels were synthesised, as described in section 2.2.1.2, from neutral hydrophilic monomers with either potassium (KCl) or sodium chloride (NaCl) incorporated into the formulation (N26 to N35 as detailed in appendix 5). KCl and NaCl were chosen as they are strong electrolytes, which dissociate in an aqueous environment to produce an electrically conductive medium. Furthermore in biological systems these electrolytes are fundamental to maintain nerve, muscle and heart cells and carry electrical impulses across to other cells. Electrolytes are distributed throughout the body in a highly ordered way; any imbalance can result in severe bodily dysfunction.

Adhesive hydrogels N26 to N30 were formulated such that the number of moles of K^+ varied per hydrogel, as listed in table 3.17. The total of the K^+ contribution was the sum of K^+ from the added KCl and TRIS.

Hydrogel Reference	No. moles K^+ from KCl/ 100g	No. moles K^+ from TRIS/ 100g	Total no. moles K^+ / 100g hydrogel
N26	0.014	0.004	0.018
N27	0.027	0.004	0.031
N28	0.041	0.004	0.045
N29	0.054	0.004	0.058
N30	0.068	0.004	0.072

Table 3.17 Number of K^+ moles per 100g hydrogel.

Adhesive hydrogels N31 to N35 were formulated such that the number of moles of Na^+ varied per hydrogel, as listed in table 3.18. For these hydrogels the total of the Na^+ contribution was solely from the added NaCl.

Hydrogel Reference	No. moles Na^+ from NaCl/ 100g
N31	0.014
N32	0.027
N33	0.041
N34	0.054
N35	0.068

Table 3.18 Number of Na^+ moles per 100g hydrogel.

Impedance tests were carried out for skin adhesives N26 to N35 as discussed in section 2.2.4. Impedance measurements were evaluated at a frequency of 50Hz and a potential difference set at approximately 1.94 V. The current and actual potential difference readings were taken every thirty seconds for a period of eleven minutes. These values were entered into a spreadsheet provided by Holman Design and the impedance calculated. The raw results are tabulated in appendix 5.

Impedance values at eight minutes were used to compare the behaviour of neutral hydrogels loaded with different ions of varying concentrations (figure 3.37). An arbitrary value of eight minutes was chosen because the results show, see appendix 5, that impedance decayed by approximately 10 % over the eleven minutes but generally stabilised by the eight minute.

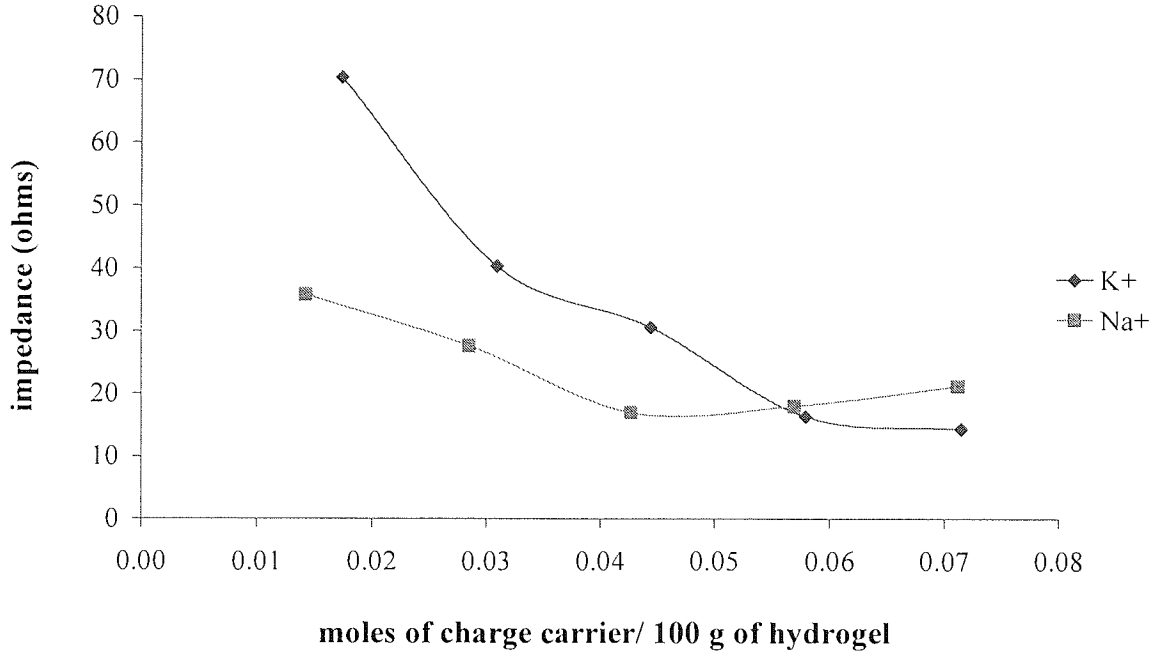

Figure 3.37 Effect of metal cations on impedance.

Figure 3.37 illustrates that for adhesive hydrogels synthesised from neutral monomers with added KCl, as the number of moles per 100g of hydrogel of K^+ increased from 0.02 to 0.06 there was a significant decrease in impedance after which it seemed to become steady when increased to 0.07. For adhesive hydrogels containing NaCl a reduction in impedance was noticed with an increase in the number of Na^+ moles from 0.01 to 0.04. A subsequent increase to 0.07 resulted in a slight increase in impedance, thus possibly tending to stabilise. Furthermore it was noted that at lower moles of charge carrier, the hydrogels containing Na^+ had lower impedance than those containing K^+.

A best-fit relationship for the data was obtained, as illustrated in figure 3.38, with the value of R^2 indicating how well the regression line approximates the real data points.

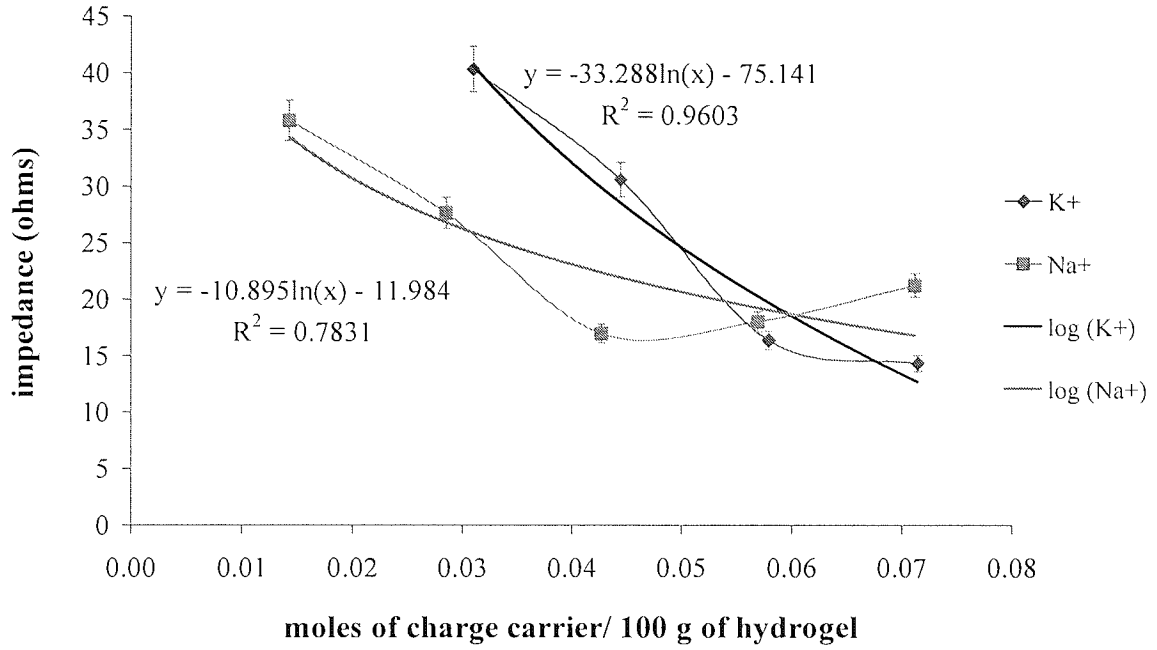

Figure 3.38 Best fit correlation of impedance against moles of charge carrier.

The impedance of neutral hydrogels containing either KCl or NaCl were compared to ionic hydrogels (FW1 to FW5) containing 42 % water, varying amounts of SPA and NaAMPS, yet their total remained the same, and 0.04 moles KCl per 100 g of hydrogel (see appendix 6). This comparison (figure 3.39) served to determine whether varying the anion had an effect on impedance. The ionic hydrogels (FW1 to FW5) were obtained from First Water, a company involved in the manufacture of biomedical electrodes for applications such as ECG, electrosurgery, defibrillation and TENS. The impedance values of these adhesives were provided by First Water and are detailed in appendix 6.

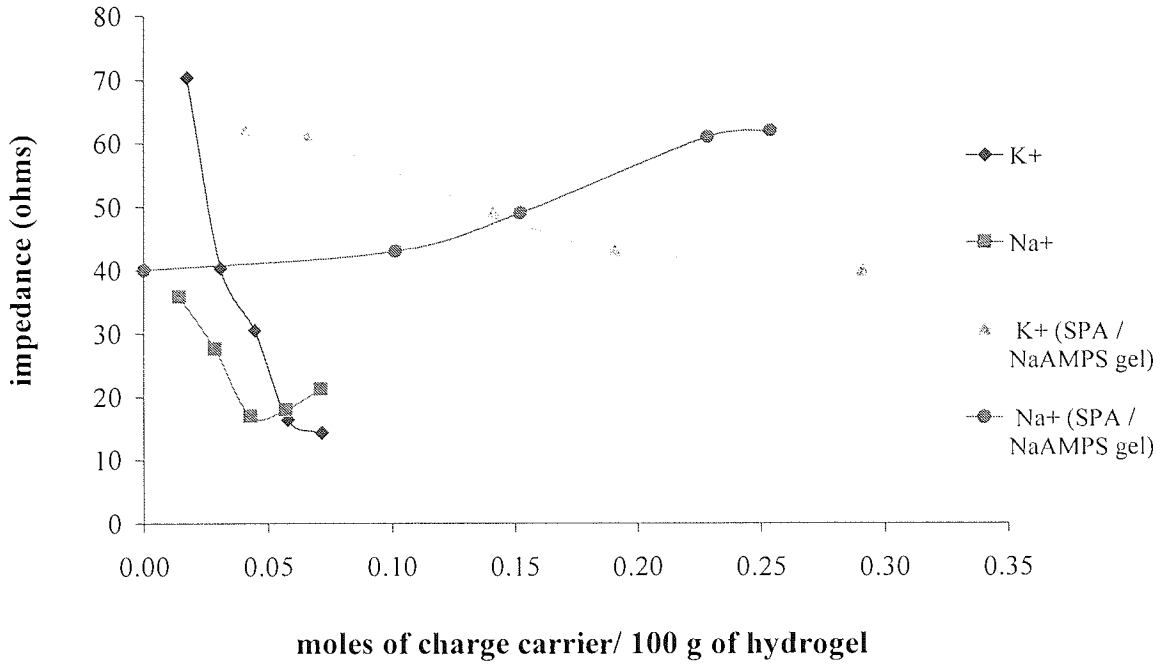

Figure 3.39 Comparing effect of varying anions on impedance.

Figure 3.39 shows that impedance reduced for hydrogel compositions FW1 to FW5 with increasing K^+ (SPA) while lowering Na^+ (NaAMPS). However substantial decrease in impedance was not apparent with increasing K^+ while decreasing Na^+ when K^+>0.2 and Na^+<0.1 moles per 100g hydrogel with 42 % water.

3.7.3.1 Comparison of K^+, Na^+ and polyanion on impedance

During the eleven minutes of testing the passage of current increased by approximately 10 % resulting in an equivalent decay in impedance for adhesive hydrogels N26 to N35. This increase in current may be a result of the adhesive flowing better on the plate in the direction of current over time; thus the reduction in impedance may be a physical phenomenon.

Examining figure 3.37 indicates that increasing amount of either charge carrier resulted in a higher passage of current, hence a drop in impedance. The results also show that at low amounts of charge carrier neutral hydrogels containing KCl had higher impedance compared to those containing NaCl. However at levels greater than 0.06 (for those containing KCl) and 0.04 (for those containing NaCl) moles per 100 g of hydrogel

impedance levelled out indicating that increasing the amount of charge carrier beyond this point will not yield further reduction in impedance. Furthermore at lower quantities of charge carrier increasing amount of K^+ results in a larger reduction in impedance compared to Na^+. These disparities could be due to the size differences in size and mobility of K^+ and Na^+.

The size difference of the ions may also have an effect on the water structuring, although as an adhesive hydrogel is normally water starved it is expected that DSC results of these hydrogels would show that at such low water content (25 %) the water is likely to be predominantly bound.

In order to determine the reliability of the experimental points, an error of 5 % was applied and an equation for the trend in impedance obtained, as shown in figure 3.38. With an R^2 value of 98 %, where R^2 is a statistical measure of how well a regression line approximates real data points, the trend for hydrogels containing KCl was satisfied by the following equation:

$$\mathbf{y = -40.3\ln(x) - 95.6} \qquad \text{Equation 3.1}$$

With an R^2 value of 78 %, the trend for hydrogels containing NaCl was satisfied by the following equation:

$$\mathbf{y = -10.9\ln(x) - 12.5} \qquad \text{Equation 3.2}$$

where:

y = impedance (Ω)

x = number of charge carrier moles per 100g of hydrogel

These equations are only valid for the given composition containing 25% water and within the limits of 0.01 to 0.07 moles of charge carrier per 100g of hydrogel. It is anticipated that increasing the water content to a certain level would reduce impedance for all amounts of metal ion; however beyond this level further reduction would be unlikely.

On inspection, impedance of neutral hydrogels containing either KCl or NaCl and those of ionic hydrogels containing SPA and NaAMPS, as illustrated in figure 3.39, showed

that neutral hydrogels with less charge carrier had lower impedance compared to hydrogels of SPA and NaAMPS. This indicated that the nature of the anion also affects impedance. With neutral hydrogels containing electrolytes the anion is mobile, however, with SPA and NaAMPS hydrogels the anion is associated to the polymer chain and is therefore immobile. Thus, the nature of both cations and anions play a role in determining the hydrogels impedance.

Due to a division in opinion between the clinician and the instrument provider further investigations in this area were not carried out. Although neutral adhesive hydrogels produced were non-cohesive, increasing the amount of water (possibly 35 %) may yield a more cohesive network due to improved rate of polymerisation of NVP, as well as reduced impedance. The cohesiveness may be further improved by reduction of NNDMA. Furthermore neutral macromers may produce skin adhesives with low residual and potentially better cohesiveness. An example of such macromer is the polyvinyl alcohol based macromer nelfilcon A, which as discussed in chapter 4, is crosslinked by photo-polymerisation to form a contact lens. It is therefore not unreasonable to anticipate that with the ability to incorporate charge carriers, neutral hydrogels may be suited for use as a return electrode with the Optis system, as mentioned in section 1.5.7.3.

The ability to easily formulate a particular balance of electrolytes into neutral adhesives may also provide these hydrogels a niche in wound dressings. Taking the adult body as a whole the molar ratio of K^+:Na^+ is around 70:80.[91] In some adult body organs (such as the brain and liver) K^+ is greater than Na^+. The "sodium-potassium pump" regulates the gradient of these two electrolytes in order to maintain an optimal electrical charge for conduction of neural impulses that prompt muscular contraction. Generally intracellular fluid has a larger amount K^+, whereas with extracellular (interstistial) fluid Na^+ is the dominant ion. The excretion of K^+ is high in urine and sweat (K^+:Na^+ is approximately 7:15 and 8:45[91] respectively) relative to its concentration in most body fluids (for example in plasma K^+:Na^+ is approximately 5:140[95]). In wounds and burns where fluid loss, as distinct from blood loss, occurs the K^+:Na^+ ratio is closer to that of serum (5:140[95]) than to normal excretion fluids, sweat and urine, but loss of K^+ from local tissue because of the mass or volume loss is a cause of concern as the body normally retains K^+ while it easily gets rid of Na^+. In conclusion for wound dressing

applications an osmotic gradient for both Na^+ and K^+ will be helpful to reduce electrolyte loss, similar to the principle applied in sports drinks.[96] In a neutral adhesive hydrogel K^+:Na^+ ratios should be closer to those of sweat and urine than to plasma. The presence of calium ions (Ca^{2+}) would also be worth considering, even if this is in a separate hydrogel phase.

Chapter Four

PVA Release for Ophthalmic Applications

4. PVA RELEASE FOR OPHTHALMIC APPLICATIONS

A wide range of water-soluble polymers have been used historically both as wetting agents and as a means to increase the viscosity of contact lens solutions. The latter increases the residence time of the solution; thus if a therapeutic agent is incorporated into the solution its period of activity or persistence in the tear film is extended. In the earlier days of polymethyl methacrylate (PMMA) hard lenses, the primary application was in the form of lens wetting solutions. Here the role of the solution was seen to act as a mechanical buffer between the lens and the cornea: assisting in the initial wetting of the lens by tears and to aid cleaning of the lens prior to insertion. The polymers used in this application included a range of cellulosics:

methyl cellulose, carboxymethyl cellulose
hydroxyethyl cellulose, hydroxymethyl cellulose
hydroxypropylmethyl cellulose

and a smaller number of entirely synthetic materials of which polyvinyl alcohol (PVA) and polyvinyl pyrrolidone (PVP) were, and still are, the most important. An early paper by Lemp and Holly[97] summarised the relevant surface tension and wetting properties.

Over time there has been a natural evolution of solutions from early hard contact lens wetting materials, some of which were based on PVA and PVP, to the current range of comfort drops and artificial tears for soft contact lenses. Of the range of such solutions available in the European Union a very large number are based on PVA as shown in table 4.1. A much lesser number are based on PVP and interestingly most of these are used in conjunction with PVA.

Solution	Manufacturer	PVA	PVP	Other
Adsorbo tears	Alcon	x		PEG, HEC
bFGF Eye drops	Torita	x		
Contafilm	Allergan	x		
Dakrina	Dakryon	x	x	
Dulcilarmes	Dulci		x	
Dwelle	Dakryon	x		
Hypotears PF	Iolab	x		
Hypo Tears	Ciba Vision	x		
Just tears	Blairex	x		
Lacrilux	Allergan	x		
Liquifilm tears	Allergan	x		
Liquifresh	Allergan	x	x	
Murine	Ross	x	x	
Neo Tears	Sola Barnes-Hind	x		
Nutratear	Dakryon	x		
PMS artificial tears	Pharmascience	x		
PMS artificial tears plus	Pharmascience	x	x	
Siccagel	Thea	x		Carbopol 974P
Siccaprotect	Ursapharm	x		
Sno Tears	Smith and Nephew	x		
Soothe	Alcon EU		x	PEG 90
Tears plus	Allergan	x	x	

Table 4.1 PVA and PVP-based ophthalmic "comfort" solutions.

It has been suggested[98] that the good surface spreading characteristics of PVA gives it the ability to drag a 10 to 20 μm aqueous layer thereby increasing the corneal tear film thickness to relieve dry eye by prolonging tear break up time. In addition tears of patients with dry eyes tend to have a higher osmolarity thus, the application of a 1 % PVA hypotonic solution with an osmolarity of 150 mOsm/L is suggested[99] to provide improved symptom relief compared to an isotonic solution of 300 mOsm/L.

One under-exploited area is the use of the contact lens as a drug delivery device. Although the concept is superficially attractive there are several problems, particularly those associated with the incorporation of hydrophobic drugs in a hydrophilic matrix and achieving adequate control over release profiles to avoid, for example, premature leaching of the drug into the lens packing solution. Another barrier to this type of experimental work is the regulatory hurdle to clinical controlled release studies using contact lenses.

It has been reported[100] that the packing solution of Focus® Dailies® contains soluble PVA that has, apparently, leached from the lens matrix, which is itself composed of cross-linked PVA. Since PVA is a component of various comfort drops (table 4.1) it is reasonable to imply some correlation exists between the release of PVA and the perceived comfort of the lenses. Evidence for this link has been reported[101] but is not detailed here. However, it is logical to attempt to use the lens matrix as a delivery vehicle to bring about the controlled release of water-soluble polymers in an attempt to modify the lens-tear interface and bring about a similar effect by different means.

The most significant generic feature of the existence (by chance rather than by design!) of a clinically available lens that releases a water-soluble polymer is that it enables the development of an *in vitro* system, that is to say a PVA release model, that relates closely to *in vivo* release behaviour. In turn this would provide a platform for the development of more effective controlled release systems for other macromolecules that may, for example, prolong the enhancement of contact lens comfort. Hence a model that allows the effective design of controlled release comfort systems would prove invaluable in tackling the reduction of comfort-related wearer dissatisfaction. In order to develop this model a technique to enable the quantification of PVA release from the lens is required. The ability to measure changes in surface properties of the lens as a result of PVA loss is also desired, as this may have an effect on the perceived comfort of the lens. An understanding of the properties of PVA is therefore essential.

4.1 PVA nature and properties

PVA is a synthetic semi-crystalline aliphatic polyol polymer produced by the hydrolysis of polyvinyl acetate (PVAc) in the presence of sodium hydroxide (NaOH) (figure 4.1). PVAc, in turn, is made by the free radical vinyl polymerisation of vinyl acetate.

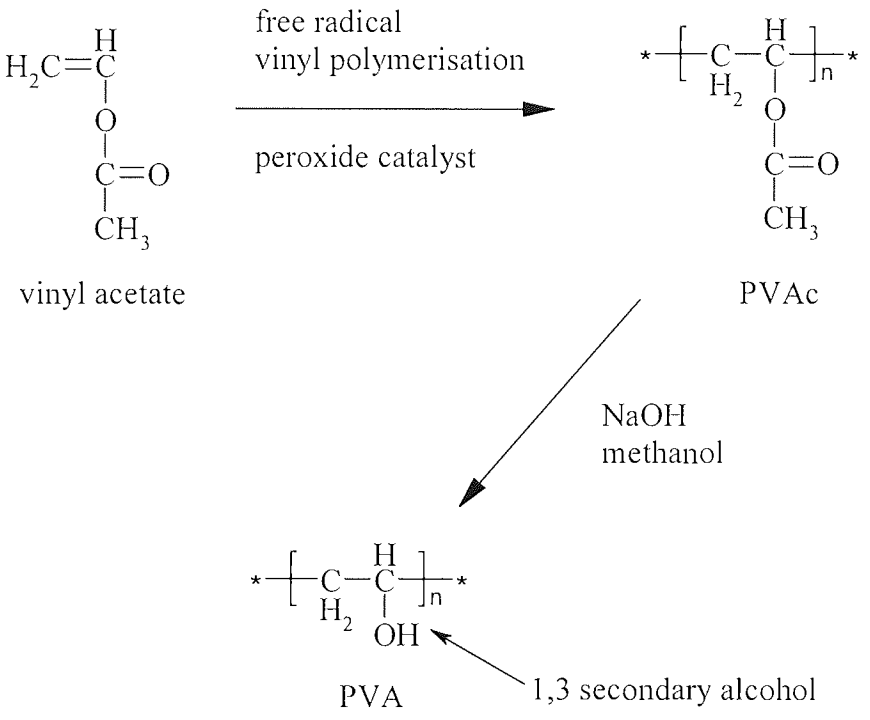

Figure 4.1 Synthesis of PVA.

PVA consists of a simple carbon-carbon (C-C) chain backbone with pendant hydroxyl (OH) groups, as shown in figure 4.1. The degree of hydrolysis determines the ratio of acetate ($OCOCH_3$) groups to OH groups. The C-C backbone is chemically and biologically quite inert; therefore it is considered non-toxic and non-carcinogenic. The longer the length of the C-C backbone the higher the molecular weight (MW). When molecular weight increases viscosity of aqueous PVA solutions increase but undesirably water solubility decreases.

The degree of hydrolysis also plays an important role in governing PVA properties. A high degree of hydrolysis will yield a high concentration of OH groups that can undergo

hydrogen-bond interactions allowing it to adhere to mucosal and tissue surfaces. However at high degrees of hydrolysis water solubility decreases because, even though OH groups have a high affinity to water, strong inter- and intra-molecular H-bonding impede its solubility in water. At lower degrees of hydrolysis the increased ratio of $OCOCH_3$ to OH groups increases and solubility increases as the hydrophobic $OCOCH_3$ groups weaken the inter- and intra-molecular H-bonding allowing for improved solubility at low degrees of hydrolysis. However PVA completely dissolves in water when heated to above 80 ^{o}C.

Since PVA contains both and hydrophilic (OH) and hydrophobic ($OCOCH_3$) moieties it forms micelles (figure 4.2) in solution.

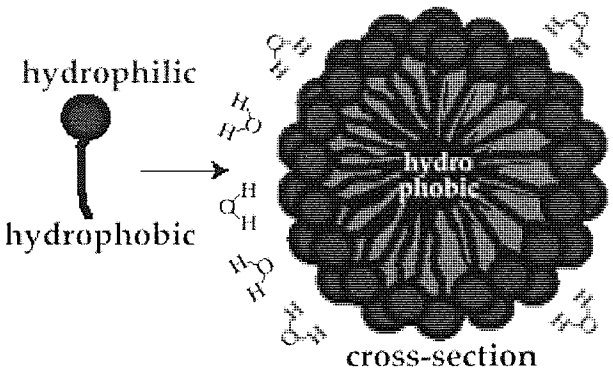

Figure 4.2 Cross-section of a micelle.

Micellisation gives it the ability to "take in" hydrophobic substances in a hydrophilic environment. It may also act as a reservoir releasing the hydrophobic substance as and when required. Hence it is routinely used as an emulsion stabiliser in formulation of pharmaceuticals and particulate polymeric drug delivery systems.[102] This ability also gives PVA based solutions lower surface tension allowing for better wetting of the cornea. PVA forms micelles at very low concentrations, known as the critical micellar concentration (CMC).[103]

However for some applications this dual functionality may be more of a disadvantage, as at hydrophobic interfaces, such as air, it undergoes chain rotation to expose the $OCOCH_3$ groups at the surface that shield the OH groups thereby reducing its capability of adhesion.

Besides the release of PVA as a soluble release agent (in the form of a linear polymer) in the eye as a means of aiding comfort, there have been more recent trends in the ophthalmic use of PVA as a drug delivery matrix[104, 105] when in the form of a crosslinked polymer. These two distinct functions come together in the nelfilcon A (Focus® Dailies®) contact lens matrix that, as mentioned previously, undergoes loss, leaching or release of soluble PVA to the ocular environment.

4.2 PVA modification and crosslinking

A unique property of PVA is that it is possible to chemically modify its backbone to form a polymer-analogue. The 1,3 secondary alcohol (figure 4.1) functional group allows for the formation of stable cyclic acetals (figure 4.3) at room temperature. This allows for a crosslinker and initiator to be added to the PVA backbone generating a PVA-crosslinker-initiator macromer, which can be polymerised. There are two advantages for doing this:

i. faster polymer conversion from solution to network
ii. can use water as a solvent hence, no need to extract the matrix to remove toxic solvents

This technique has already been employed by CIBA Vision to produce Focus® Dailies® (31% nelfilcon A, 69 % water) contact lenses (figure 4.3).

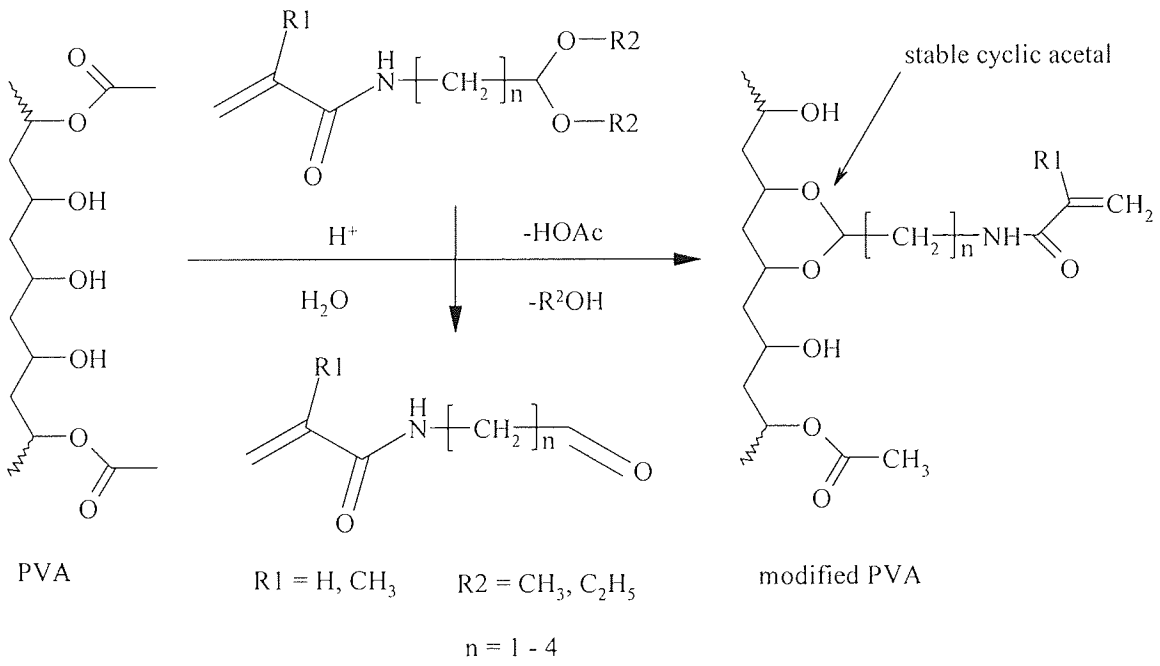

Figure 4.3 Modification of PVA backbone.[106]

The nelfilcon A macromer is simply dosed into a quartz mould and a beam of UV-light is passed through to crosslink the polymer in what is known as the "Lightsteam process"[106] (figure 4.4). This therefore provides a standard matrix with the potential to release water-soluble therapeutic agents in a controlled manner. However, due to inefficiencies of the process it is likely that residual PVA remains within the matrix which is released during storage and in eye.

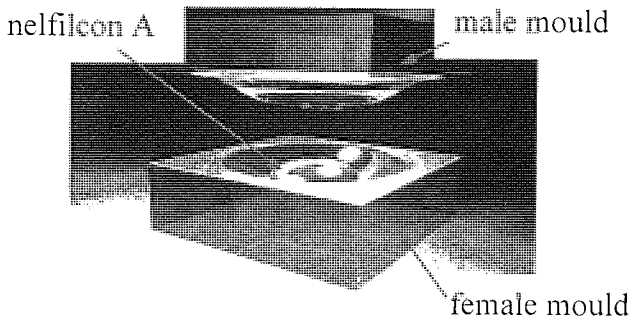

a) nelficon A dosed into quartz mould

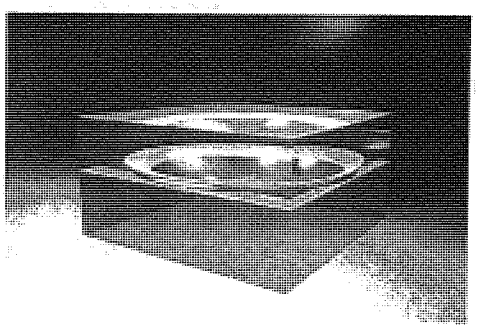

b) moulds lowered to within microns

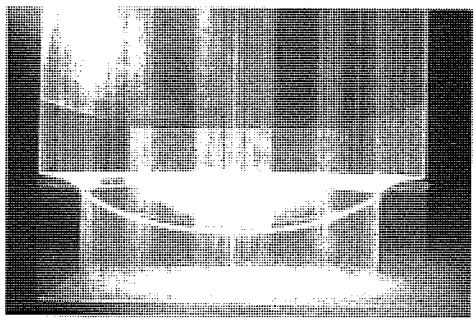

c) ultraviolet light passes through the moulds

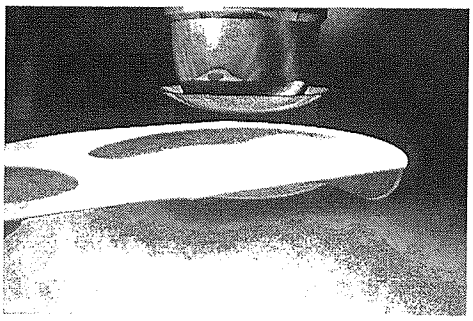

d) lens is placed into packaging

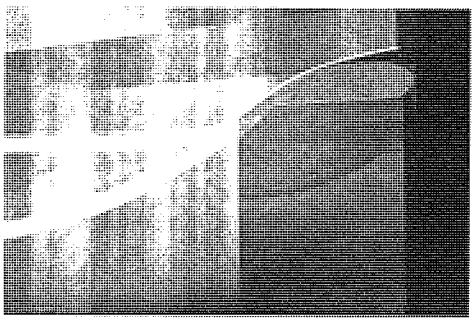

e) close-up of masked lens edge

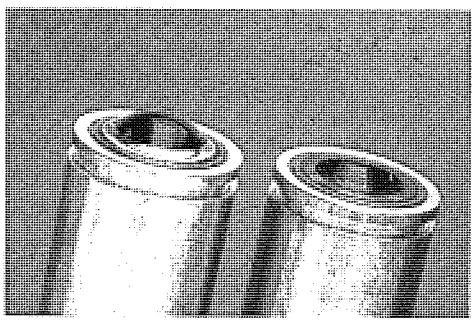

f) actual view of re-usable quartz lens mould

Figure 4.4 The Lightstream process.[107]

4.3 Quantification of PVA using refractive index

In order to study the release of a range of water-soluble polymers an assay technique is needed that is both qualitative and independent of specific chemical features of the polymer chain. In size exclusion chromatography of polymers refractive index (RI) is widely used for this purpose (the principle of this technique is detailed in section 2.2.6). For the purpose of this investigation a highly sensitive microrefractometer (Index Instruments automatic GPR 11–37X) was adapted for this purpose (figure 4.5).

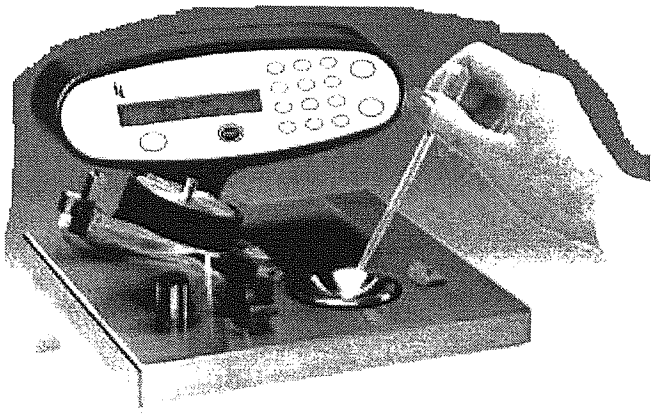

Figure 4.5 An example of an automatic microrefractometer.

The RI of a series of PVA standards of two molecular weights, 47000 (47k) and 61000 (61k), was measured (as outlined in section 2.2.6) at 25 °C in both isotonic phosphate-acetate (PABS) buffered saline and HPLC grade water (figure 4.6).

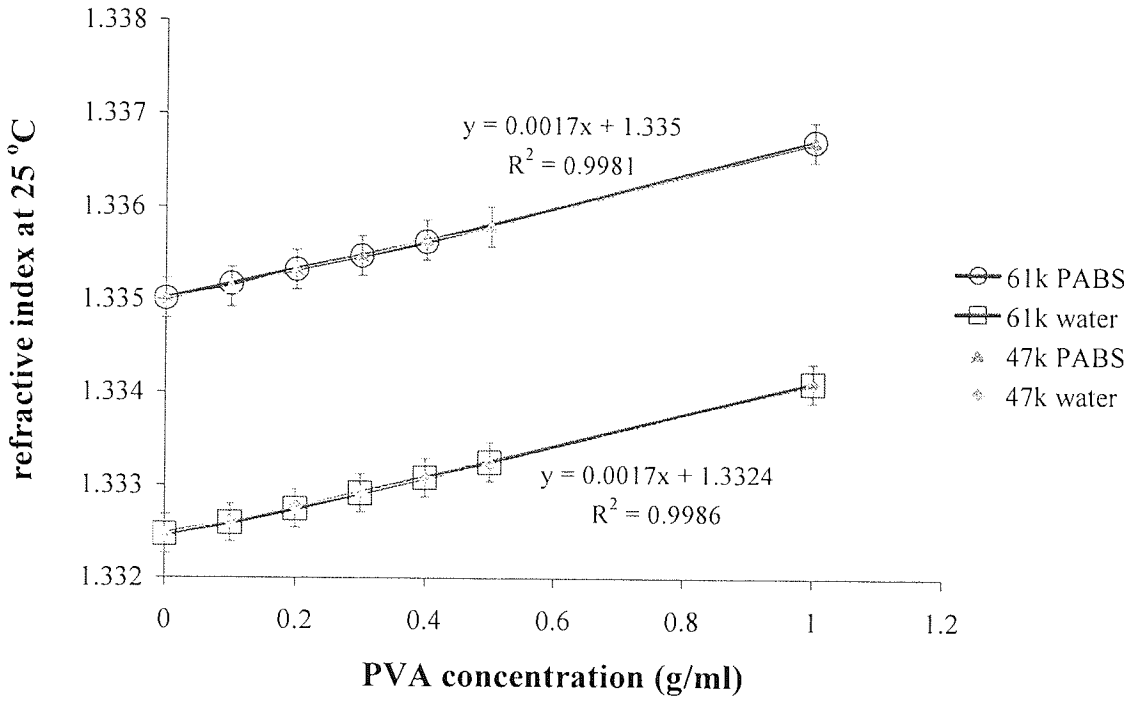

Figure 4.6 RI of 47k and 61k PVA in HPLC water and phosphate-acetate buffered saline.

The relationship between RI and concentration was found to be linear, however the technique was not capable of differentiating molecular weights. This is advantageous because it means that the technique can be used to measure the concentration of PVA released independent of molecular weight.

Linear relationships are characterised by the equation:

$$\mathbf{y = mx + c} \qquad \text{Equation 4.1}$$

where:

m is the gradient

c is the intersection point on the y axis when x = 0

Applying standard error to the data yielded the trend of RI with concentration. With an R^2 value of 99 %, where R^2 is a statistical measure of how well a regression line approximates real data points, the trend for PVA in isotonic PABS was satisfied by the following equation:

$$\mathbf{y = 0.0017x + 1.3350} \qquad \text{Equation 4.2}$$

With an R^2 value of 99 %, the trend of PVA in HPLC grade water was satisfied by the following equation:

$$\mathbf{y = 0.0017x + 1.3324} \qquad \text{Equation 4.3}$$

where:

y is RI of medium post extraction

x is PVA concentration (g/ml)

Hence, by measuring the RI of the extraction medium (y), it is possible to determine the concentration of PVA (x) in a given sample by rearranging and substituting for y in the above equations.

These equations are only valid for concentrations up to 1 % (w/v) PVA in both isotonic PABS and HPLC grade water at 25 °C. Equally it should be noted that the constant, c, is equivalent to the RI of the given release media without any PVA and this may be subject to slight variation on a batch to batch or on a daily basis. Thus it was deemed sensible to equate PVA concentration in terms of RI increment (equation 4.4).

$$\mathbf{x = \frac{y - RI\ extraction\ medium}{0.0017} = \frac{RI\ increment}{0.0017}} \qquad \text{Equation 4.4}$$

The use of mass spectrometry to detect and quantify PVA was also investigated (section 2.3.3). However very broad spectra were obtained and as yet there is insufficient clarity to enable different origins of eluted species to be determined.

4.4 Development of an *in vitro* release model

Having established a suitable assay technique, an *in vitro* method to model the *in vivo* release of PVA from a contact lens into the tear layer was developed. Given that commercial lenses were used it was possible to compare *in vitro* and *in vivo* PVA loss and thereby validate the method.

4.4.1 Large volume extraction

Initially PVA from commercial lenses was extracted using a large volume of media. Three Focus® Dailies® contact lenses were dried on filter paper and subsequently placed into lens cases containing 2 ml of extraction medium. To begin with both HPLC grade water and isotonic PABS were used as the extraction media. In an attempt to physically drive the PVA out of the lenses (to mimic blinking) the lens cases were subsequently placed on a shaker at 200 rpm for fifteen minutes. This was equivalent to an extraction media turnover rate of 8 ml per hour. After this period the contact lenses were removed and placed into separate cases with fresh amount of extraction media and placed on a shaker for a further fifteen minutes. This procedure was repeated for six hours. The cases remained on the shaker overnight in order to obtain a PVA release profile over a 24-hour period. The extraction media turnover rate overnight was equivalent to 8 ml per hour.

The RIs of the extraction media post extraction were measured as detailed in section 2.2.6. The RIs of the media post extraction were almost equal to that of the extraction media pre extraction. This was probably due to the fact that the concentration of the PVA released was very low compared to the extraction volume in terms of percentage that the refractometer was not able to detect the PVA released.

It was subsequently decided that a smaller extraction volume, similar to that of tear flow rate in the eye, should be used. In addition it was decided that isotonic PABS would be used as the extraction medium.

4.4.2 Small volume extraction

Tear flow rate of the eye is of the order of 1 µl/min, which may be conveniently approximated to 100µl per hour. Hence using this principle 100 µl of extraction media (isotonic PABS) was placed into two Eppendorf microtubes. A Focus® Dailies® contact lens was carefully placed into each microtube, as demonstrated in figure 4.7. The microtubes were then vortexed at 2400 rpm for fifteen seconds and left to stand for an hour before vortexing for a further fifteen seconds.

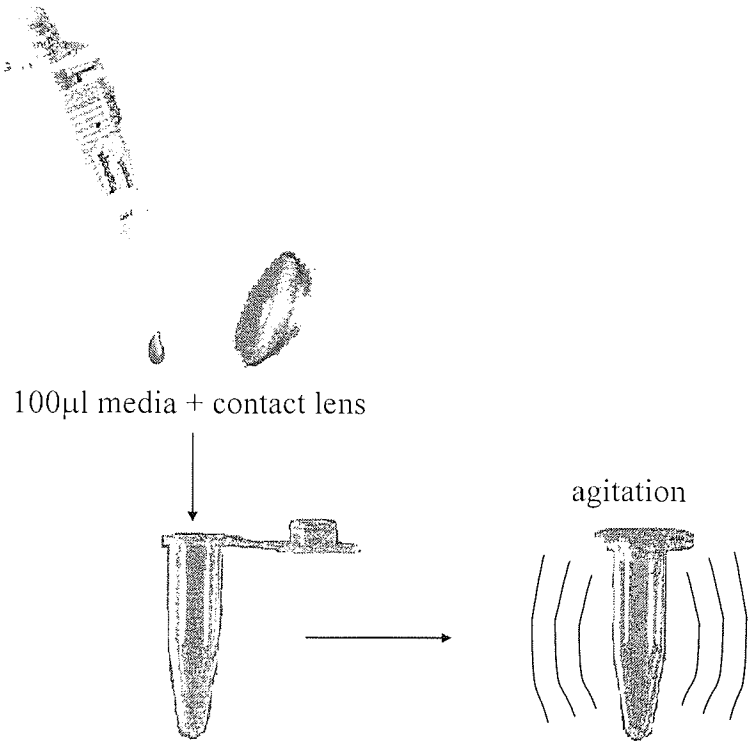

Figure 4.7 Schematic of in vitro PVA release.

The contact lenses were removed from the microtubes and placed in a second set of microtubes containing 100 µl of fresh extraction media and the procedure repeated over a six-hour period. The RI of the extraction media post extraction was measured as detailed in section 2.2.6. The RI increment was determined by subtracting the RI of the extraction medium from the RI of the extraction medium post extraction. These RI increments were then totalled, by adding that of the second hour to that of the first then that of the third hour to the combined RI increment of the second and first hour and so

on (see appendix 7), to give the cumulative RI. The extraction profiles of two Focus® Dailies® from the same strip in 100 µl of media are shown in figure 4.8.

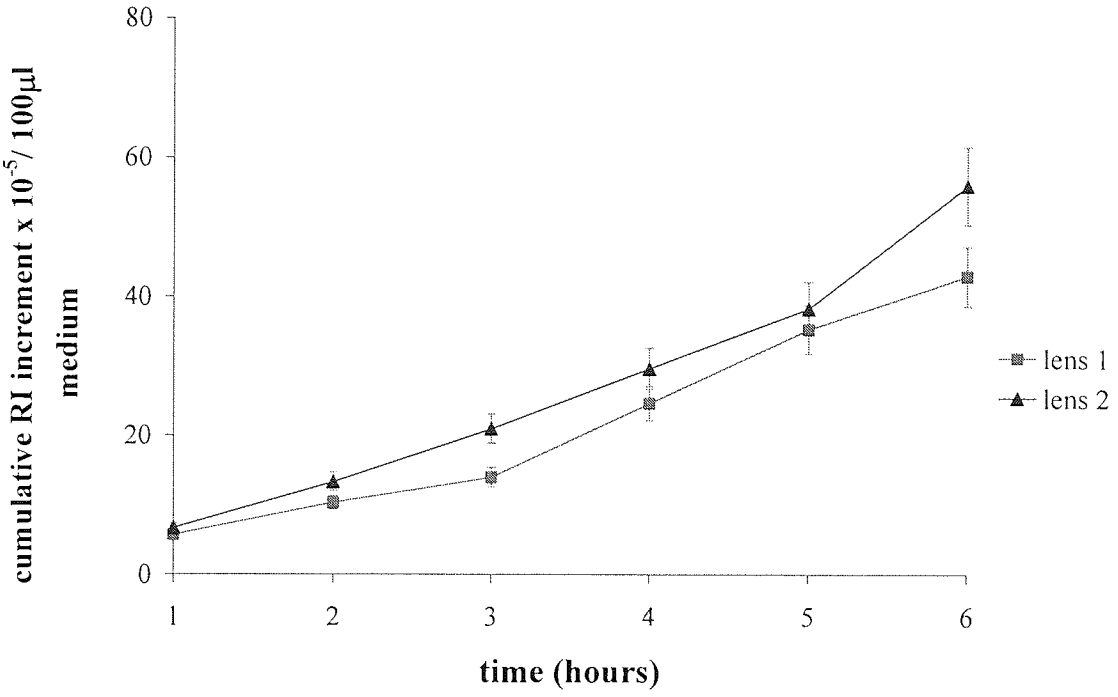

Figure 4.8 Extraction of PVA from a -3.00 Focus® Dailies® contact lens in a smaller volume of medium.

Figure 4.8 illustrates that there was a relatively linear relationship between PVA extracted with time. The difference in the release profile of the two lenses may be due to lens-to-lens variation innate of the manufacturing process, although a 10 % error has been applied.

The blinking motion of the eye results in shearing of the lens therefore, the need to design a physical step release the PVA from the lens surface was required. So far this had been done by either:

i. leaving the lens in a large volume of extraction medium on a shaker through out the extraction period or
ii. placing the lens in a much smaller volume of extraction medium and vortexing for fifteen seconds at the beginning and end of an hour.

Although extracting in a smaller volume enabled PVA to be detected using RI it was necessary to compare various methods of "physical extraction" in order to identify one which closely simulated blinking.

4.4.3 Agitation

It was assumed that the type of agitation that would best match in eye blinking would be one that drove out the most PVA *in vitro* at worst case scenario, that is to say a lens containing little unpolymerised PVA. Worn Focus® Dailies® lenses are likely to have a lower amount of unpolymerised PVA compared to unworn lenses. Thus worn lenses were used for this set of experiments. The lenses were stored in distilled water post wear. Prior to extraction the lenses were re-equilibrated overnight in isotonic PABS, the extraction medium. Three methods of extraction were compared.

i. Lens placed in microtube with 100 µl isotonic PABS and vortexed for five seconds at the beginning and end of a one-hour extraction period. Lens was then removed and placed in another microtube containing fresh extraction medium and process repeated over five hours.

ii. Lens placed in microtube with 100 µl isotonic PABS and left in an ultrasonic cleaner for five minutes at the start of each hour. Lens was then removed and placed in another microtube containing fresh extraction medium and process repeated over five hours.

iii. Lens placed in microtube with 100 µl isotonic PABS and left to stand for one hour. Lens was then removed and placed in another microtube containing fresh extraction medium and process repeated over five hours.

RI of the extraction media post extraction was measured as detailed in section 2.2.6. The cumulative RI increment was then determined (see appendix 7). The extraction profiles in 100µl of media using different agitation techniques are illustrated in figure 4.9.

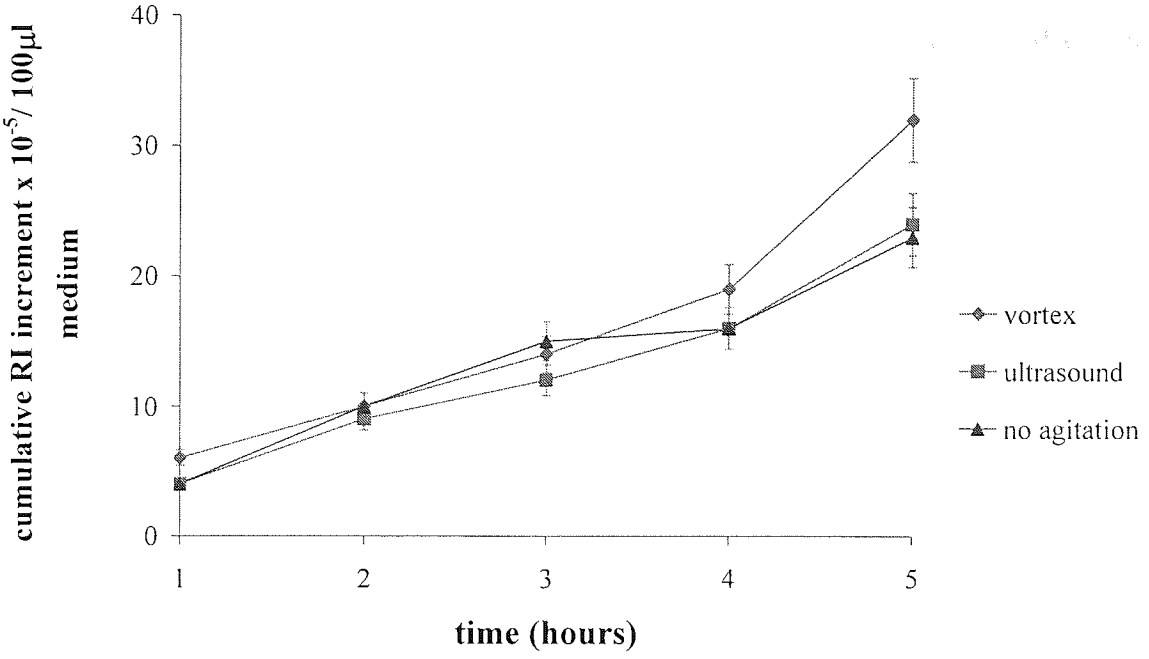

Figure 4.9 Comparison of various agitation methods on PVA release.

For the first three hours the method of agitation did not have a significant effect on PVA release from the contact lens, however after this initial release period there was a marked difference. The vortexed lens released the most PVA followed by the lens placed in the ultrasonic cleaner which was closely followed by the lens that was not agitated.

The similarity in the amount of PVA release during the first three hours suggested that an equilibrated lens releases PVA from the surface of the lens. After this initial release period the concentration of surface PVA diminishes, thus agitation caused residual PVA within the lens matrix to migrate to the surface. Hence the most ferocious method of agitation shifted more PVA to the surface.

From these results it was decided that an *in vitro* system that would most closely simulate *in vivo* eye behaviour would be to place the lens in 100 µl extraction medium and vortex for fifteen seconds at the beginning and end of a one hour extraction period. The lens would then be removed and placed in 100 µl of fresh extraction medium and the process repeated for the required period.

4.5 PVA release during storage

The packing solution of Focus® Dailies® contains soluble PVA, as mentioned earlier. RI measurements Focus® Dailies® lenses packing solution from various years and lots were taken (see appendix 7) to establish whether there is a relationship between storage time and amount of PVA in packing solution (figure 4.10).

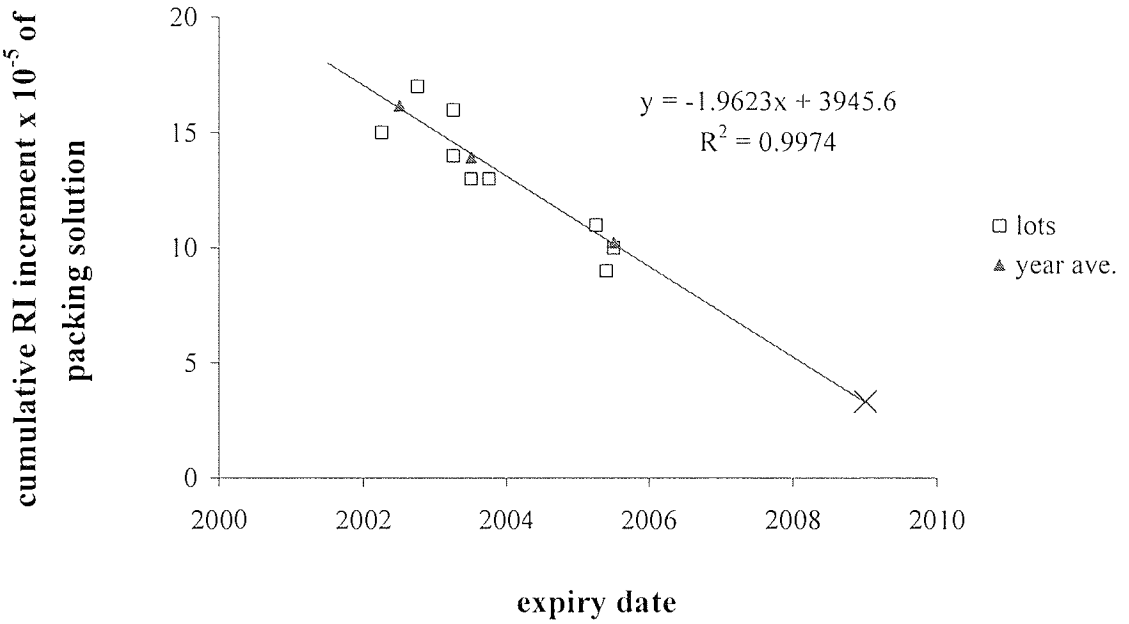

Figure 4.10 Correlation of packing solution RI and expiry date.

From the above graph (figure 4.10) the correlation between expiry date and RI of the packing solution was linear. RI values of the packing solution of older lenses were higher, indicating an elevated concentration of PVA, compared to newer lenses.

These measurements were taken at the beginning of 2004. Lenses produced at this period would expire at the beginning of 2009. By extrapolating the graph forward to 2009 the packing solution of the lens produced at the same time the tests were carried out would have a RI increment of approximately $4x10^{-5}$. Given that this was slightly higher than that of isotonic PABS, it suggested that a step in the manufacturing process might enhance the release of PVA from the contact lens.

Contact lenses are required to undergo a sterilisation process post manufacture. In the case of Focus® Dailies® the lenses are autoclaved post-packaging. Since this occurs at high temperatures the lens is placed under "stress" which may enhance the release of PVA from the surface. Hence, the effect of autoclaving on PVA release was investigated.

4.6 Effect of autoclaving on PVA release

In order to verify that autoclaving caused PVA from the lens to leach into packing solutions, three mature commercial, that is to say already autoclaved, Focus® Dailies® lenses were removed from their packing solution and placed in 0.5 ml fresh isotonic PABS. The lenses were then autoclaved with pressurised steam (15 psi) at a temperature of 121 °C for twenty minutes with eight minutes of free steam and left overnight. RI measurements of the isotonic PABS were taken and the RI increment determined as before (see appendix 7).

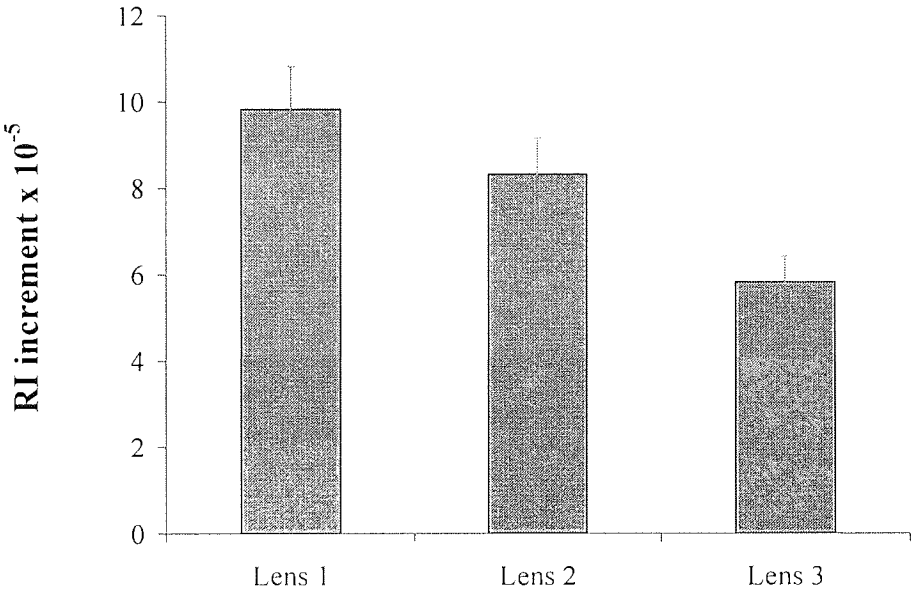

Figure 4.11 Effect of autoclaving on PVA release.

Figure 4.11 demonstrates that the RI of the fresh isotonic PABS increased as a result of autoclaving. The process of autoclaving undoubtedly caused the lens to release PVA into the packing solution.

Heat is likely to induce ageing and according to figure 4.10 the RI of packing solution increases by approximately 1.96×10^{-5} per year; thus an increase of RI by 4×10^{-5} as a result of autoclaving "ages" the lens by approximately 2 years. However, as shown in

figure 4.11 the inter lens RI increment varied. This was likely to be due lens-to-lens variation as all lenses were from same lot but lens 1 was from a different strip.

To determine whether re-autoclaving the lens would affect the release rate of PVA, PVA release from a standard commercial and re-autoclaved commercial Focus® Dailies® lens in 100 µl isotonic PABS were compared, as shown in figure 4.12, using the *in vitro* release system (section 4.4.2). RI of the extraction media post extraction was measured as detailed in section 2.2.6. The cumulative RI increment was then determined (see appendix 7).

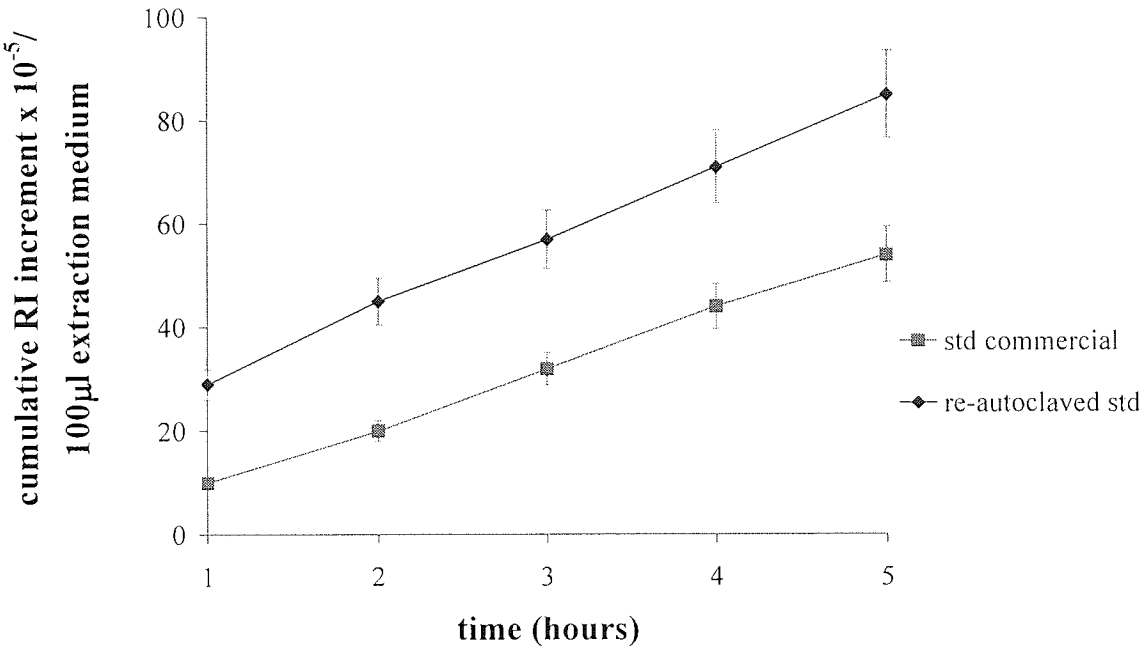

Figure 4.12 PVA release from a standard and re-autoclaved Focus® Dailies® lenses.

The re-autoclaved lens released more PVA during the first hour of extraction. This re-illustrated that autoclaving tends to boost PVA concentration at the lens' surface. However for both lenses the rate of release (gradient of the line) was very similar (figure 4.12).

Although the autoclaving process seemed to increase the concentration of PVA at the lens' surface, it was desired to determine whether this procedure resulted in better equilibrated lenses, that is gave a more constant PVA release, or whether it caused the

extraction of PVA leading to a lower residual release than a non-autoclaved matrix. This was verified by extracting non-autoclaved and autoclaved Focus® Dailies® test lenses (figure 4.13) in 100 µl of isotonic PABS using the *in vitro* release system (section 4.4.2). For direct comparison between not autoclaving and autoclaving, non-autoclaved Focus® Dailies® test lenses were obtained from Ciba Vision and then autoclaved using the same process outlined at the beginning of this section. RI of the extraction media post extraction was measured as detailed in section 2.2.6. The cumulative RI increment was then determined (see appendix 7).

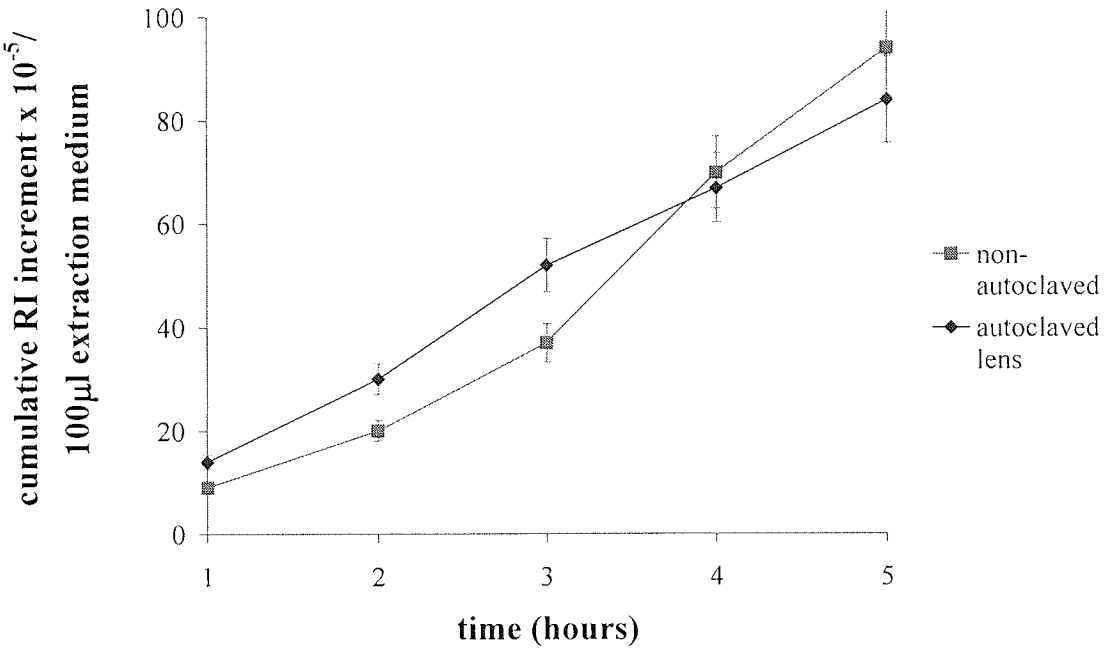

Figure 4.13 PVA release from a non-autoclaved and autoclaved Focus® Dailies® test lenses.

The plot of figure 4.13 illustrates that the autoclaved lens did not have a significantly higher initial amount of PVA released compared to the non-autoclaved lens, as would have been expected from previous results (4.11 and 4.12) figure. However the rate of release from the autoclaved lens was almost even, unlike that of the non-autoclaved lens throughout the extraction period. Thus, it appeared that the autoclaving process equilibrates the residual PVA in the matrix leading to a uniform post-autoclaved rate of release.

Although it may seem surprising that the initial amount of PVA released for the autoclaved lens was not higher, there are two potential factors which may have contributed to this. These are:

i. These lenses are test lenses produced on a different line to commercial Focus® Dailies® lenses.
ii. The duration, temperature, and/or number of cycles of the manufacturing autoclaving procedure may differ from the one employed, for example the cycle may occur twice with the first one equilibrating the residual PVA in the matrix and the next cycle "ages" the lens.

4.7 Enhancing PVA at the surface of the contact lens

The results from the previous section indicated that the limiting factor of PVA release from the contact lens was the PVA concentration at the lens' surface. This in turn was governed by the rate of movement of residual PVA from within the matrix to the surface. Thus if by some mechanism the surface of the lens could be increased, the amount of PVA released should also increase.

Inadvertently, during the extraction of two commercial Focus® Dailies® lenses in 100 µl isotonic PABS using the *in vitro* release system (section 4.4.2) one happened to tear during the second to third hour extraction period. The cumulative RI increment profile is shown in figure 4.14. RI of the extraction media post extraction was measured as detailed in section 2.2.6, the primary results are tabled in appendix 7.

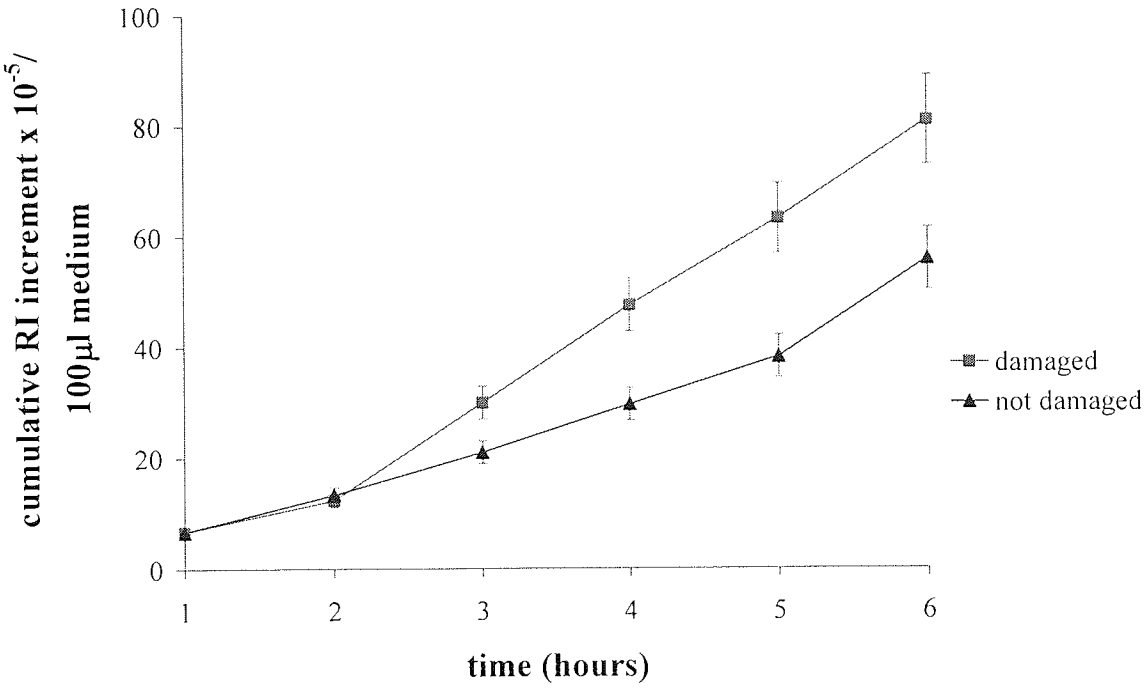

Figure 4.14 Effect of PVA release when the surface of the contact lens is increased.

During the first two hours of extraction both lenses released a similar amount of PVA. After this period the damaged lens release more PVA. Compared to the non-damaged lens, the damaged lens effectively has a larger surface area. From these results (figure 4.14) it is proposed that:

i. PVA release is determined by the PVA concentration at the surface of the lens
ii. the marked increase of PVA release from the "interior" of the lens when it tore suggests that there is a relatively larger amount of PVA within the matrix that could potentially be released.

A larger amount of PVA at the surface of the contact lens may potentially reduce dry eye discomfort experienced by contact lens wearers. Given that there are physical limitations to increasing the surface area of a contact lens, the effect of increasing surface PVA by incorporating mobile PVA into the lens matrix was investigated. It was anticipated that the additional PVA may cause an increase of PVA release from the lens surface, hence may improve end of day discomfort for lens wearers. This hypothesis is evaluated in the next section.

4.8 Incorporation of mobile PVA into the lens matrix

Two sets of Focus® Dailies® test lenses containing an additional 0.2 % mobile 47k and 61k uncrosslinked PVA were obtained from CIBA Vision. The packing solution RI of each type of lens was measured, as detailed in section 2.2.6, and compared to a commercial (control) contact lens (figure 4.15). The primary results are tabled in appendix 7.

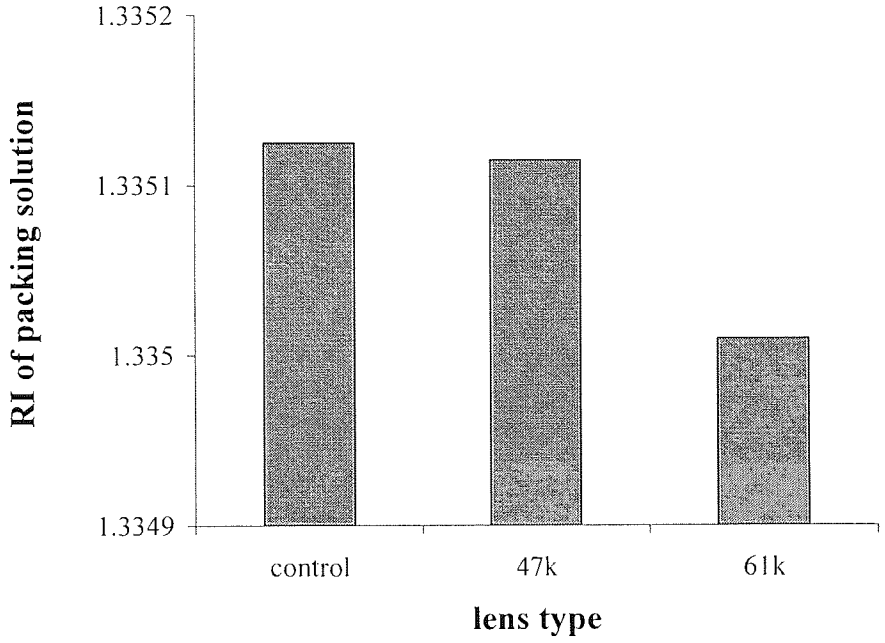

Figure 4.15 RI of packing solution of Focus® Dailies® lenses containing mobile PVA of varying molecular weight.

The packing solution RI was lower for both lenses containing added mobile compared to the control lens. However, the difference was more noticeable with the lens containing the higher molecular weight (61k) mobile PVA. There are three possible explanations for this type of behaviour:

i. The higher molecular weight (MW) PVA are not as mobile as lower MW ones, thus passive diffusion from the matrix to the surface takes longer.

ii. Higher MW PVA might act as a type of crown ether complexing around the Na^+ in the isotonic PABS effectively lowering the concentration of NaCl in the water hence, lowering the RI of isotonic PABS closer to that of water (1.33250 at 25 °C).

iii. The 61k lenses may have been contaminated with process water at the time of packaging.

The release profile of these lenses was also determined, as demonstrated in figure 4.16, using the *in vitro* release model (section 4.4.2). RI of the extraction media post extraction was measured as detailed in section 2.2.6 and the cumulative RI increment determined (see appendix 7).

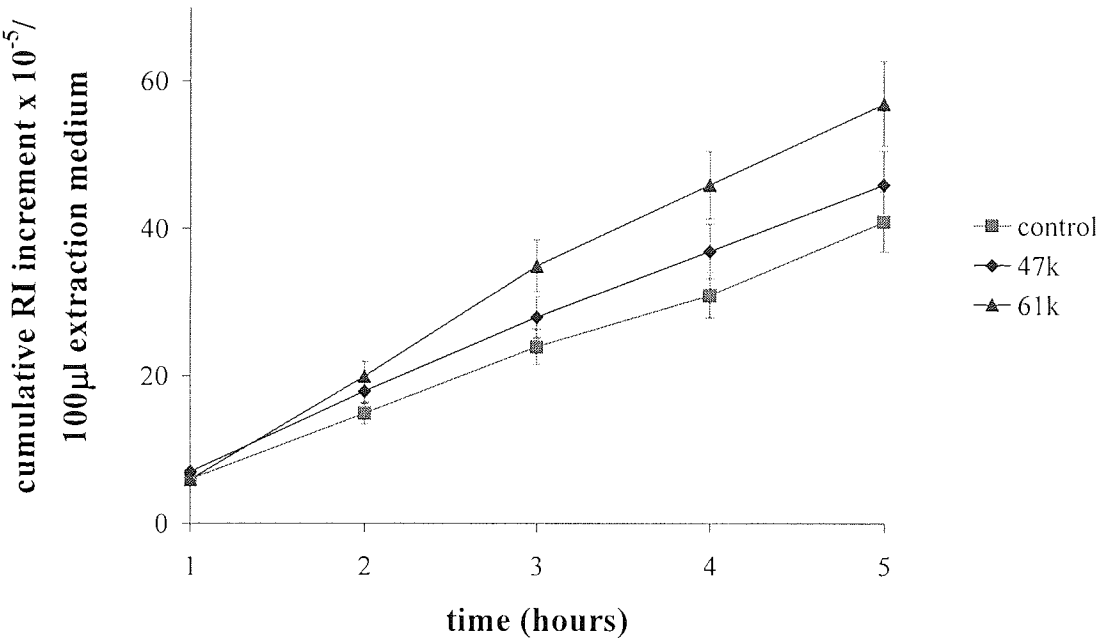

Figure 4.16 Release profile of lenses containing mobile PVA.

Figure 4.16 illustrates that overall the lens containing added 61k PVA released the most, followed by the 47k and then the control lens. There are two potential reasons for this to have occurred:

i. The higher MW PVA may not be compatible with the lens matrix, thus with agitation it is quickly displaced to the lens surface.

ii. Since the 61k lens had a lower packing solution RI compared to the packing solution of the 47k lens, the 61k matrix had more residual PVA within its matrix.

By comparing and contrasting the trends in RI for the packing solution (figure 4.15) and the extraction medium (figure 4.16) from the *in vitro* release system, it can be suggested that the 61k lens packing solution RI is lower as the 61k PVA is not as mobile as the 47k PVA, thus more of 61k PVA remains within the matrix. Agitation assists the displacement of the 61k PVA from the matrix to the surface of the lens. However, even with agitation the 61k PVA does not reach the surface immediately. During the first to third hour the plot of the 61k lens release had a steeper gradient compared to that of the 47k lens. This may be due to a "burst" release occurring as after this the release rate was similar to that of the 47k lens (figure 4.16).

4.9 PVA release from worn lenses

To this point (sections 4.5, 4.6, 4.7 and 4.8) it has been established that:

i. older lenses had a higher amount of PVA in the packing solution; indicating a higher amount of PVA at the surface of the lens
ii. PVA release was limited by its concentration at the surface
iii. autoclaving the lens equilibrated the PVA in the matrix leading to a uniform post-autoclaved rate of release and also "aged" the lens as it enhanced the PVA concentration at the surface.
iv. there was a relatively large reservoir of residual PVA within the matrix available for release
v. adding mobile PVA to the matrix increased the concentration at the surface of the lens

These deductions were obtained from investigations carried out on unworn Focus® Dailies® lenses. It therefore seemed logical to evaluate the release rate of PVA from contact lenses with a depleted amount of PVA. Given that PVA is released from the lens during wear it was assumed that worn Focus® Dailies® lenses would have less PVA in its matrix.

Commercial Focus® Dailies® contact lenses were worn for eight hours and then placed in an empty airtight vial overnight. These "fresh" *ex vivo* lenses were extracted the following day in 100µl isotonic PABS using the *in vitro* release system (section 4.4.2). RI of the extraction media post extraction was measured as detailed in section 2.2.6. In order to determine the cumulative RI of the ninth hour the cumulative RI for the eight hour of the worn lenses was calculated using the trendline equation obtained for the first six hours of unworn lenses extracted *in vitro*. This was then added to the RI increment of the first hour of *in vitro* extraction of the worn lens to obtain the cumulative RI for the ninth hour (see appendix 7). A comparison between PVA release rates of worn and unworn lenses is demonstrated in figure 4.17.

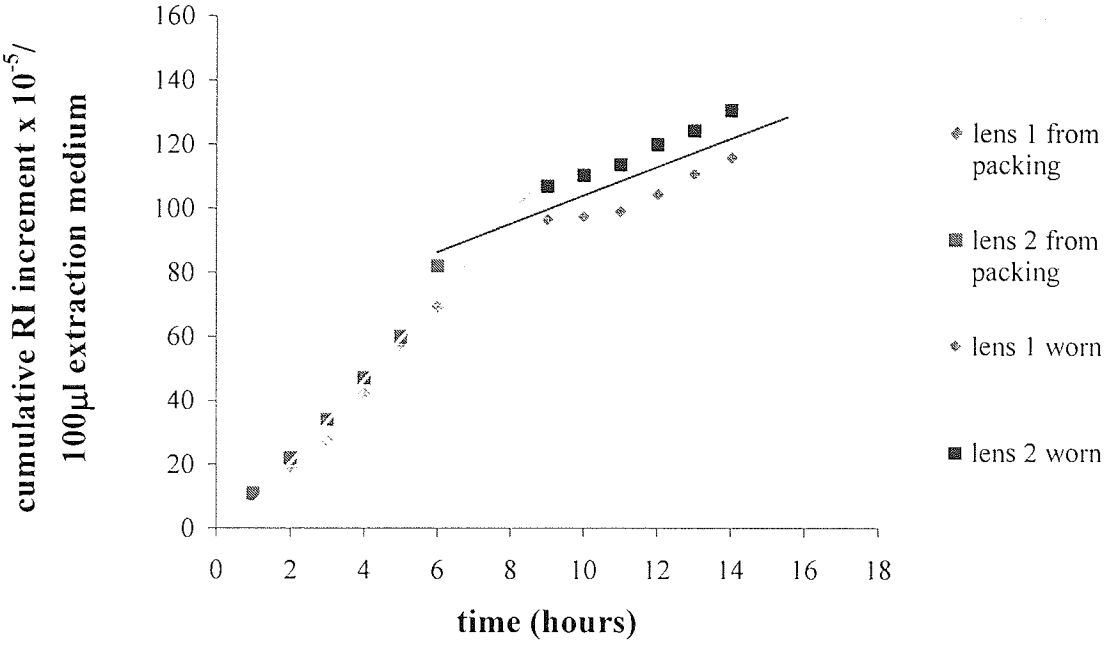

Figure 4.17 Release rates from unworn and worn lenses.

Figure 4.17 shows that the worn contact lenses continued to release PVA after eight hours of wear. However, the gradient of the average linear plot was not as steep as that of the extracted unworn lenses. This indicated that the rate of release from the worn contact lenses was lower, which in turn implied that the worn lens had "lost" most of its surface PVA in eye and that surface depletion of PVA in eye occurred by an "active" mechanism that outstripped the ability of passive diffusion to maintain surface concentration. In addition "lens 1 worn" released less PVA then "lens 2 worn"; this may have been due to the lenses being of different powers. "Lens 1 worn" was of a lower power, therefore a thinner lens than "lens 2 worn" thus, likely to have had less residual PVA.

These results also indicated that the *in vitro* model could not keep up with the in eye extraction. Nonetheless this *in vitro* model gave some simulation of *in vivo* release (much faster than passive diffusion) proving a useful tool for comparing the various factors that contribute to the mechanism of PVA release *in vivo*. In addition this model showed that although the worn lenses continued to release PVA, it was at a lower rate; hence there was potentially a lower amount of PVA on the front surface of the lens. Since the surface of the contact lens may affect both the feel of the sliding motion of the

eyelid and the spreading of the tear film during a blink cycle, potentially having a major effect on lens comfort, it was deemed useful to compare the coefficients of friction of a lens surface as it get worn. Therefore the ability to measure the coefficient of friction (μ) of contact lenses *in vitro* would prove useful for comparing different lens surfaces and subsequently the effect on patient comfort.

4.10 Frictional properties of Focus® Dailies® lenses

The study of friction and lubricity involves the measurement of the resistance to motion of contacting surfaces. This is expressed in terms of μ the coefficient of friction (see section 2.2.7). During a blink cycle there is sliding motion between the eyelid and the front surface of the eye. When a lens is inserted in the eye it is not able to support the pressure of the eyelids during blinking and this causes it to move resulting in a resistance to friction between the lens and the eyelid. The properties of the lens' front surface are likely to affect the frictional forces between the eyelid and the lens, potentially changing the blinking feel. Although the frictional forces involved during blinking are very small their cumulative effect on contact lens wear is expected to have longer-term (such as end of day) implications.

When a contact lens is introduced into the eye its front surface is coated with tear fluid, which contains a superficial lipid layer (see section 1.5.5). The mechanics of the tear film also plays an important role in the interaction between the lens surface and the eyelid. When the eyelid closes the tear lipid layer is compressed and when the eyelid opens it spreads. The lipid spreading behaviour of individuals produces visible interference patterns as demonstrated figure 4.18.

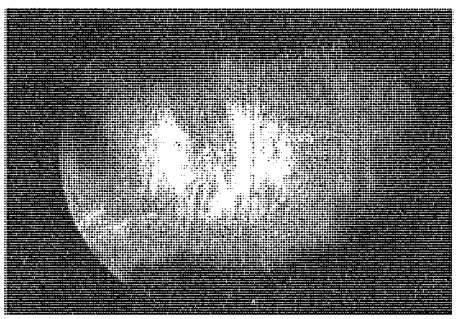

Figure 4.18 Spreading behaviour of a healthy tear film.[108]

If wear of the contact lens' front surface causes inadequate spreading, rapid tear evaporation that compromises the tear layer can sometimes be observed and this results in dry eye as shown in figure 4.19.

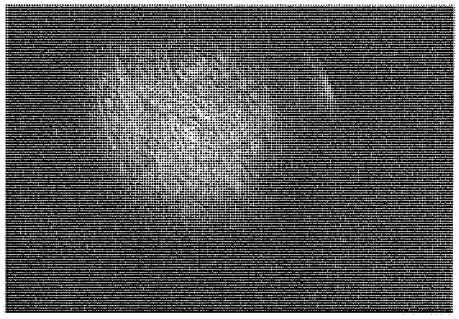

Figure 4.19 Tear film spreading behaviour in a "dry" eye.[108]

This invariably causes a rise in μ between the eyelid and the contact lens' surface during a blink cycle. Furthermore it can be deduced from the Stribeck curve (section 2.2.7) that a reduction in the thickness of the lubricating layer may alter the lubricating regime and therefore lubricating mechanism.

Although instrumentation is available for determining the μ of artificial joint components, there are as yet no established *in vitro* techniques that reflect the important aspect of the interaction between the contact lens and the anterior eye. In conjunction with an instrument manufacturer a high sensitivity tribometer was identified and adapted for the study of contact lens biotribology (see section 2.2.7). This subsequently enabled the comparison of μ of a lens surface "modified" by PVA and one that was not. In addition the effect of PVA deteriorating at the surface of the lens as a result of wear could also be investigated.

4.10.1 Effect of PVA on the coefficient of friction

In order to compare the μ of a lens surface "modified" by PVA and one that was not, the μ for unworn Focus® Dailies® and Biomedics®55 (45% oculfilcon D, which is HEMA and MA based, 55% water) lenses were determined.

To measure the μ of a contact lens it was placed on the convex mould of the nanotribometer. The substrate, a smooth rigid polymer film (Melinex®), was clipped onto a moving table and 50 μl of the lubricating solution placed on the substrate. The table was raised until the contact lens came into contact with the lubricating solution (see section 2.2.7). The table was then allowed to move enabling the substrate to

"carry" the meniscus of the lubricating solution over the lens, similarly to the eyelid carrying the tear meniscus over the lens or cornea.

The μ was taken as an average of six passes of at least three lenses. Both the static (μS) and dynamic (μD) coefficients of friction (see section 2.2.7) were determined as it is not yet clear which one is most significant. The effect of three lubricating solutions: HypoTears®, because its interfacial behaviour is very similar to that of tears, the respective packing solutions and isotonic PABS on the μ of both types of lenses were compared (figures 4.20 and 4.21).

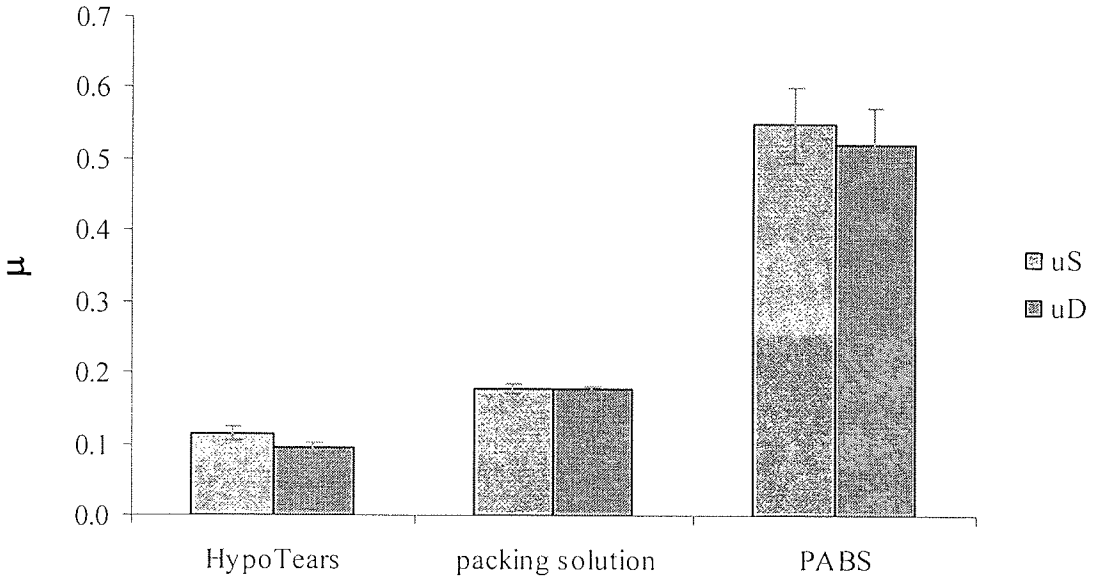

Figure 4.20 The coefficient of friction of a Focus® Dailies® lens with various lubricating solutions.

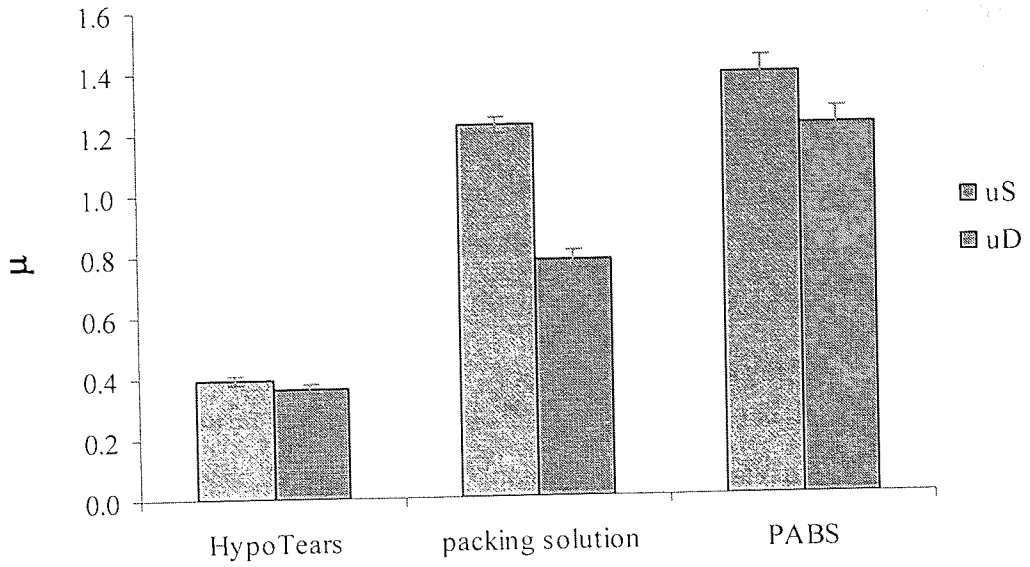

Figure 4.21 The coefficient of friction of a Biomedics®55 lens with various lubricating solutions.

Comparing figures 4.20 and 4.21 clearly shows that μ for the Biomedics®55 lens was significantly higher than the Focus® Dailies®. This suggested that the lubricating ability of the PVA present at the surface of the lens lowered μ substantially.

A second observation was that there was a marked difference in the μ of the two lens materials with their respective packing solutions. The μ of Biomedics®55 in its packing solution was similar to that with isotonic PABS, whereas with Focus® Dailies® the μ with its packing solution was closer to that with HypoTears®. This may have been due to the surface tension of the Biomedics®55 packing solution being very similar to that of isotonic PABS, whereas the Focus® Dailies® packing solution is modified by soluble PVA, which leaches from the lens and reduces the surface tension, which in turn reduced the μ.

Thirdly, the static friction (μS) for the Biomedics®55 lens with its packing solution and PABS was substantially higher than its dynamic friction (μD), whereas with Focus® Dailies® the two were comparable. However, with HypoTears® the difference between μS and μD for the Biomedics®55 lens was lower and overall its μ was lower with

HypoTears® than with its packing solution. This clearly illustrated the importance of the lubricating layer's properties. HypoTears® contains 1 % PVA, therefore has a lower surface tension than the Biomedics®55 packing solution, consequently it reduced the force required to begin moving the lens against Melinex®, thereby significantly reducing μS. However the μ of Focus® Dailies® with HypoTears® was still lower than that of Biomedics®55. This suggested that the PVA on the surface of the lens has a larger influence on μ than the PVA in the lubricant.

Generally with surfactant-free isotonic PABS μ was much higher and experimental results had a lower degree of reproducibility. This was probably due "slip-stick" behaviour as a result of the isotonic PABS having very little surface activity.

4.10.2 Effect of lens wear on the coefficient of friction

A 16 hour clinical study[109] of patients wearing a Focus® Dailies® Aqua Release lens (Focus® Dailies® lenses containing additional non-functionalised PVA) in one eye and a Biomedics®55 lens in the other enabled the evaluation of the μ of worn lenses against unworn lenses for both types of lenses.

The contact lens was placed on the convex mould of a nanotribometer as already detailed. The substrate, a smooth rigid polymer film (Melinex®), was clipped onto a moving table and 50 μl of HypoTears® placed on the substrate. The table was raised until the contact lens came into contact with the HypoTears® (see section 2.2.7). The table was then allowed to move enabling the substrate to "carry" the meniscus of the lubricating HypoTears® over the lens.

The static (μS) and dynamic (μD) coefficient of friction (see section 2.2.7) were taken as an average of six passes of at least three lenses. The coefficients of friction of unworn and worn Focus® Dailies® Aqua Release (AR) lens and Biomedics®55 lens were compared and contrasted (figures 4.22 and 4.23).

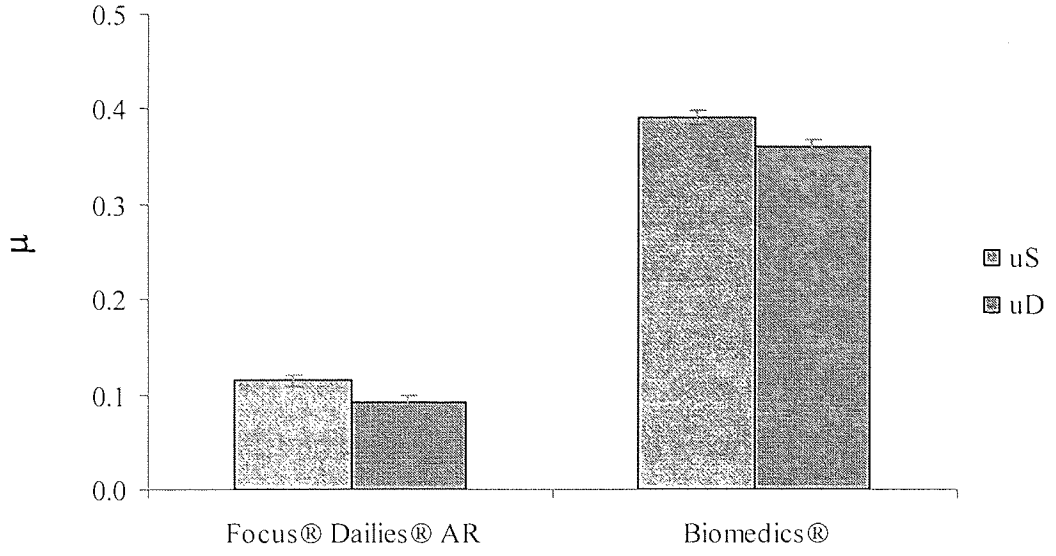

Figure 4.22 The coefficient of friction of unworn Focus® Dailies® Aqua Release and Biomedics®55 lenses.

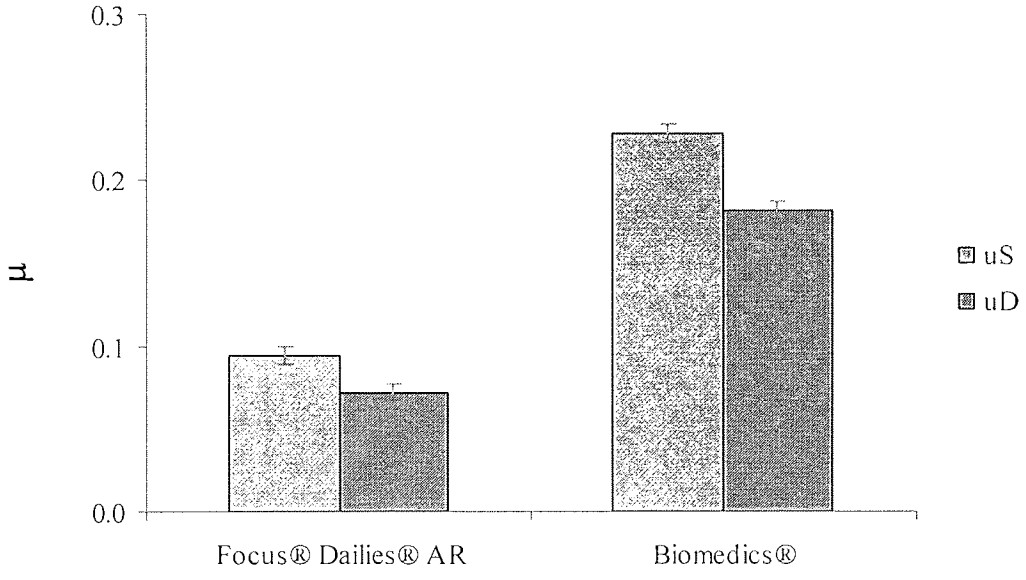

Figure 4.23 The coefficient of friction of worn Focus® Dailies® Aqua Release and Biomedics®55 lenses.

Comparing figure 4.22 and 4.23 illustrated that the μ of an unworn or worn Biomedics®55 lens was significantly higher than the Focus® Dailies® Aqua Release

lens. This again exemplifies that the presence of PVA on the surface of Focus® Dailies® Aqua Release lenses lubricated the surface, therefore reduced the μ. Furthermore the clinical study[109] indicated a very significant forced choice preference for the Focus® Dailies® Aqua Release lens over the Biomedics®55 lens, both on insertion and at the end of 16 hours wear. This in turn suggested that comfort enhancement appears to be more related to modification of lens surface by temporary anchoring of emergent PVA molecules than the modification of tear layer *per se*.

For both type of lenses the μ of the worn lens was lower than unworn lens. This was probably because initial protein and lipid deposition reduces the μ somewhat, however if a lens is worn over longer periods of time (days) the progressive degradation of protein and lipid may lead to a deterioration of surface properties, including lubrication. In addition further protein and lipid deposition may destabilise the tear film causing a breakdown in lubrication and it is this breakdown in lubrication that is likely to have the most dramatic effect in increasing μ.

Chapter Five

Analysing Release from a Monolithic Device

5. ANALYSING RELEASE FROM A MONOLITHIC DEVICE

This chapter deals with release of actives such as, but not restricted to, drugs from a hydrogel matrix. Its particular relevance to the introduction and chapters 3 and 4 of this thesis is that the case of release from a hydrogel that might be used in an electroporation or TENS device, in which the effect of the device is to promote the ready diffusion of actives across the dermal barrier but not by an ionic driving force (chapter 3) is considered. Here as in the release of PVA from a PVA matrix the process is one of diffusion. Whereas in chapter 4 that diffusion was aided mechanically (by action of the eyelid or vortex mixer), here the diffusion of the gel is considered not to be affected by electrical or agitation techniques.

The ability to manipulate the composition of hydrogels allows for the release characteristics of the device to be tailored in order to load a particular active, which is then released at or to a specific site at a predetermined rate and time (see section 1.5). It has been previously discussed (chapter 4) that *in vitro* models combined with sensitive detection techniques provide useful data on the release characteristics and release mechanism of a particular system. However, probably the most challenging aspect in the area of controlled delivery is the ability to predict the release kinetics of an active agent. This would provide valuable knowledge for both the design requirements of a particular formulation and the empirical verification of the release mechanism.

A powerful method that is widely employed to obtain information on the mass transport involved in release, assisting prediction of the release kinetics, is mathematical modelling. Although this can considerably aid the optimisation of existing as well as the development of new active delivery systems, there is no universal mathematical model and the choice of an appropriate mathematical model will depend on the type of active, type of excipients and formulation of the device.

This chapter examines the release characteristics of hydrogels for both dermal and ocular applications occurring by diffusion through the bulk of the matrix (see section 1.5.1).

5.1 Diffusion through hydrogels

The release of a species from a hydrogel occurs by its permeation through the bulk of the polymer network. This results from a combination of its diffusion, which is mainly governed by the mass transfer limitations at the boundary between the device and its surroundings,[9] and the degree of solubility of the species in the network. This may be expressed in the form:[110]

$$\mathbf{p = d\ x\ s} \qquad \text{Equation 5.1}$$

where:

p = permeability constant

d = diffusion coefficient

s = solubility

The diffusion of an active agent through a polymeric release device can be described by Fick's law, which assumes that the limiting factor of transport is simply diffusion. For transport in one dimension this can be mathematically stated as:[9, 110]

$$\mathbf{J_i = -d_i \frac{\partial c_i}{\partial x}} \qquad \text{Equation 5.2}$$

where:

J_i = flux of species i per unit area

d_i = diffusion coefficient of species i

c_i = concentration of species i

x = position normal to the effective area of diffusion

In matrix release systems the active is uniformly distributed throughout the polymer network (see section 1.5.1). However for matrix release systems of simple geometries their rate of release is proportional to $t^{-½}$ [32], that is it is time dependent, hence their release kinetics are generally not zero-order. This is probably because the active released from the surface layer has a shorter distance to travel, whereas active released subsequently from deeper layers has a longer distance, therefore takes longer to travel. In situations where

rate of release is time dependent Fick's second law is used to analyse the system. Fick's second law[9, 110] states that the change in species concentration is equal to the change in local flux, hence:

$$\frac{\partial \mathbf{c}_i}{\partial \mathbf{t}} = -\frac{\partial \mathbf{J}_i}{\partial \mathbf{x}}, \text{by substituting from equation 5.2} \Rightarrow \mathbf{d}_i \frac{\partial^2 \mathbf{c}_i}{\partial^2 \mathbf{x}} \qquad \text{Equation 5.3}$$

where:

t = release time

It should be noted that equations 5.2 and 5.3 are only true[9] for release from a device with thin planar geometry (minimum aspect ratio 1:20([111])) and for a diffusion coefficient that is independent on concentration. By applying appropriate initial and boundary conditions, which provide an accurate reflection of the imposed *in vitro* or *ex vivo* experimental conditions, solutions to these equations can be obtained.[110] Although these equations have been widely used due to computational ease, an expression of Fickian diffusion which includes a concentration-dependent diffusion coefficient is:

$$\frac{\partial \mathbf{c}_i}{\partial \mathbf{t}} = \mathbf{d}_i(\mathbf{c}_i)\frac{\partial^2 \mathbf{c}_i}{\partial^2 \mathbf{x}} \qquad \text{Equation 5.4}$$

where:

$d_i(c_i)$ = concentration-dependent diffusion coefficient

The dependence of the diffusion coefficient on concentration is influenced by the structural characteristics of the hydrogel devices and can be estimated by various published methods[9], hence will not be discussed any further.

Mathematical modelling is a complex process, which does not always produce a convenient formula. In order to simplify the analysis of release from controlled release polymeric devices a simple power law expression:

$$\frac{\mathbf{M}_t}{\mathbf{M}_\infty} = k\,\mathbf{t}^n \qquad \text{Equation 5.5}$$

has been proposed[112] to empirically describe the first 60 % of fractional solute release behaviour.

where:

$\frac{M_t}{M_\infty}$ = fractional active release

k = a constant characteristic of the active-polymer system

t = release time

n = diffusional exponent characteristic of the release mechanism and geometry

Determining the value of the exponent n provides information about the physical mechanism controlling release from a particular device (table 5.1[8, 112]).

Diffusional exponent, n			**Release mechanism**	**Time dependence**
Thin film	**Cylindrical sample**	**Spherical sample**		
0.5	0.45	0.43	Fickian diffusion	$t^{1/2}$
0.5 < n < 1.00	0.45 < n < 1.00	0.43 < n < 1.00	anomalous diffusion	t^{n-1}
1	1	1	zero order release (case II transport)	time independent
n > 1	n > 1	n > 1	super case II transport	t^{n-1}

Table 5.1 Transport mechanisms from non-swellable controlled release devices of various geometries.

The release profiles of the various release mechanisms are illustrated in figure 5.1.

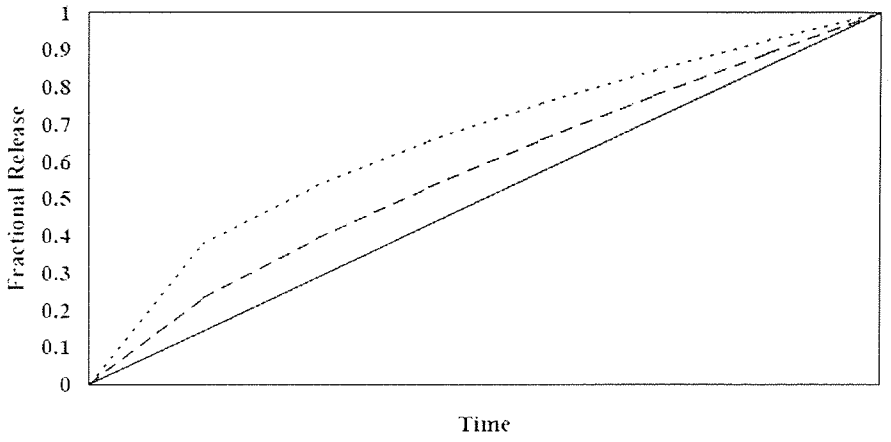

Figure 5.1 Release behaviour of a) Fickian diffusion (.....) b) Anomalous diffusion (- - - -) and c) zero-order release (———).[8]

Anomalous and zero-order diffusion are normally referred to as non-Fickian. Non-Fickian behaviours are classed further into two-stage, sigmoidal and zero-order.[113] These are identified by plotting the fractional amount of active released as a function of the square root of time (figure 5.2).

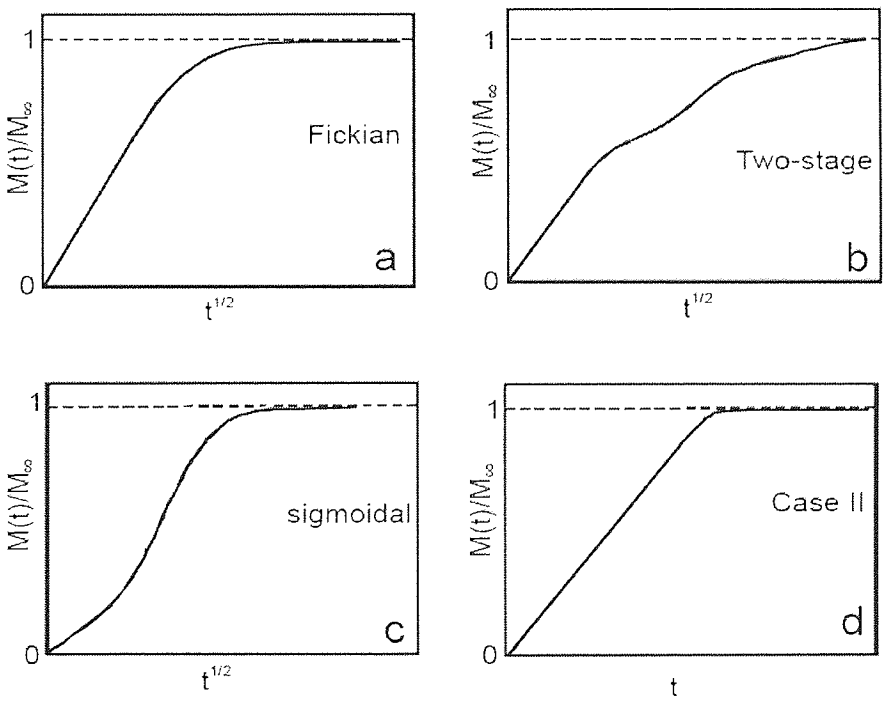

Figure 5.2 Release characteristics of a) Fickian b) two-stage c) sigmoidal d) case II diffusion.

5.2 Species selection

The physicochemical properties of the active play a large part in the successful application of controlled release. Characteristics of actives that make them suitable for iontophoretic delivery have been outlined in section 1.5.7.1, however the ability to identify actives that will permeate through the release vehicle (polymer matrix) as well as biological membranes to its point of action at an acceptable rate is of colossal importance.

For steady state diffusion, that is constant J_i and d_i and constant membrane thickness, equation 5.2 can be integrated over the thickness δ to give:[8, 62, 111]

$$\mathbf{J_i = K_{pc} d_i \frac{\Delta c_i}{\ell}} \qquad \text{Equation 5.6}$$

where:

Δc_i = transmembrane concentration difference

ℓ = thickness of the hydrogel

K_{pc} = the solute partition coefficient, which is expressed as:

$$\mathbf{K_{pc} = \frac{solute\ concentration\ in\ the\ polymer}{solute\ concentration\ in\ the\ receptor\ medium}} \qquad \text{Equation 5.7}$$

From equation 5.6 it can be stated that for a species to permeate through a membrane it requires reasonable values of both the diffusion and the partition coefficients. Thus it can be deduced that a species will not diffuse through a microporous polymer membrane unless it is thermodynamically compatible with the polymer.[111] It is for this reason that polar actives are readily transported through hydrophilic polymers unlike hydrophobic species. A typical example of incompatibility is the "dumping" effect, where a large amount of the species is released from the device once it comes into contact with the release site/ medium. It has been suggested[62] that the ideal characteristics for an active penetrating the stratum corneum are that it should possess:

i. a low molecular mass, preferably less than 600 Da particularly when d is high
ii. a balanced K_{pc}, as if it is too large it may not be cleared by viable tissues

iii. adequate solubility in vehicle and membrane such that its concentration in the delivery vehicle remains large enough to maintain an adequate concentration gradient (driving force)

iv. a low melting point which results in good solubility.

Equation 5.6 may also be defined using thermodynamic activities:[62]

$$\mathbf{J_i = \frac{a_i d}{\gamma h}} \qquad \text{Equation 5.8}$$

where:

a_i = thermodynamic activity of species i in its vehicle

γ = effective activity coefficient in the skin barrier

h = thickness of the recipient membrane

This equation suggests that[62] that, to achieve the maximum penetration rate the active should be at its highest thermodynamic activity. In a saturated solution dissolved molecules are in equilibrium with pure solid which is at its maximum activity, thus the solute molecules are also at maximum activity. Therefore, vehicles containing actives as a finely ground suspension should have the same penetration rate if d, γ and h remain constant. In reality this is difficult to achieve as the delivery vehicle interacts with the stratum corneum to some extent.

For supersaturated solutions the theoretical maximum flux may increase by several factors. Supersaturated solutions result from the design of the active-vehicle system or arise when a cosolvent evaporates while the system is in contact with the biological membrane; hence the system is not at equilibrium. Purposely designing supersaturated active-vehicle systems should, however, ensure that they are stable in order to reduce crystallisation of the active.

In addition to the physicochemical properties of the active their pharmacokinetic, pharmacological and toxicological properties need to be considered.[114]

The pharmacokinetic properties are:

i. rate of absorption from various dosage forms

ii. rate and mechanism of active elimination (biological half-life)
iii. obstacles to bioavailability such as first-pass hepatic metabolism

The pharmacological and toxicological properties are:

i. minimum effective therapeutic concentration
ii. influence of the active peaking against its steady state levels in blood
iii. desirability of steady state kinetics
iv. minimum toxic concentration
v. frequency and type of toxicity encountered

It has been shown that the impedance of a hydrogel is affected by the presence of ions as well as their nature (chapter 3). In view of the fact that a fair number of actives tend to ionise under delivery conditions it would be interesting to determine how the presence of ions influences the delivery of an active. An overview of mathematical models that may be used to quantitatively determine the release of actives, at this stage either in the unionised or ionised state, from an adhesive hydrogel into a biological membrane, such as skin, follows.

5.3 Mathematical models for delivery of actives

Delivery models serve to provide an indication of the viability of an active to penetrate the skin's stratum corneum or the eye's anterior surface under active or passive delivery. The Nernst-Planck model describes electrically assisted delivery while the pH-partitioning model evaluates passive delivery.

5.3.1 Electrotransport model

The electrotransport of ions across a membrane occurs by three mechanisms (section 1.5.7.1). These are the passive, electromigration and electroosmosis contributions. The Nernst-Planck model[64] is a simple equation describing assisted transport of ions through a membrane. It defines the flux of species i as:

$$\mathbf{J}_i = -\mathbf{d}_i \frac{\partial \mathbf{c}_i}{\partial \mathbf{x}} - \mathbf{z}_i \mathbf{m} \mathbf{F} \mathbf{c}_i \frac{\partial \mathbf{E}}{\partial \mathbf{x}} \qquad \text{Equation 5.9}$$

where:

m = the mobility of the species

z_i = the valence of species i

F = Faraday's constant

E = the electrostatic potential

For a non-electrolyte z = 0, thus equation 5.9 is reduced to equation 5.2, Fick's first law of diffusion (passive contribution). Similarly for an ion with a uniform concentration gradient $\frac{\partial c_i}{\partial x} = 0$, thus equation 5.9 is reduced to:

$$\mathbf{J}_i = -\mathbf{z}_i \mathbf{m} \mathbf{F} \mathbf{c}_i \frac{\partial \mathbf{E}}{\partial \mathbf{x}} \qquad \text{Equation 5.10}$$

which is the equation for electrophoresis (electromigration contribution). Thus, equation 5.9 postulates that during the simultaneous existence of a concentration gradient and an electric field, ionic flux is a sum of flux occurring from each effect. However, in reality techniques such as iontophoresis and electroporation have a large number of operating

variables. Equation 5.9 assumes that the sole driving forces on the ionic species i is the negative gradient of its own chemical potential. The possible coupling of chemical potential gradients of other species is not considered. When a potential difference is applied across a charged porous membrane it causes electroosmosis, electrically induced water flow, in the same direction of ion transport. At physiological pH skin has a negative charge, thus by nature is permselective to cations. Electroosmotic flow occurs from anode to cathode thereby further enhancing the flux of cations as well as inducing some of the neutral molecules flux. Consequently, to allow for this effect the Nernst-Planck equation has been modified[64] to:

$$\mathbf{J}_i = -\mathbf{d}_i \frac{\partial \mathbf{c}_i}{\partial \mathbf{x}} - \mathbf{z}_i \mathbf{m} \mathbf{F} \mathbf{c}_i \frac{\partial \mathbf{E}}{\partial \mathbf{x}} \pm \mathbf{c}_i \mathbf{J}_v \qquad \text{Equation 5.11}$$

where:

J_v = velocity of convective flow

The Nernst-Planck model is a very simplified model used to predict the flux of electrically assisted delivery. It is suitable for most small unionised actives (molecular weight < 1000) or weak electrolytes (acids or bases) as these properties directly influence passive diffusion. In addition as cell membranes are hydrophobic lipid bilayers they are much more permeable to the unionised form of actives.

In order to tailor the model towards taking into account crucial factors that affect the flux of an active across a membrane, flux arising from the nature of the active is subsequently explored.

5.3.2 Passive diffusion model

An unionisable compound (or the non-ionised form of an acid or a base) reaches equilibrium across a lipid membrane that is proportional to its concentration gradient. However, actives tend to exist in the ionised form when exposed to their "pH-opposite" chemical environment. Figure 5.3 illustrates that acids are increasingly ionised with increasing pH (basic environment), whereas bases are increasingly ionised with decreasing pH (acidic environment).

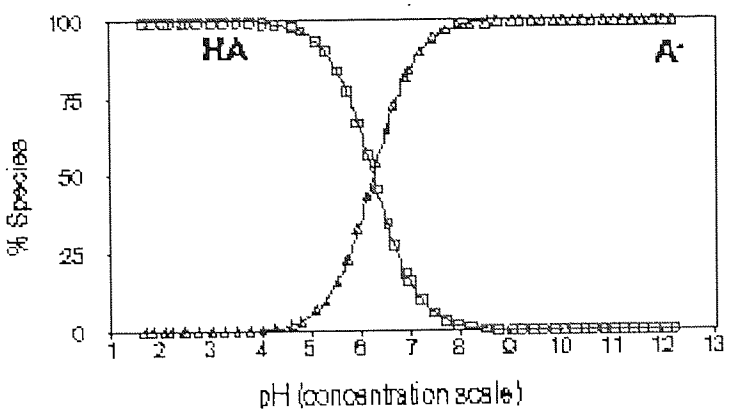

$$HA \rightleftharpoons H^+ + A^-$$

a) acid conjugate base

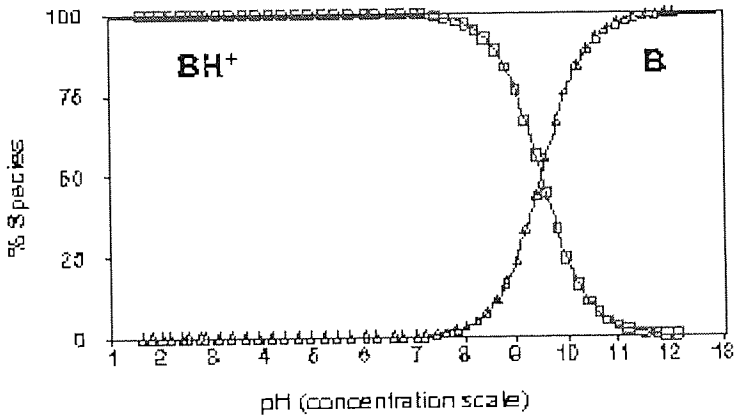

$$BH^+ \rightleftharpoons H^+ + B$$

b) conjugate acid base

Figure 5.3 Percentage ionisation of a) acids and b) bases with change in pH.

The ratio of ionised to unionised moieties is described by the Henderson-Hasselbach equation, which is of the form:

$$\mathbf{pH - pK_a = log\left(\frac{[conjugate\ base]}{[acid]}\right)_{acid} = log\left(\frac{[base]}{[conjugate\ acid]}\right)_{base}} \quad \text{Equation 5.12}$$

where:

pK_a = pH at which the active is 50 % ionised which can be determined using the following equation:

$$\mathbf{pK_a = -logK_a = \left(-\log \frac{[H^+][conjugate\ base]}{[acid]} \right)_{acid} \quad or \quad \left(-\log \frac{[H^+][base]}{[conjugate\ acid]} \right)_{base}}$$

Equation 5.13

where:

K_a = acidity constant

From equation 5.12 it can be deduced that the active will equilibrate within a given environment (hydrogel matrix or biological membrane) according to the pH of the environment and the pK_a of the active, thus the equilibrating process is not dependent of the initial state of the active. The pK_a measures the tendency of a species to keep a proton (H^+) at its ionisation centre as the pH changes, as implied in equation 5.13, hence for acids the larger its value the less likely it is to become ionised, the inverse being true for bases.

Generally an ionised active is polar and therefore water-soluble, whereas a non-ionised active is non-polar and more lipid-soluble. Given that a fair number of actives become ionised within the skin's pH range (4 to 7.4) the pH partitioning theory can be used to describe the transdermal delivery of ionisable actives.[115] The model, based on equation 5.14, states that total flux is a composite of the transport of unionised and ionised contributions.

$$\mathbf{J_T = \left(k_p{}^N \times c^N\right) + \left(k_P{}^I \times c^I\right)}$$

Equation 5.14

where:

J_T = total flux of a species, mg/cm^2h

$k_p{}^N$ = permeability of the unionised species, cm/h

$k_p{}^I$ = permeability of the ionised species, cm/h

c^N = concentration of the unionised species, mg/ml

c^I = concentration of the ionised species, mg/ml

From equation 5.12 the relative ratio of ionised and unionised species at a certain pH and pK_a can be determined. The fraction of the species that is ionised is given by the following equations:

$$f^I\,(acid) = 1/\left[1+10^{(pK_a - pH)}\right] \qquad \text{Equation 5.15}$$

$$f^I\,(base) = 1/\left[1+10^{(pH - pK_a)}\right] \qquad \text{Equation 5.16}$$

Using either equation 5.15 or 5.16 for a acid or base respectively and knowing the initial concentration it is possible to determine c^N and c^I. However equations to determine the respective permeabilities are less readily available. An equation to calculate $k_p{}^N$ (cm/h) through a lipid membrane has been proposed as:[115]

$$\log k_p = -2.7 + 0.71 \log K_{o/w} - 0.0061\,MW \qquad \text{Equation 5.17}$$

where:

$K_{o/w}$ = species' octanol-water partition coefficient

MW = molecular weight of the species

$K_{o/w}$ is the partition coefficient of the unionised species between octanol and water (see section 1.5.6). Octanol as a solvent has been deemed[115] a better model of the lipids in biological membranes compared to dioleylphosphatidyl choline (DOPC) which has a bilayer structure similar to the lipid bilayer found in skin. Other organic solvents, such as ethomeen,[16] may be more appropriate, however physicochemical properties of actives with these solvents are not readily available, hence need to be determined experimentally. Since this is outside the scope of this work physicochemical properties based on octanol have been used throughout.

$K_{o/w}$ may be defined as either $logP^N$ or logD. $LogP^N$ is independent of pH, and is therefore constant.

$$\log P^{N} = \log \frac{[\text{unionised species}]_{octanol}}{[\text{unionised species}]_{water}} \qquad \text{Equation 5.18}$$

On the other hand logD is the distribution coefficient of the ionised and unionised species between octanol and water; therefore it gives an indication of the apparent partition coefficient for all protolytic forms. It is pH dependent, thus pH specific.

$$\log D = \log \frac{[\text{unionised + ionised species}]_{octanol}}{[\text{unionised + ionised species}]_{water}} \qquad \text{Equation 5.19}$$

Figure 5.4 shows the change in logD with pH for various drugs that possess the same logD at pH 7.4. The significant variation of logD over the physiological pH range emphasises the importance of the pH of the drugs environment and the pK_a of the drug.

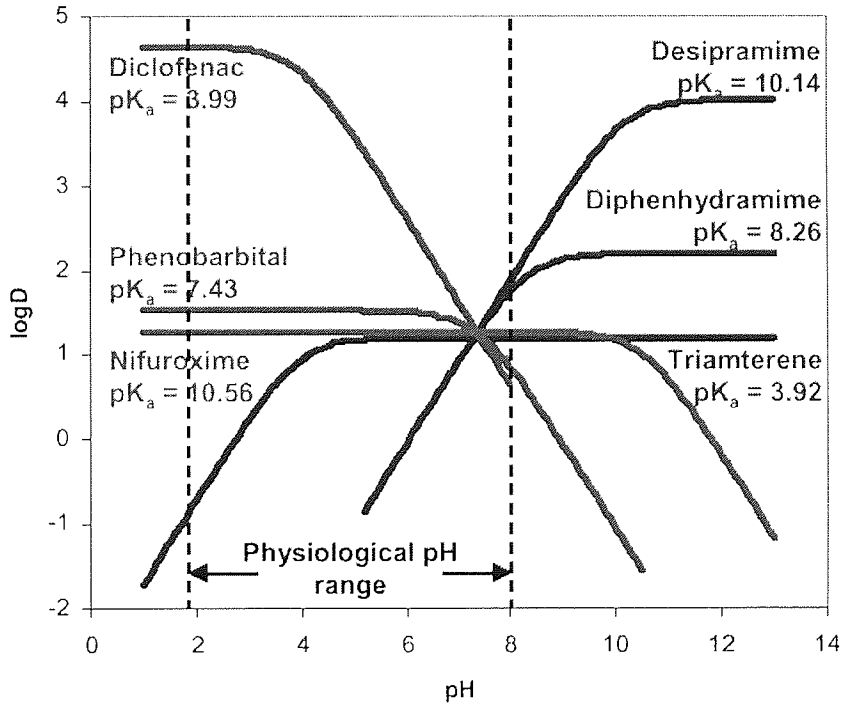

Figure 5.4 Changes in logD with pH for various drugs (—— acidic and —— basic).

Substituting $\log P^{N}$ (equation 5.18) for $\log K_{o/w}$ in equation 5.17 provides a constant value for $\log k_p^{N}$ which is independent of pH. Alternatively substituting logD (equation 5.19) for $\log K_{oct}$ in equation 5.17 provides a value for $\log k_p^{N+I}$ (equation 5.20), which is pH dependent.

$$\log k_p^{N+I} = -2.7 + 0.71\,\log D - 0.0061\,MW \qquad \text{Equation 5.20}$$

The definition of k_p^I has been not been cited in the literature, as it has been considered[115] to be unclear. However in order to determine the total flux of a permeant using equation 5.14 the value of k_p^I is required. Thus, it is proposed that by subtracting $\log k_p^N$ from $\log k_p^{N+I}$ (equation 5.20 – equation 5.17) an indication of $\log k_p^I$, and therefore k_p^I, can be obtained providing all the necessary values to resolve equation 5.14. The value of this model has been illustrated by determining the flux for a common acidic drug (ibuprofen) and a common basic drug (lidocaine).

5.3.2.1 Predicted flux of ibuprofen through a lipid membrane

Ibuprofen (figure 5.5) is classed as a non-steroidal anti-inflammatory drug (NSAID)[116] which has analgesic, antipyretic and anti-inflammatory properties. It has been widely indicated for the symptomatic relief of acute or chronic conditions where pain and inflammation are present, for example rheumatoid arthritis, osteoarthritis as well as muscular disorders. The advantages of NSAIDs are that they do not cause sedation or respiratory depression and the odds for abuse or physical dependence are extremely low. However as oral administration of ibuprofen causes gastric irritation it is contraindicated for many patients. Thus it has been formulated into a large number of topical preparations for localised treatment.

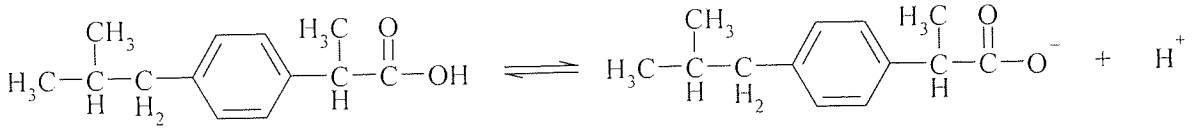

acid conjugate base

Figure 5.5 Unionised acid and ionised conjugate base pair of ibuprofen.

In order to predetermine its flux through a lipid-based membrane by using equation 5.14 it was necessary to acquire the various physicochemical parameters mentioned above. For

the purpose of this investigation values based on the literature or from predictive software were used. These values for ibuprofen were as follows:

MW = 206.3 (see section 2.1.3)

pK_a = 4.45 (measured[117])

$logP^N$ = 3.79 (predicted[118])

By substituting $logP^N$ into equation 5.17:

$logk_p^N$ = -1.268 ∴

k_p^N = 0.054 cm/h

In order to determine $logk_p^{N+I}$ to obtain $logk_p^I$ it was necessary to establish logD at various pH's. For this analysis logD was calculated using predictive software.[119] In order to predict logD as pH varies predetermined values $logP^N$, pK_a and $\delta_{o/w}$ were required. $\delta_{o/w}$ is the log of the ratio of the partition coefficient of neutral species to the partition coefficient of ionic species[117] in an octanol-water system, expressed as:

$$\delta_{o/w} = \log \frac{P^N}{P^I} \qquad \text{Equation 5.21}$$

where:

$$\log P^I = \log \frac{[\text{ionised species}]_{\text{octanol}}}{[\text{ionised species}]_{\text{water}}} \qquad \text{Equation 5.22}$$

A high $\delta_{o/w}$ indicates that the ionised species has a lower affinity for the lipid phase compared to its unionised form. For this study values of $\delta_{o/w}$ were obtained from the literature. For ibuprofen:

$\delta_{o/w}$ = 4.02 (measured[117])

With these values the logD obtained using predictive software[119] were comparable to those available in the literature.[115, 117]

In order to obtain a flux-pH profile, the equations given above were entered into a Microsoft Excel spreadsheet and the following steps taken to determine the flux at each pH:

i. the value for logD at a particular pH was substituted into equation 5.20 to yield $\log k_p^{N+I}$
ii. $\log k_p^{N}$ was subtracted from $\log k_p^{N+I}$ providing the $\log k_p^{I}$, the antilog of which gives the k_p^{I} for that pH
iii. f^{I} at a particular pH was obtained from equation 5.15 (as ibuprofen is an acid) and by choosing an arbitrary initial concentration c^{I} was subsequently determined
iv. the value of c^{N} was calculated by simply subtracting that of c^{I} from 1.
v. substituting these parameters into equation 5.14 for each pH in turn enabled the determination of a flux versus pH relationship
vi. varying initial concentrations enabled the flux–pH outline to be determined for various concentrations (figure 5.6). For this study load concentration values of 1 to 5 mg/ml of ibuprofen were chosen.

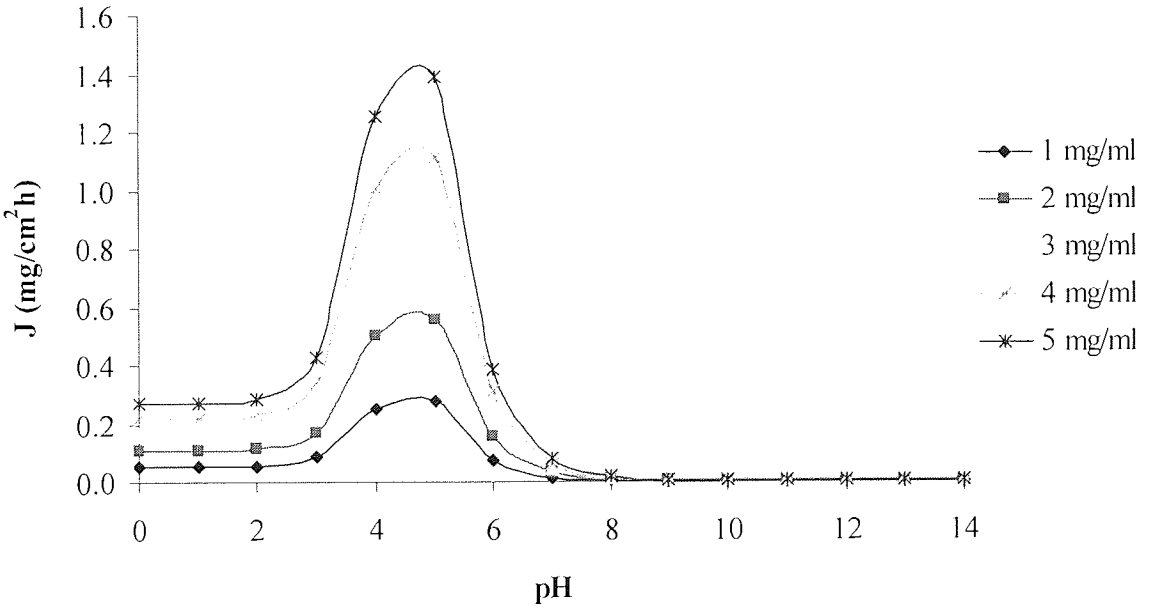

Figure 5.6 Flux profile of ibuprofen as pH is varied for five load concentrations.

Based on the physicochemical values stated above, the pH-partitioning model showed that the flux of ibuprofen through a lipid membrane, not surprisingly, increases with concentration. It also illustrated that flux increased significantly between pH 3 and 5,

dropped rapidly at pH 6 and reduced to virtually zero thereafter. In order to explain this behaviour its fraction ionised–pH relationship (figure 5.7) was determined by using equation 5.15.

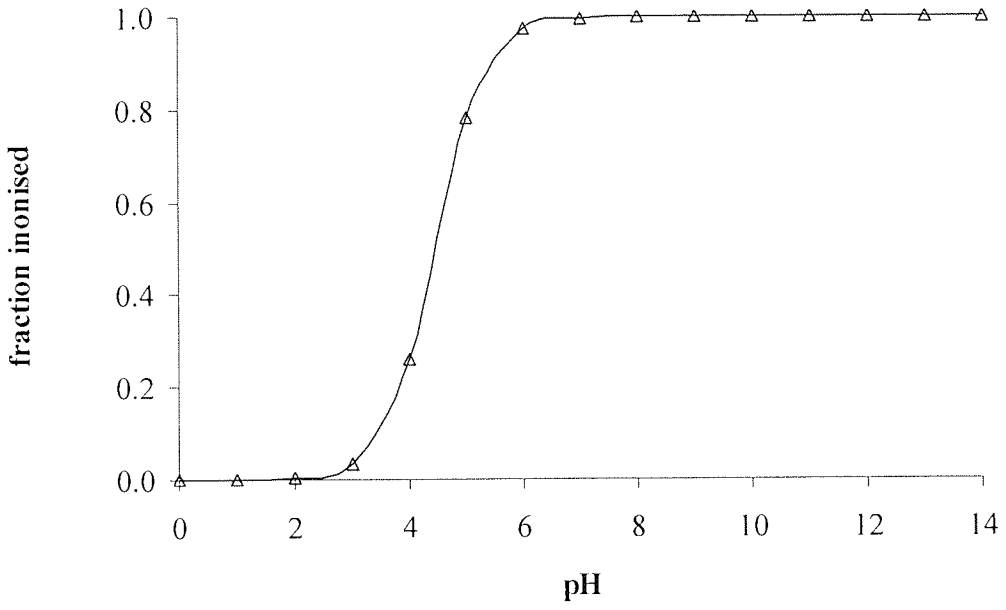

Figure 5.7 Outline of the ionised fraction of ibuprofen as pH increases.

The ionised fraction increases from 3 % to 97 % between pH 3 and 6 remaining at 100 % from then on. Maximum flux occurred at pH 5, which corresponds to a 78 % ionised fraction. This was slightly surprising as it is generally accepted that the flux of the unionised form of a compound through a lipoidal membrane should be larger than its ionised counterpart. However, at pH 4 only 26 % of ibuprofen should have been ionised and the flux was not too dissimilar to that at pH 5, hence the maximum flux may actually lie somewhere between pH 4 and 5 corresponding to an ionisation fraction of 26 to 78 %. It should also be noted that maximum flux falls within a pH region similar to that of its pK_a (4.45). On the other hand this discrepancy may suggest that the process is more complex than Ko/w values are able to deal with.

5.3.2.2 Predicted flux of lidocaine through a lipid membrane

Lidocaine (figure 5.8) is an amide based local anaesthetic.[116] Local anaesthetics work by reversibly inhibiting the transmission of signals along nerves; thus ensuing analgesia (loss of pain sensation) and paralysis (loss of muscle power) without causing loss of consciousness. Lidocaine is commonly used for topical and dental anaesthesia. The advantages of local anaesthetics are that they have rapid onset, little potential for abuse and do not produce hypertension or local vasoconstriction. In addition topical anaesthesia in cataract surgery eliminates the risks associated with the retrobulbar injection while allowing for early recovery of visual acuity.[120]

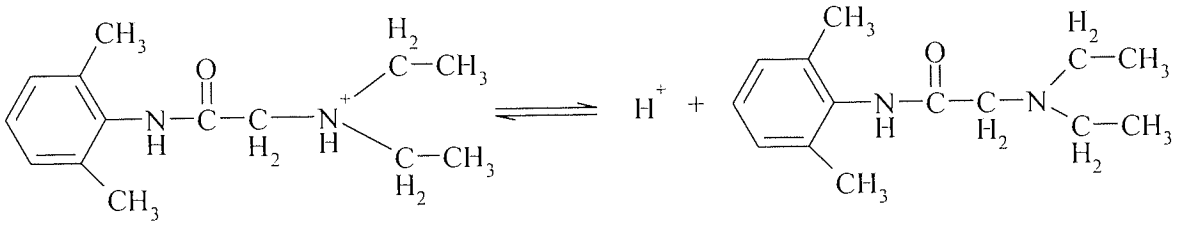

Figure 5.8 Unionised base and ionised conjugate acid pair of lidocaine.

In order to predetermine the flux of lidocaine as pH varies by using equation 5.14 it is necessary to acquire the physicochemical parameters discussed above. For the purpose of this investigation values based on the literature or from predictive software were used. For lidocaine the values were as follows:

MW = 234.3 (see section 2.1.3)
pK_a = 7.96 (measured[117])
$logP^N$ = 1.66 (predicted[118])
$\delta_{o/w}$ = 2.98 (measured[117])

With these values the logD obtained using predictive software[119] were comparable to those available in the literature.[115, 117]

By substituting $logP^N$ into equation 5.17:

$logk_p^N = -2.951$ ∴

$k_p^N = 0.0011$ cm/h

To determine the remaining variables steps i to v as for ibuprofen were followed. The only difference being that c^I was determined using equation 5.16 (as lidocaine is a base). Load concentrations of 1 to 5 mg/ml were chosen once more to illustrate the flux–pH profile of lidocaine (figure 5.9) at various concentrations.

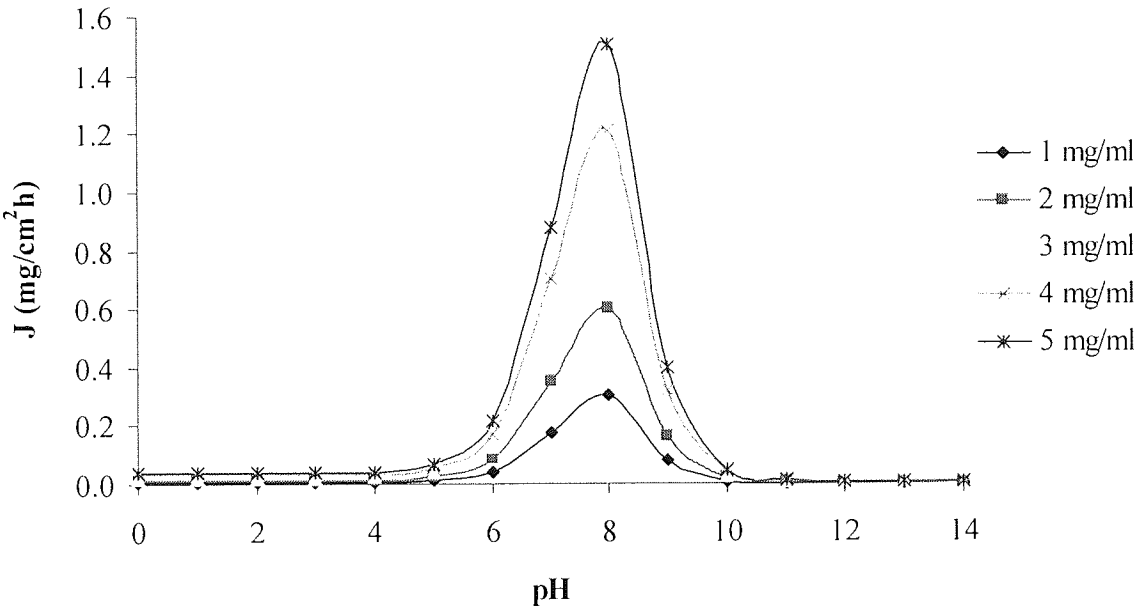

Figure 5.9 Flux profile of lidocaine as pH is varied for five load concentrations.

For lidocaine the pH-partitioning model also demonstrated that the flux of lidocaine through a lipid membrane increases with concentration. Flux increased significantly between pH 6 and 8, dropped rapidly at pH 9 and reduced to virtually zero thereafter. Once again this was correlated to its fraction ionised–pH relationship determined using equation 5.16 (figure 5.10).

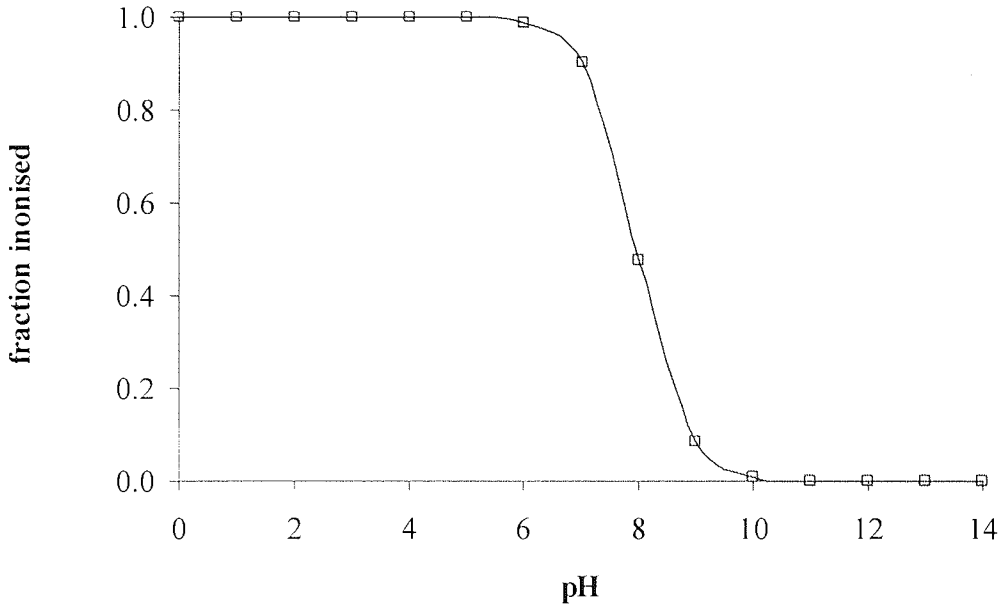

Figure 5.10 Outline of the ionised fraction of lidocaine as pH increases.

The ionised fraction of lidocaine reduces from 100 % to 8 % between pH 6 and 9 subsequently remaining at 0 %. Maximum flux occurred at pH 8, this corresponds to an ionised fraction of 48 % which is also similar to the pK_a. Thus, for lidocaine the model also indicated that at 2 pH units above or below its pK_a flux is reduced notably.

Although it is expected that the flux of the unionised form of a compound through a lipoidal membrane should be larger than its ionised counterpart, this model can still be regarded as invaluable since it gives an insight of the behaviour of an active. However, the limitations of this model need to be taken into account. These are:

i. the partitioning of the species in the polymer or lipoidal and aqueous components may be more complex than partitioning between octanol and water
ii. an increase in concentration will increase the flux of the species only up to a point where the diffusion of the species becomes a limiting factor.

The physicochemical properties of the active also provide an indication on the compatibility of the active with its delivery vehicle (hydrogel membrane). Thus, in order to acquire a better understanding of the release of an active from a delivery vehicle into a biological membrane, the release of actives from hydrogels are subsequently explored.

5.4 Release of actives from hydrogels explored

The factors that influence the release of an active from a hydrogel delivery vehicle depend on the properties of three systems involved. These are:[16]

i. the active, for example molecular weight, $K_{o/w}$, pK_a and load concentration
ii. the hydrogel matrix, for instance composition, EWC, degree of hydration and pH
iii. the release environment, that is the pH, aqueous or organic nature and in particular how it differs from the environment within the hydrogel.

A series of partitioning stages are, therefore, involved during the release process as illustrated in figure 5.11.

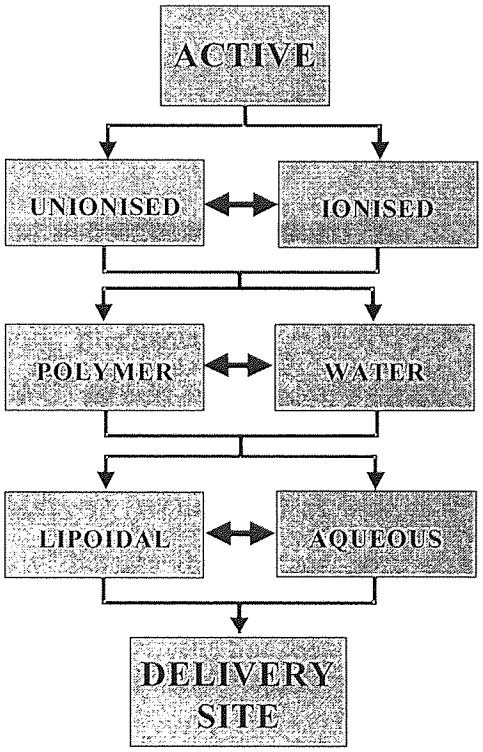

Figure 5.11 Flow chart depicting the partitioning stages occurring during release.[16]

In the first stage the active partitions between the polymeric and aqueous components of the hydrogel according to its $logP^N$ and logD. These are in turn dependent on the solubility of the active and the latter also being influenced by the pK_a of the active and the pH of the environment within the hydrogel as discussed in section 5.3.2.

The second stage involves the release of the active from the vehicle and partitioning between the lipoidal and aqueous parts of the biological membrane. Once again this is influenced by its $logP^N$ and logD.

Generally the more hydrophobic compounds (unionised) will have a greater affinity for the polymeric (stage 1) or lipoidal (stage 2) component, whereas the more hydrophilic compounds (ionised) will have an affinity for the aqueous component (both stages).

Transportation of an active from the delivery vehicle to its site of action is collectively influenced by each stage. Thus knowing how an active behaves facilitates tailoring the release to suit a particular application as each stage can be manipulated. However, controlling the properties of the hydrogel based delivery vehicle may be less challenging compared to manipulating the properties of the active and of the biological membrane. Although the physical structure of a biological membrane may be temporarily modified by methods such as electroporation (section 1.5.7.2), the degree of modification may vary depending on body site and also from individual to individual.

An active may be dissolved or dispersed in a hydrogel matrix system (section 1.5.1) and release may occur by a solution-diffusion mechanism or through the water filled pores.[32] The latter being the primary mechanism in water-swollen hydrogels.[16] Thus the equilibrium water content (EWC) as well as degree of hydration and state of water (section 1.2) will have large impact on rates of diffusion. The EWC of a hydrogel is determined by the nature of its chemical backbone (section 1.2) as well as its crosslink density (section 1.3.1). The crosslink density dictates the average pore size, ξ, defined as the linear distance between neighbouring crosslinks (figure 5.12). The ratio between ξ and r, the hydrodynamic radius of the active, is an important factor governing release kinetics.

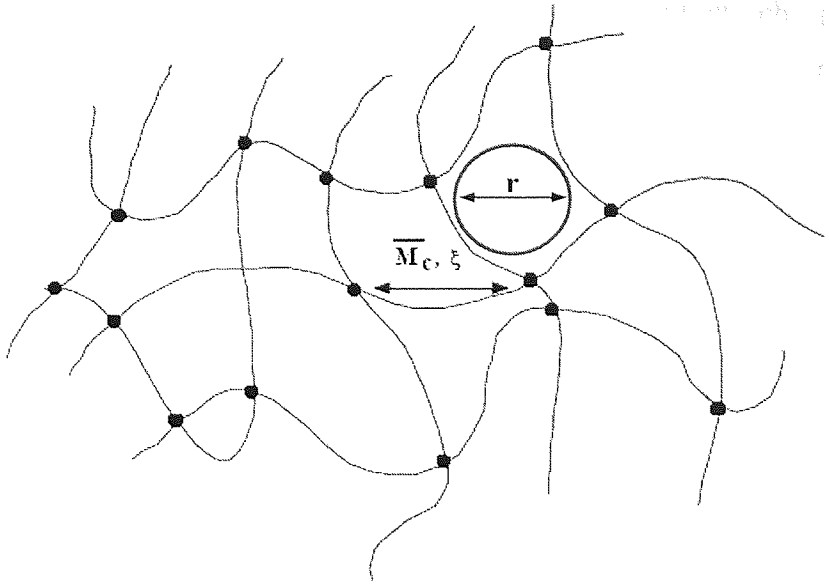

Figure 5.12 Schematic representation of a crosslinked hydrogel structure showing the relationship between ξ and r.

The average pore size is an important parameter in delivery as it gives an indication of the mean space available for diffusion of molecules within the water filled pores. Large molecules are expected to have slow release kinetics due to the space limitation imposed by ξ.

The chemical backbone can be modified, by copolymerising monomers with different hydrophilicities, to achieve the desired EWC. This also allows for the introduction of more hydrophobic monomers to the backbone to allow the incorporation of more hydrophobic actives, however this needs to be weighed against the potential reduction of EWC.

In order to investigate the effect of manipulating hydrogel composition for release purposes, release characteristics from hydrogels with different compositions were investigated. The most economical method to explore release kinetics is through using model compounds such as dyes instead of specific actives. The added advantage of using dyes is that a simple analysis technique, such as colorimetry, instead of more complex ones, for example high-performance liquid chromatography (HPLC), facilitates the investigation process. For this study three fully hydrated hydrogel compositions in the form of contact lenses were investigated. A single model composite, basic fuchsin, was chosen based on lidocaine due to its increased interest for use in cataract surgery. The

contact lenses were loaded with the dye and subsequently released into phosphate buffered saline (PBS), a pH 7.4 medium similar to that of blood, as detailed in the ensuing subsections.

5.4.1 Immobilising a model active within a hydrogel

There are four[121] techniques commonly used to load a hydrogel with an active. These are physical entrapment, electrostatic attraction, physical adsorption and chemical bonding. A combination of these techniques may also be used.

The physical entrapment of a compound may occur during the polymerisation of the vehicle or by absorption from a solution into a pre-polymerised matrix. The advantage of imbibition over "copolymerising" is that the solute has a lowered risk of its therapeutic properties suffering any detrimental alteration. However, for imbibition the crosslink density must enable the solute to become trapped within the hydrogel.

For this study the technique chosen to load the contact lenses was imbibition; this being the most logical approach as the vehicle was preformed and the technique itself was the least demanding. The dye found to be most suited to model lidocaine, as it was the smallest one containing a nitrogen group attached to a benzene ring, was basic fuchsin (figure 5.13).

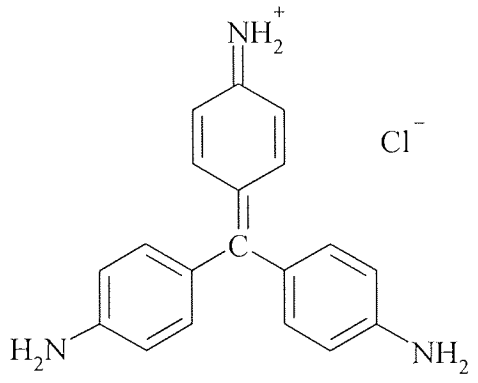

Figure 5.13 The structure of basic fuchsin.

Its physicochemical properties are:

MW = 323.82

$\log P^N$ = -0.11[118]

pK_a = 2.9[122]

λ_{max} = 544 nm[123]

where:

λ_{max} = absorption maximum

Properties of the contact lenses used as release vehicles are detailed in table 5.2.

Composition	Water content
HEMA : NVP 55% : 45%	60%
HEMA : NVP 90% : 10%	42%
100% HEMA	38%

Table 5.2 Composition of contact lenses used for characterising release of model compound.

In order to optimise the loading of the contact lens with dye, the water from the lens was replaced with a bridging solvent (methanol). The lenses were rinsed in distilled water, to remove salts contained in the packing solution, blotted on filter paper and then dehydrated for twenty-four hours in a dessicator to remove all the water. This was followed by fifteen hours (overnight) rehydration in methanol. The contact lenses were then placed on a shaker at 200 rpm in methanol solutions saturated with dye (2 % w/v) and stored in the same solution until time of use to avoid early release of the dye. However it was anticipated that a minimum of twenty-four hours was required for equilibrium to be reached between the lens and the saturated solution. The lenses were then rehydrated in distilled water for five minutes to return their original size, therefore minimise effects from discrepancies of hydration levels. This also served to remove excess dye from the surface of the contact lens. The lenses were reblotted on filter paper to remove excess surface water. This procedure is neatly outlined in figure 5.14

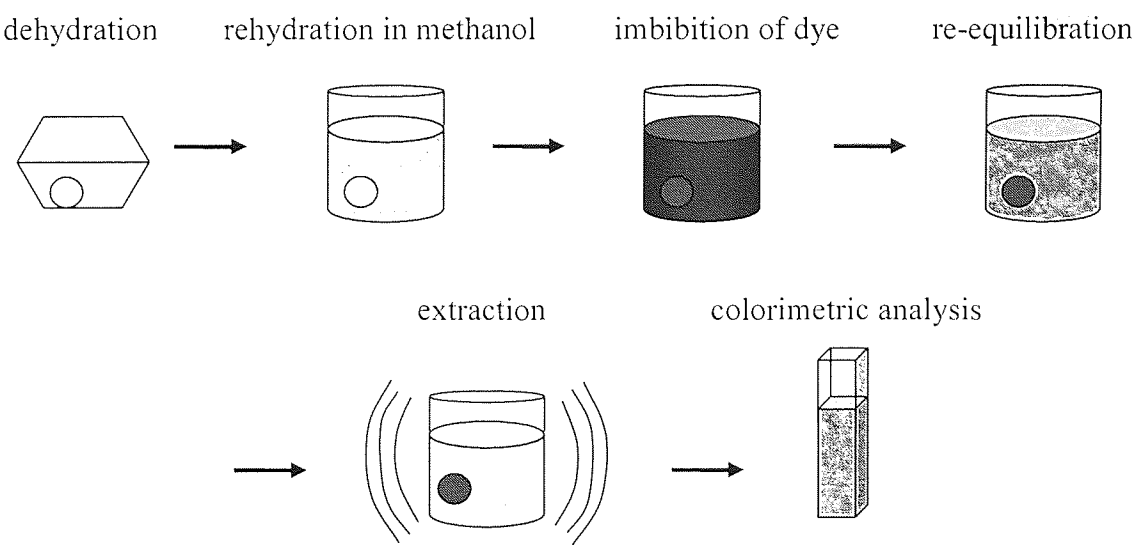

Figure 5.14 Schematic representation of the imbibition process.

5.4.2 Evaluating release of the model active

The release of basic fuchsin from the contact lenses was measured by observing the absorbance of the release media over time. To translate the measured absorbance to concentration a calibration chart was constructed.

5.4.2.1 Calibration curve

A calibration curve was constructed by measuring the absorbance of five known concentrations of basic fuchsin in PBS (pH 7.4). A 0.001 w/w % stock sample was prepared by dissolving 0.001 g of basic fuchsin in 100 ml PBS (10 μg/ml). Dilutions of 3:1, 1:1, 1:3, 1:9 basic fuchsin stock to PBS were carried out to make up four more concentrations of 7.5, 5, 2.5 and 1 μg/ml. Samples of each concentration were placed in cuvettes and their absorbance measured on a Cecil CE404 spectrophotometer (see section 2.2.8). Uncontaminated samples of PBS were used as the control. The colorimetric filter chosen was that which was most sensitive to the range of wavelengths most strongly absorbed by the dye. For basic fuchsin, which has an absorption maximum at 544 nm, this was found to be the Ilford Bright filter 624. To construct the calibration chart, the measured absorbance values were plotted against the known concentrations of the samples (figure 5.15).

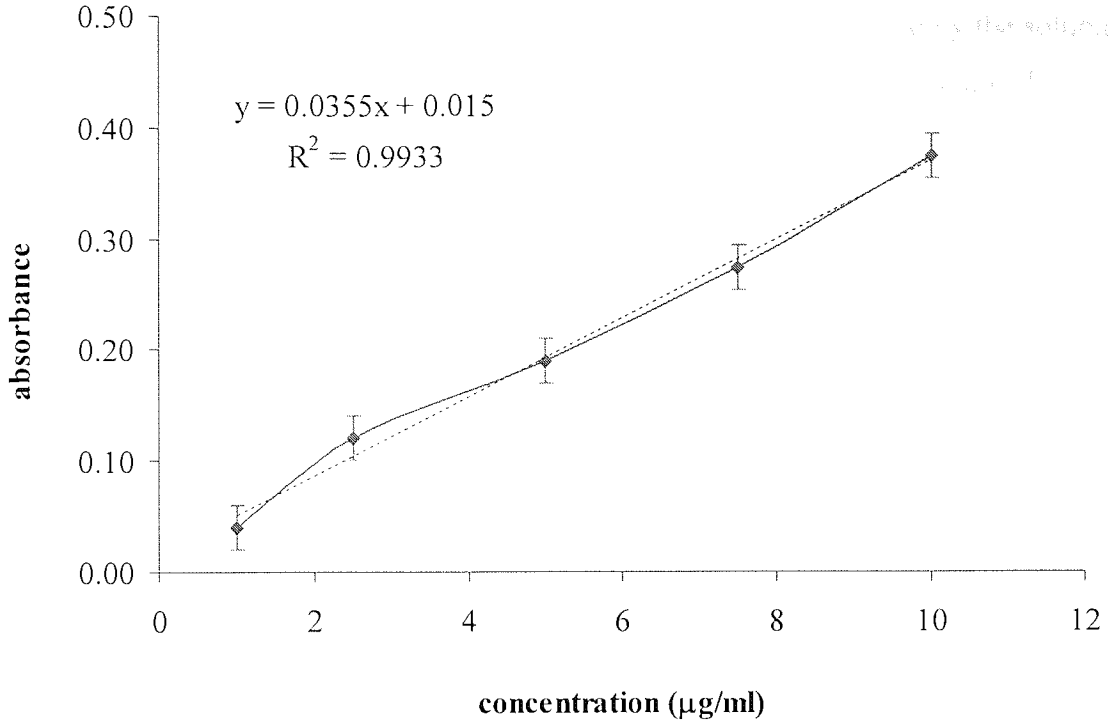

Figure 5.15 Calibration curve of basic fuchsin in phosphate buffered saline measured with an Ilford Bright filter 624.

where:

y = absorbance

x = concentration, µg/ml

With an R^2 value of 99 %, where R^2 is a statistical measure of how well a regression line approximates real data points, the relationship between absorbance and concentration of basic fuchsin in phosphate buffered saline was satisfied by the following equation:

$$\mathbf{y = 0.0355x + 0.015} \qquad \text{Equation 5.23}$$

This equation is only valid for basic fuchsin in PBS with concentrations up to 0.001 %.

5.4.2.2 The extraction profile

The three types of lenses were loaded with basic fuchsin dye, as described in section 5.4.1, and placed into three separate vials containing 10 ml of PBS. The extraction process was

then allowed to continue on a shaker at 200 rpm for one hour. A large medium sample and the constant stirring ensured that the release kinetics would not be limited by the solubility of the dye and also minimised the formation of a stagnant mass boundary transfer layer, thereby maintaining optimum sink conditions. After one hour the lenses were removed and placed in vials containing fresh release media. This process was continued for six hours, after which the process was carried out at larger time intervals up to a total of two hundred and sixty six hours. The absorbance of the release media of each lens post extraction was then measured on the Cecil CE404 spectrophotometer with an Ilford Bright filter 624. The basic fuchsin concentration of each sample was obtained using figure 5.15. The cumulative release concentration (desoprtion) profile is shown in figure 5.16.

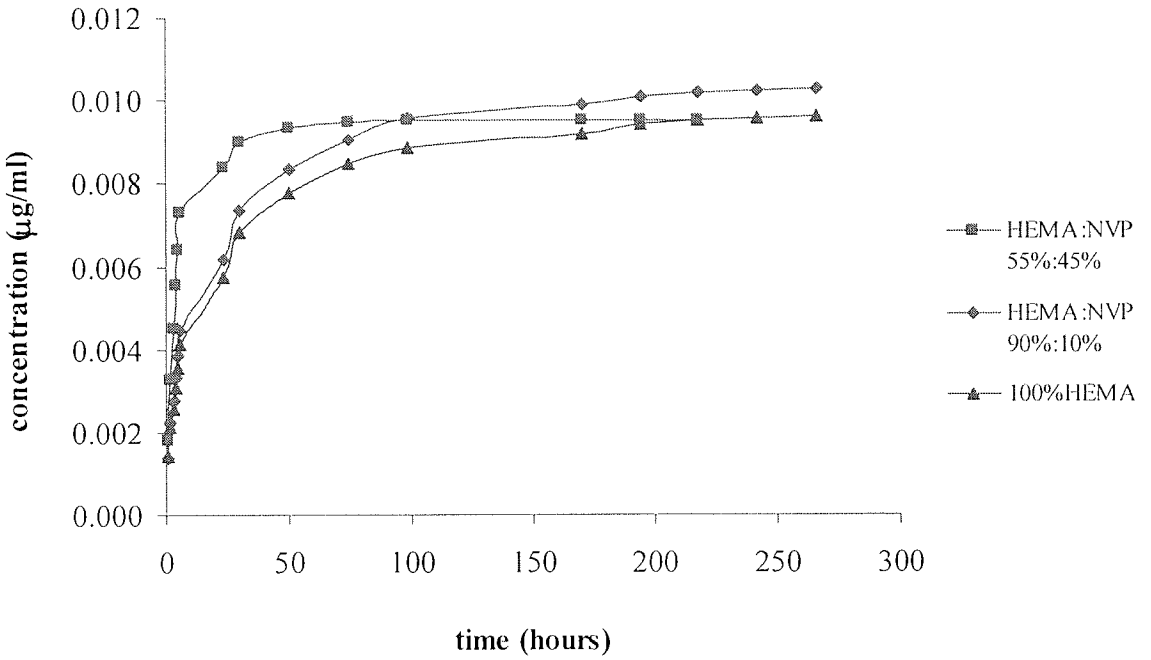

Figure 5.16 Basic fucshin release profile from three contact lens materials.

For all three materials the release profile consisted of two phases. The first phase rapid initial "burst" release was followed by a substantial second phase of approximately first order release. A third stage of no, or very little, release could also be identified whereby the polar interaction of the dye with the hydrophilic monomers of the polymer backbone was more influential. This indicated that the extraction process did not reach completion, as there was some interaction between the active and the polymer backbone.

From figure 5.1 this type of profile was either Fickian or anomalous. In order to identify the type of release mechanism (figure 5.2) the cumulative concentration was plotted against time$^{1/2}$ (figure 5.17).

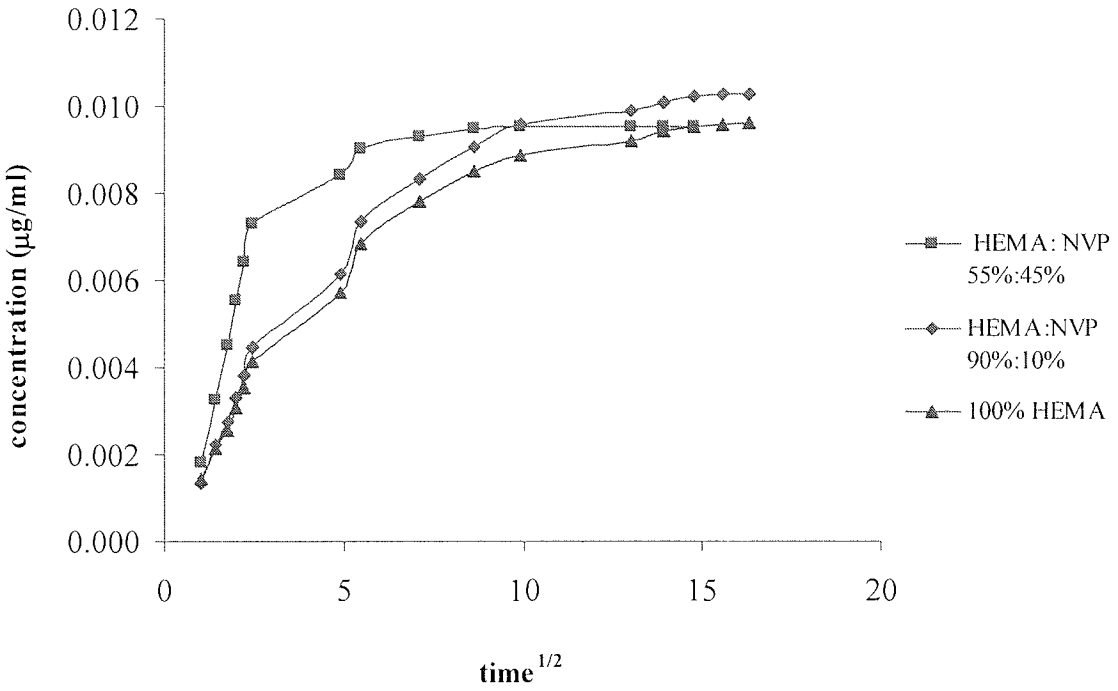

Figure 5.17 Release profile with concentration as a function of time$^{1/2}$.

The pattern of the profiles seen in figure 5.17 for 90 % HEMA:10 % NVP and 100 % HEMA were typical of the anomalous two-stage type release. That of 55 % HEMA:45 % NVP, which although was primarily of the two-stage release, was slightly more Fickian particularly during the first few twenty-four hours. This was thought to be mainly due to the differences in water content and it demonstrated a slight preference for release through the aqueous component. The impact of changes in composition on release kinetics was significant as it demonstrated that modifying the constituents of a hydrogel altered its release characteristics. Thus, the formation of a library of knowledge on the way in which release is affected by composition would provide an important tool for designing hydrogel delivery vehicles to a suit particular application.

Given that the release kinetics from these contact lenses were time dependent, thus similar to that of monolithic devices (section 5.1), release from contact lenses may be modelled by solving for Fick's second law of diffusion (equation 5.3) provided that the coefficient of

diffusion is known. For the case where the species is dissolved in the matrix (which is the case when the hydrogel is equilibrated in a saturated solution and uptake of the active occurs by imbibition) and for slab geometry, desorption of the species can be expressed by two equations[124] valid for the different phases of the desorption curve. The early time approximation accounts for the initial 60 % of the total active released.

$$\frac{\mathbf{M}_t}{\mathbf{M}_\infty} = \mathbf{4}\left(\frac{\mathbf{dt}}{\pi \ell^2}\right)^{1/2} \quad \text{for } 0 \le \frac{M_t}{M_\infty} \le 0.6 \qquad \text{Equation 5.24}$$

The late time approximation accounts for the remaining phase of the desorption curve.

$$\frac{\mathbf{M}_t}{\mathbf{M}_\infty} = \mathbf{1} - \frac{\mathbf{8}}{\pi^2}\mathbf{exp}\left(\frac{-\pi^2 \mathbf{dt}}{\ell^2}\right) \quad \text{for } 0.4 \le \frac{M_t}{M_\infty} \le 1.0 \qquad \text{Equation 5.25}$$

By differentiating equations 5.24 and 5.25 with respect to time, the release rates at any time can be obtained.

$$\frac{\mathbf{dM}_t}{\mathbf{dt}} = \mathbf{2M}_\infty\left(\frac{\mathbf{dt}}{\pi \ell^2 \mathbf{t}}\right) \quad \text{for } 0 \le \frac{M_t}{M_\infty} \le 0.6 \qquad \text{Equation 5.26}$$

$$\frac{\mathbf{dM}_t}{\mathbf{dt}} = \frac{\mathbf{8DM}_\infty}{\ell^2}\mathbf{exp}\left(\frac{-\pi^2 \mathbf{dt}}{\ell^2}\right) \quad \text{for } 0.4 \le \frac{M_t}{M_\infty} \le 1.0 \qquad \text{Equation 5.27}$$

The use of model compounds, both here and in the literature,[16] to investigate the release characteristics of different hydrogel materials enables the identification of parameters that affect release kinetics to be identified, therefore aid compositional manipulation to provide the required kinetics for a particular application. This study was limited to one model compound, three fully hydrated hydrogel materials and one type of release medium. The trends obtained here, however, compliment those obtained with other model compounds in different hydrogel materials.[16] The potential for using dye models in partially hydrated hydrogels (skin adhesives) has also been suggested in the literature.[16] Although the use of dyes as active models provides a wealth of information at a fraction of the cost there are limitations inherent of the process. These are:

i. it is not easy to quantify the amount of dye absorbed by imbibition

ii. equilibration of the samples to their original size post loading may result extract some of dye interfering with the "burst" phase.

Chapter Six

Conclusions and Suggestions for Further Work

6. CONCLUSIONS AND SUGGESTIONS FOR FURTHER WORK

6.1 Conclusions

6.1.1 Skin adhesive hydrogels for use as return bioelectrodes

The Optis ocular iontophoresis system (section 1.5.7.3) presently uses conventional NaAMPS TENS medical return bioelectrodes to complete the circuit. However the main drawback of these electrodes is that they produce high polarisation at the interface resulting in a local high impedance. This causes the patient to experience discomfort at the location of the return electrode at low current levels. Although sensation is a requirement for some electrotherapeutic applications, such as TENS, this thesis has investigated the potential of designing non-polarisable hydrogels which may serve to minimise the pain experienced with ocular iontophoresis.

Although NaAMPS hydrogels possess the required adhesiveness and a relatively high concentration of sodium ions (Na^+), the conductivity behaviour is limited as the Na^+ is linked to a large AMPS anion, as illustrated in chapter 2. When polymerised the large sulphonate anion become fixed to the polymer backbone; hence a NaAMPS polymer is associated with a fixed charge density that is composition dependent. In order to extend the range of adhesive hydrogels for use as bioelectrodes in therapeutic applications the aim of the work carried out here was to design conductive skin adhesives containing neutral monomers such as NVP and NNDMA in an attempt to "dilute" the fixed charge density. The potential to design an adhesive containing neutral monomers would produce a more versatile skin adhesive as the effect of adding different types and amounts of mobile charge carriers, for example alkali salts, on impedance could be investigated.

Generally a skin adhesive hydrogel should be cohesive and readily removable. It should provide good skin contact and for optimal biocompatibility should not have residual monomers. The adhesive hydrogels referred to in this thesis were photo-polymerised, as it would be impractical to thermally polymerise skin adhesives during mass production. Although, in order to determine their EWC, hydrogel membranes were thermally polymerised and then fully hydrated in 0.9 %, 2 % and 5 % w/v (approximately 0.15, 0.34 and 0.86 M) NaCl. This served to determine whether "diluting" the fixed charge density

lowered the residual capacity of the hydrogels for water uptake, as in partially hydrated skin adhesives adhesion is promoted by removal of interfacial moisture.

Hydrogel membranes consisting of anionic monomers "diluted" with neutral monomers had EWCs above 80 %, indicating that the neutral monomers were sufficiently hydrophilic to maintain the aggressiveness to absorb interfacial water. Although, EWC decreased with increasing saline concentration (figure 3.2) the decrease was not as large as anticipated due to the evolution of the forces that contribute to swell as the osmolarity of the hydrating medium increases.

Given that "diluting" ionic monomers with neutral ones produced hydrogel membranes with a high residual capacity to absorb interfacial moisture, partially hydrated were formulated and the functional changes were evaluated by measuring peel strength and viscoelastic properties of the gel.

6.1.1.1 Peel adhesion

The mean maximum peel strength, that is the tensional force required to remove the adhesive at a peel angle of 90°, for the anionic adhesive hydrogels was below 8 N/25mm (section 3.4.1.1) and that of the neutral adhesive hydrogels was below 2 N/25mm (section 3.5.1.1). The neutral adhesive hydrogels were, unlike the ionic hydrogels, not cohesive. It was observed that the more cohesive the hydrogel the more likely it was to fail adhesively and have consistent peel strengths. Whereas non-cohesive adhesive hydrogels were "leggy" (extended), tended to fail cohesively and had inconsistent peel strengths. However, it is thought that ionic skin adhesives have higher peel strengths compared to neutral hydrogels due to an increased hyperosmotic effect.

Peal strength seemed to reach a maximum when the NaAMPS to SPA ratio was approximately 1:1 and also to lesser extent when the ratio of NVP to NNDMA was approximately 1:1 (section 3.4.1.1). At this ratio the induced dipolar attraction, between polar groups of NaAMPS and SPA molecules and those of NVP and NNDMA molecules on opposing chains, is at a maximum. The higher mean peel strength may be due to the hydrogels having improved cohesiveness, as the dipolar attraction has an effect of a secondary crosslink strengthening the network allowing, them to comply better to skin

surface. However the interaction between all the components was deemed to have a dominating effect on peel strength.

6.1.1.2 Dynamic mechanical testing

Rheology measurements provide details of the viscoelastic properties of hydrogels. Values of tan δ (ratio of viscous modulus to elastic modulus) give an indication of the cohesiveness of the hydrogel. Skin adhesive hydrogels with values of tan δ below 0.40 were preferred as they were more cohesive.

Generally tan δ of the anionic adhesive hydrogels decreased gradually with frequency and then sharply at very high frequency (section 3.4.2.1). This trend was desirable as it demonstrated that the adhesive hydrogel would be adequately malleable during application (lower frequencies), allowing it to form a good bond with skin, and would remain cohesive on removal (higher frequencies). On the other hand tan δ of neutral adhesive hydrogels increased with frequency and then fell sharply at very high frequencies (section 3.5.2.1). This was due to much lower differences in G' than G" of neutral adhesive hydrogels compared to the anionic adhesive. Thus, the neutral adhesive hydrogels were less cohesive compared to anionic ones and notably "leggier". Hence this suggests that an ionic monomer is desired for cohesion. Furthermore the lack of acrylic acid in neutral adhesive hydrogels may have added to their lowered cohesiveness. In addition the optimum amount of crosslinker-initiator mixture was the same as that used for anionic adhesive hydrogels, however this value might not be optimum for a neutral system.

Comparing tan δ to average peel strength suggested that at low tan δ values, peel strength was reasonably consistent as the adhesive hydrogels were not "leggy". However, at higher tan δ values peel strength became unpredictable, as the adhesive hydrogels were likely to "leg" (section 3.4.2.1).

6.1.1.3 Residuals

Neutral adhesives hydrogels produced were "leggy", therefore non-cohesive. In addition a dermal response emerged forty-eight hours post-application of the neutral hydrogels to skin (section 3.5.1.1). This suggested that, unlike the anionic hydrogels, residual

monomers were precipitating from the bulk hydrogel. To determine the monomer most likely to cause the polymer backbone to swell and render it "leggy", discs of neutral and anionic hydrogels were placed in their constituent monomers and the diameter noted (section 3.6). For the neutral hydrogel swell increased along the series AMO < NVP < NNDMA. For the anionic hydrogel swell increased along the series glycerol < NaAMPS < NNDMA.

For both types of adhesive hydrogels NNDMA was found to be the monomer most likely to cause swell and therefore "legging". This is probably because the carbonyl group on NNDMA is less shielded as the amide group is less sterically hindered, thus it forms hydrogen bonds more easily and so it is likely to interact with the same sites as water within the hydrogel.

Gas chromatography was used to quantify the relative amounts of residual monomer. At a similar monomer feed, residual NNDMA was greater than that of residual NVP. This indicated that NNDMA is less likely to polymerise under the conditions used. NNDMA contains alternating double bonds that are able to stabilise the initiator's free radical and, therefore, do not break easily to form another bond during polymerisation. Thus the use of NNDMA under similar conditions is not recommended for the fabrication of skin adhesives for use with the Optis system.

6.1.1.4 Impedance

Impedance measurements (section 3.7) showed that the anionic hydrogels produced had lower impedance compared to the 3M red dot electrode, deemed as not acceptable by Optis, and other commercialised electrodes. This indicated that composition was likely to affect impedance. However there was no significant change in impedance between the anionic hydrogels produced for the purposes of this research, as their fixed charge density was comparable.

Increasing the hydrogel thickness resulted in an impedance increase. However, increasing the surface area of the hydrogel electrode caused impedance to decrease. This may be a result of a reduction in current density. Increasing current frequency also caused impedance to drop. However, impedance reduction was most significant at lower than at

higher frequencies. This clearly demonstrates the need to design adhesive bioelectrodes for the intended application. The results obtained for increasing electrode surface area and current frequency were analogous to those in the literature.
There were no readings for either potential or current when the neutral hydrogels were tested. This indicated that current was not passing through suggesting that water is not sufficient to pass on current. The incorporation of charge carriers was, therefore, investigated.

Increasing amount of charge carrier in neutral hydrogels resulted in a reduction in impedance due to an elevated passage of current. At low amounts of charge carrier KCl containing hydrogels had higher impedance compared to those containing NaCl. Additionally at low quantities of charge carrier increasing amount of K^+ resulted in a larger reduction in impedance compared to Na^+. This difference could be due to the size and mobility differences.

The impedance of neutral hydrogels containing charge carriers was lower, even at significantly lower amounts of charge carrier, compared to anionic hydrogels containing SPA and NaAMPS. This suggests that the nature of the anion also affects impedance. With neutral hydrogels the anion is mobile, however with SPA and NaAMPS hydrogels the anion is associated with the polymer chain and is therefore immobile. Thus, the nature of both cations and anions play a role in determining the hydrogels impedance.

Although neutral adhesive hydrogels produced were non-cohesive, neutral macromers may produce skin adhesives with low residual and potentially better cohesiveness. It is, therefore, not unreasonable to anticipate that with the ability to incorporate charge carriers, neutral hydrogels may be suited for use as a return electrode with the Optis system. Furthermore, the ability to formulate a particular balance of electrolytes into neutral adhesives may also provide these hydrogels a niche in wound dressings. In wounds and burns where fluid loss (as distinct from blood loss) occurs, the K^+:Na^+ ratio is closer to that of serum than to normal excretion fluids, sweat and urine, but loss of K^+ from local tissue because of the mass or volume loss is a cause of concern as the body normally retains K^+ while it easily gets rid of Na^+. In conclusion for wound dressing applications an osmotic gradient for both Na^+ and K^+ will be helpful to reduce electrolyte loss, similar to the principle applied in sports drinks.

6.1.2 Macromolecular release

A wide range of water-soluble polymers have been used historically both as wetting agents and as a means of increasing viscosity in contact lens solutions. One under-exploited area is the use of the contact lens as a drug delivery device. The lens matrix could be used as a delivery vehicle to, for example, bring about the controlled release of water-soluble polymers in an attempt to modify the lens-tear interface and bring about a similar effect by a different means. In turn this would provide a platform for the development of more effective controlled release systems for other actives without the immediate need for clinical studies which are subjected to stringent regulations. The most significant generic feature of the existence (by chance rather than by design!) of a clinically available lens, Focus® Dailies®, that releases a water-soluble polymer, PVA, is that it enables the development of an *in vitro* system, specifically a PVA release model, that relates closely to *in vivo* release from a contact lens into the tear layer.

The *in vitro* method found (section 4.4) to most closely simulate *in vivo* eye behaviour involved placing the lens in an Eppendorf microtube containing 100 µl extraction medium and vortexing for fifteen seconds at the beginning and end of a one hour extraction period. The lens would then be removed and placed in another microtube containing 100µl of fresh extraction medium and the process repeated for the required period. RI of the extraction media post extraction was used to determine the amount of PVA released from the lens.

Using this *in vitro* model it was established (section 4.5) that the older the lens the higher the packing solution concentration of PVA. Furthermore, it was realised that the packing solution of lenses that were just manufactured were likely to contain PVA. This indicated that a step in the manufacturing process enhanced the release of PVA from the contact lens. Contact lenses are required to undergo a sterilisation process post manufacture. In the case of Focus® Dailies®, the lenses are autoclaved post-packaging. Since this occurs at high temperatures the lens is placed under "stress" which may enhance release of PVA from the surface (section 4.6).

A larger amount of PVA at the surface of the contact lens may potentially reduce dry eye discomfort experienced by contact lens wearers. Given that there are physical limitations

to increasing the surface area of a contact lens, the incorporation of mobile PVA into the lens matrix was investigated (section 4.8). A comparison of incorporating 0.2 % (w/w) of two molecular weights of PVA, 47000 (47k) and 61000 (61k), was made. The packing solution RI of the 61k lens was lower than the 47k lens. This may have been because 61k PVA is not as mobile as the 47k PVA, thus more of 61k PVA remained within the matrix. The *in vitro* release model showed that the 61k lens released more PVA than the 47k lens, thus agitation assisted the displacement of the 61k PVA from the matrix to the surface of the lens. However, even with agitation the 61k PVA did not reach the surface immediately. During the first to third hour the release profile (figure 4.16) of the 61k lens release has a steeper gradient compared to that of the 47k lens. This may have been due to the "burst" release phenomenon as after this the release rate was similar to that of the 47k lens.

The *in vitro* release model also demonstrated (section 4.9) that worn contact lenses continued to release PVA after eight hours of wear, albeit at a lower release rate than unworn lenses. This implied that worn lenses "lose" most surface PVA in eye and that surface depletion of PVA in eye occurs by an "active" mechanism that outstrips ability of passive diffusion to maintain surface concentration. Although this indicated that the *in vitro* model cannot keep up with the in eye extraction, this *in vitro* model gives some simulation of *in vivo* release (much faster than passive diffusion) proving a useful tool for comparing the various factors that contribute to the mechanism of PVA release *in vivo*.

The lower release rate of PVA from worn lenses suggested that there is potentially a lower amount of PVA on the lens' front surface. Since the surface of the contact lens may affect both the feel of the sliding motion of the eyelid and the spreading of the tear film during a blink cycle, potentially having a major effect on lens comfort, determining the coefficient of friction, μ, of contact lenses *in vitro* would not only enable the comparison of different lens surfaces but also their effect on patient comfort.

A comparison (section 4.10) between Focus® Dailies® and a non-PVA based lens, Biomedics®55, illustrated that the μ for the Biomedics®55lens was significantly higher than the Focus® Dailies®. Thus, the lubricating ability of PVA present at the surface of the lens lowered μ substantially. Furthermore, PVA at the surface of the lens was found to

have a larger influence on μ compared to PVA in the lubricating solution (section 4.10.1). For both type of lenses the μ of the worn lens was lower than the unworn lens. This was probably because initial protein and lipid deposition reduces the μ somewhat, however, for lenses worn over longer periods of time (days) the progressive degradation of protein and lipid is likely to cause a deterioration of surface properties, including lubrication. In addition further protein and lipid deposition would destabilise the tear film causing a breakdown in lubrication and it is this breakdown in lubrication that is likely to have the most dramatic effect in increasing μ.

6.1.3 Kinetics of release from hydrogels

Recently there has been a lot of research[21, 36, 41, 62-64, 69] focused towards transporting drugs across skin into the bloodstream. Although this is not impossible it is difficult to achieve. In many cases however, drugs are required to simply get to the dermis or epidermis. This study involved designing adhesive hydrogels for use as a return electrode in ocular iontophoresis (chapter 3). Iontophoresis is a technique that may be used to drive a charged drug into the upper skin layers using current. A general rule is that electrotherapy enhances the passive permeation of an active by about ten fold depending upon current density. Since the differences in biological activity of different drugs are already known, the ability to predict the passive permeation is desirable as this would enable the estimation of electrically assisted permeation.

The passive release of a drug from a hydrogel based delivery vehicle is influenced by the interaction between the drug, the hydrogel matrix and the release environment (section 5.4). The result of this is that a series of partitioning stages are involved during the release process. The first stage is concerned with the partitioning of the drug between the polymeric and aqueous components of the hydrogel. The second stage involves the drug release from the vehicle and partitioning between the lipoidal and aqueous parts of the biological membrane. This extent of partitioning is influenced by the $logP^N$ and logD (octanol-water partition coefficients) of the drug. The first term is not pH dependent as it describes the non-ionised form of the drug. The latter term is influenced by the pK_a of the drug; therefore pH of the partitioning environment as it includes the ionised form of the drug.

In order to evaluate passive drug permeation the use of the pH-partitioning flux model was investigated (section 5.3.2) for the delivery of common drugs such as ibuprofen (acid) and lidocaine (basic).

The model showed that for either ibuprofen or lidocaine flux, through a lipid membrane, was at maximum when the pH was similar to that of their respective pK_a values with notable reduction two pH units above or below the pK_a values. Although this model provides an insight of the behaviour of an active, there are limitations that need to be taken into account. These are:

i. the partitioning of the species in the polymer or lipoidal and aqueous components of a biological membrane is more complex than partitioning between octanol and water
ii. an increase in concentration will increase the flux of the species only up to a point where the diffusion of the species becomes a limiting factor.

In order to investigate the effect of hydrogel composition on release kinetics, release characteristics from hydrogels with different compositions were investigated (section 5.4.2). Model compounds such as dyes instead of specific drugs were used, as this was more cost effective. The added advantage of dyes is that a simple analysis technique, colorimetry, instead of a more complex one could be employed facilitating the investigation process. For this study three fully hydrated hydrogel compositions in the form of contact lenses were investigated. A single model composite, basic fuchsin, based on lidocaine due to its increased interest for use in cataract surgery was chosen. The contact lenses were loaded with the dye and subsequently released into phosphate-buffered saline, a pH 7.4 medium similar to that of blood. For all three materials the release profile obtained by plotting amount released against time$^{1/2}$ was typical of a two-stage type release pattern. This involves a first phase rapid initial "burst" release, which is followed by a substantial second phase of approximately linear first order release. A third stage of no or very little release could also be identified whereby the polar interaction of the dye with the hydrophilic monomers of the polymer backbone was more influential. Thus, the extraction process did not reach completion. Given that this form of release profile is typical of release pattern observed with monolithic (matrix) systems, that is it is time dependent, the release kinetics from contact lenses can be modelled by solving for Fick's second law of diffusion provided that the coefficient of diffusion is known.

6.2 Suggestions for further work

It has been recommended that neutral adhesive hydrogels incorporated with charge carriers would be the preferred choice as a return electrode with the Optis system. However, the neutral adhesives produced during this research were non-cohesive. Acrylic acid is thought to improve the cohesiveness of skin adhesives; thus the effect of adding acrylic acid on cohesiveness of neutral hydrogels could be evaluated. Furthermore, the potential to produce cohesive neutral hydrogels from novel neutral macromers would be another interesting area of study. In addition, the lack of cohesiveness may have been due to the inefficacy of the polymerisation process; hence varying the crosslinker–photoinitiatior ratios as well as amounts and also the use of other crosslinkers and photoinitiators could be investigated to optimise the polymerisation process. This could also be extended to exploring other methods of initiation, for example redox, that would allow hydrogels to be used in other applications such as in-situ polymerisation for use as synthetic spine disc or as a "smart" drug delivery agent to deliver the right amount of drug when the appropriate signal is given.

Impedance measurements of the adhesive hydrogels produced showed that impedance increased with thickness, however it was not determined whether or not there is an optimal thickness. Impedance was only measured for ten minutes gel impedance over longer periods could be considered, as some treatments may require a longer application of current. Incorporating NaCl and KCl into neutral hydrogels showed that impedance varied depending on type and amount of cation. Formulating compositions of neutral hydrogels containing other salts in order to investigate the effect of bigger cations as well as effect of different anions would be worthy of further analysis. The ionic adhesive hydrogels were formulated with anionic monomers associated with a mobile cation; hence it would be worth comparing the effect of cationic monomers associated with a mobile anion on impedance.

The impedance measurement device used was limited to a maximum of 2V. Although it was possible to vary frequency it was not possible to vary pulse width or type of current. Hence a robust device that would allow for different iontophoresis and electroporation conditions to be selected would be desired the for further impedance characterisation.

Furthermore the system could also be used to deliver species through a membrane into a release medium.

Although the benefits of iontophoretic and electroporation drug delivery have been known for a number of years, these techniques have not been the major method of drug delivery as only approximately ten drugs are loaded into skin adhesives and that a system for home use has not been available. However a more recent development, that is not yet on the market at the time of submitting this thesis, has been the incorporation of micropowered cells into patches ("powerpaper" technology) providing an integrated system consisting of drug, vehicle and delivery mechanism. Thus a logical extension to the work carried out here would be to take forward gel design and harness the gels to deliver actives such as ibuprofen and lidocaine. The manipulation of hydrogel compositions to improve vehicle-drug compatibility would allow for an increase of the number of actives administered using electrotherapeutic methods. The use of similar techniques such as ultrasound and magnetophoresis could be assessed in order to establish if a technique or possibly a combination of techniques produces sustained drug delivery. This could also entail determining whether choice of techniques is drug specific. The modification of existing or development of new *in vitro* models to determine the permeation of various drugs across an appropriate membrane using a single or a combination of techniques would be equally appealing.

The existence of a clinical lens that releases a water-soluble polymer (PVA) enabled the development of an *in vitro* system that relates closely to *in vivo* release behaviour. This suggested that a sufficiently large amount of linear polymer remained within the lens matrix post extraction. This could be verified by etching the lens' surface, to "expose" bulk PVA at the lens surface, then re-extracting the lens *in vitro* and compare changes in release rate. In addition characterisation of the differences, if any, of release from the front and back surface of lenses has not yet been carried out. Although an attempt at comparing the coefficient of friction of unworn and worn lenses was made, that of the lenses extracted *in vitro* was not determined. Similarly evaluating the energetics of the lens surface at different stages of release would provide a fuller picture on the rate of change of the surface.

The release kinetics of smaller molecules from contact lenses was also considered. A model compound (dye) was absorbed by the lens and then released. The release was allowed to take place at low agitation. Having established an *in vitro* release system that provides a closer resemblance to the *in eye* mechanical extraction by the action of the eyelids, the release kinetics of the dye from the lens using this model would be worthy of further assessment. Furthermore, incorporating ophthalmic dyes into contact lenses might reduce the regulatory issues associated with clinical trials of therapeutic lenses.

References

1. Peppas, N.A., Langer, R, *New challenges in biomaterials.* Science, 1994. **264** (5154): p. 1715-1720.

2. Wichterle, O., Lim, D., *Hydrophilic gels for biological use.* Nature, 1960 (9 Jan.): p. 117.

3. Peppas, N.A., Mikos, A.G, *Preparation methods and structure of hydrogels*, in *Hydrogels in Medicine and Pharmacy, Vol. 1, Fundamentals*, N.A. Peppas, Editor. 1986, CRC Press: Boca Ranton, Florida. p. 1-25, Chapter 1.

4. Corkhill, P.H., Hamilton, C.J. and Tighe, B.J., *The design of hydrogels for medical applications.* Critical Reviews in Biocompatability, 1990. **5**(4): p. 363-436.

5. Hoffman, A.S., *Hydrogels for biomedical applications.* Advanced Drug Delivery Reviews, 2002. **43**: p. 3-12.

6. Peppas, N.A., *Hydrogels*, in *Biomaterials Science: An Introduction to Materials in Medicine*, B.D. Ratner, Hoffman, A.S., Lemons, J.E., Schoen, F.J., Editor. 1997, Academic Press: London. p. 60 - 64.

7. Parthiban, L., *Preparation, structure and properties of polymeric hydrogels and their biomedical applications.* The Chemist, 1997(May/ June): p. 11-16.

8. Lowman, A.M., Peppas, N.A., *Hydrogels*, in *Encyclopaedia of Controlled Drug Delivery*, E. Mathiowitz, Editor. 1999, Wiley: New York. p. 397-418, Part B.

9. Peppas, N.A., Bures P., Leobandung W., Ichikawa H., *Hydrogels in pharmaceutical applications.* European Journal of Pharmaceutics and Biopharmaceutics, 2000. **50**: p. 27-46.

10. Kishida, A., Ikada, Y., *Hydrogels for biomedical and pharmaceutical applications*, in *Polymeric Biomaterials*, S. Dumitriu, Editor. 2002, Marcel Dekker, Inc.: New York. p. 133-145, Chapter 6.

11. Pedley, D.G., Skelly P.J., Tighe, B.J., *Hydrogels in biomedical applications.* The British Polymer Journal, 1980. **12**: p. 99-110.

12. Tighe, B.J., *Towards the bionic man - a new biomedical technology*, in *Biomedical Technology*, R. Greenshields, Editor. 1992. p. 186-192.

13. Corkhill, P.H., Jolly, A.M., Ng, C.O., *Synthetic hydrogels: 1-hydroxyalkyl acrylate and methacrylate copolymers - water binding studies.* Polymer, 1987. **28**: p. 1758-1766.

14. Muller-Plate, F., *Different states of water in hydrogels.* Macromolecules, 1998. **31**: p. 6721-6723.

15. Quinn, F.X., Kampff, E., Smyth, G., McBrierty, V.J., *Water in hydrogels 1. A study of water in poly(N-vinyl-2-pyrrolidone/ methyl methacrylate) copolymers.* Macromolecules, 1988. **21**: p. 3191-3198.

16. Cartwright, H.R., *Hydrogels for dermal applications*. 2003, Aston University: Birmingham, U.K.

17. Fleming, M.C., *Skin adhesive hydrogels for biomedical applications*. 1999, Aston University: Birmingham, UK.

18. Anseth, K.S., Bowman, C.N., Brannon-Peppas, L., *Mechanical properties of hydrogels and their experimental determination.* Biomaterials, 1996. **17**: p. 1647-1657.

19. Sperling, L.H., *Interpenetrating polymer networks and related materials*. 1981, Plenum Press: New York.

20. Peppas, N.A., *Preface*, in *Hydrogels in Medicine and Pharmacy, Vol.1, Fundamentals*, N.A. Peppas, Editor. 1986, CRC Press: Boca Ranton, Florida.

21. Tan, H.S., Pfister, W.R., *Pressure sensitive adhesives for transdermal drug delivery systems.* Pharmaceutical Science and Technology Today, 1999. **2**(2): p. 60 -69.

22. Park, K., Park, H., *Test methods of bioadhesion*, in *Bioadhesive Drug Delivery systems*, V. Lenaerts, Gurny, R., Editor. 1990, CRC Press: Boca Ranton, Florida. p. 43-64, Chapter 3.

23. Park, K., Cooper, S.L., Robinson, J.R., *Bioadhesive hydrogels*, in *Hydrogels in Medicine and Pharmacy, Vol. 3, Properties and Applications*, N.A. Peppas, Editor. 1986, CRC Press: Boca Ranton, Florida. p. 151-175, Chapter 8.

24. Chickering III, D.E., Mathiowitz, E, *Definitions, mechanisms and theories of bioadhesion*, in *Bioadhesive Drug delivery Systems Fundamentals, Novel Approaches and Development*, E. Mathiowitz, Chickering III, D.E.,Lehr, C-M, Editor. 1999, Marcel Dekker, Inc.: New York. p. 1-10, Chapter 1.

25. Venkatraman, S., Gale, R., *Skin adhesives and skin adhesion 1. Transdermal drug delivery systems.* Biomaterials, 1998. **19**: p. 1119-1136.

26. Mikos, A.G., Peppas, N.A., *Scaling concepts and molecular theories of adhesion of synthetic polymers to glycoproteinic networks*, in *Bioadhesive Drug Delivery Systems*, V. Lenaerts, Gurny, R., Editor. 1990, CRC Press: Boca Ranton, Florida. p. 25-42, Chapter 25.

27. Williams, F.R., *Skin conducting electrode and electrode assembly, US Patent 4,117,846*. 1978, Consolidated Medical Equipment.

28. Gupta, P.K., Leung, S-H. S., Robinson, J.R., *Bioadhesives, mucoadhesives in drug delivery to the gastrointentestinal tract*, in *Bioadhesive Drug Delivery Systems*, V. Lenaerts, Gurny, R., Editor. 1990, CRC Press: Boca Ranton, Florida. p. 65-92, Chapter 4.

29. Tighe, B.J., *The design of polymers for contact lens applications.* The British Polymer Journal, 1976(Sept.): p. 71-77.

30. Tighe, B.J., *Hydrogels as contact lens materials*, in *Hydrogels in Medicine and Pharmacy, Vol. 3, Properties and Applications*, N.A. Peppas, Editor. 1986, CRC Press: Boca Ranton, Florida. p. 53-82, Chapter 3.

31. Hsieh, D.S.T., *Controlled release systems: past, present and future*, in *Controlled Release Systems: Fabrication Technology, Vol. 1*, D.S.T. Hsieh, Editor. 1988, CRC Press: Boca Ranton, Florida. p. 1-16, Chapter 1.

32. Langer, R.S., Peppas, N.A., *Present and future applications of biomaterials in controlled drug delivery systems.* Biomaterials, 1981. **2**(Oct.): p. 201-214.

33. Heller, J., *Drug delivery systems*, in *Biomaterials Science: An introduction to Materials in Medicine*, B.D. Ratner, Hoffman, A.S., Lemons, J.E., Schoen, F.J., Editor. 1997, Academic Press: San Diego, California. p. 346-370, Chapter 7.8.

34. Chen, L.H., Chien, Y.W., *Transdermal iontophoretic permeation of luteinizing hormone releasing hormone: characterisation of electric parameters.* Journal of Controlled Release, 1996. **40**: p. 187-198.

35. Williams, A.C., *Transdermal and topical drug delivery.* 2003, Pharmaceutical Press: London.

36. Ranade, V.V., *Drug delivery systems 6: transdermal drug delivery.* Journal of Clinical Pharmacology, 1991. **31**(5): p. 401-418.

37. Duncan, R., Seymour, L.W., *Controlled release technologies. A Survey of research and commercial applications.* 1989, Elsevier Advanced Technology: Oxford.

38. Stella, V.J., Mikkelson, T.J., Pipkin, J.D., *Prodrugs: the control of drug delivery via bioreversible chemical modification*, in *Drug Delivery Systems: Characteristics and Biomedical Applications*, R.L. Juliano, Editor. 1980, Oxford University Press: New York. p. 112-176, Chapter 4.

39. Rutter, N., *Applied physiology: the new born skin.* Current Paediatrics, 2003. **13**: p. 226-230.

40. Maillard-Salin, D.G., Bécourt, Ph., Couarraze, G., *A study of the adhesive-skin interface: correlation between adhesion and passage of a drug.* International Journal of Pharmaceutics, 2000. **200**: p. 121-126.

41. Naik, A., Kalia, Y.N., and Guy, R.H., *Transdermal drug delivery:overcoming the skin's barrier function.* Pharmaceutical Science and Technology Today, 2000. **3**(9): p. 318-326.

42. Urtti, A., Salminen, L., *Minimising systemic absorption of topically administered ophthalmic drugs.* Survey of Ophthalmology, 1993. **37**(6): p. 435-456.

43. Felt, O., Einmahl, S., Gurny, R., Furrer, P., Baeyens, V., *Polymeric systems for opthalmic drug delivery*, in *Polymeric Biomaterials*, S. Dumitriu, Editor. 2002, Marcel Dekker, Inc.: New York. p. 377-421, Chapter 15.

44. Mitra, A.K., *Opthalmic drug delivery devices*, in *Drug Delivery Devices Fundamentals and Applications*, P. Tyle, Editor. 1988, Marcel Dekker, Inc.: New York. p. 455-470, Chapter 15.

45. Lee, V.H.L., *Precorneal, corneal and post corneal factors*, in *Ophthalmic Drug Delivery Systems*, A.K. Mitra, Editor. 1993, Marcel Dekker, Inc.: New York. p. 59-81, Chapter 3.

46. Järvinen, K., Järvinen, T., Urtti, A., *Ocular absorption following topical delivery.* Advanced Drug DeliveryReviews, 1995. **16**: p. 3-19.

47. Saettone, M.F., Burgalassi, S., Chetoni, P., *Ocular bioadhesive drug delivery systems*, in *Bioadhesive Drug delivery Systems Fundamentals, Novel Approaches and Development*, E. Mathiowitz, Chickering III, D.E., Lehr, C-M., Editor. 1999, Marcel Dekker, Inc.: New York. p. 601-640, Chapter 22.

48. Hughes, P.M., Mitra, A.K., *Overview of ophthalmic drug delivery and iatrogenic ocular cytopathologies*, in *Ophthalmic Drug Delivery Systems*, A.K. Mitra, Editor. 1993, Marcel Dekker, Inc.: New York. p. 1-27, Chapter 1.

49. Burrows, J., Tsibouklis, J.,Smart J.D., *Drug delivery to the eye.* The Drug Delivery Companies Report, Pharmaventures, 2002. (Spring/ Summer).

50. Robinson, J.C., *Ocular anatomy and physioslogy relevant to ocular drug delivery*, in *Ophthalmic Drug Delivery Systems*, A.K. Mitra, Editor. 1993, Marcel Dekker, Inc.: New York. p. 29-57, Chapter 2.

51. Keister, J.C., Cooper, E.R., Missel, P.J., Lang,J.C., Hager, D.F., *Limits on optimising ocular drug delivery.* Journal of Pharmaceutical Sciences, 1991. **80**(1): p. 50-53.

52. Saettone, M.F., *Progress and problems in ophthalmic drug delivery.* Business Briefing: Pharmatec, 2002: p. 167 - 171.

53. Zignani, M., Tabatabay, C., Gurny, R., *Topical semi-solid drug delivery: kinetics and tolerance of ophthalmic hydrogels.* Advanced Drug Delivery Reviews, 1995. **16**: p. 51-60.

54. Jain, M.R., *Drug delivery through soft contact lenses.* British Journal of Ophthalmology, 1988. **72**: p. 150-154.

55. Hiratani, H., Alvarez-Lorenzo, C., *The nature of backbone monomers determines the performance of imprinted soft contact lenses as timolol drug delivery systems.* Biomaterials, 2004. **25**: p. 1105-1113.

56. Hecht, G., *Ophthalmic preparations*, in *Remington: The Science and Practice of Pharmacy*, A.R. Gennaro, Editor. 2000, Lippincott Williams & Wilkins: Baltimore, Maryland. p. 821-835, Chapter 43.

57. http://www.xenophilia.com/zb0061.htm, correct at time of thesis submission.

58. Sangster, J., *Octanol-water partition coefficients; fundamentals and physical chemistry*. 1997, Wiley: New York.

59. Pagliara, A., Reist, M., Geinoz, S., Carrupt, P.A., Testa, B., *Evaluation and prediction of drug permeation.* Journal of Pharmacy and Pharmacology, 1999. **51**(12): p. 1339-1357.

60. Singh, C.P., Shah, D.O., *Surface chemical aspects of ocular drug delivery systems*, in *Ocular Therapeutics and Drug Delivery a Multi-Disciplinary Approach*, I.K. Reddy, Editor. 1996, Technomic: Lancaster. p. 31-49, Chapter 2.

61. Lawrence, M.S., Miller, J.W., *Ocular tissue permeabilities.* International Ophthalmic Clinics, 2004. **44**(3): p. 53-61.

62. Barry, B.W., *Novel mechanisms and devices to enable successful transdermal drug delivery.* European Journal of Pharmaceutical Sciences, 2001. **14**: p. 101-114.

63. Kalia, Y.N., Naik, A., Garrison, J., Guy, R.H., *Iontophoretic drug delivery.* Advanced Drug Delivery Reviews, 2004. **56**: p. 619-658.

64. Banga, A.K., *Electrically assisted transdermal and topical drug delivery*. 1998, Taylor & Francis: London.

65. Banga, A.K., Bose, S., Ghosh, T.K., *Iontophoresis and electroporation: comparisons and contrasts.* International Journal of Pharmaceutics, 1999. **179**(1): p. 1-19.

66. Singh, P., Maibach, H.I., *Iontophoresis in drug delivery: basic principles and applications.* Critical Reviews in Therapeutic Drug Carrier Systems, 1994. **11**(2&3): p. 161-213.

67. http://www.empi.com, correct at time of thesis submission.

68. Baeyens, V., Percicot, C., Zignani, M., Deshpande, A.A., Kaltsatos, V.and Gurny, R., *Ocular drug delivery in veterinary medicine.* Advanced Drug Delivery Reviews, 1997. **28**(3): p. 335-361.

69. Prausnitz, M.R., *A practical assessment of transdermal drug delivery by skin electroporation.* Advanced Drug Delivery Reviews, 1999. **35**(1): p. 61-76.

70. http://optis.ifrance.com/optis/Technology, correct at time of thesis submission.

71. *Personal communication Prof. Jean-Marie Parel, Bascom Palmer Eye Institute, University of Miami, Florida, U.S.A.*

72. Jadoul, A., Bouwstra, J., Preat, V., *Effects of iontophoresis and electroporation on the stratum corneum. Review of the biophysical studies.* Advanced Drug Delivery Reviews, 1999. **35**(1): p. 89-105.

73. Curdy, C., Kalia, Y.N., Guy. R.H., *Post-iontophoresis recovery of human skin in vivo.* European Journal of Pharmaceutics and Biopharmaceutics, 2002. **53**: p. 15-21.

74. Prausnitz, M.R., *The effects of electric current applied to skin: a review for transdermal drug delivery.* Advanced Drug Delivery Reviews, 1996. **18**(3): p. 395-425.

75. Nguyen, K.T., West, J.L., *Photopolymerisable hydrogels for tissue engineering applications.* Biomaterials, 2002. **23**: p. 4307- 4314.

76. *Photoinitiators for UV curing. A formulator's guide.* Ciba guide.

77. Zosel, A., *Molecular structure, mechanical behavior and adhesion performance of PSAs.* 2000(27/09), http://www.adhesivesmag.com/CDA/ArticleInformation/coverstory/BNPCoverStoryItem/0,2103,11474,00.html (correct at time of thesis submission).

78. Horstmann, M., Muller, W., Asmussen, B., *Principles of skin adhesion and methods for measuring adhesion of transdermal systems*, in *Bioadhesive Drug delivery Systems Fundamentals, Novel Approaches and Development*, E. Mathiowitz, Chickering III, D.E., Lehr, C-M., Editor. 1999, Marcel Dekker, Inc: New York. p. 175-195, Chapter 8.

79. *Bohlin instruments CVO Rheometer operating manual.*

80. http://whatis.techtarget.com/definition/0,sid9_gci212333,00.html, correct at time of thesis submission.

81. *Cecil instruments CE404 spectrophotometer operating manual.*

82. http://www.shu.ac.uk/schools/sci/chem/tutorials/chrom/gaschrm.htm, correct at time of thesis submission.

83. *Personal communication Dr. D.E. Walton, Aston University, Birmingham B4 7ET.*

84. *Bruker Flex III user's guide.*

85. Macha, S.F., Limbach, P.A., *Matrix-assisted laser desorption/ ionisation mass spectrometry of polymers.* Current Opinion in Solid State and Materials Science, 2002. **6**: p. 213-220.

86. Nagy, D.J., *Aqueous SEC triple detection of polyvinyl alcohol.* American Laboratory, 2003(Jan.): p. 38- 43.

87. Schriemer, D.C., Li, L., *Detection of high molecular weight narrow polydisperse polymers up to 1.5M Daltons by MALDI mass spectrometry.* Analytical Chemistry, 1996. **68**(17): p. 2721-2725.

88. McEwen, C.N., Jackson, C., Larsen, B.S., *Instrumental effects in the analysis of polymers of wide polydispersity by MALDI mass spectrometry.* International Journal of Mass Spectrometry and Ion Processes, 1997. **160**: p. 387-394.

89. Creton, C., Fabre, P., *Tack.* http://www.mdi.espci.fr/~creton/publications/P34.pdf, correct at time of thesis submision.

90. Ratner, B.D., *Hydrogel surfaces*, in *Hydrogels in Medicine and Pharmacy, Vol.1, Fundamentals*, N.A. Peppas, Editor. 1986, CRC Press: Boca Ranton, Florida. p. 85-34, Chapter 4.

91. *Geigy scientific tables, volume 1: units of measurement, body fluids, composition of the body, nutrition*, C. Lentner, Editor. 1981, Ciba-Geigy Ltd.: Basle.

92. Benning, B.K., *Novel high water content hydrogels.* 2000, Aston University: Birmingham, UK.

93. Lugao, A.B., Rogero S.O., Malmonge, S.M., *Rheological behaviour of irradiated wound dressing poly(vinyl) pyrrolidone hydrogels.* Radiation Physics and Chemistry, 2002. **63**: p. 543-546.

94. Schulz, D.N., Kitano, K., Danik, J.A., Kaladas, J.J., *Copolymers of N-vinylpyrrolidone and sulfonate monomers.* Polymers in Aqueous Media, 1989: p. 165-173.

95. *Appendix*, in *Biomaterials science: an introduction to materials in medicine*, B.D. Ratner, Hoffman, A.S., Lemons, J.E., Schoen, F.J., Editor. 1997, Academic Press: London.

96. http://www.brianmac.demon.co.uk/drinks.htm, correct at time of thesis submission.

97. Lemp, M.J., Holly, F.J., *Ophthalmic polymers as ocular wetting agents.* Annals of Ophthalmology, 1972. **4**: p. 15-20.

98. Kaur, I.P., Singh, M., Kanwar, M., *Formulation and evaluation of ophthalmic preparations of acetazolamide.* International Journal of Pharmaceutics, 2000. **199**: p. 119-127.

99. http://www.pharmj.com/Editorial/20000205/education/eye_otc.html#Ref53, correct at time of thesis submission.

100. Maissa, C., Tonge,S., Guillon, M. and Tighe, B.J., *Surface properties of daily disposable contact lenses.* in *Abstracts of the BCLA Annual Clinical Conference.* 1998. Brighton, UK.

101. Tighe, B.J., Wolffsohn, J.S., *Eye-contact lens interface: the influence of macromolecules.* in *International Society for Contact Lens Research.* 2005. Coolum, Australia.

102. Shastri, V., *Non degradable biocompatible polymers in medicine: past, present and future.* Current Pharmaceutical Biotechnology, 2003. **4**(5): p. 331-337.

103. Campbell, D., *Thesis to be published*, Aston University: Birmingham, UK.

104. Lee, V.H.L., Li, S. Y., Sasaki, H., Saettone, M.F. and Chetoni, P., *Influence of drug release rate on systemic timolol absorption from polymeric ocular inserts in the pigmented rabbit.* Journal of Ocular Pharmacology, 1994. **10**(2): p. 421- 429.

105. Goldenberg, M., Beekman, A., Rennwantz, E., *Polyvinyl alcohol/borate ophthalmic drug delivery system, WO patent 94/10976.* 1994, Ciba Geigy Corporation.

106. Bühler, N., Haerri, H., Hofmann, M., Irrgang, C., Mühlebach, A., Müller, B., Stockinger, F., *Nelfilcon A: a new material for contact lenses.* Chimia, 1999. **53**(6): p. 269-274.

107. *Ciba vision education presentation.*

108. Josephson, J.E., *Observation of the specular reflection from the anterior surface of the preocular film*, in *Preocular Tear Film in Health, Disease and Contact Lens Wear*, F.J. Holly, Editor. 1986, Dry Eye Institute: Lubbock, Texas. p. 554-562, Chapter 49.

109. Peterson, R.C., Wolffsohn, J.S., Nick, J., Winterton L., Lally, J., *Clinical performance of daily disposable soft contact lenses using sustained release technology.* Contact Lenses and Anterior Eye, awaiting publication 2006.

110. Crank, J., *The mathematics of diffusion.* 2nd ed. 1975: Oxford University Press.

111. Peppas, N.A., *Diffusion through polymers*, in *Transdermal Delivery of Drugs, Vol. 1*, A.F. Kydonieus, Berner, B., Editor. 1987, CRC Press. p. 17-28.

112. Ritger, P.L., Peppas, N.A., *A Simple equation for description of solute release I. Fickian and non-Fickian release from non-swellable devices in the form of slabs, spheres, cylinders or discs.* Journal of Controlled Release, 1987. **5**: p. 23 -36.

113. van der Wel, G.K., Adan, O.C.G., *Moisture in organic coatings - a review.* Progress in Organic Coatings, 1999. **37**(1): p. 1-14.

114. Mills, S.N., Davis, S.S., *Controlled drug delivery*, in *Polymers in Controlled Drug Delivery*, L. Illum, Davis, S.S., Editor. 1987, IOP Publishing Ltd.: Bristol. p. 1, Chapter 1.

115. Hadgraft, J., Valenta, C., *pH, pK(a) and dermal delivery.* International Journal of Pharmaceutics, 2000. **200**(2): p. 243-247.

116. http://en.wikipedia.org, correct at time of thesis submission.

117. Avdeef, A., Box, K.J., Comer, J.E.A., Hibbert, C., Tam, K.Y., *pH metric logP 10. Determination of liposomal membrane-water partition coefficients of ionisable drugs.* Pharmaceutical Research, 1998. **15**(2): p. 209-215.

118. http://www.syrres.com/esc/est_kowdemo.htm, correct at time of thesis submission.

119. http://www.raell.demon.co.uk/chem/calcs/index.htm, correct at time of thesis submission.

120. Barequet, I.S., Soriano, E.S., Green, W.R., O'Brien, T.P., *Provision of anaesthesia with single application of lidocaine 2% gel.* Journal of Cataract Refractive Surgery, 1999. **25**(May): p. 626-631.

121. Gombotz, W.R., Hoffman, A., *Immobilization of biomolecules and cells on and within synthetic polymeric hydrogels*, in *Hydrogels in Medicine and Pharmacy, Vol. 1, Fundamentals*, P. N.A., Editor. 1986: Boca Ranton, Florida. p. 95-126, Chapter 5.

122. Metivier-Pignon, H., Faur-Brasquet, C., Cloirec P.L., *Adsorption of dyes onto activated carbon cloths: approach of adsorption mechanisms and coupling of ACC with ultrafiltration to treat coloured waste waters.* Separation and Purification Technology, 2003. **31**(1): p. 3-11.

123. *Sigma-Aldrich chemical catalogue 2005, product no. 215597.*

124. Baker, R.W., Lonsdale, H.K., *Controlled release mechanism and rates*, in *Controlled Release of Biologically Active Agents*, A.C. Tanquary, Lacey, R.E., Editor. 1974, Plenum Press: New York. p. 15-71, Chapter 2.

APPENDICES

APPENDIX 1

Gas Chromatography Analysis

% Menthol peak area at various concentrations for different solvents

Solvent & Sample Concentrations	SOLVENT					MENTHOL				
				Std area					With std solvent area	
	Retention	Area	Area			Retention	Area	Area		
Methanol	Time / min	units^2	%	units^2	%	Time / min	units^2	%	units^2	%
0.5 w/w % menthol	2.3	563.7	95.8	353.5	95.8	3.0	24.7	4.2	15.5	4.2
5w/w % menthol	2.4	353.5	91.1	353.5	91.1	3.0	34.5	8.9	34.5	8.9
10w/w % menthol	2.3	402.2	80.1	353.5	80.1	3.0	100.2	19.9	88.0	19.9
Ethyl acetate										
0.5 w/w % menthol /	2.3	435.3	97.9	580.7	97.9	3.0	9.5	2.1	12.7	2.1
5w/w % menthol/	2.2	580.7	91.4	580.7	91.4	2.9	54.7	8.6	54.7	8.6
10 w/w % menthol/	2.4	477.5	77.0	580.7	77.0	3.0	142.5	23.0	173.3	23.0

APPENDIX 2

Fully Hydrated Hydrogels

COMPOSITIONS

Sample Reference	SPA g	NaAMPS g	TRIS g	NVP g	Acrylic Acid g	NNDMA g	Water g	AZBN g	DATr g
FH1	0.25	1.25	0.5	2.25	0.25	0.5	1.905	0.025	0.05
FH2	0.5	1	0.5	2.125	0.25	0.625	1.724	0.025	0.05
FH3	0.75	0.75	0.5	2	0.25	0.75	1.543	0.025	0.05
FH4	0.25	1.25	0.5	0	0.25	2.75	1.905	0.025	0.05
FH5	0.5	1	0.5	0	0.25	2.75	1.724	0.025	0.05
FH6	0.75	0.75	0.5	0	0.25	2.75	1.543	0.025	0.05
FH7	0. 5	1	0.5	2.75	0.25	0	1.724	0.025	0.05
FH8	0.5	1	0.5	1.75	0.25	1	1.724	0.025	0.05

Increasing NVP / reducing NNDMA amounts

Sample Reference	NVP : NNDMA
FH7	2.75 : 0
FH2	3.4 : 1
FH5	0 : 2.75

Increasing SPA / reducing NaAMPS amounts

Sample Reference	NaAMPS : SPA
FH4	5 : 1
FH5	2 : 1
FH6	1 : 1

Increasing NVP and SPA / reducing NNDMA and NaAMPS amounts

Sample Reference	NVP : NNDMA	NaAMPS : SPA
FH1	4.5 : 1	5 : 1
FH2	3.4 : 1	2 : 1
FH3	2.7 : 1	1 : 1

APPENDIX 3

Adhesive Hydrogels with Reduced Fixed Charge Density

Ionic adhesive hydrogel compositions

Sample Reference	SPA g	NaAMPS g	NVP g	NNDMA g	Acrylic Acid g	Glycerol g	Water g	Ebecryl 11: Irgacure , 10:3, Mixture g
IN1	5	14.5	10	10	5	25	30.5	0.15
IN2	10	11.6	10	10	5	25	28.4	0.15
IN3	15	8.7	10	10	5	25	26.3	0.15
IN4	5	14.5	5	15	5	25	30.5	0.15
IN5	10	11.6	5	15	5	25	28.4	0.15
IN6	15	11.6	5	15	5	25	23.4	0.15
IN7	5	14.5	15	5	5	25	30.5	0.15
IN8	10	11.6	15	5	5	25	28.4	0.15
IN9	15	8.7	15	5	5	25	26.3	0.15

Description of ionic adhesive hydrogels

During photo-polymerisation of these hydrogels a pungent smell was given off.

All these hydrogels were transparent and slightly yellow in colour.

Hydrogels IN1 to IN9 were cohesive.

Ionic adhesive hydrogel compositions

Sample Reference	SPA g	NaAMPS g	NVP g	NNDMA g	Acrylic Acid g	Glycerol g	Water g	Ebecryl II: Irgacure , 10:3, Mixture g
IN10	12.5	11.6	2.5	7.5	5	25	35.9	0.15
IN11	12.5	8.7	2.5	7.5	5	25	38.8	0.15
IN12	12.5	5.8	2.5	7.5	5	25	41.7	0.15
IN13	15	11.6	5	5	5	25	33.4	0.15
IN14	15	8.7	5	5	5	25	36.3	0.15
IN15	15	5.8	5	5	5	25	39.2	0.15
IN16	17.5	11.6	7.5	2.5	5	25	30.9	0.15
IN17	17.5	8.7	7.5	2.5	5	25	33.8	0.15
IN18	17.5	5.8	7.5	2.5	5	25	36.7	0.15

Description of ionic adhesive hydrogels

All these hydrogels were transparent and slightly yellow in colour.

Hydrogels IN10 to IN15 were non-cohesive, therefore legged. Hydrogels IN16 to IN18 were more cohesive.

Increasing SPA / reducing NaAMPS and water

Sample Reference	Water : NaAMPS : SPA
IN1 & 7	6.1 : 2.9 : 1
IN2 & 8	2.8 : 1.2 : 1
IN3 & 9	1.8 : 0.6 :1

Increasing NNDMA / reducing NVP

Sample Reference	NVP : NNDMA
IN7 & 8	3 : 1
IN1 & 2	1 : 1
IN4 & 5	0.3 : 1

Increasing water / reducing NaAMPS

Sample Reference	Water : NaAMPS
IN10 & 13 & 16	1 : 0.3
IN11 & 14 & 17	1 : 0.2
IN12 & 15 & 18	1 : 0.1

Increasing NVP and SPA / reducing water and NNDMA

Sample Reference	Water : SPA	NNDMA : NVP
IN10	2.9 : 1	3 : 1
IN13	2.2 : 1	1 : 1
IN16	1.8 : 1	0.3 : 1
IN11	3.1 : 1	3 : 1
IN14	2.4 : 1	1 : 1
IN17	1.9 : 1	0.3 : 1
IN12	3.3 : 1	3 : 1
IN15	2.2 : 1	1 : 1
IN16	2.1 : 1	0.3 : 1

Increasing water, NaAMPS and NNDMA / reducing SPA and NVP

Sample Reference	NaAMPS : water : SPA	NVP : NNDMA
IN17	0.5 : 1.9 : 1	3 : 1
IN10	0.9 : 2.9 : 1	0.3 : 1

Mean peel strengths

Hydrogel		Max. N/25mm	Ave. N/25mm	Min. N/25mm
IN1	Mean	3.8	2.3	1.4
	Std Dev.	0.6	0.6	0.5
IN2	Mean	5.2	3.7	2.6
	Std Dev.	1.5	0.7	0.4
IN3	Mean	3.1	1.9	1.0
	Std Dev.	0.7	0.5	0.4
IN4	Mean	3.2	2.3	1.0
	Std Dev.	0.5	0.4	0.2
IN5	Mean	3.7	2.8	1.1
	Std Dev.	0.9	0.7	0.2
IN6	Mean	3.7	2.2	1.3
	Std Dev.	1.2	0.5	0.1
IN7	Mean	1.4	0.9	0.4
	Std Dev.	0.1	0.2	0.0
IN8	Mean	2.2	1.4	0.7
	Std Dev.	0.3	0.2	0.1
IN9	Mean	3.6	2.6	1.3
	Std Dev.	0.4	0.2	0.3
IN10	Mean	6.6	4.9	1.9
	Std Dev.	0.6	0.5	0.7
IN11	Mean	2.6	1.5	0.7
	Std Dev.	0.5	0.2	0.1
IN12	Mean	3.0	1.7	1.0
	Std Dev.	0.4	0.3	0.2
IN13	Mean	7.9	6.0	2.0
	Std Dev.	2.0	1.0	1.0
IN14	Mean	4.3	3.4	2.1
	Std Dev.	0.4	0.3	0.6
IN15	Mean	4.2	3.1	2.0
	Std Dev.	0.6	0.3	0.3
IN16	Mean	6.2	5.1	2.5
	Std Dev.	0.6	0.3	0.5
IN17	Mean	3.6	2.8	1.5
	Std Dev.	0.5	0.3	0.2
IN18	Mean	2.4	1.8	1.1
	Std Dev.	0.4	0.3	0.3

Typical mean elastic modulus (Pa)

Frequency Hz	IN1	IN2	IN3	IN4	IN5	IN6	IN7
0.5	9295.2	9020.8	14698.0	10165.9	11981.7	17422.0	13331.7
0.6	9788.6	9431.7	15376.7	10726.3	12749.3	18027.7	13934.7
0.8	10360.1	9782.8	16419.3	11370.0	13403.0	18278.3	14543.3
0.9	10882.5	10289.9	17369.0	11894.7	14154.7	18788.0	15138.0
1.1	11538.0	10875.7	18489.3	12475.0	14933.0	19579.3	15780.7
1.4	12164.5	11501.0	19518.0	13137.7	15802.7	20536.3	16448.3
1.7	12788.5	12219.5	20574.3	13784.3	16736.7	21477.3	17118.3
2.1	13422.0	12937.0	21553.7	14484.0	17725.7	22449.0	17828.7
2.6	14141.0	13625.5	22465.3	15176.0	18724.0	23538.0	18531.7
3.2	14800.0	14297.5	23319.3	15919.3	19703.3	24593.7	19250.0
3.9	15516.5	15022.0	24295.0	16704.0	20768.3	25743.7	20042.7
4.8	16219.0	15709.0	25167.0	17514.0	21777.3	26828.0	20766.7
6.0	16958.5	16410.0	26131.3	18344.0	22812.0	27990.3	21556.7
7.3	17681.0	17071.5	27020.0	19163.3	23787.0	29098.7	22324.7
9.1	18507.0	17768.5	28045.3	20124.3	24822.3	30334.3	23180.3
11.1	19295.5	18411.0	29059.7	21070.3	25722.0	31481.0	24007.7
13.6	20191.5	19103.5	30238.7	22193.0	26624.0	32694.3	24962.7
16.7	21155.5	19976.0	31599.7	23590.3	27557.0	34047.3	26208.0
21.4	22854.0	21749.5	34057.0	26311.0	29114.7	36502.0	28794.3
25.0	24861.5	23869.0	36458.0	29147.3	30679.7	39003.0	31684.0
Std Dev.							
0.5 Hz	920.5	1992.6	2173.7	485.9	1062.1	683.1	760.7
25 Hz	781.4	5687.1	2934.2	1435.7	2154.7	941.2	992.4

Frequency Hz	IN8	IN9	IN10	IN11	IN12	IN13	IN14
0.5	16039.0	15248.0	3361.3	2248.7	1636.3	4349.5	3300.9
0.6	16763.3	16466.7	3719.0	2419.4	1878.4	4824.8	3653.2
0.8	17529.0	17587.3	4128.7	2592.4	2173.6	4884.9	4128.0
0.9	18256.3	18411.3	4552.0	2751.6	2406.4	5545.3	4612.3
1.1	19006.7	19232.0	4990.7	2955.0	2687.1	6110.5	5044.3
1.4	19813.7	20022.7	5445.5	3149.5	2967.7	6627.6	5450.3
1.7	20629.0	20832.7	5905.7	3371.4	3272.1	7126.7	5870.8
2.1	21488.0	21711.7	6393.3	3621.8	3582.4	7648.2	6289.3
2.6	22351.0	22557.3	6884.5	3860.1	3882.7	8163.5	6720.7
3.2	23172.0	23384.3	7369.7	4137.5	4196.3	8684.7	7160.1
3.9	24119.0	24300.3	7898.0	4439.2	4544.1	9256.4	7623.2
4.8	24974.0	25143.0	8417.7	4750.5	4892.8	9813.8	8078.1
6.0	25928.0	26105.3	8941.9	5098.8	5272.1	10402.3	8582.7
7.3	26812.7	26994.3	9467.5	5466.3	5659.8	10980.7	9093.9
9.1	27749.0	27996.3	10053.1	5906.5	6126.9	11617.3	9673.0
11.1	28663.7	28970.7	10586.0	6370.7	6647.3	12289.0	10295.4
13.6	29646.3	30112.3	11167.0	6958.0	7321.8	13115.0	11072.0
16.7	30830.7	31474.3	11872.0	7782.3	8272.6	14209.0	12119.3
21.4	33210.3	34137.0	13371.7	9640.4	10279.2	16459.0	14326.0
25.0	35847.7	36998.7	15200.0	11835.7	12573.0	19007.3	16888.0
Std Dev.							
0.5 Hz	1232.7	1442.5	212.1	86.9	686.2	586.8	1527.2
25 Hz	822.6	641.3	610.1	805.7	2098.5	58.0	753.3

Frequency Hz	IN15	IN16	IN17	IN18
0.5	4067.8	7739.8	5444.0	4240.9
0.6	4406.9	8136.0	5732.8	4970.9
0.8	4564.3	8641.1	6160.8	5368.7
0.9	4821.3	9096.3	6491.9	5693.2
1.1	5083.2	9558.6	6932.7	6053.0
1.4	5374.5	10092.2	7402.3	6405.5
1.7	5685.1	10624.3	7917.7	6794.9
2.1	6075.6	11152.7	8413.3	7201.3
2.6	6411.2	11672.5	8899.4	7589.4
3.2	6784.2	12206.2	9418.9	7974.8
3.9	7196.0	12837.0	9953.6	8402.7
4.8	7613.8	13375.0	10509.5	8822.1
6.0	8045.4	14017.0	11102.7	9296.6
7.3	8499.8	14656.7	11680.3	9765.2
9.1	8975.3	15306.0	12299.7	10284.4
11.1	9459.6	15963.3	12909.3	10815.4
13.6	9968.1	16629.3	13556.7	11447.0
16.7	10511.7	17329.0	14228.0	12171.3
21.4	11184.3	18188.7	15073.0	13423.3
25.0	11944.0	18868.0	15725.3	14578.7
Std Dev.				
0.5 Hz	514.6	1778.2	1069.2	728.9
25 Hz	842.9	3070.0	1904.7	2925.2

Mean viscous modulus (Pa)

Frequency Hz	IN1	IN2	IN3	IN4	IN5	IN6	IN7
0.5	3865.1	3780.6	5741.4	4349.3	5471.8	6302.3	4245.6
0.6	4027.6	3879.8	5954.1	4462.6	5691.9	6443.7	4485.4
0.8	4191.1	3971.2	6130.7	4629.3	5833.9	6565.8	4605.3
0.9	4394.7	4064.6	6386.6	4834.0	6032.1	6673.9	4846.2
1.1	4545.7	4229.5	6690.7	4986.3	6223.2	6875.8	5000.8
1.4	4717.6	4398.4	7134.4	5184.3	6439.0	7116.8	5189.6
1.7	4919.9	4604.8	7260.7	5389.8	6672.6	7469.3	5394.5
2.1	5074.0	4817.5	7565.7	5593.4	7004.8	7771.7	5625.2
2.6	5330.7	5025.3	7891.7	5815.6	7270.2	8186.6	5842.2
3.2	5496.2	5230.6	8088.2	6057.1	7561.7	8550.5	6084.6
3.9	5719.6	5461.6	8425.3	6299.4	7844.4	9059.4	6350.6
4.8	5976.7	5669.9	8735.2	6602.5	8152.4	9486.8	6624.8
6.0	6245.2	5925.4	9113.0	6872.1	8478.7	10068.4	6904.7
7.3	6471.9	6149.5	9541.2	7152.7	8814.1	10649.7	7203.6
9.1	6766.6	6418.0	10029.2	7457.0	9167.1	11334.7	7546.2
11.1	7016.8	6612.4	10449.3	7712.6	9483.4	11966.3	7821.0
13.6	7216.9	6725.8	10903.0	7904.4	9704.0	12578.3	7974.5
16.7	7281.7	6638.0	11140.5	7921.6	9752.6	13057.0	7945.9
21.4	6962.1	5882.6	11065.9	7332.3	9207.6	13064.0	7123.8
25.0	6227.6	4651.1	10398.9	6259.2	8178.2	12277.7	5733.9
Std Dev.							
0.5 Hz	298.5	667.4	730.7	107.0	512.6	166.1	184.7
25 Hz	767.3	2052.8	4927.1	448.7	1497.0	26.2	174.2

Frequency Hz	IN8	IN9	IN10	IN11	IN12	IN13	IN14
0.5	5105.3	4248.2	1754.3	963.0	827.1	1817.9	1398.1
0.6	5263.6	4672.6	1932.8	1068.0	970.9	2021.7	1544.5
0.8	5482.4	4918.4	2109.3	1132.4	1083.1	2048.1	1707.7
0.9	5702.8	5154.3	2277.2	1218.9	1231.3	2374.6	1905.4
1.1	5924.9	5377.8	2493.1	1322.5	1355.0	2569.2	2070.2
1.4	6160.0	5605.8	2689.7	1415.3	1494.5	2744.8	2226.0
1.7	6408.1	5831.2	2870.3	1516.3	1633.9	2917.4	2372.9
2.1	6618.6	6084.8	3083.0	1632.7	1775.9	3087.8	2523.4
2.6	6875.4	6378.6	3281.2	1745.6	1907.9	3252.6	2667.7
3.2	7154.7	6662.3	3475.7	1872.4	2048.2	3416.1	2813.7
3.9	7471.5	7029.4	3681.1	2004.3	2206.4	3606.9	2977.5
4.8	7771.7	7353.0	3879.4	2133.6	2341.1	3774.6	3121.6
6.0	8126.7	7689.0	4085.7	2264.7	2478.7	3946.9	3276.0
7.3	8476.7	8127.8	4274.9	2385.7	2602.9	4102.5	3425.3
9.1	8854.8	8560.2	4478.1	2487.6	2710.5	4243.9	3551.0
11.1	9203.0	8971.9	4584.6	2546.8	2767.2	4323.7	3627.4
13.6	9476.8	9321.4	4590.3	2489.0	2748.1	4311.5	3606.6
16.7	9505.6	9492.4	4373.3	2234.1	2550.6	4096.1	3404.0
21.4	8812.8	9060.9	3423.8	1235.1	1727.2	3159.0	2493.6
25.0	7459.5	8018.8	2134.2	208.5	655.3	1903.1	1229.2
Std Dev.							
0.5 Hz	493.0	361.8	152.3	47.0	295.8	249.5	609.2
25 Hz	943.1	1002.5	579.3	74.8	342.3	490.9	114.2

Frequency Hz	IN15	IN16	IN17	IN18
0.5	1398.1	1668.9	3262.1	2361.5
0.6	1544.5	1728.1	3242.6	2404.5
0.8	1707.7	1817.9	3466.6	2541.3
0.9	1905.4	1944.4	3515.2	2652.6
1.1	2070.2	2011.0	3639.2	2762.8
1.4	2226.0	2119.5	3743.5	2950.9
1.7	2372.9	2229.8	3918.1	3096.6
2.1	2523.4	2363.4	4048.0	3267.4
2.6	2667.7	2489.9	4223.6	3387.5
3.2	2813.7	2627.4	4376.2	3578.7
3.9	2977.5	2757.7	4572.0	3740.5
4.8	3121.6	2919.2	4779.1	3948.7
6.0	3276.0	3065.3	5000.7	4092.7
7.3	3425.3	3202.4	5208.9	4281.0
9.1	3551.0	3329.0	5439.8	4455.2
11.1	3627.4	3400.8	5620.6	4598.0
13.6	3606.6	3383.0	5745.9	4681.8
16.7	3404.0	3186.6	5776.4	4631.3
21.4	2493.6	2394.9	5317.1	4063.8
25.0	1229.2	1435.0	4589.3	3285.6
Std Dev.				
0.5 Hz	179.1	674.4	298.7	454.9
25 Hz	442.0	373.7	580.5	538.5

Impedance

Hydrogel area = $25cm^2$

Time min	IN1	IN2	IN3	IN4	IN6	IN7
0	17.6	27.5	16.6	23.6	36.6	21.2
0.5	17.3	27.0	16.2	23.3	36.9	20.8
1	17.2	26.7	16.2	23.0	36.8	20.7
1.5	17.2	26.5	16.2	22.8	36.8	20.6
2	17.2	26.3	16.1	22.6	36.8	20.5
2.5	17.1	26.2	16.1	22.4	36.7	20.4
3	17.1	26.1	16.1	22.3	36.7	20.4
3.5	17.1	25.9	16.1	22.2	36.6	20.4
4	17.1	25.8	16.1	22.0	36.6	20.3
4.5	17.1	25.7	16.1	21.9	36.6	20.3
5	17.1	25.6	16.1	21.8	36.6	20.2
5.5	17.1	25.5	16.1	21.7	36.6	20.2
6	17.1	25.4	16.1	21.6	36.6	20.2
6.5	17.1	25.4	16.1	21.6	36.6	20.2
7	17.1	25.3	16.1	21.5	36.6	20.1
7.5	17.1	25.2	16.1	21.4	36.6	20.2
8	17.0	25.1	16.0	21.3	36.6	20.2
8.5	17.0	25.0	16.1	21.2	36.6	20.1
9	17.1	25.0	16.1	21.1	36.6	20.1
9.5	17.1	24.9	16.0	21.0	36.7	20.1
10	17.1	24.9	16.0	20.9	36.7	20.0
10.5	17.1	24.8	16.0	20.9		20.0
11	17.1		16.0	20.8		20.0

Time min	IN11	IN13	IN14	IN15	IN16	IN17	IN18
0	10.3	9.3	10.9	11.4	17.5	11.8	10.8
0.5	10.1	9.3	10.8	11.0	17.0	9.8	10.8
1	10.0	9.3	10.7	10.9	16.9	11.2	10.7
1.5	9.9	9.4	10.7	10.8	16.7	11.2	10.6
2	9.9	9.4	10.6	10.8	16.6	11.0	10.6
2.5	9.8	9.4	10.6	10.7	16.5	11.0	10.6
3	9.8	9.4	10.6	10.7	16.5	10.9	10.6
3.5	9.8	9.4	10.5	10.7	16.4	10.9	10.5
4	9.8	9.4	10.5	10.7	16.3	10.8	10.5
4.5	9.7	9.5	10.5	10.7	16.3	10.8	10.5
5	9.7	9.5	10.5	10.7	16.2	10.7	10.5
5.5	9.7	9.5	10.5	10.7	16.2	10.7	10.5
6	9.7	9.5	10.4	10.7	16.1	10.7	10.5
6.5	9.7	9.5	10.4	10.7	16.1	10.7	10.5
7	9.7	9.5	10.4	10.7	16.1	10.6	10.5
7.5	9.7	9.5	10.4	10.7	16.0	10.6	10.5
8	9.7	9.5	10.4	10.7	16.0	10.6	10.4
8.5	9.7	9.5	10.4	10.7	16.0	10.6	10.4
9	9.6	9.6	10.4	10.7	15.9	10.6	10.4
9.5	9.6	9.6	10.4	10.7	15.9	10.5	10.4
10	9.6	9.6	10.4	10.7	15.9	10.5	10.4
10.5	9.6	9.6	10.4	10.7	15.8	10.5	10.4
11	9.6		10.4	10.7	15.8	10.5	10.4

Time min	**IN1 10Hz**	**IN1 2kHz**	**IN3** 5 x thicker, 25cm^2	**IN3** 66cm^2
0	29.2	14.5	57.5	7.4
0.5	28.7	14.3	57.1	7.5
1	28.5	14.2	57.2	7.6
1.5	28.6	14.1	57.0	7.6
2	28.5	14.1	57.0	7.7
2.5	28.5	14.0	57.1	7.7
3	28.6	14.0	57.1	7.7
3.5	28.6	14.0	57.1	7.7
4	28.5	13.9	57.1	7.8
4.5	28.5	13.9	57.1	7.8
5	28.5	13.9	57.1	7.8
5.5	28.5	13.9	56.8	7.8
6	28.6	13.8	57.0	7.8
6.5	28.6	13.8	57.0	7.9
7	28.6	13.8	57.1	7.9
7.5	28.6	13.8	57.2	7.9
8	28.6	13.8	57.2	7.9
8.5	28.6	13.8	57.2	7.9
9	28.7	13.7	57.2	7.9
9.5	28.7	13.7	57.4	8.0
10	28.7	13.7	57.4	8.0
10.5	28.7	13.7	57.4	8.0
11	28.7	13.7	57.6	8.0

APPENDIX 4

Neutral Adhesive Hydrogels

COMPOSITIONS

Sample Reference	AMO g	PEG MA 400 g	NVP g	NNDMA g	TRIS g	Glycerol g	Water g	Ebecryl 11: Irgacure , 10:3, Mixture g
N19	12.5	20	2.5	7.5	5	27.5	25	0.15
N20	15	15	5	5	5	30	25	0.15
N21	12.5	20	2.5	7.5	5	25	27.5	0.15
N22	15	15	5	5	5	25	30	0.15
N23	12.5	15	2.5	7.5	5	32.5	25	0.15
N24	17.5	15	7.5	2.5	5	27.5	25	0.15

DESCRIPTION OF NEUTRAL ADHESIVE HYDROGELS

These hydrogels were clear, glassy looking and non-cohesive. They also contained residual monomers, N19 and N21 having more than the other two.

Increasing glycerol, AMO and NVP/ reducing $MPEG_{400}MA$ and NNDMA

Sample Reference	glycerol : AMO : $MPEG_{400}MA$	NVP : NNDMA
N19	6.1 : 2.9 : 1	0.3 : 1
N20	2.8 : 1.2 : 1	1: 1

Increasing water, AMO and NVP/ reducing $MPEG_{400}MA$ and NNDMA

Sample Reference	water : AMO : $MPEG_{400}MA$	NVP : NNDMA
N21	1.4 : 0.6 : 1	0.3 : 1
N22	2 : 1 :1	1: 1

Increasing water / reducing glycerol amounts

Sample Reference	water : glycerol
N19	1 : 1.11
N21	1 : 0.91
N20	1 : 1.12
N22	1 : 0.83

Mean elastic modulus (Pa)

Frequency Hz	N19	N20	N21	N22
0.50	793.43	1830.90	788.41	1860.03
0.61	782.86	2042.40	839.79	1951.80
0.76	852.47	2176.95	888.59	2080.67
0.93	913.70	2295.20	929.46	2163.30
1.14	982.65	2468.75	996.42	2270.20
1.40	1050.71	2578.90	1045.78	2375.63
1.72	1130.87	2735.98	1116.93	2484.63
2.13	1212.07	2903.73	1189.43	2619.77
2.61	1296.70	3064.78	1266.63	2765.87
3.19	1384.93	3235.58	1353.47	2912.00
3.95	1491.13	3427.18	1455.13	3071.67
4.84	1596.73	3631.98	1567.10	3250.10
6.00	1728.83	3850.13	1712.67	3452.33
7.32	1870.87	4074.85	1867.30	3663.77
9.09	2047.97	4310.58	2080.97	3924.93
11.11	2234.03	4522.30	2325.57	4218.53
13.64	2478.10	4709.20	2628.67	4536.63
16.67	2732.80	4899.30	3069.10	4905.17
21.43	3208.67	5019.83	3819.67	5534.30
25.00	3551.93	5096.85	4513.10	6049.77

Mean viscous modulus (Pa)

Frequency Hz	N19	N20	N21	N22
0.50	327.30	637.53	275.59	499.21
0.61	368.68	710.49	315.89	577.55
0.76	406.73	803.75	340.67	619.29
0.93	454.69	896.20	387.13	691.06
1.14	513.02	963.87	436.11	758.82
1.40	578.53	1083.83	484.43	840.02
1.72	615.31	1197.68	542.66	930.71
2.13	722.24	1316.33	601.53	1028.25
2.61	798.18	1443.20	664.15	1123.93
3.19	879.03	1569.43	731.98	1237.60
3.95	966.60	1716.63	804.06	1365.83
4.84	1056.27	1869.90	879.98	1474.33
6.00	1155.57	2032.80	965.21	1607.63
7.32	1256.93	2187.28	1040.34	1726.80
9.09	1352.30	2328.83	1109.83	1845.90
11.11	1434.83	2454.68	1138.30	1939.87
13.64	1481.77	2507.68	1117.17	1948.60
16.67	1428.87	2385.10	963.63	1788.27
21.43	1181.10	1797.28	500.35	1196.21
25.00	817.17	977.18	250.24	448.05

Residuals

Feed as %
Residual as % area

Retention time (min)	Monomer	N20		N24		N25	
		Feed	Residuals	Feed	Residuals	Feed	Residuals
3.1	**NNDMA**	5.0	2.0	7.5	1.5	2.5	2.0
3.4	**NVP**	5.0	0.4	2.5	0.2	7.5	1.0
4.2	**AMO**	15.0	0.4	12.5	0.5	17.5	0.9

Keeping the ratio of AMO % feed: residual % area at 3:3, in order to compare % feed: residual % area of each monomer.

Retention time (min)	Monomer	N20		N24		N25	
		Feed	Residuals	Feed	Residuals	Feed	Residuals
3.1	**NNDMA**	1.00	15.94	1.80	9.49	0.43	6.52
3.4	**NVP**	1.00	2.84	0.60	1.05	1.29	3.19
4.2	**AMO**	3	3	3	3	3	3

APPENDIX 5

Neutral Adhesive Hydrogels Containing Metal Ions

Compositions of neutral adhesive hydrogel with KCl

Sample Reference	AMO g	$MPEG_{400}MA$ g	NVP g	NNDMA g	TRIS g	Glycerol g	Water g	KCl	Ebecryl 11: Irgacure , 10:3, Mixture g
N26	15	15	5	5	5	30	25	1	0.15
N27	15	15	5	5	5	30	25	2	0.15
N28	15	15	5	5	5	30	25	3	0.15
N29	15	15	5	5	5	30	25	4	0.15
N30	15	15	5	5	5	30	25	5	0.15

Compositions of neutral adhesive hydrogel with NaCl

Sample Reference	AMO g	$MPEG_{400}MA$ g	NVP g	NNDMA g	TRIS g	Glycerol g	Water g	NaCl	Ebecryl 11: Irgacure , 10:3, Mixture g
N31	15	15	5	5	5	30	25	0.8	0.15
N32	15	15	5	5	5	30	25	1.6	0.15
N33	15	15	5	5	5	30	25	2.4	0.15
N34	15	15	5	5	5	30	25	3.1	0.15
N35	15	15	5	5	5	30	25	3.9	0.15

Impedance

Time min	N26	N27	N28	N29	N30
0	71.1	44.4	33.4	17.2	15.0
0.5	71.2	42.9	31.8	17.0	15.0
1	71.1	42.1	31.8	16.8	15.0
1.5	71.1	41.5	31.7	16.8	15.0
2	71.1	41.3	31.6	16.8	14.9
2.5	71.1	41.2	31.7	16.7	14.8
3	70.8	41.2	31.4	16.6	14.7
3.5	70.8	41.3	31.2	16.6	14.7
4	70.8	40.9	31.2	16.6	14.6
4.5	70.8	40.9	31.1	16.6	14.6
5	70.8	40.8	31.2	16.5	14.5
5.5	70.6	40.6	30.9	16.5	14.5
6	70.6	40.6	30.9	16.5	14.5
6.5	70.6	40.5	30.8	16.4	14.4
7	70.6	40.4	30.7	16.4	14.4
7.5	70.3	40.4	30.6	16.4	14.4
8	70.3	40.3	30.6	16.4	14.3
8.5	70.3	40.3	30.7	16.3	14.3
9	70.1	40.2	30.4	16.3	14.3
9.5	70.1	40.1	30.3	16.3	14.3
10	70.1	40.1	30.3	16.3	14.2
10.5	69.8	40.0	30.2	16.3	14.2
11	69.8	39.9	30.2	16.2	14.2
11.5	69.8	39.9	30.2	16.2	14.2
12	69.6	39.8	30.2	16.2	14.1

Time (min)	N31	N32	N33	N34	N35
0	38.6	25.6	18.2	18.8	20.3
0.5	38.1	25.5	17.9	18.8	19.6
1	37.8	25.8	17.8	18.8	20.0
1.5	37.6	26.0	17.7	18.7	20.6
2	37.4	26.2	17.6	18.7	20.9
2.5	37.2	26.3	17.5	18.6	21.1
3	36.9	26.4	17.5	18.5	21.2
3.5	36.8	26.4	17.4	18.5	21.3
4	36.7	26.5	17.4	18.4	21.3
4.5	36.5	26.6	17.3	18.4	21.4
5	36.5	26.7	17.3	18.3	21.4
5.5	36.3	26.9	17.2	18.3	21.3
6	36.2	27.2	17.2	18.2	21.3
6.5	36.1	27.3	17.1	18.1	21.3
7	36.0	27.4	17.1	18.1	21.3
7.5	35.8	27.5	17.0	18.0	21.3
8	35.8	27.6	17.0	18.0	21.2
8.5	35.6	27.7	16.9	17.9	21.2
9	35.6	27.8	16.9	17.9	21.2
9.5	35.5	27.8	16.8	17.8	21.1
10	35.4	28.0	16.8	17.8	21.1
10.5	35.3	28.0	16.8	17.8	21.1
11	35.2	28.1	16.7	17.7	21.0
11.5	35.1	28.2	16.7	17.7	21.0
12	35.0	28.3	16.7	17.6	21.0

APPENDIX 6

SPA and NaAMPS Adhesive Hydrogels

Composition and Impedance

						K^+			Na^+			
Sample Reference	Water g	NaAMPS g	SPA g	KCl g	crosslinker-initiator mixture g	SPA g	KCl g	Total g	Na^+ g	Total Cations g	Polyanion SO_3^- g	Impedance Ohms
FW1	42	58	0	3	0.15	0.0	1.6	1.6	5.8	7.4	52.2	62
FW2	42	52.2	5.8	3	0.15	1.0	1.6	2.6	5.2	7.8	51.8	61
FW3	42	34.8	23.2	3	0.15	3.9	1.6	5.5	3.5	9.0	50.6	49
FW4	42	23.2	34.8	3	0.15	5.9	1.6	7.4	2.3	9.8	49.8	43
FW5	42	0	58	3	0.15	9.8	1.6	11.3	0.0	11.3	48.3	40

APPENDIX 7

Macromolecular Release

In vitro release in small volume of media and effect of lens damage

Release media (isotonic phosphate-acetate buffered saline) RI = 1.33507

	Hours	RI	RI increment x 10^{-5}	(cumulative)	Temp (^{o}C)
lens 1	1	1.33513	6	6	24.9
	2	1.33512	5	10	25.0
	3	1.33511	4	14	25.0
	4	1.33518	11	25	25.0
	5	1.33518	11	35	24.9
	6	1.33515	8	43	24.9
lens 2 (not damaged)	1	1.33514	7	7	24.9
	2	1.33514	7	13	24.9
	3	1.33515	8	21	24.9
	4	1.33516	9	30	24.9
	5	1.33516	9	38	24.9
	6	1.33525	18	56	24.9
lens 3 (damaged)	1	1.33514	7	7	24.9
	2	1.33513	6	12	24.9
	3	1.33525	18	30	24.9
	4	1.33525	18	48	24.9
	5	1.33523	16	63	24.9
	6	1.33525	18	81	24.9

Different methods of agitation

Release media (isotonic phosphate-acetate buffered saline) RI = 1.33503

Type of Agitation	Hours	RI	RI increment x 10^{-5}		Temp (^{o}C)
				(cumulative)	
vortex	1	1.33509	6	6	25.0
	2	1.33507	4	10	25.0
	3	1.33507	4	14	25.0
	4	1.33508	5	19	25.0
	5	1.33516	13	32	25.0
ultrasound	1	1.33507	4	4	25.0
	2	1.33508	5	9	25.0
	3	1.33506	3	12	25.0
	4	1.33507	4	16	25.0
	5	1.33511	8	24	25.0
no agitation	1	1.33507	4	4	25.0
	2	1.33509	6	10	25.0
	3	1.33508	5	15	25.0
	4	1.33504	1	16	25.0
	5	1.33510	7	23	25.0

Packing solution of lenses with different expiry dates

Release media (isotonic phosphate-acetate buffered saline) RI = 1.33507

Lots				Year average		
Expiry date	Prescription	RI	RI increment x 10^{-5}	Expiry date	RI	RI increment x 10^{-5}
2002.25	-3.75	1.33522	15			
2002.75	-3.25	1.33524	17	2002.5	1.33523	16
2003.25	-0.50	1.33521	14			
2003.25	-3.00	1.33523	16			
2003.5	-5.00	1.33520	13			
2003.75	-3.50	1.33520	13	2003.5	1.33521	14
2005.25	-3.75	1.33518	11			
2005.4	-5.00	1.33516	9			
2005.5	-3.00	1.33517	10	2005.5	1.33517	10

RI – expiry date relationship y = -1.9623x + 3945.6
∴ RI of packing solution expiring in 2009 = (-1.9623 x 2009) + 3945.) = 3.3393

Packing solution of autoclaved lenses

Release media (isotonic phosphate-acetate buffered saline) RI = 1.33491

	Autoclaved saline RI		Average RI	RI increment x 10^{-5}
lens 1	1.33501	1.33501	1.33501	10
lens 2	1.33501	1.33498	1.33500	8
lens 3	1.33497	1.33497	1.33497	6

In vitro release from a standard commercial lens and a re-autoclaved standard commercial lens

Release media (isotonic phosphate-acetate buffered saline) RI = 1.33495

	Hours	RI	RI increment x 10^{-5}	(cumulative)	Temp °C
std	1	1.33505	10	10	24.9
commercial	2	1.33505	10	20	24.9
lens	3	1.33507	12	32	24.9
	4	1.33507	12	44	24.9
	5	1.33505	10	54	24.9
re-autoclaved	1	1.33524	29	29	24.9
standard	2	1.33511	16	45	24.9
lens	3	1.33507	12	57	24.9
	4	1.33509	14	71	24.9
	5	1.33509	14	85	24.9

In vitro release from a non autoclaved and autoclaved test lens

Release media (isotonic phosphate-acetate buffered saline) RI = 1.33495

	Hours	RI	RI increment x 10^{-5}		Temp °C
				(cumulative)	
non autoclaved lens	1	1.33504	9	9	24.9
	2	1.33506	11	20	24.9
	3	1.33512	17	37	24.9
	4	1.33528	33	70	24.9
	5	1.33519	24	94	24.9
autoclaved lens	1	1.33509	14	14	24.9
	2	1.33511	16	30	24.9
	3	1.33517	22	52	24.9
	4	1.33510	15	67	24.9
	5	1.33512	17	84	24.9

Packing solution of lenses with additional linear PVA

lens type	RI	Temp °C
control	1.33512	24.9
	1.33513	24.9
mean	*1.33513*	
47k	1.33513	24.9
	1.33511	24.9
	1.33512	24.9
mean	*1.33512*	
61k	1.33501	24.9
	1.33501	24.9
mean	*1.33501*	

In vitro release from lenses with additional linear PVA

Release media (isotonic phosphate-acetate buffered saline) RI = 1.33502

lens type	hours	RI	RI increment x 10^{-5}	(cumulative)	Temp °C
control	1	1.33508	6	6	24.9
	2	1.33511	9	15	24.9
	3	1.33511	9	24	24.9
	4	1.33509	7	31	24.9
	5	1.33512	10	41	24.9
47k	1	1.33509	7	7	24.9
	2	1.33513	11	18	24.9
	3	1.33512	10	28	24.9
	4	1.33511	9	37	24.9
	5	1.33511	9	46	24.9
61k	1	1.33508	6	6	24.9
	2	1.33516	14	20	24.9
	3	1.33517	15	35	24.9
	4	1.33513	11	46	24.9
	5	1.33513	11	57	24.9

In vitro release from unworn and worn lenses

Release media (isotonic phosphate-acetate buffered saline) RI for unworn lenses = 1.33503

Release media (isotonic phosphate-acetate buffered saline) RI for worn lenses = 1.33506

	HRS	RI	RI increment 10^{-5}	x (cumulative)	Temp °C
	1	1.33513	10	10	24.9
lens 1 unworn	2	1.33512	9	19	24.9
	3	1.33511	8	27	24.9
	4	1.33518	15	42	24.9
	5	1.33518	15	57	24.9
	6	1.33515	12	69	24.9
y = 12.114x - 5.0667	*8*			*92*	
	9	1.33510	4	96	24.9
	10	1.33507	1	98	24.9
lens 1 worn	11	1.33507	1	99	24.9
	12	1.33511	5	104	24.9
	13	1.33512	6	111	24.9
	14	1.33511	5	116	24.9
	1	1.33514	11	11	24.9
lens 2	2	1.33514	11	22	24.9
	3	1.33515	12	34	24.9
	4	1.33516	13	47	24.9
	5	1.33516	13	60	24.9
	6	1.33525	22	82	24.9
y = 13.771x - 5.5333	*8*			*105*	
	9	1.33508	2	107	24.9
	10	1.33509	3	110	24.9
	11	1.33509	3	114	24.9
lens 2 worn	12	1.33512	6	120	24.9
	13	1.33510	4	124	24.9
	14	1.33512	6	131	24.9